

Himalayan

JOURNAL OF SCIENCES

PEER REVIEWED JOURNAL OF SCIENCE | Volume 5 • Issue 7 • 2008 | www.himjsci.com | ISSN 1727 5210

SPECIAL ISSUE

Extended Abstracts



The 23rd Himalaya-Karakoram-Tibet Workshop

8-11 AUGUST 2008, LEH (LADAKH), INDIA

About INASP

Please see below for a brief description of INASP's work and details of two current projects.

Support for libraries

As repositories of knowledge, libraries have an important role to play in increasing the accessibility and dissemination of development research. INASP works with libraries to ensure that policy-makers and researchers have access to global knowledge that can help improve the lives of millions of people.

Training in new technology

INASP works with partners in developing countries to identify skill gaps in areas such as such as ICT (Information and Communication Technologies) and online resources, and we train individuals so that they can fulfil their role in putting research at the heart of efforts to reduce poverty.

Access to international research

As well as supporting new research in developing countries, INASP improves access to existing international research. In doing so, it provides researchers and policy-makers with important evidence of what is needed to improve people's lives and livelihoods.

Supporting publishing

As well as having access to research-based knowledge from across the world, researchers in developing countries must also be able to publish and communicate the results of their own work. INASP works with researchers and publishers in developing countries to ensure that local research has maximum impact.

For more information on INASP's work, please go to www.inasp.info



Introducing www.nepjol.info - Research from Nepal online

NepJOL was launched in 2007. There are currently more than 880 articles of which 570 are in full text. More articles are being added daily.

What is NepJOL?

The NepJOL website provides participating journals with the opportunity to take control of their own area within NepJOL, to load, edit and update their own journal information. Researchers can read free abstracts and access full text articles from participating journals, while authors can submit their articles online by following a few simple steps.

For more information please go to www.nepjol.info

JOLs (Journals Online) projects are also available in Vietnam (www.vjol.info), Bangladesh (www.banglajol.info) and in Africa (www.ajol.info). For more information, please visit their websites.



www.AuthorAID.info provides mentoring and support throughout the publication process for researchers in developing countries.

What is AuthorAID?

AuthorAID at INASP is a project which aims to assist researchers from developing countries to communicate their work more effectively. The goals are two-fold: to increase the success rate of researchers in obtaining publication and, ultimately, to increase the visibility and influence of research undertaken within the developing world.

Get involved

If you are a senior researcher who would like to get involved with the project, or if you are an early career researcher who would like to find a mentor, please contact us at: authoraid@inasp.info or go to

www.authoraid.info/get-involved

INASP, 60 St Aldates, Oxford, OX1 1ST, UK

Tel: +44 (0)1865 249909

Fax: +44 (0)1865 251060

Email: inasp@inasp.info

Web: www.inasp.info

Himalayan

JOURNAL OF SCIENCES

Volume 5

•

Issue 7 (Special Issue)

•

2008

•

ISSN 1727 5210

EXTENDED ABSTRACTS

The 23rd Himalayan – Karakoram – Tibet Workshop

8-11 august 2008
Leh, Ladakh
India

ORGANIZING COMMITTEE

A.K. Jain, India

Mark E. Barley, Australia

Mary L. Leech, USA

Sandeep Singh, India (Organizing Secretary)

GUEST EDITORS

Sandeep Singh

Arvind K. Jain

Bharat B. Shrestha

PRICE

Personal: US \$ 25.00

Institutional: US \$ 50.00

For HKT-23 Workshop Participants: IRs.1000.00

The 23rd Himalayan – Karakoram – Tibet Workshop



Hosted by

The organizing committee of
The 23rd Himalayan – Karakoram – Tibet Workshop

Department of Earth Sciences
Indian Institute of Technology Roorkee
Roorkee, INDIA

Sponsored by

Council of Scientific and Industrial Research, New Delhi
Oil and Natural Gas Corporation, India
Ministry of Earth Sciences, Government of India
National Hydroelectric Power Corporation
Indian National Science Academy, New Delhi
International Lithosphere Program (ILP)
National Geophysical Research Institute, Hyderabad

PREFACE

The Himalaya-Karakoram-Tibet region is the most fascinating and unique tectonic domain on Earth and is characterized by numerous geodynamic processes. The orogen has developed as a result of the interaction between the Indian and Asian plates during the past 150 million years. The Tibetan Plateau, popularly known as the “roof of the world,” is marked by doubling of crust and subduction-related magmatism, and is currently undergoing an eastward extrusion along major strike-slip and normal faults, east-west extension and devastating earthquakes.

The juncture of the Tibet plateau and the zone of crustal shortening (the Himalayas) is marked by the Karakoram fault and the Shyok and Indus Tsangpo Suture Zones, where the Neo-Tethyan oceanic lithosphere of the Indian Plate was subducted beneath the Asian Plate. The subduction of this ocean is manifested in the evolution of the Dras and Shyok volcanic arcs, imbrication of sections of the oceanic lithosphere of about 140-120 Ma, and deposition of trench sediments. All this is followed sequentially by emplacement and intrusion of calc-alkaline and Andean-type Trans-Himalayan batholiths from Pakistan to the easternmost parts of the Himalaya in Arunachal Pradesh. Once the Tethyan Ocean closed along the suture zones, immense crustal shortening followed within the Himalayan Collision zone to the south, with (i) continental subduction ca. 57 Ma along the northern edge producing ultrahigh pressure metamorphic terrain in Pakistan, India and Nepal, (ii) intense remobilization, Cenozoic progressive regional metamorphism and leucogranite generation from the Proterozoic continental crust within the Himalayan Metamorphic Belt (HMB), (iii) emplacement of the HMB nappes along the Lesser Himalayan Proterozoic Sedimentary Belt adjacent to the Main Central Thrust (MCT), (iv) cooling and exhumation of the terrain due to tectonics and/or monsoon precipitation and ensuing erosion, (v) deposition and evolution of the Himalayan foreland basins, and (vi) ongoing crustal deformation along major tectonic boundaries resulting in the present-day seismicity.

The Himalayan orogen is also the cradle for new geodynamic concepts such as the proposed role of deformation processes in the inversion of prograde metamorphic isograds including ductile shearing, leucogranite generation, monsoon-controlled erosion and channel flow. For the uplift of convergent orogenic belts, exhumation processes are linked with erosion and/or tectonic activity for unroofing the deeply-buried sequences, where one of the mechanisms may dominate over the other. In mountainous and humid active convergence zones, surface erosion processes require concomitant removal of eroded detritus through an efficient fluvial drainage system, which is an effective alternative to tectonic exhumation in the modification of structural and internal deformation patterns

Since the inception of the Himalayan-Karakoram-Tibet Workshop in 1985, this platform has become an important

focus of discussion among active researchers from the countries of the mountain chain as well as international groups. The present workshop, the 23rd in the series, is being held in the cold desert heartland of Ladakh, located on the Indus Tsangpo Suture Zone and the extensive Andean-type Ladakh Batholith, emplaced around 60 Ma at around 10 km depth.

Ladakh, the cold desert, consists of the two districts of Leh and Kargil in State of Jammu and Kashmir. Leh with an area of 45110 km² makes it the largest district in the country in terms of area. The Leh district has international borders with Pakistan and China in the north and is bounded by Lahul and Spiti region of Himachal Pradesh in southeast. Ladakh lies on the rain shadow side of the Himalayan region and has both arctic and desert climatic conditions, which in combination with the high altitude, poor oxygen and vegetation, low humidity as well as high solar radiation, make the region inhospitable. In the background, the nine-story Leh Palace is a distinguished historical monument of the 17th century Tibetan architecture and is said to have inspired the famous Potala Palace of Lhasa.

In ancient times, the present Leh district was a part of Greater Ladakh from Kailash Mansarover to Swaat (Dardistan) and was neither under the Domain of Tibet nor under its influence. Lying on the ancient trade silk route between Tibet and Central Asia, with the majestic Leh Palace in the background, beautiful Leh is an ideal setting for this workshop from the geological, historical, cultural, religious and adventure points of view.

This volume of Himalayan Journal of Science contains one hundred and twenty four extended abstracts, which will be the subject of discussion during three-day presentation during the workshop. One hundred and forty scholars have responded to our call for the workshop, while about 120 delegates are likely to participate in the workshop. Out of these, 40 delegates will join us to the Field Excursion through the fabulous geology of the Indian and Asian plate margins.

The Organizing Committee expresses its deep sense of gratitude to many organizations for their generous financial support of this workshop and also travel assistance for many participants. The Editorial Board of the Himalayan Journal of Sciences has been most cooperative in their timely publication of this volume. Finally, the workshop could not have been held without the unwavering support of the Indian Institute of Technology Roorkee.

Organizing Committee of the
23rd Himalayan-Karakoram-Tibet Workshop

Sandeep Singh
Arvind K Jain
Mary L Lecch
Mark E Barley

EDITORIAL POLICY

Himalayan Journal of Sciences (ISSN 1727 5210) is a peer-reviewed multi-disciplinary journal published twice yearly. HJS focuses on biodiversity, natural resource management, ecology and environment, and other fields related to Himalayan conservation, and development. HJS invites authors to communicate their knowledge and uncertainties from all the sciences.

HJS publishes works in the following genres:

- i) *Research papers*: report on original research
- ii) *Review papers*: thorough account of current developments and trajectories in any field covered in the journal
- iii) *Articles*: narrowly-focused account of a current development in any field covered in the journal
- iv) *Editorial*: opinionated essay on an issue of public interest
- v) *Essay*: similar to editorial but longer and more comprehensive; may include tables and figures
- vi) *Commentary and Correspondence*: persuasive and informed commentary on any topical issues or on articles published in prior issues of the journal
- vii) *Policy*: critical review of some topic of high public interest, hybrid of essay and review article, with the basis of highly valid facts and figures
- viii) *Resource review*: evaluation of books, websites, CDs, etc. pertinent to the scope of HJS
- ix) *Publication preview*: description/epitome of the forthcoming important books
- x) *Calender*: notice of forthcoming conferences, seminars, workshops, and other events related to science and the Himalayas.

Permission

Permission to make digital or hard copies of part or all of any article published in HJS for personal use or educational use within one's home institution is hereby granted without fee, provided that the first page or initial screen of a display includes the notice "Copyright © 2008 by the Himalayan Association for the Advancement of Science," along with the full citation, including name of author(s). We assert the authors' moral right to post their papers on their personal or home institution's Web pages and to make and distribute unlimited photocopies of their papers. In all of the above cases, HimAAS expects to be informed of such use, in advance or as soon as possible.

To copy or transmit otherwise, to republish, to post on the public servers, to use any component of a paper in other works, or to use such an article for commercial or promotional purposes requires prior specific permission. HimAAS does not grant permission to copy articles (or parts of articles) that are owned by others.

Special Acknowledgments

In the business of dissemination of new knowledge relevant to Himalaya, we are assisted in our publication and pre-publication work by certain commercial collaborators. By offering HJS generous discounts (and in some cases waiving all fees), they have significantly reduced our publication costs. We have tried to reciprocate in a small measure by including notices of their services. Scanpro Pvt. Ltd. and Jagadamba Press: Thank you for standing with us in this venture!

Printed at: Jagadamba Press
Hattiban, Lalitpur, Tel: 55250017, 55250018

Layout and Designed by Bharat Shrestha
Kathmandu, Nepal

Color separation: ScanPro Pvt Ltd.
Pulchowk, Lalitpur, Nepal
Tel: 5548861, 5551123, 5552335

NOTICE

This is a special issue of the Himalayan Journal of Sciences, containing extended abstracts of papers to be presented at the 23rd Himalaya-Karakoram-Tibet Workshop to be held in Leh, Ladakh, India August 08-11, 2008. The issue was produced by guest editors and its contents have not been subjected to peer review.

Himalayan

JOURNAL OF SCIENCES

Volume 5

Issue 7 (Special Issue)

2008

ISSN 1727 5210



*Himalayan Journal
of Sciences*

Volume 5, Issue 7, 2008

Page: 01-182

Cover Image

Leh Palace, Ladakh: the site of
23rd HKT Workshop. Courtesy
of Sandeep Singh.

Organizing Secretary, 23rd
Himalayan Karakoram Tibet
Workshop.

(email: san662005@gmail.com)



Published by
Himalayan Association for
the Advancement of Sciences
(HimAAS)
Lalitpur, Nepal
GPO Box No. 5275

extended abstracts

Scion Image Analysis in rocks of the hanging wall and foot wall of the MCT, central Nepal
Kamala Kant Acharya and Bernhard Grasemann, Page 15

Geological setting of the Siang Dome located at the Eastern Himalayan Syntaxis
Subhrangsu K. Acharyya and Puspendu Saha, Page 16

Geochemical-isotopic characteristics and K-Ar ages of magmatic rocks from Hundar valley,
Shyok Suture Zone, Ladakh.
*T Ahmad, S Sivaprabha, S Balakrishnan, N X Thanh, T Itaya, H K Sachan, D K Mukhopadhyay and
P P Khanna, Page 18*

New SHRIMP ages for Ladakh and Karakoram Batholiths - inherited zircons indicate
involvement of older crust
T Ahmad, L White, M Forster, T R Ireland and G Lister, Page 19

Preliminary paleomagnetic study of Cretaceous dykes in SE-Tibet
E Appel, I Dunkl, L Ding, C Montomoli, R El Bay and R Gloaguen, Page 20

Carbon and sulfur isotope records of Ediacaran carbonates of Lesser Himalayas: implications
on oxidative state of the contemporary oceans
DM Banerjee, Page 21

Kinematics of the crust in southern Tibet and Higher Himalayan
Crystalline – a paleomagnetic approach
*Rachida El Bay, Erwin Appel, R Carosi, L Ding, D István, R Gloaguen, C Montomoli, L Paudel and
B. Wauschkuhn, Page 22*

White Sandstone in Subathu Sub-Basin: an example of tectonically driven forced regressive wedge
MK Bera, A Sarkar and PP Chakraborty, Page 24

Evolution of the Lesser Himalaya
ON Bhargava and W.Frank, Page 26

Bursting of glacial lakes—a consequence of global warming: a case history from the Lunana
area, Gasa Dzongkhag, Bhutan
ON Bhargava, SK Tangri and AK Choudhary, Page 28

Implications of biostratigraphy in the Himalayan Paleogene Foreland Basin
SB Bhatia and ON Bhargava, Page 29

Spatio – Temporal Variation of Vegetation during Holocene in the Himalayan Region
Amalava Bhattacharyya and SK Shah, Page 31

Songpan Garze fold belt: New petrological and geochronological data
Audrey Billerot, Julia de Sigoyer, S Duchêne, O Vanderhaeghe and Manuel Pubellier, Page 32

extended abstracts Continued...

Crustal velocity structure from surface wave dispersion tomography in the Indian Himalaya

Warren B Caldwell, Simon L Klempner, Shyam S Rai and Jesse F Lawrence, Page 33

Non-coaxial heterogeneous deformation in the Num orthogneiss (Arun valley, Mt. Makalu area, eastern Nepal)

R Carosi, C Frassi, C Montomoli, PC Pertusati, C Groppo, F Rolfo and D Visonà, Page 34

Ductile-brittle deformation in the hanging-wall of the South Tibetan Detachment System (Southern Tibet)

R Carosi, C Montomoli, E Appel, I Dunkl and Ding Lin, Page 35

Three-Dimensional Strain Variation across the Kathmandu Nappes: Insight to Nappe Emplacement Mechanism

Deepak Chamlagain Page 36

Crustal configuration of NW Himalaya based on modeling of gravity data

Chamoli Ashutosh, AK Pandey, VP Dimri and P. Banerjee, Page 39

Tectonometamorphic evolution of collisional orogenic belts in the Korean Peninsula: Implications for East Asian tectonics

Moonsup Cho, Page 40

The Sedimentary Record of Deglaciation in the Western Himalaya recorded in the Indus Delta, Pakistan

PD Clift, L Giosan, IH Campbell, J Blusztajn, M Pringle, AR Tabrez, A Alizai, MM Rabbani and S Vanlaningham, Page 41

Seismic reflection evidence for a Dangerous Grounds mini-plate in the South China Sea and implications for extrusion tectonics in SE Asia

Peter Clift, GH Lee, NA Duc, U Barckhausen, H Van Long, and Sun Zhen, Page 42

Examination of relocated earthquake hypocenters in the Pamir-Hindu Kush seismic zone using 3-D plots

S Das, Page 43

Unzipping Lemuria from its Himalaya suture to understand mammalian origins

Maarten J de Wit and Judith Masters, Page 44

Addressing Tectonic and Metamorphic Controversy in the Pakistan Himalaya

Joseph A Dipietro, Page 45

Active tectonics and origin of Tso Morari Lake observed by Remote sensing and GIS techniques

CS Dubey and DP Shukla, Page 47

Diagenetic and metamorphic overprint and deformation history of Permo-Triassic Tethyan sediments, SE Tibet

István Dunkl, Ding Lin, Chiara Montomoli, Klaus Wemmer, Gerd Rantitsch, Borja Antolin, Rachida El Bay and Erwin Appel, Page 49

Impact of coeval tectonic and sedimentary-driven tectonics on the development of overpressure cells, on the sealing, and fluid migration –Petroleum potential and environmental risks of the Makran Accretionary Prism in Pakistan

N Ellouz-Zimmermann, A Battani, E Deville, A Prinzofher and J Ferrand, Page 50

The Tso Morari Nappe of the Ladakh Himalaya: formation and exhumation

Jean-Luc Epard and Albrecht Steck, Page 52

Implications of geochemical signatures in the Trans-Himalayan Lohit batholith, Arunachal Pradesh, India

TK Goswami, Page 53

Cretaceous - Tertiary carbonate platform evolution and the age of India – Asia collision along the Ladakh Himalaya (NW India)

Owen R Green, Michael P Searle, Richard I Corfield and Richard M Corfield, Page 54

P-T evolution across the Main Central Thrust zone (Eastern Nepal): hidden discontinuities revealed by petrology

Chiara Groppo, Franco Rolfo and Bruno Lombardo, Page 55

Kyanite-bearing anatectic metapelites from the Eastern Himalayan Syntaxis, Eastern Tibet, China : textural evidence for partial melting and phase equilibria modeling

Carl Guilmette, Indares Aphrodite, Hébert Réjean and CS Wang, Page 56

New occurrence of eclogitic continental rocks in NW Himalaya: The Stak massif in northern Pakistan

Stéphane Guillot, Nicolas Riel, Kéiko Hattori, Serge Desgreniers, Yann Rolland, Jérémie Van Melle, Mohamad Latif, Allah B. Kausar and Arnaud Pêcher, Page 57

Evolution of the Indian Monsoon System and Himalayan-Tibetan Plateau uplift during the Neogene

Anil K Gupta, Page 58

Structural and metamorphic equivalence across the LHS-HHCS contact, Sikkim Himalaya – indicator of post-deformation metamorphism or the wrong MCT?

Saibal Gupta and Suman Mondal, Page 59

Continental Relamination Drives Compositional and Physical-Property Changes in the Lower Crust

Bradley Hacker, Peter B Kelemen and Mark D Behn, Page 60

Comparison of regional geoelectric structure of Himalayan region

T Harinarayana and RS Sastry, Page 61

extended abstracts Continued...

Pre-collisional Crustal Structure Adjacent the Indus-Yalu Suture
T Mark Harrison, Donald J Depaolo and Amos B Aikman, Page 62

Discovery of crustal xenolith-bearing Miocene post-collisional igneous rocks within the Yarlung Zangbo Suture Zone southern Tibet: Geodynamic implications
Réjean Hébert, L Guillaume, B Rachel, C Guilmette, É Bédard, C Wang, T D Ullrich and Jaroslav Dostal, Page 63

Constraints to the timing of India-Eurasia collision determined from the Indus Group: a reassessment
Alexandra L Henderson, Yani Najman, Randall R Parrish, Andrew Carter, Marcelle Boudagher-Fadel, Gavin Foster, Eduardo Garzanti and Sergio Andò, Page 64

Structure of the crust and the lithosphere in the Himalaya-Tibet region and implications on the rheology and eclogitization of the India plate
György Hetényi, J Vergne, John L. Nábělek, R Cattin, F Brunet, L Bollinger and M Diament, Page 65

Present-day E-W extension in the NW Himalaya (Himachal Pradesh, India)
Esther Hintersberger, Rasmus Thiede, Manfred Strecker and Frank Krüger, Page 67

3-D Velocity Structure of the Crust and upper Mantle in Tibet and its Geodynamic Effect
Zheng Hongwei, He Rizheng, Zhao Dapeng, Li Tingdong and Rui Gao, Page 69

Electrical Structure of Garhwal Himalayan region, India, inferred from Magnetotelluric
M Israil, DK Tyagi, PK Gupta and Sri Niwas, Page 70

Heterogeneous Himalayan crust using shear wave attenuation in the Pithoragarh region of Kumaon
A Joshi, M Mohanty, AR Bansal, VP Dimri and RK Chadha, Page 72

Lithostratigraphy of the Naga-Manipur Hills (Indo-Burma Range) Ophiolite Belt from Ukhrul District, Manipur, India
A Joshi and KT Vidyadharan, Page 73

Pre-Himalayan tectonometamorphic signatures from the Kumaun Himalaya
Mallickarjun Joshi, Page 75

Northeast Tibetan Crustal Structure from INDEPTH IV Controlled-Source Seismic Data
Marianne Karplus, S Klemperer, Z Wenjin, Wu Zhenhan, Shi Danian, Su Heping, L Brown, Chen Chen, Jim Mechie, R. Kind, F Tilmann, Yizhaq Makovsky, R Meissner, and INDEPTH Team Page 76

Geochronologic, structural and metamorphic constraints on the evolution of the South Tibetan detachment system, Bhutan Himalaya
Dawn A. Kellett, Djordje Grujic, Isabelle Coutand and Clare Warren, Page 78

Paired terraces of the Seuti Khola, Dharan, eastern Nepal
M P Koirala, SK Dwivedi, P Dhakal, G Neupane, YP Dhakal, SP Khanal, N K Regmi, G Ojha, S Shrestha and RK Dahal, Page 80

Late Quaternary climatic changes in the eastern Kumaun Himalaya, India as deduced from multi-proxy studies
BS Kotlia, J Sanwal, B Phartiyal, L M Joshi, A Trivedi, and C Sharma, Page 81

Palaeozoic granites and their younger components - A study of Mandi and Rakcham granites from the Himachal Himalaya
A Kundu, NC Pant and Sonalika Joshi, Page 82

Out-of-sequence deformation and expansion of the Himalayan orogenic wedge: insight from the Changgo culmination, south-central Tibet
Kyle P Larson and Laurent Godin, Page 84

Is the Ramgarh thrust equivalent to the Main Central thrust in central Nepal?
Kyle P Larson and Laurent Godin, Page 85

Telescoping of isotherms beneath the South Tibetan
Richard D Law, Micah J Jessup, Michael P Searle, John M Cottle and David Waters, Page 86

Does the Karakoram fault interrupt mid-crustal channel flow in the western Himalaya?
Mary L Leech, Page 88

Miocene exhumation of the granulite-eclogite of the Ama Drime range (high Himalayas) through polyphased syn-convergence normal faulting
Philippe Hervé Leloup, Elise Kali, N Arnaud, G Mahéo and E Boutonnet, Page 89

Lateral heterogeneity in lithospheric structure in SE Tibet
Anne Meltzer, Brian Zurek, Stephane Sol and Lucy Brown, Page 90

Polyphase deformation history of the "Tibetan Sedimentary Sequence" in the Himalayan chain (South-East Tibet)
Chiara Montomoli, E Appel, A Borja, I Dunkl, R El Bay, Ding Lin and Gloaguen, Page 91

How significant is erosion in extrusion- insights from analogue and analytical models
S Mukherjee, Hemin A Koyi, CJ Talbot and AK Jain, Page 92

extended abstracts Continued...

Flexural-slip folding and fold-accommodation faulting in the Tethyan Sedimentary Zone, NW Himalayas
Dilip K Mukhopadhyay, Page 93

The Paleogene record of Himalayan erosion; Burma and Bangladesh
Yani Najman, R Allen, M Bickle, M BouDagher-Fadel, A Carter, E Garzanti, M Paul, J Wijbrans, Ed Willett, G Oliver, R Parrish, S H Akhter, S Ando, D Barfod, E Chisty, L Reisberg, G Vezzoli and J Uddin, Page 94

The Main Central Thrust Revisited: New Insights from Sikkim Himalaya
Sudipta Neogi and V Ravikant, Page 95

Deformation partitioning at the rupture front in NW Himalaya: evidence from tectono-geomorphic and paleoseismic investigations
Anand K Pandey, Prabha Pandey, Guru Dayal Singh, GV Ravi Prasad, K Dutta and DK Ray, Page 97

Geochemical characters of muscovite from the Pan African Mandi Granite, and its emplacement and evolution
NC Pant and A Kundu, Page 98

Segmented Nature of the Himalaya and Gangetic Plain
B Parkash, RS Rathor, AK Awasthi, P Pati, B Bhosle, RP Jakhmola, S Singh and V Acharya, Page 99

Significance of the clay mineral distribution in the fluvial sediments of the Neogene Himalayan Foreland Basin (central Nepal)
Pascale Huyghe, Romain Guillot, Matthias Bernet and Ananta Prasad Gajurel, Page 100

Deformation and exhumation of the Higher and Lesser Himalayan Crystalline sequences in the Kumaon region, NW-Himalaya based on structural and fission-track analysis
Patel RC, Nand Lal and Yogesh Kumar, Page 101

Tectonics vs. erosion: evidences from apatite fission track and Rb-Sr (Biotite and Muscovite) thermochronology, Arunachal Himalaya
Pebam J, AK Jain, R Kumar, Sandeep Singh and Nand Lal, Page 103

Stress field evolution in the North West Himalayan syntaxis (Northern Pakistan)
A Pêcher, S Guillot, F Jouanne, G Mahéo, JL Mugnier, Y Rolland, P Van der Beek and J Van Melle, Page 106

Soft sediment deformation structures in the Late Quaternary sediments of Ladakh: evidence of multiple phases of palaeoearthquakes in the North western Himalayan Region
Binita Phartiyal and Anupam Sharma, Page 107

Complex Seismic Discontinuities in the Mantle Transition Zone beneath NW Himalaya and Ladakh- Karakoram
KS Prakasam, SS Rai, Keith Priestley and VK Gaur, Page 108

High Crustal Seismic Attenuation in Ladakh- Karakoram
SS Rai, Ashish, Amit Padhi and P Rajgopala Sarma, Page 109

The Deep structure of Western Himalaya – Ladakh-Karakoram
SS Rai, VK Gaur, Keith Priestley and Lev Vinnik, Page 110

Deep seismic reflection profiling over the Siwalik fold belt of NW Himalaya
B Rajendra Prasad, V Vijaya Rao and HC Tewari, Page 111

Occurrence of Permian palynofossils from the Saltoro Formation, Shyok-Suture-Zone, Ladakh Himalaya, India
Ram- Awatar, Page 113

Central crystallines as the exclusive source terrain for the sandstone-mudstone suites of siwalik group: geochemical evidence
Nikesh Ranjan and DM Banerjee, Page 114

Northern Margin of India in the Pre-Himalayan times
Vibhuti Rai and Aradhana Singh, Page 115

The petrogenesis of a crustal-derived Palaeoproterozoic Bomdila orthogneiss, Arunachal Pradesh, NE Lesser Himalaya
Shaik A Rashid, Page 116

The great 1950 Assam Earthquake revisited: field evidences of liquefaction and search for paleoseismic events
DV Reddy, Pasupuleti Nagabhushanam, Devender Kumar, BS Sukhija, PJ Thomas, AK Pandey, RN Sahoo, GV Ravi Prasad and K Datta, Page 117

Occurrences of sulphide minerals in the Stak and Tso Morari eclogites: Implications for the behaviour of sulphur and chalcophile elements in subduction zones
Nicolas Riel, Keiko Hattori, Stephane Guillot, Mohamad Latif and Allah B Kausar, Page 118

SHRIMP zircon ages of eclogites in the Stak massif, northern Pakistan
Nicolas Riel, Kéiko Hattori, Stéphane Guillot, Nicole Rayner, Bill Davis, Mohamad Latif and Allah B. Kausar, Page 119

Structural, paleogeographic and topographic evolution of the northern Tibetan Plateau margin: Evidence from the southern Tarim basin, northern Hexi Corridor, and Qaidam basin
Bradley D Ritts, Paul M Bovet, Malinda L Kent-Corson, Brian J Darby, Jeremy Hourigan, Guangsheng Zhuang, Stephan A Graham and Yongjun Yue, Page 121

extended abstracts Continued...

- New recognition of NNE-strike belt of negative aeromagnetic anomaly in Tibetan plateau
HE Ri-Zheng, GAO Rui and ZHENG Hong-Wei, Page 123
- Identification of necessary conditions for supershear wave rupture speeds: Application to Californian and Asian Fault
David Robinson and Shamita Das, Page 125
- Discovery of granulitized eclogite in North Sikkim expands the Eastern Himalaya high-pressure province
Franco Rolfo, Rodolfo Carosi, Chiara Montomoli and Dario Visonà, Page 126
- Seismic Tomography of Garwhal-Kumaun Himalayas: Is the basal detachment a wistful thinking?
S Mukhopadhyay, J Sharma and BR Arora, Page 128
- Lake-level changes in the past 50 ka reconstructed from the lacustrine delta deposits in Kathmandu Valley, Nepal
Tetsuya Sakai, Ananta P Gajurel, Hideo Tabata, Nobuo Ooi and Bishal N Upreti, Page 129
- Mineralogy and Geochemistry of mafic to hybrid microgranular enclaves and felsic host of Ladakh batholith, Northwest Himalaya: Evidence of multistage complex magmatic processes
Santosh Kumar and Brajesh Singh, Page 130
- Geochemistry and Petrogenesis of Granitoids from Kameng Corridor of Arunachal Himalaya, Northeast India
Santosh Kumar and Manjari Pathak, Page 132
- Analysis of gravity and magnetic data along Runtse-Upshi-Leh-Kardung la and Runtse-Upshi-Igu-Shakti-Chang la – Durbuk profiles – Presence of ophiolites within Ladakh batholith and suture zones
Rambhatla G Sastry and Md Israil, Page 133
- Analysis of gravity and magnetic data along Mahe-Sumdo-Tso Morari
Rambhatla G Sastry and Md Israil, Page 135
- Anatomy, Age and Evolution of the Baltoro granite batholith, Pakistani Karakoram
Michael Searle, Andrew Thow, Randall Parrish, Steve Noble and David Waters, Page 137
- Analysis of Climate change from high elevation sites of North West Himalaya based on tree ring data
SK Shah, A Bhattacharyya and V Chaudhary, Page 138
- Geohistory of Tso-Morari Crystalline, Eastern Ladakh, India: a plausible model for ultra-high pressure rocks in the Himalaya
Ram S Sharma, Page 139
- Geochemistry of Late Quaternary Spituk palaeolake deposit of Ladakh, NW Himalaya
Anupam Sharma and Binita Phartiyal, Page 141
- Remote Sensing based Study of Retreat of and Accompanying Increase in Supra-glacial Moraine Cover over a Himalayan Glacier
A Shukla, RP Gupta and MK Arora, Page 142
- Vertical stratigraphic variations and sedimentation model of the Lower Siwalik sequence in Kumaun Himalaya, India
UK Shukla and DS Bora, Page 143
- Amphibole compositions as indicators of deep crustal and mantle processes in subduction zones: case study – Tso Morari metamafics, Ladakh, Himalaya
Preeti Singh, NC Pant, A Kundu, T Ahmad and PK Verma, Page 144
- Tectonic Activity In The Ganga Plain Foreland Basin During Quaternary
Indra Bir Singh, Page 145
- Weathering in the Ganga Alluvial Plain: Geochemical signatures linking of the Himalayan source and the Bay of Bengal sink
Indra Bir Singh, Sandeep Singh and Munendra Singh, Page 146
- Geomorphic indicators of active growth and lateral propagation of fault-related folds: Mohand Ridge anticline, NW Himalaya
Tejpal Singh and A. K. Awasthi, Page 147
- Neotectonic activity and its geomorphic response in the Tangtse valley, Ladakh Himalaya
Vimal Singh, Page 148
- Sediment sourcing in the Gangetic alluvium, Himalayan Foreland Basin – competition between Himalayan and cratonic hinterland
R Sinha, Y Kettanah, MR Gibling, S K Tandon, M Jain, P S Bhattacharjee, AS Dasgupta and P Ghazanfari, Page 149
- Silurian acanthomorphitae acritarch from the Shiala Formation, Tethys Garhwal Himalaya, India
HN Sinha, Page 150
- Landslides in the Kashmir Earthquake of 8th October 2005
Amita Sinhal, Ashok D Pandey and Sachin M Pore, Page 152
- Neogene sedimentary evolution of the Guide Basin and its implications on uplift of the NE Tibetan Plateau, China
Chunhui Song, Qingquan Meng, Xiaomin Fang, Shuang Dai and Junping Gao, Page 154
- A possible Permian suture in the Lhasa Block, Tibet: Evidence from eclogite and probable ophiolite
Chen Songyong, Yang Jingsui, Li Tianfu, Xu Xiangzhen, Li Zhaoli and Ren Yufeng, Page 155

extended abstracts Continued...

Long Term GPS Deformation
Rates in the Karakoram terrane of Ladakh
*Sridevi Jade, VK Gaur, MSM Vijayan and
P Dileep Kumar, Page 156*

The metamorphism of the Tso Morari
ultra-high pressure nappe of the Ladakh Himalaya
Albrecht Steck and Jean-Luc Epard, Page 157

The Tectonics of the Tso Morari Ultra High
Pressure Nappe in Ladakh, NW Indian Himalaya
Albrecht Steck and Jean-Luc Epard, Page 159

The Trans-Hudson Orogen of North America and the
Himalaya-Karakoram-Tibetan Orogen of Asia: Structural and
thermal evolution of the collisional lower and upper plates
*Marc St-Onge, Michael Searle, Natasha Wódicka, Jeroen van Gool,
Adam Garde and David Scott, Page 161*

Melting and Exhumation of the upper structural
levels of the Greater Himalaya Sequence and Makalu granite:
constraints from thermobarometry, metamorphic
modeling and U-Pb geochronology
*Michael J Streule, Michael P Searle, Matthew
SA Horstwood and David Waters, Page 162*

Strong ground motion observation and estimation:
From predictive relationships and
modelling to real-time shakemaps
*Suhadolc Peter, Costa Giovanni and
Moratto Luca, Page 163*

Degree of Magnetic anisotropy as a strain intensity gauge:
An example from the Footwall of MCT Zone along
Bhagirathi valley, Garhwal Himalaya, India
Nihar R Tripathy and Tejpal Singh, Page 164

Petrology and geochronology of eclogitic and
retrograde micas from Tso Morari UHP
Complex, Ladakh Himalaya
*Igor M Villa, Julia de Sigoyer and
Stéphane Guillot, Page 167*

Examining the Tectonic Wedging
Hypothesis in the NW India Himalaya
A Alexander G Webb and An Yin, Page 168

Tectonic sequence diagrams and the constraints
they offer for the structural and metamorphic
history of the Kullu Valley, NW India
L White, G Lister, M Forster and T Ahmad, Page 169

Different eclogite types from the Pakistan Himalaya
and implications for exhumation processes
*Franziska DH Wilke, Patrick J O'Brien and
M Ahmed Khan, Page 170*

River discharge and erosion rates in the
Sutlej basin, NW Himalaya
Hendrik Wulf and Dirk Scherler Page 172

The Central Crystallines around Hapoli,
Subansiri, Eastern Himalayas
*An Yin, CS Dubey, AAG Webb, PK Verma,
TK Kely and TM Harrison, Page 174*

Surface-tectonic coupling at the Namche Barwa –
Gyala Peri massif and geologic hazards associated with a
proposed dam on the Yarlung-Tsangpo river in SE Tibet
*Peter Zeitler, Anne Meltzer, Brian Zurek, Lucy Brown,
Noah Finnegan, Bernard Hallet, Page Chamberlain,
William Kidd and Peter Koons, Page 176*

Paleomagnetic and Geochronologic Results From Late Paleozoic
and Mesozoic Rocks of the Central Tibet: Implications for the
Paleogeography of the Qiangtang Terrane
*Xixi Zhao, Pete Lippert, Rob Coe, Chengshan Wang, Zhifei Liu,
Haisheng Yi, Yalin Li, Bin Deng, and Igor Villa, Page 177*

Whole-rock elemental and zircon Hf isotopic geochemistry of
mafic and ultramafic rocks from the Early Cretaceous Comei
large igneous province in SE Tibet: constraints on mantle source
characteristics and petrogenesis
*Di-Cheng Zhu, Xuan-Xue Mo, Zhi-Dan Zhao, Yaoling Niu and
Sun-Lin Chung, Page 178*

Scion Image Analysis in rocks of the hanging wall and foot wall of the MCT, central Nepal

Kamala Kant Acharya* and Bernhard Grasemann

Department of Geodynamics & Sedimentology, Structural Processes Group, Vienna University, AUSTRIA

* For correspondence, email: Acharyk4@univie.ac.at

In central Nepal, the Kathmandu Crystalline Thrust Sheet comprises rocks of the Higher Himalayan Crystalline, overlying lower metamorphic grade rocks of the Nawakot Complex, separated by the Main Central Thrust (MCT). All these rocks, which are sometimes combined in the 'Kathmandu Nappe', have been folded to form the NW-SE trending, essentially upright Mahabharat Synform. A public downloading software Scion imaging has been used to quantitative image analyse of thin sections from the area especially in the vicinity of the thrust. Scion Image is an image processing and analyzing program (Scioncorp.com).

Images of seven thin sections from different parts of central Nepal were analysed using Scion Image. These thin sections were prepared from the three samples collected from the hanging wall i.e. Kathmandu Complex rocks and four samples from the foot wall i.e. Nawakot Complex rocks of the MCT. The ellipse major axis, ellipse minor axis, and orientation of the ellipse major axis of quartz and feldspar grains were measured using this software from the thin sections. The ellipticity and Bretherton shape index were calculated from the obtained values.

The analysis shows that, rocks of the Nawakot Complex (Lesser Himalaya) record a monoclinic symmetry while rocks of the Kathmandu Complex (Higher Himalaya) record an orthorhombic symmetry. In one sample collected from the thrust zone of the MCT, quartz grains show orthorhombic while feldspar grains show monoclinic symmetry. In all the samples feldspar behave as a rigid particle whilst quartz grains show evidence of ductile deformation. Flattening and elongation of quartz grains is strong parallel to the foliation. Rocks of the Kathmandu Complex and of the MCT thrust

zone show higher rheological role of quartz than in rocks of the Nawakot Complex. Some rocks of the Kathmandu and Nawakot Complex shows asymmetry indicating non-coaxial deformation. Other possible indicators of non-coaxial deformation, such as extensional crenulation cleavage, S-C shear bands, porphyroclasts with asymmetric pressure shadows and porphyroblasts with curved inclusion trails have also been observed in thin-sections. The strain partitioning between individual phases, typical of lower metamorphic grade rocks such as the chlorite grade Nawakot Complex diminishes as the metamorphic grade increases to garnet and biotite grade in the Kathmandu Complex and deformation becomes more nearly homogenous. In the sample from MCT zone, where both quartz and feldspar grains have been analysed, feldspars show a higher ellipticity than quartz. The average ellipticity of quartz in all of these rocks is more or less similar but in feldspar rocks of the Kathmandu Complex shows higher average ellipticity than rocks of the Nawakot Complex. Comparatively feldspar grains show higher variation in ellipticity and Bretherton Shape Index than that of quartz. In these rocks, shear sense indicators show both pure shear flattening fabrics and non-coaxial south-directed simple shear fabrics.

From these observations, it can be said that rocks of both the hanging wall and footwall show a significant pure shear component early in the deformation and simple shear component during exhumation. Therefore, the MCT can be characterized as Stretching Fault Thrusting (Means 1989), where wall rocks lengthen perpendicular to the shear direction, and MCT partially acted as Stretched Fault Thrust.

Geological setting of the Siang Dome located at the Eastern Himalayan Syntaxis

Subhrangsu K. Acharyya* and Puspendu Saha

Department of Geological Sciences, Jadavpur University, Kolkata 700032, INDIA

* For correspondence, email: skacharyya@yahoo.com

The Siang Dome located at the Eastern Himalayan Syntaxis is a large structure involving entire Himalayan packet from the Paleogene rocks to the south at the core of the Siang Window to the ophiolitic suture rocks and the Trans-Himalayan granitoids around Tuting at its northern periphery. About a kilometer thick shear zone with intense granitic injection is exposed in the Siang River section located at the tectonic base of the Yang Sang Chu Fm., overriding the Central Crystallines. This zone is tentatively equated to the South Tibetan Detachment. Macroscopically the Himalayan thrust pile at the Siang Dome has a prominent orogen-transverse antiformal structure trending NW-NNW. It is truncated to the west by the N to NE trending Tuting-Basar dextral fault. The Siang Window at the core exposes a duplex antiform of Paleogene rocks that are placed beneath the low grade Proterozoic Himalayan rocks tectonically separated by the arched splay of the MBT roof-thrust.

Two structurally discordant units frame the Siang Window. The crystalline thrust packet and the subjacent Lesser Himalayan thrust sheets of low-grade Proterozoic and locally present Permian metasediments on the hanging wall of the arched MBT to the north constitute one congruous unit and preserve identical structure. The duplex antiform of the Paleogene rocks beneath the arched MBT, which are further truncated to the south against the Neogene Siwalik Sub-Himalayas by the ENE-SSW trending and north dipping frontal MBT and North Pashighat Thrust (NPT) represent the other tectonic unit. The antiform of Paleogene rocks are dissected by subsidiary imbricate faults that are oblique to both MBT at the roof and NPT at the floor, truncating and dislocating MBT, but remaining asymptotic to NPT. These are responsible for generating the Siang duplex antiform and its northern fault bend antiformal closure (Figure 1, 2). Tuting-Basar tear fault also breaches folded thrusts, and off sets the Siang and the Namche Barwa Domes at its northeastern end, whereas, to the south the frontal Gondwana thrust belt, frontal belt MBT and MFT remain unaffected, and therefore represent the youngest thrust structures.

The lower unit of the Paleogene sequence at the Siang Window, the base of which is not yet well defined, is mainly composed of white to pink colored, skolitho-bearing and mature Miri like quartzite. It is also frequently intruded by dykes and sills feeding the overlying Abor Volcanics. The stratigraphic base of this quartzite with type Miri Quartzite is yet to be defined. Calcareous bands or limestones occurring at the upper part of this quartzite and at the lower parts of the Abor Volcanics have yielded rich larger foraminifera record characterized by *Assilina depressa*, *A. regularia*, *Orbitosiphon cf. tibetica*, *Nummulites*

thalicus etc., indicating Late Paleocene to Early Eocene age. The Yinkiong Formation overlying the volcanics consists of mainly argillo-arenaceous volcanisediments with marl and limestone intercalations. Foraminifera assemblage in these, characterized by *Nummulites atacicus*, *N. maculatus*, *Assilina spira*, *A. daviesi*, *A. subassamica*, indicate Early to Mid Eocene age (Acharyya 1994, 2007). The MBT zone between the early Paleogene rocks and the overriding pre-Tertiary rocks, particularly the Permian Gondwana rocks, Proterozoic quartzite-dolostone bearing Buxa like rocks, often develop mélangé with tectonic assemblage of these rocks. Narrow zones of intermixed Permian and Eocene fossils are recorded from frontal belt MBT zones, which extend over 250 km (Acharyya 1994).

The Himalayan crystalline thrust tectonically floored by the MCT has many similarities with typical features of the Type-C crystalline Thrust Sheets as recognized by Hatcher and Hooper (1992). The foreland thrusts are driven ahead of Type C sheets as crystalline and foreland thrust merge into the Coulomb wedge of the foreland. At the Eastern and NE Himalayas located in Darjeeling-Sikkim area and Arunachal Pradesh, the pile of thrust sheets, from higher to lower structural levels comprising the crystalline, the low-grade Proterozoic metamorphic rocks, Late Paleozoic metasediments and the Neogene floor sediments, are cofolded together. The macroscopic folds in the former area have orogen-parallel and transverse trends. In the present area, the latter are the dominant fold style. In mesoscopic scale four generations of folds have been recognized from the former area and broadly similar fold styles are also inferred from the Siang Dome, but here the orogen parallel early folds are generally rotated to orogen-transverse orientation. The earliest F1 folds are tight isoclinal with axial plane cleavage which is the main cleavage/schistosity S1. Fold axes generally trend northward. Stretching lineation and mullions denoting transport direction of thrusts are developed parallel to F1 axes, but the latter often show variable trends. The F1 are well developed in the Paleogene rocks, particularly in the Yinkiong Formation. F2 folds developed on S1 are generally asymmetric, upright, inclined to recumbent in geometry. Often there is development of spaced cleavage S2, and striping, and mineral lineation. F3 fold are open, upright and trend NW-NNW. In the present area because of superposition, F2 and F3 fold axes are both transversely oriented and are thus often difficult to differentiate. Evidence of F2-F3 cross folding in the Paleogene rocks of the Siang Window is revealed by the presence of well formed dome structures at the top section of the Miri Quartzite (*sensu lato*) and basal sections of the Abor Volcanics (Figure 1, 2). The presence of co-axial folding of F1 by F3 is recorded from single outcrops. The

latest F4 fold structures are generally orogen-parallel in trend, but have recumbent geometry with subhorizontal axial plane. These are better developed in zones of steeply dipping sheet schistosity and bedding. The F4 folds are not recorded from the Tertiary sediments, whereas, F1 to F4 affect the thrust pile of Proterozoic, Late Paleozoic and Paleogene rocks. Therefore, F1 to F4 folds are late- to post-thrust structures (Acharyya 2007).

The buried basement ridge of the Shillong-Mikir massif in NE India, trends NE-N-ward and finally plunges beneath the Siang Window. Regional trend and depths to basement immediately south of the Siang Window are obtained from seismic reflection data (Baruah et al. 1992). The Paleogene rocks in the Siang Window are thrust over the Neogene pile and older sediments overlying the basement (Figure 1). Some test wells on north bank of Brahmaputra River have also confirmed the presence of late Paleocene-early Eocene marine shelf sediments. Lateral continuity and thickening sequence of the Eocene marine shelf in Arunachal Sub-Himalayas, around the Siang Window is strongly indicated by the presence of thrust slivers of Eocene sediments and presence of similar marine fauna in them, which occur close to and beneath MBT zone from widely separated

sections. The thrust arcuation of the Siang Window located at the Eastern Himalayan Syntaxis was therefore influenced initially by the involvement of the subsurface indenture of the NE leading edge of Indian continent, which acted as an oblique crustal ramp over which the pile of Himalayan nappes climbed. A basement saddle and depression occurs instead south of western part of the Siang Window and the complementary synform located further west (Acharyya 2007). The geometry of the Siang Dome was modified subsequently by ductile deformations.

References

Acharyya SK. 1994. The Cenozoic foreland basin and tectonics of the Eastern Sub-Himalaya: problems and prospects. *Himalayan Geology* 15: 3-21

Acharyya SK. 2007. Evolution of the Himalayan Paleogene foreland basin, influence of its litho-packet on the formation of thrust-related domes and windows in the Eastern Himalayas – A review. *Journal of Asian Earth Sciences* 31: 1-17

Baruah JMB, Handique GK, Rath S, Mallick RK. 1992. Exploration for Palaeocene-lower Eocene hydrocarbon prospects in the eastern parts of Upper Assam basin. *Indian Journal of Petroleum Geology* 1: 117-129

Hatcher RD (Jr) and Hooper RJ. 1992. Evolution of crystalline thrust sheets in the internal parts of mountain chains. In: Mc Clay KR. (ed.), *Thrust tectonics*, Chapman and Hall, London p 217-233

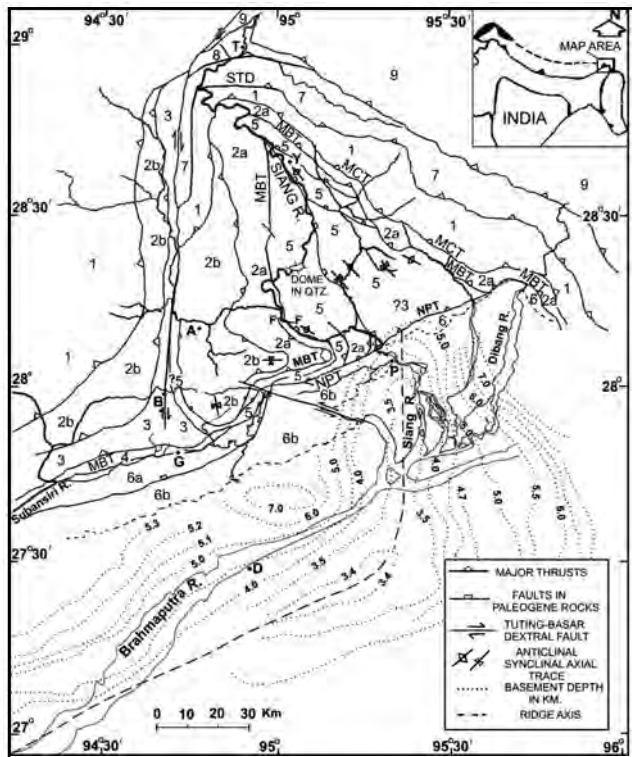


FIGURE 1. Simplified geological map of the Siang Dome and foothill plains. Regional Depth contours in km close to basement in the foothill plains and Basement Ridge Axis are based on reflection seismic data after Baruah et al., 1992. - 1-High-grade rocks and gneisses (Central Crystallines), 2a- Low-grade quartzite-dolomite metasediments (Buxa Fm., equivalent, Proterozoic), 2b- Low-medium grade meta-argillite (Proterozoic), 3- Miri Quartzite (? Early Paleozoic), 4- Late Paleozoic Gondwana equivalent metasediments, 5- Paleogene rocks, 6a- Tectonised early Neogene sediments in the northern belt (Lower Siwalik), 6b- Late Neogene (Upper and Middle Siwalik) in the southern belt, 7- Low- to high-grade graphitic metasediments (Yang Sang Chu Fm.), 8- Mafic and ultramafic rocks (Ophiolite), 9- Trans-Himalayan granitoids and gneisses. Abbreviations: MBT- Main Boundary Thrust, NPT- North Pashighat Thrust, MCT- Main Central Thrust, STD- South Tibetan Detachment, A- Along, B- Basar, D-Dibrugarh, G- Garu, P-Pashighat, T-Tuting, Y-Yinkiong.

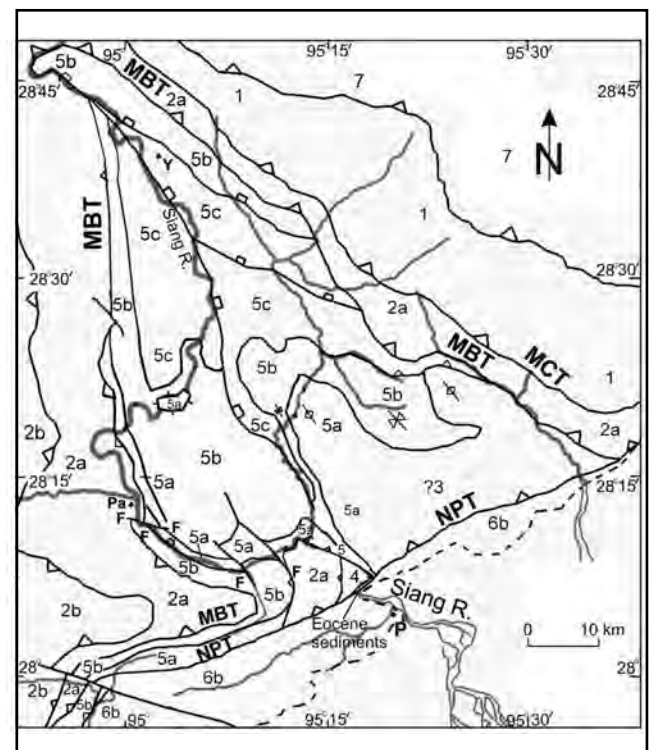


FIGURE 2. Simplified geological map of the Siang Window. Legend same as in Figure 1. Paleogene rocks differentiated to: 5a- Quartzite (Late Paleocene-Early Eocene: may include older Lower Paleozoic Miri Quartzite), 5b- Abor Volcanics, 5c- Yinkiong Fm.

Geochemical-isotopic characteristics and K-Ar ages of magmatic rocks from Hundar valley, Shyok Suture Zone, Ladakh

T Ahmad^{1*}, S Sivaprabha², S Balakrishnan³, N X Thanh⁴, T Itaya⁴, H K Sachan⁵,
D K Mukhopadhyay² and P P Khanna⁵

¹ Department of Geology, University of Delhi, Delhi, INDIA

² Department of Earth Sciences, Indian Institute of Technology Roorkee, Roorkee, INDIA

³ Department of Earth Sciences, Pondicherry University, Pondicherry, INDIA

⁴ Research Institute of Natural Sciences, Okayama University of Science, Okayama, JAPAN

⁵ Wadia Institute of Himalayan Geology, Dehradun, INDIA

* For correspondence, email: tahmad100@yahoo.co.in

Hundar section rocks of the Shyok Suture Zone comprise predominantly diorite, granodiorite with minor gabbro-dolerite, two types of granite, volcano-clastic sediments and tuffs that are intruded by diabasic dykes. Diorite samples contain pyroxene, amphiboles and plagioclase as major phases. Quartz and alkali feldspar, showing myrmekitic intergrowth are found in granites. Gabbro-dolerite comprises feldspar, biotite, hypersthene and hornblendes. Andesitic dykes have euhedral plagioclase phenocryst within fine-grained groundmass.

Major and trace element display trends expected for igneous rocks from mafic to felsic compositions. Data indicate fractionation of olivine, pyroxene, feldspars and Fe-Ti oxide phases during evolution of the magma. Normalized REE plots depict light REE enrichment and middle - heavy REE moderate fractionation. Multi-element patterns also display enrichment of large ion lithophile elements (LILE) and depletion of high field strength elements (HFSE) with significant negative Sr and Eu anomalies.

Hundar samples do not define any collinear array for Rb-Sr or Sm-Nd isotope evolution indicating multiplicity of sources for

magmas. $\epsilon_{Nd}(t = 100)$ varies from +3.7 to -7.4, while the ϵ_{Sr} varies from -7 to +50. ϵ_{Nd} vs. ϵ_{Sr} diagram plots for Hundar samples partly overlaps the mantle array and partly that of Ladakh pluton. The samples of Ladakh pluton have extended ϵ_{Nd} and ϵ_{Sr} values up to -8 and +165 respectively. Probably magmas of the Hundar section were variably contaminated by enriched and long lived continental crustal components.

Eight samples from the Hundar section yield K-Ar ages from 60.8 Ma to 65.8 Ma. The medium-grained granite shows younger age (60.8 and 61.8 Ma) compared to the coarser-grained granite of 63.9 Ma. Three coarse-grained diorite samples yield the age from 64.4 to 65.8 Ma. Two microdiorite samples in the center of Hundar section yield the age of 64.0 and 64.4 Ma. The coarse grained granite samples having magma mingling structure with the microdiorite gives the similar ages of 63.9 and 64.4 Ma respectively. Two coarse grained diorite display the oldest age (65.8 Ma) in the area. These age data indicate that the magmatic rocks of the Hundar section are much older than the dominant magmatic phase (~58 Ma) of the Ladakh batholith and therefore could be unrelated.

New SHRIMP ages for Ladakh and Karakoram Batholiths - inherited zircons indicate involvement of older crust

T Ahmad^{1*}, L White², M Forster², T R Ireland² and G Lister²

¹ Department of Geology, University of Delhi, Delhi, INDIA

² Research School of Earth Sciences, The Australian National University, Canberra, AUSTRALIA

* For correspondence, email: tahmad100@yahoo.co.in

We report new U-Pb zircon SHRIMP ages for the Ladakh and Karakoram batholiths. The samples of the Ladakh Batholith were collected from the Khardung La and Chang La tops and those of the Karakoram Batholith were collected along the Tangtse gorge and Darbuk-Shyok section.

Separated zircon crystals display zoned zircon crystals typically observed in igneous rocks. The age obtained for the Khardung La and Chang La top samples is circa 58 Ma. These ages are similar to the age data published by earlier workers, confirming a strong phase of magmatism in the Ladakh Batholith at approximately 58 Ma. No inherited older zircons were observed in these samples, confirming the observations of earlier studies.

A Karakoram Batholith sample was collected near Tangste Gompa. This sample is a coarse grained porphyritic granite and gave an age of circa 32 Ma. One zircon grain from this sample gave a late Permian age, and this may indicate the involvement of older crust in the batholith.

Muscovite-biotite-garnet bearing leucocratic granite dykes are best exposed in the Tangtse gorge where many leucocratic granitic dykes dissect each other (Figures 1 and 2). One sample was collected from near the middle of the gorge between the northern and southern strands of the Karakoram fault. This sample gave an age of circa 18 Ma.

This is consistent with earlier published age data that was associated with movement on the Karakoram fault.

Another sample of the Karakoram Batholith was collected further to the north, near the Karakoram fault. This sample has gneissic characteristics and is richer in mafic phases (biotite-hornblende). The age of this sample is circa 102 Ma. This age is consistent with data published by earlier workers indicating that there was also a major magmatic phase in the Karakoram Batholith at around 102 Ma.

One leucocratic granitic dyke sheet sampled between Darbuk and Shyok villages has a mixture zircon crystals that gave a range of ages. Some of these zircon grains are possibly inherited. These range of ages found in these samples range between 15 Ma and 97 Ma. All of these dates have been reported from at least one of the other sampled localities by various methods. Interestingly several grains gave ages that have not been previously reported (ranging between 250 – 970 Ma). These older ages may indicate that older crust was involved in the generation of part of the Karakoram Batholith (possibly the southern portion of the Tibetan slab?). Recent suggestions that collision was as late as 35 Ma may need more consideration in the light of magmatic zircon ages of 32-36 Ma.



FIGURE 1. Leucocratic granitic dykes, Tangtse gorge



FIGURE 2. Close up of Figure 1

Preliminary paleomagnetic study of Cretaceous dykes in SE-Tibet

B Antolín^{1*}, E Appel¹, I Dunkl², L Ding³, C Montomoli⁴, El Bay¹ R and R Gloaguen⁵

¹ Institut f. Geowissenschaften, Sigwartstrasse 10, D-72076 Tübingen, GERMANY

² University of Göttingen, Goldschmidtstrasse 3, D-37077 Göttingen, GERMANY

³ Institute of Tibetan Plateau Research, Chinese Academy of Sciences, Shuangqing Rd. 18, Beijing 100085, CHINA

⁴ University of Pisa, via S. Maria 53, 56126 Pisa, ITALY

⁵ University of Freiberg, Bernhard-von-Cottastrasse 2, 09596 Freiberg, GERMANY

* For correspondence, email: borja.antolin@uni-tuebingen.de

The SE Tibetan area is a key region to better understand Tibetan Plateau formation. Lateral motion is evident by the alignment of major rivers in Southeast Asia and GPS velocities indicating motion around and away from the Eastern syntaxis. We try to find vertical axes rotations utilizing paleomagnetic studies combined with geological-petrological investigations to clarify the process of uplift of the Himalaya-Tibetan Plateau in the south eastern Tibet.

A total of 17 sites with about 10 cores per site were drilled in Lower Cretaceous diorite dykes. These dykes intruded widespread into the Triassic flysch of the Tethyan Himalaya. A total of 11 dykes were drilled in Nagarze area and 6 sites more to the east (south of Tsetang-Gyaca) (Figure 1).

Rock magnetic analysis demonstrates the presence of pyrrhotite as the principle carrier of the remanence. IRM saturates from 300 mT to 500 mT and thermal demagnetization of SIRM is mainly achieved around the Curie temperature of pyrrhotite (325°C). Most of the samples show also a decay of the SIRM around 580°C indicating the additional presence of magnetite.

The values of the intensity of the natural remanent magnetization varies strongly from 0.5 to 446 mA/m. In about 50% of the samples it is possible to isolate a significant pyrrhotite component, usually unblocking between 250°C and 350°C. Equal area projection mostly shows a scattered distribution of the pyrrhotite components. In three sites the characteristic pyrrhotite remanence components are well grouping and in four sites a small circle distribution can be observed. We relate the origin of the pyrrhotite remanence to last metamorphic cooling in the area (K/Ar ages indicate ~24 Ma). Sulphur for pyrrhotite formation has been likely delivered from the adjacent schists during peak metamorphism. The remanence is therefore probably secondary,

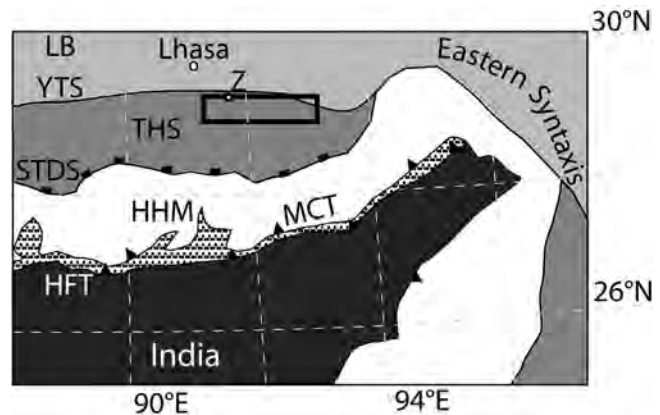


FIGURE1. Simplified geological map of the East Himalaya and SE-Tibet (modified after Yin and Harrison 2000). HFT, Himalaya Frontal Thrust; MCT, Main Central Thrust; HHM, High Himalaya Metamorphic rocks; STDS, South Tibetan Detachment System; THS, Tethyan Himalayan Sequences; YTS, Yarlung Tsangpo Suture zone; LB, Lhasa Block; Z, locality of Tsetang or Zetang. The black rectangle indicates the studied area.

either being a thermoremanence or a thermo-chemical remanence. More paleomagnetic analysis is required to elucidate vertical axes rotations in SE-Tibet.

References

- Yin A and TM Harrison. 2000. Geologic evolution of the Himalayan-Tibetan orogen. *Annual Reviews in Earth and Planetary Sciences* 28: 211-280

Carbon and sulfur isotope records of Ediacaran carbonates of Lesser Himalayas: implications on oxidative state of the contemporary oceans

DM Banerjee

Department of Geology, University of Delhi, Delhi-110007, INDIA
E-mail: dhiraj1942@yahoo.co.in

High resolution geochemical data from fossil-poor Blaini-Krol and fossiliferous Lower Tal succession in the Lesser Himalayas closely conform to the geochemical trends demonstrated by the rock sequences at Oman, Newfoundland, South China and Western United States. Geochemistry of all these known Ediacaran sections suggest long term oxidation of the terminal Proterozoic oceans which led to gradual depletion of dissolved organic carbon reservoir. It is interpreted that the increase in the dissolved organic carbon was responsible for the radiation of acritarchs and algal population (McFadden et al 2008). Such coupling of oceanic oxidation event and the evolution of organisms can be suggested only when chemostratigraphy is adequately supported by biostratigraphy. Lower Himalayan sections do not offer such an opportunity due to low sulphate but high sulfide contents in the Krol carbonates and the consequent paucity of preserved organic life in these strata. The Krol basin carbonates show fairly stable organic carbon isotopes, but three profound negative carbonate carbon excursions and a positive excursion close to the rock junction of Lower Tal phosphorite. Two of these excursions are associated with facies changes, hence suspected to be artifacts, while one negative excursion in the transgressive facies represent biogeochemical anomaly comparable through different continents (Kaufmann et al. 2006). On the other hand, sulfate sulfur isotopes

associated with the carbonates are compatible with large buffered dissolved organic carbon reservoir and low sulfate concentrations but high sulfide sulfur. Sharp negative isotopic shift in the upper part of the Krol succession therefore records pulsed oxidation of the deep oceanic dissolved organic carbon reservoir, leading to sudden proliferation of small Shelly Fossils and associated eukaryotic diversity in the Lower Tal phosphate/Chert which follow the sharp negative carbonate carbon excursion. Two negative excursions in the lower Cambrian Tal succession reflect changes in the oceanic chemistry while one small excursion is an artifact and influenced by the facies. On the other hand, at the bottom of the whole succession, representing the end phase of the Blaini Formation, a prominent negative carbonate carbon excursion has matching trends in most of the continents and reflects last phase of the glacial activity in the terminal Proterozoic time.

References

- McFadden KA, J Huang, X Chu, G Jiang, AJ Kaufman and C Zhou. 2008. Pulsed oxidation and biological evolution in the Ediacaran Doushantuo Formation. *Proceedings National Academy of Sciences USA*, 105(9): 3197-3202
- Kaufman AJ, G Jiang, N Christie-Blick, DM Banerjee, V Rai. 2006. Stable isotope record of the terminal Neoproterozoic Krol platform in the Lesser Himalayas of northern India. *Precambrian Research* 147: 156-185

Kinematics of the crust in southern Tibet and Higher Himalayan Crystalline –a paleomagnetic approach

Rachida El Bay^{*1}, Erwin Appel¹, Rodolfo Carosi², Lin Ding³, Dunkl István⁴, Richard Gloaguen⁵, Chiara Montomoli², Lalu Paudel⁶ and Bastian Wauschkuhn⁵

¹ Institute for Applied Geoscience, University of Tuebingen, GERMANY

² Dipartimento di Scienze della Terra, University of Pisa, ITALY

³ Institute of Tibetan Plateau Research, Chinese Academy of Sciences, CHINA

⁴ Geoscience Center, University of Goettingen, GERMANY

⁵ Institute for Geology, Technical University of Freiberg, GERMANY

⁶ Central Dept. of Geology, Tribhuvan University, Kathmandu, NEPAL

* For correspondence, email: rachida.el-bay @uni-tuebingen.de

Secondary pyrrhotite remanences from the Tethyan Himalaya acquired during Eocene (western Himalaya) and Oligocene to early Miocene (central and eastern Himalaya) were evaluated for block rotations. Oroclinal bending is well reflected by paleomagnetic data in the western part of the Himalaya also showing a uniform counterclockwise rotation of India versus the Tethyan Himalaya. In contrast, data from the central part and preliminary results from the eastern part indicate an abrupt change to unexpected clockwise rotations versus India where oroclinal bending would predict no rotation or slight counterclockwise rotations (Schill et al. 2004). It can be hypothesized that these clockwise rotations are a result of a large dextral shear zone related to lateral extrusion of the Tibetan Plateau, with an onset in central Nepal. However, the existing gap in suitable data from the eastern part of the Himalaya was hindering a closer evaluation of this question. The hypothesis is reconsidered in the light of new findings.

In southern Tibet field work has been carried out on an E-W section between 86° and 89°E (Figure 1) encompassing the Nayalam section, the Karta valley, the Dinggye extensional zone and the Yadong/Pagri area. Low grade Ordovician to Mid-Triassic metacarbonates and slates were sampled. The south Tibetan series are bounded to

the south by the South Tibetan Detachment System (STDS) and to the north by the Yarlung Tsangpo Suture Zone (YTSZ) and there is a widespread occurrence of north Himalayan gneiss domes. The S-N transect at ca. 87°E is ranging from few km south of Lukla (Solu Khumbu, HHC) to Lhatse close to the YTSZ. Sampling included the high grade metamorphic gneisses from the HHC, the Tethyan sedimentary series (Ordovician to Carboniferous) and the upper Triassic flysch between Tingri and Lhatse.

The mechanism of secondary remanence acquisition in low-grade metamorphic rocks of the Tethyan Himalaya is quite well understood. Pyrrhotite is formed during prograde metamorphism. A thermoremanence is blocked during last cooling if the peak metamorphic temperature has reached the Curie temperature (T_c) of pyrrhotite (ca. 320 °C). If the peak temperature was lower than T_c a thermo-chemical mechanism is likely and the time of remanence acquisition might predate the cooling age. For these reason we applied illite crystallinity and K/Ar dating to determine peak metamorphic temperatures and ages of metamorphic cooling. In the high grade gneisses of the HHC pyrrhotite is believed to be formed during the transition from ductile to brittle deformation (retrograde stage). A thermoremanence is likely acquired and its age

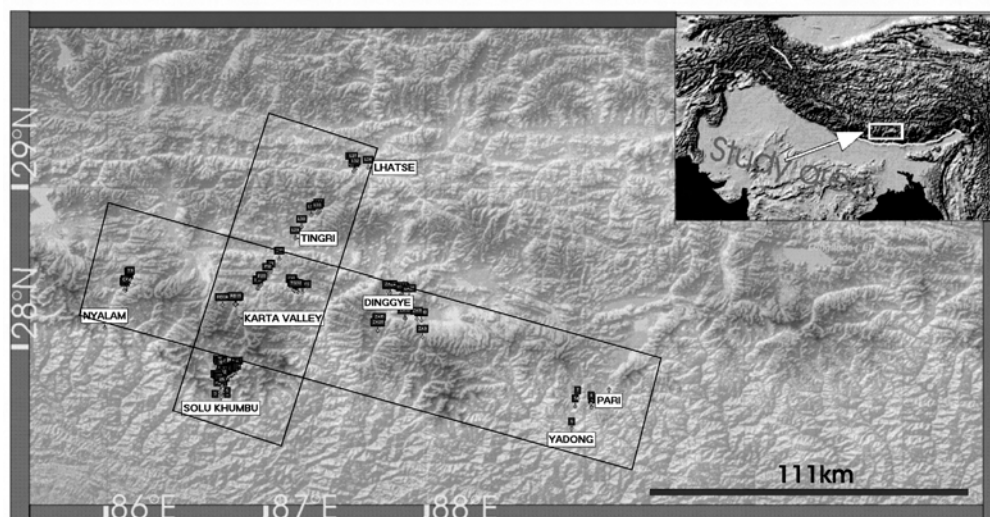


FIGURE 1. Shuttle Radar Topography Mission (SRTM) image from the study area showing sampled E-W traverse and S-N transect

will correspond to the age of the last metamorphic cooling event.

“Anomalous” inclinations, indicating strong tilting after remanence acquisition, are observed across the E-W traverse. Taking into account the proximity of the sampled sites to the STDS, especially at the Nyalam section (Nyalam detachment) and in the Karta valley, a regional trend linked to a “folded” STDS can be assumed. Therefore, remanence acquisition predates the onset of the STDS or is coeval with it.

Remarkably, remanences are mainly dispersed on small circles with a tilt axis oriented approximately in N-S direction. This is not in agreement with long-wavelength tilting parallel to the strike of the main Himalayan tectonic units. It can be suggested that this small-circle distribution is an expression of doming in the crust (caused by channel flow?).

Inclinations at Nyalam section and Karta valley indicate a second phase of tilting superposed to the E-W tilting.

Small circle analysis (Waldhör et al. 2006) enables quantification of vertical axis rotation. A clockwise rotation is evident along the S-N transect at ca. 87°E at Karta valley and further

north in the flysch series between Tingri and Lhatse. First results from the northern part of the HHC in Khumbu area indicate a pattern of rotation comparable to those observed at the Karta valley. Counterclockwise rotation obtained for the Dinggye- and Yadong/Pagri areas are in contradiction with the above mentioned hypothesis of a uniform large dextral shear zone.

In summary, the hypothesis of a large dextral shear zone linked to the extrusion of the Tibetan Plateau can be yet not proved or rejected. A major effect attributed to a normal fault/thrust system became more evident.

References

- Schill E, E Appel, C Crouzet, P Gautam, F Wehland and M Staiger. 2004. Oroclinal bending and regional significant clockwise rotations of the Himalayan arc – constraints from secondary pyrrhotite remanences. *Geological Society of America Special Publication* on orogenic curvature
- Waldhör M and E Appel. 2006. Intersection of remanence small circles: new tools to improve data processing and interpretation in paleomagnetism. *Geophysical Journal International* 33-45

White Sandstone in Subathu Sub-Basin: an example of tectonically driven forced regressive wedge

MK Bera^{1*}, A Sarkar¹ and PP Chakraborty²

¹ Department of Geology and Geophysics, Indian Institute of Technology, Kharagpur-721302, INDIA

² Department of Applied Geology, Indian School of Mines, Dhanbad 826 004, INDIA

* Corresponding author: e-mail: melinda_bera@yahoo.com

Sediments of the Himalayan peripheral foreland basin, developed due to progressive thrust-loading (DeCelles and Giles 1996, Dickinson 1974) and subsequent exhumation/upliftment of the mountain chain, records signature of hinterland tectonics vis-a-vis basin filling processes. The synchronicity of the foreland sediments with widespread early Oligocene glaciation suggests that hypothesis of tectonics-climate connection, whereby the cooling was driven by drop in atmospheric CO₂ via enhanced silicate weathering of the rising Himalayan orogen (Raymo and Ruddiman 1992, Pagani et al. 2005), has considerable merit. As a test-case Paleogene Sub-Himalayan foreland sediments of marine Subathu and continental Dagshai formation rocks were studied to identify the teleconnection between tectonics and climate, if any. The Subathu-Dagshai transition here is marked by the presence of a ~31 Ma old (Najman et al. 2004) characteristic quartz rich mature sandstone locally termed as the "White Sandstone". It marks the termination of marine Subathu Formation and initiation of continental molasses Dagshai Formation and represents an important evolutionary stage in the geodynamic history of the foreland basin (DeCelles and Giles 1996, Sinclair 1997). However, the status of White Sandstone has always been uncertain varying between marine Subathu (a beach or tidal flat; Singh and Khanna 1980, Srivastava and Casshyap 1983) to fluvial Dagshai (Najman et al. 2000, 2004). Further, raging debates exist about the possible continuity/discontinuity between Subathu and Dagshai formations (see Bera et al. 2008 and references therein). Since the White Sandstone plays a crucial role in this debate the present study focused on process based sedimentology of this unit. Detailed bed form geometry and sedimentary structure shows that the White Sandstone unit is made up of three distinct components viz., Lower shoreface (between fair weather wave base and storm wave base), Upper shoreface (above fair weather wave base) and Foreshore/beach. Lower shoreface deposits are characterized by intercalation of centimeter thick fine sand and shale couplets, although definite signature of hummocky cross stratified (HCS) unit is not recorded in the present study. These units lie between two erosional surfaces. The lower erosional surface is sharp and it places the units directly over the offshore/shelf sediments. Presence of gutter cast and rip-up clast at the base of these units suggest the lower erosional surface must be a storm weather wave base or regressive surface of marine erosion (RSME) (Plint 1988). The upper erosional surface is marked by the truncation of the fine sand shale intercalation of lower shoreface with decimeter thick lenticular unit of upper shoreface and dips towards the basinal depocenter. The presence of this surface above basal RSME allowed us to interpret it as a fair

weather wave base or "surf diastem" (of Swift et al. 2003). Recent studies (Fraser et al. 2005, Tamura et al. 2007) show that this fair wave base is an important component of shoreface sand deposits, as it helps in assessing the change in progradation of the upper shoreface deposits during forced regression. Our study shows that the basal RSME is not a single erosional surface developed due to fall in storm wave base; at places, where lower shoreface is absent, fair weather wave base amalgamates with it. The amalgamation depends upon the preservation of lower shoreface which, in turn, governed by both sediment supply and rate of sea level fall during forced regression. As mentioned earlier, the upper shoreface deposits are characterized by the decimeter thick lenticular sandy units. The meter thick thinning and fining upward nature of these lenticular beds and internal truncation of these bed sets suggest its probable longshore bar origin (Tamura et al. 2007). The presence of wave ripples on top of the beds and foreshore/beach deposits above it indicate its upper shoreface environment. The foreshore/beach deposits are characterized by decimeter thick parallel bed sets with very low angle cross stratification and sometimes show parting lineation. This unit is overlain by either interfluvial sediments with extensive caliche development or cut by Dagshai channel sandstone. The presence of basal RSME and fluvial incision and/or caliche development on the top of white sandstone unit indicate it as a product (an FSST wedge) of forced regression (Hunt and Tucker 1992, Catuneanu 2002). Our spatially extensive new petrographic dataset suggest a sudden increase in metamorphic detritus from the White Sandstone unit onwards indicating initiation of exhumation of the Himalayan metamorphic core during this time. Our study has three important implications. First, the ~31 Ma white sandstone is marine not fluvial and hence the unconformity occurs above it not below. Second, the forced regression was possibly tectonically driven due to sudden hinterland uplift. Third, the timing of this tectonically driven forced regression coincides with the rapid rise in sea water Sr isotope ratio (from 0.7077 to 0.708) further strengthening the hypothesis that uplift driven silicate shedding might have causal link with the early Oligocene cooling.

References

- Bera MK, A Sarkar, PP Chakraborty, RS Loyal and P Sanyal. 2008. Marine to continental transition in Himalayan foreland. *Geological Society of America Bulletin*. (In press).
- Catuneanu O. 2002. Sequence stratigraphy of clastic systems: Concepts, merits, and pitfalls. *Journal of African Earth Sciences* 35: 1–43
- DeCelles PG and KA Giles. 1996. Foreland basin systems. *Basin Research* 8: 105–123

- Dickinson WR. 1985. Interpreting provenance relations from detrital modes of sandstones. In: Zuffa GG (eds) *Provenance of arenites: Dordrecht, NATO ASI series C, 148, D. Reidel* p333–361
- Fraser C, PR Hill and M Allard. 2005. Morphology and facies architecture of a falling sea level strandplain, Umiujaq, Hudson Bay, Canada. *Sedimentology* 52: 141–160
- Hunt D. and ME Tucker. 1992. Stranded parasequences and the forced regressive wedge systems tract: Deposition during base level fall. *Sedimentary Geology* 81: 1–9
- Najman Y, M Bickle and H Chapman. 2000. Early Himalayan exhumation: Isotopic constraints from the Indian foreland basin. *Terra Nova* 12: 28–34
- Najman Y, K Johnson, N White and G Oliver. 2004. Evolution of Himalayan foreland basin, NW India. *Basin Research* 16: 1–24
- Pagani M, JC Zachos, KH Freeman, B Tripple and S Bohaty. 2005. Marked decline in atmosphere carbon dioxide concentrations during the Paleogene. *Science* 309: 600–603
- Plint AG. 1988. Sharp-based shoreface sequences and 'offshore bars' in the Cardium Formation of Alberta: Their relationship to relative changes in sea level. In: Wilgus CK, BS Hastings CGStC Kendall, HW Posamentier, CA Ross and JC Van Wagoner (eds), *Sealevel changes—An integrated approach. SEPM (Society for Sedimentary Geology) Special Publication 42: 357–370*
- Raymo ME and WF Ruddiman. 1992. Tectonic forcing of late Cenozoic climate. *Nature* 359: 117–122
- Sinclair HD. 1997. Tectonostratigraphic model for underfilled peripheral foreland basins: An Alpine perspective. *Geological Society of America Bulletin* 109: 324–346
- Singh HP and AK Khanna. 1980. Palynology of the Paleogene marginal sediments of Himachal Pradesh, India. Lucknow. *Proceedings Fourth International Palynological Conference* 1: 462–471
- Srivastava VK and SM Casshyap. 1983. Evolution of the pre-Siwalik Tertiary basins of Himachal Himalaya. *Journal of Geological Society of India* 24: 134–147
- Tamura T, F Nanayama, Y Saito, F Murakami, R Nakashima and K Watanabe. 2007. Intra-shoreface erosion in response to rapid sea-level fall: depositional record of a tectonically uplifted strand plain, Pacific coast of Japan. *Sedimentology* 54: 1149–1162
- Swift DJP, BS Parsons, A Foyle and GF Oertel. 2003. Between beds and sequences: stratigraphic organization at intermediate scale in the Quarternery of the Virginia coast, USA. *Sedimentology* 50: 81–111

Evolution of the Lesser Himalaya

ON Bhargava^{1*} and W Frank²

¹ 103, Sector 7, Panchkula 134109, India, 253/8 Ferrogasse Vienna 1040, AUSTRIA

* For correspondence, e-mail: onbhargava@yahoo.co.in

The earliest rocks found in the Lesser Himalaya are gneisses and crystallines in which the 1860 Ma Jeori-Wangtu-Bandal Granite-gneiss Complex (JWBC) is intrusive. It forms the basement complex for the oldest Lesser Himalayan rocks and are a possible extension of the Peninsular rocks. In stratigraphic/parautochthonous position it is found only in the Himachal and J&K (Kishtwar). In the Eastern Himalaya, the basement rocks occur as tectonic slivers. Once the JWBC was cratonised there was a formation of paleosol prior to the 1800 Ma rifting. The JWBC is also involved in thrusting and forms a tectonic marker (Baragaon/Gahr) throughout the Himalaya.

The history of the Himalaya commenced with a rifting manifested by 1800 Ma Rampur and equivalent volcanics. This event created a shallow marine basin in which the Rampur Group and equivalent sequences (Sundernagar, Dharagad, Berinag, Kuncha, Daling, Shumar groups) along with tholeiites were laid. Duration of the Rampur Group sedimentation is uncertain, but the basin certainly terminated prior to 1500 Ma i.e. the age of the basal part of the overlying Shali Group and its equivalents. The Kulu Thrust sheet involving the JWB basement was possibly nucleated between 1800 Ma and 1500 Ma.

After a hiatus, the sedimentation of the carbonate sequences of the Shali and equivalent successions (Larji, Deoban, Calc "Series", Nawakot, Baxa) took place. The stromatolites in these 3000 m thick carbonate sequences, indicate an age range between 1500-1000 Ma. It looks improbable that only 3000 m thick sequences should have been deposited during 500 Ma time-span, which almost equals the entire Phanerozoic. Several sedimentological breaks in between the carbonate sequences are probable and many of the shale horizons in these carbonate sequences may represent paleosols.

The carbonate sedimentation ceased with another rifting around 1000 Ma. The rifting caused outpouring of the Tattapani and Peontra tholeiitic volcanics. The rise of thermal dome formed the Chaur Granite. The Jutogh Thrust Sheet was possibly nucleated at this juncture. The raised Rampur and Deoban and equivalent terrains provided clasts to the Basantpur and Mandhali diamictites culminating in the deposition of the Simla-Jaunsar groups in the same basin. The detrital mica in the Sanjauli Formation (Simla Group) and Nagthat Formation (Jaunsar Group) are 860 Ma old, thus indicating these formations to be younger to this age. The mica and illite have chemical signatures of the Erinpura Granite. This basin was possibly confined mainly between Nepal and Jammu, as its equivalents are not known in the Eastern Himalaya. The sedimentation possibly terminated around 750 Ma to allow time to raise the Simla and Jaunsar groups and their consequent extensive erosion before the sedimentation of 700-650 Ma Blaini sequence. This regression was accompanied by rising of upland between the Himalaya basin and the Aravalli terrain.

The clasts in the glaciomarine Blaini diamictites are from the Himalayan source, suggesting the glaciers to have emanated from the raised Simla-Jaunsar upland, which had cut off supply from the peninsular part. There were two glaciations intervened by an interglacial period. After the deposition of the cap carbonate, there was a regression and the basin was confined to a smaller part in which Infra-Krol and Krol sequences were deposited. At the termination of the Krol sedimentation, close to the Precambrian-Cambrian boundary, the Outer Krol Belt part was raised and the Tal sedimentation continued in the Krol Basin sited over the Jaunsar Group. This basin too was confined mainly between Nepal and Himachal. Upwelling currents from an open sea, as indicated by presence of cerium, concentrated the phosphorite in the Tal Group. The open sea was separated from the Tal Basin by a submarine ridge. Another basin towards SE of the Krol basin was created, in which the Chilar Formation was deposited. The Chilar quartzitearenites enclose 1860 Ma detrital mica, whereas the Tal quartzitearenite have 860 Ma detrital mica. Presence of age specific micas in the Chilar and Tal sediments indicates that a barrier separated the basins of these two formations to preclude intermixing of micas of two different ages. The Outer Krol Belt, which lacks the Tal sediments, formed this barrier. The Tal basin relatively subsided, which resulted in greater depth of burial, leading to higher grade of anchimetamorphism in the Jaunsar Group as compared to the Simla Group. The Tal quartzarenites are younger than 525 Ma--the age of enclosed detrital zircons. Zircons of the same age are found in the Middle Cambrian Kunzam La Formation of the Tethyan Himalaya also, thereby indicating a common provenance. The submarine ridge referred to above, mainly made up of Vaikrita Group with Early Palaeozoic granites, became aerial and contributed sediments to the Tal basin as well as the Kunzam La basin on the Tethyan side during the Middle Cambrian.

The Tal basin terminated around 520 Ma due to late Cambrian thrusting event, which was experienced over the entire length of the Himalaya. Suturing in the northern part of the then Indian Plate caused this tectonic event. The folds generated during this event are co-axial with the Himalayan folds. The suturing and resultant thrusting caused a regional hiatus covering the Late Cambrian and generation of Early Paleozoic granites all over the Himalaya in the Vaikrita Crystalline. The Vaikrita Thrust Sheet too was nucleated at this time and on its back carried the Kunzam La basin, which contributed clasts to the Thango Formation of the Tethyan basin.

After this event the Lesser Himalayan terrain became a positive area, with drainage heading towards the Tethyan part. At the beginning of the Permian, associated with rifting in the Gondwanaland, old lineaments, mainly in the present foothill parts opened and provided pathway to Permian sea right from

Arunachal to Uttarkhand. The sea lasted only during the Early Permian, its withdrawal coinciding with Midian regression and sedimentological break in the Tethyan part. Thereafter Lesser Himalaya again became a positive area.

The rifting/drifted during Cretaceous again re-opened old lineaments for the transgression of Late Cretaceous Sea between Uttarkhand and Arunachal. The sea withdrew around 70 Ma. Thereafter erosion in subtropical climate led to the formation of bauxite. The subduction of the Indian plate had already commenced, the Lesser Himalayan part arched and the foreland basin formed at the present foothill region; its embayments extended quite far over the Mesoproterozoic carbonate belts and Neoproterozoic Simla-Krol, Cambrian Tal, Permian Bijni and Cretaceous Nilkanth parts. The Subathu sediments derived material from the northern and partly from southern (peninsula) sources and from the Waziristan-Khost area. The sedimentation in a marine basin continued up to 44 Ma, thereafter (Passage Beds) the paralic conditions set in that lasted till 40 Ma. In shallower part of the basin there was a break in sedimentation during the Late Eocene. The thrust sheets, which were nucleated in the Precambrian times were reactivated and were partly bared. The

Dagshai and equivalent basins were mainly deposited in estuaries and extensive flats. The Dagshai and the Passage Beds had their provenance in sedimentary sequences and also from the rising crystalline thrust sheets. The overlying Kasauli Formation represents brackish water environment with distinct supply mainly from the low grade crystalline. As the thrust sheets further emerged as a consequence of continued subduction of the Indian Plate, these advanced towards the south and the foreland basin shifted towards farther south in which typical molassic sediments of the Siwalik were deposited.

Due to impact of advancing crystalline thrust sheets the Shali and Simla groups' rocks moved partly over the Paleogene of the foreland basin and Krol Belts slid on their floors as superficial thrust sheets. The Late Cambrian folds, which are co-axial with the Himalayan folds, got accentuated and also selectively overturned, whereas the Himalayan folds (e.g. Jutogh, Krol, Tons and Kulu thrusts) remained largely open and upright. The Himalaya acquired the present elevation and various weathering processes became active, with the removal of overburden due to extensive erosion the stresses were released and various faults were reactivated from time to time.

Bursting of Glacial Lakes-- A Consequence of Global Warming: A Case History from the Lunana Area, Gasa Dzongkhag, Bhutan

ON Bhargava¹, SK Tangri² and AK Choudhary³

¹ 103 Sector 7, Panchkula 134109, INDIA

² 3 Sector 33, Chandigarh, INDIA

³ Resident Geologist, Tala Hydroelectric Project Authority, Tshimalakha, Chimakoti, BHUTAN

The lower reaches of the Lunana area expose multiple folded migmatite and biotite gneiss of the Thimphu Group, extensively intruded by granitic and pegmatitic rocks. This sequence in the upper reaches of the Table Mountain is overlain by the Tethyan metasediments.

The straight course of the Pho Chhu between Luggye and Lhedhi lakes in the Lunana area is probably controlled by a fault. A N-S strike-slip fault during Quaternary seems to have formed the Raphstreng Lake as a pull apart sag-pond.

Severe hot summers during the year 1994 led to excessive melting of glaciers. The exceptional melting contributed enormous amount of melt water to the lake basins, which caused breach of the morainic dam and consequent enlargement of the outlet of the Luggye Tsho and the Tshopda Tsho. The breach was followed by floods on October 7, 1994. These floods destabilized the slopes on either bank of the Pho Chhu near Tshopda Tsho outlet making them prone to landslides. The flash floods also eroded the left lateral moraine of the Raphstreng Tsho, which had disturbed the original angle of repose. The Raphstreng area is also

prone to ice avalanches, rock glaciers, surge of which can damage the rim and also cause spillover of water.

The morainic material comprises poorly graded gravel, deficient in finer fraction. The unit weight or in place density of the material and permeability values varies from 17.67 kN/m³ to 19.66 kN/m³ and 7.39 to 8.36 Lugeon respectively in the Raphstreng Tsho, 24.66 kN/m³ and 1.81 Lugeon in the Thorthormi Tsho and 21.39 kN/m³ and 1.14 Lugeon in the Lyggey Tsho. The permeability values suggested semi-pervious nature of the material. The values of cohesion and friction angle are 0.02 kN/cm² and 370 respectively.

The mitigating measures suggested were: (i) management of active landslide in the Tshopda-Tsho-Thorthormi Tsho complex, (ii) construction of dykes, check dams and (iii) partial draining of the Raphstreng Tsho complex and construction of dykes and check dams in Thnza-Tshoju complex. Plantation along the slopes, regular monitoring of the lakes, seismic and micro-climatic observations are recommended as long term measures. These measures were implemented in the years 1996-97. Since then the lakes of this area have remained intact.

Implications of biostratigraphy in the Himalayan Paleogene Foreland Basin

SB Bhatia^{1*} and ON Bhargava²

¹ 441 Sector 6, Panchkula-134109, INDIA

² 103 Sector 7, Panchkula-234109, INDIA

* For correspondence, email: sudhashi0903@hotmail.com

The paper discusses the role and significance of biostratigraphy in deciphering the structures, facies models and dating event stratigraphic surfaces of the intricately deformed Paleogene sediments comprising the Subathu, Dagshai and Kasauli formations (Late Thanetian-Early Miocene) of the Surajpur Tectonic Unit of the Himalayan Foreland Basin. The larger foraminifera, particularly the Nummulitidae, which occur in great abundance in distinct foraminiferal bands in the Subathu Formation are chronologically significant and facilitate recognition of Shallow Benthic Faunal Zones (SBZ–Serra-Kiel et al. 1998) throughout the Tethyan Zone, including the Himalayan Foreland Basin (Bhatia and Bhargava 2005, 2006).

In the case of the structurally deformed Paleogene sediments of the Surajpur Tectonic Unit (Mukhopadhyay and Misra, 2005), it is all the more imperative to identify and recognize the biostratigraphically significant foraminifera and other taxa to determine the younging direction of the beds. Failure to do so led Raiverman and Raman (1971), Singh (1996) and Raiverman (2002) to erroneous conclusions by suggesting an inter-tonguing relationship between the various exposed green Subathu (G1-G5) and the red Dagshai sediments (R1-R5) on the Simla-Bilaspur Highway, implying thereby that the G1-R1-G2-R2... sequence was towards the younging direction. This concept was soon contradicted by Batra (1989) on the basis of the faunal zones, which were repeated in all the G1-G5 units clearly suggesting that they were all of the same age (Late Cuisian-Early Lutetian) and that the repetition of the red and green beds was due to folding and faulting. Later works of Bagi (1992), Najman et al. (1993) and others confirmed this view. Singh's (1996) work, based on the premise that the increase of the proloculus size in the megalospheric generation (Form A) in larger foraminifera, is of phylogenetic significance, is misconstrued in as much as it relies on the proloculus-size increase in a single species-identified by him as *Nummulites atacicus*, which neither corresponds in size to the types from Europe nor to the Shallow Benthic Zone (SBZ) 8, Middle Ilerdian, of which it is one of the characteristic zonal fossil. The bulk of larger foraminifera in the exposed Subathu Formation- G1-G5 in the Bilaspur-Simla Highway are of Middle-Late Cuisian (SBZ 11-12) and Early Lutetian age (SBZ 13 = *Assilina spira abarardi* = Zone III of Batra, identified by him as *Assilina blondeaui*).

The inter-tonguing concept of green Subathu and red Dagshai was extended to embrace the grey facies of the Kasauli Formation also in the section near Charring Crossing in Dagshai Cantonment (Raiverman 2002, p. 12, figs. 2.1, 2.5c). This would seem to imply that the Kasauli Formation, generally accepted to be of Early Miocene age, is roughly homotaxial with the Early to Middle Eocene Subathu Formation—an untenable stratigraphic

situation. We critically examined the Charring Crossing section and did not find any evidence of interfingering between the green and red Subathu (actually the Passage Beds with characteristic molluscs) and the grey beds of the Kasauli Formation. On the contrary, the two are juxtaposed along a thrust plane as evidenced by profuse silckensides observed in all the rocks, particularly the sandy beds exposed in this section. The Subathu Formation along with the overlying Dagshai Formation, exposed north and northeast of the Charring Crossing, was found to have ridden over the Kasauli Formation along a ramp-flat-ramp thrust, which may be designated as the Dagshai Thrust.

In so far as the relationship between the various morphotypes of the Nummulitidae (Nummulites and *Assilina* and various paleofacies models) are concerned, the work by Luterbacher (1984) in Southern Pyrenees shows a correlation between morphological characters (size and shape, whether lenticular or flat discoidal), classified into four morphotypes and the established facies models in the Paleogene of the Pyrenees. Our work in the Kaushalia River section shows that the beds of the lowermost SBZ 10 (Early Cuisian) containing *Nummulites planulatus* and *N. burdigalensis burdigalensis* were deposited in a beach, prodelta setting, while those of SBZ 11 and 12 (Middle to Late Cuisian) with abundant *A. laxispira*, *A. cuvillieri*, besides bryozoa, crabs etc., in a lagoon to bay carbonate shoal setting, and those of SBZ 13 (Early Lutetian)-*A. spira abarardi* bed (flat discoidal >8 mm diameter) in a beach, shore face, near shore shoal environment.

The larger foraminiferal fauna thus corroborates the views expressed three decades earlier on sedimentological criteria by Singh (1978) that most of the Subathu sediments were laid down in shelf mud, tidal flats, and coastal sand bars. This view has stood the test of the time as confirmed by several workers from the homotaxial beds in Jammu, Hazara-Kashmir Syntaxis and Nepal. These homotaxial beds were deposited in a shallow, wave and storm dominated tidally influenced lagoon/barrier beach with near shore carbonate-shoal setting.

The above conclusions are in stark contradiction to the contention of Bera et al. (2008) of documenting for the first time large varieties of basinal turbidites in the Subathu—an interpretation that is not corroborated by sedimentological and paleontological evidences. The occurrence of hummocky cross-bedded sandstones (Late Cuisian) immediately below the *A. spira abarardi* bed in the Kaushalia River section (Bagi 1992) and in the oyster-bearing beds in the Jammu sector (Singh and Andotra, 2000) testify to frequent storm events in the Subathu basin. We are also in strong disagreement with the conclusion of Bera et al. (2008) that “Fixing an age for the termination of marine beds, based on reworked fossils (e.g. *A. spira*) in calciturbidite units is not justifiable and the upper limit of the Subathu Formation

must be significantly younger than ca 44 Ma.” In support of the above contention, Bera et al. (2008) have shown the occurrence of *A. spira* in a calciturbidite bed at the base of the black grey Subathu shale in most of their sections, which is hypothetical, factually incorrect and militates against the basic principles of stratigraphy. The surmise of Bera et al. (2008) regarding the upper age limit of Subathu is not borne out by the fossil records in the overlying Passage Beds, which delimit the termination of HST, including the Passage Bed around ca 40 Ma (Bhatia and Bhargava 2005). The *A. spira* abrardi bed (SBZ 13) in the Subathu Formation in all the sections occurs in the same chronological order above the beds containing foraminifera of Cuisian age (SBZ 12) as it does elsewhere in the Tethyan Zone (European biozonation), hence could not be reworked by any stretch of imagination.

In so far as the Event Stratigraphic framework is concerned, the entire Subathu sequence including the coal and carbonaceous shale at the base and the Passage Beds at the top represent Highstand Systems Tract (HST), the maximum flooding surface (MFS) is seen in sections where the base is exposed, viz., Jammu, Kakra and other sections and is represented by the occurrence of limestone beds containing *Daviesina garumnensis* (Bhatia and Bhargava 2005, 2006) representing SBZ 4 of Late Thanetian age.

We concur with Bera et al. (2008) that the ubiquitous white sandstone bed in the Kaushalia River and other sections, occurring at the top of the Passage Beds with a sharp contact, is of marine origin and that it represents the Falling-Stage Systems Tract (FSST) in the Event stratigraphy framework. However, we

disagree with their age assignment of 31 Ma to the white sandstone and of 28 Ma to the overlying Dagshai, as none of these dates are corroborated with the fossil record (Bhatia and Bhargava 2005).

References

- Bera MK, A Sarkar, PP Chakraborty, RS Loyal and P Sanyal. 2008. Marine to continental transition in Himalayan Foreland. *Geological Society of America* (In Press, available On Line)
- Bhatia SB and ON Bhargava. 2005. Regional Correlation of the Paleogene sediments of the Himalayan Foreland Basin. *Palaontological Society of India, Special Publication 2*: 105-123
- Bhatia SB and ON Bhargava. 2006. Biochronological continuity of the Paleogene sediments of the Himalayan Foreland Basin: paleontological and other evidences. *Journal of Asian Earth Sciences* 26: 477-487
- Bhatia SB and ON Bhargava. 2007. Reply to Y.Najman, 2007, Comments on “Biochronological continuity of the Paleogene sediments of the Himalayan Foreland Basin: paleontological and other evidences”- Bhatia, S.B. and Bhargava, O.N., 2006, *Journal of Asian Earth Sciences*. 26,477-487. *Journal of Asian Earth Sciences* 31: 87-89
- Luterbacher H 1984. Palaeoecology of foraminifera in Paleogene of Southern Pyrenees. Benthos 83. *Second International Symposium Benthic Foraminifera* April 1983 p389-392
- Mukhopadhyay DK and P Misra. 2005. A balanced cross section across the Himalayan frontal fold-thrust belt, Subathu area, Himachal Pradesh, India: thrust sequence, structural evolution and shortening. *Journal of Asian Earth Sciences* 25: 735-746

Spatio – Temporal Variation of Vegetation During Holocene in the Himalayan Region

Amalava Bhattacharyya* and Santosh K Shah

Birbal Sahni Institute of Palaeobotany 53, University Road, Lucknow-226 007, INDIA

** For correspondence, email: amalava@yahoo.com*

Palaeovegetation records derived from pollen assemblages provide potential information on palaeoclimate due to its characteristically multivariate and multiscale nature with respect to both temporal and spatial scales. A good number of studies on climate changes based on palynology are available from the higher elevation sites of the Himalaya, but these are mostly from its Northwestern part and data from the Northeast Himalayan region are scanty. This paper gives a glimpse of palaeovegetation-palaeoclimate changes in the alpine Himalayan region during the Holocene based on evidence of pollen data from sub-surface sediments. Further, interpretation of fossil pollen data based on the calibration of modern climate vs. modern pollen data could be used in quantitative climate reconstruction from the pollen diagrams of this region have also been emphasized

In general in the Northwest Himalayan region, the climate was warm-moist during most part of Holocene with short phases interruption of colder and drier climate around 8.3-7.3 ka B.P, 6 - ~3 ka B.P and 850 years B.P. In contrary data from the Northeast Himalaya is available only for Late Holocene, around 1.8 Ka B.P. the climate was comparatively warmer and moister similar to condition prevailing at present. There is further amelioration of climate around 1.1 Ka B.P. corresponding to Medieval warm period. Around 0.55 Ka B.P. there is a trend towards cooler and comparatively less moist climate corresponding to the little Ice Age. This is followed by an amelioration of climate comparable to present day climatic condition.

Songpan Garze fold belt: New petrological and geochronological data

Audrey Billerot^{1*}, Julia de Sigoyer², Stéphanie Duchêne³, Olivier Vanderhaeghe¹ and Manuel Pubellier²

¹ G2R, Nancy Université, FRANCE

² ENS-CNRS, Labo. Géologie, 75005-Paris, FRANCE

³ CRPG, Nancy, FRANCE

* For correspondence, email: audrey.billerot@g2r.uhp-nancy.fr

The Songpan Garze fold belt, located in the north Tibet, is the most enigmatic block of the Tibetan plateau. It is located between the Qaidam block (to the North), the Qiangtang block (to the South) and the Yangtze block (to the East). It has been accreted to Eurasia during the Indosinian orogeny in the upper Trias. The Songpan Garze block mainly consists of deformed Triassic flyschoid sediments (5-15 km thick). Many granitoids cross cut the Songpan Garze flysch. Some of them present the same isotopic signature than the Yangtze block basement (Zhang et al. 2006, Zhang et al. 2007). The Songpan Garze block is interpreted as a relict of the Yangtze peninsula, crushed between Qaidam and Qiantang blocks during the PaleoTethys closure. Songpan Garze sediments were deposited as submarine fan in the depression comprised between the converging blocks (Roger et al. 2008).

In the Danba area (Sichuan Province China), north-west to the Longmen Shan belt (that represents the eastern boundary of the Tibetan plateau) high grade metamorphic rocks are outcropping. Those metamorphic terrains could represent a cross section of exhumed deep structure of the Songpan Garze block. Petrological and geochronological studies carried on by Huang et al. (2003a) and Huang et al. (2003b) show a polyphased metamorphic evolution. M1 stage is characterized by the occurrence of kyanite and garnet (3-5 kb 570-600°C). It is dated at 204-190 Ma and is thus related to the Indosinian orogeny. M2 stage is characterized by heating, rocks reached the sillimanite grade and migmatitic conditions (4.8-6.3 kb 640-725 °C) (Huang et al., 2003b) and is dated at 168-158 Ma. However, Wallis et al. (2003) obtained an age of 65 Ma (on monazite that contain inclusions of sillimanite) for a high grade metamorphism event close to Danba. The question of the age of high temperature is then a matter of debate.

In the Quingaling dome (North Danba), migmatites of sedimentary rocks are observed. Field observations suggest that migmatization also affected metabasic intrusions. We are processing

a petrological and geochemical study on this metamorphic dome in order to precise the successive P-T conditions, and to determine if the basic intrusions are the cause of heating or if they are affected by the migmatization (partial melting or crystallization).

Moreover, cathodoluminescence observations of zircons from a leucosome of the Quingaling dome reveal growth zoning that correspond to different step of crystallisation. We interpreted them as metamorphic overgrowth around an inherited core. The different sub-domain will be dated by U-Pb dating (SIMS Cameca 1270).

References

- Huang, M., Maas, R., Buick, I.S. and Williams, I.S., 2003a. Crustal response to continental collisions between the Tibet, Indian, South China and North China blocks: geochronological constraints from the Songpan-Garze Orogenic Belt, Western China. *Journal Of Metamorphic Geology* 21(3): 223-240
- Huang, M.H., Buick, I.S. and Hou, L.W., 2003b. Tectonometamorphic evolution of the eastern Tibet Plateau: Evidence from the central Songpan-Garze Orogenic Belt, western China. *Journal Of Petrology* 44(2): 255-278
- Roger, F., Jolivet, M. and Malavieille, J., 2008. Tectonic evolution of the Triassic fold belts of Tibet. *Comptes Rendus Geoscience* 340: 180-189.
- Wallis, S. et al., 2003. Cenozoic and Mesozoic metamorphism in the Longmenshan orogen: Implications for geodynamic models of eastern Tibet. *Geology* 31(9): 745-748
- Zhang, H.F., Harris, N., Parrish, R. and Zhang, L., 2006. Association of granitic magmatism in the Songpan-Garze fold belt, eastern Tibet Plateau: Implication for lithospheric delamination. *Geochimica Et Cosmochimica Acta* 70(18): A734-A734
- Zhang, H.F. et al., 2007. A-type granite and adakitic magmatism association in Songpan-Garze fold belt, eastern Tibetan Plateau: Implication for lithospheric delamination. *Lithos* 97(3-4): 323-335

Crustal velocity structure from surface wave dispersion tomography in the Indian Himalaya

Warren B Caldwell^{1*}, Simon L Klemperer¹, Shyam S Rai² and Jesse F Lawrence¹

¹ Department of Geophysics, Stanford University, CA 94305-2215, USA

² National Geophysical Research Institute, Hyderabad 500007, INDIA

* For correspondence, email: warrenc@stanford.edu

Background

A network of 15 broadband seismographs in a ~500 km long, N-S array recorded 12 months of data in 2002–2003 (Rai et al. 2006). The array traverses the NW Himalaya, from the Indian plain in the south, across the Indus-Tsangpo Suture and the Tso Moriri Dome, to the southern flank of the Karakoram in the north. Magnetotelluric (MT) studies in this region reveal low-resistivity zones which may be indicative of fluids, graphite, or partial melts in the mid-crust. We have tested these hypotheses by creating 1-D models of crustal shear wave velocity. The models contain low-velocity zones at 25–40 km depth; these may be indicative of fluids or partial melts.

Methods

Our models are obtained by inverting group velocity dispersion curves of Rayleigh waves in the period range of roughly 4–60 s. Numerous magnitude 4 events, several magnitude 5 events, and one magnitude 6 event occurred 900 km or less from the array. We find dispersion curves by analyzing the z-component of fundamental mode Rayleigh waves using Robert Herrmann's Computer Programs in Seismology (Herrmann and Ammon 2002). We invert the dispersion curves using these programs to create 1-D models of crustal shear wave velocity structure. The inversion is done to 150 km depth, but we consider only the upper 60 km of the models.

Results

Our results reveal, as expected, demonstrably different crustal structure in the Indian shield and the Himalaya and Tibetan Plateau, and our 1-D models suggest that a low-velocity zone is present immediately north of the Indus-Tsangpo Suture (Figure 1).

Future work

We are currently performing tomographic inversions for the region using these data. These results will offer resolution not available in our 1-D models. The 1-D results, with their simpler underlying assumptions, will provide a test of the tomography results.

References

- Herrmann, RB and CJ Ammon. 2002. Computer Programs in Seismology: Surface Waves, Receiver Functions and Crustal Structure. St. Louis University, St. Louis, MO. <http://www.eas.slu.edu/People/RBHerrmann/ComputerPrograms.html>.
- Rai SS, K Priestley, VK Gaur, S Mitra, MP Singh and M Searle. 2006. Configuration of the Indian Moho beneath the NW Himalaya and Ladakh. *Geophysical Research Letters* 33 (L15308): doi:10.1029/2006GL026076.

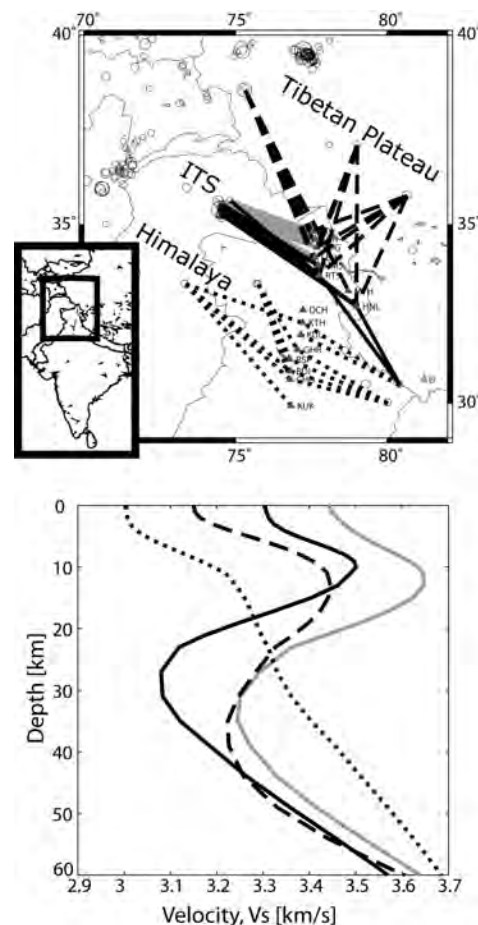


FIGURE 1. Upper: Locations of seismograph stations and epicenters of earthquakes scaled by magnitude (all magnitudes are between 3.8 and 6.4). Lines are earthquake paths used for this study. We designate 3 principal geologic regions: 'Tibetan Plateau,' 'Indus-Tsangpo Suture' (ITS), and 'Himalaya.' Lower: Mean of the shear wave velocity models in each regional group. Line styles follows the map. Event-station paths in the thrust and foreland basin (dotted lines) show a normal velocity profile that increases with depth. Event-station paths north of the ITS in the Gangdese Batholith (gray solid lines) show the highest velocity, and, along with paths from the Tibetan Plateau (dashed lines), have a low-velocity zone at 30–40 km. Event-station paths in the ITS (black solid lines) have a pronounced low-velocity zone at 25–30 km.

Non-coaxial heterogeneous deformation in the Num orthogneiss (Arun valley, Mt. Makalu area, eastern Nepal)

R Carosi^{1*}, C Frassi¹, C Montomoli¹, PC Pertusati¹, C Groppo², F Rolfo² and D Visonà³

¹ Department of Earth Sciences, University of Pisa, Via S. Maria, 53 I-56126 Pisa, ITALY

² Department of Mineralogical and Petrological Sciences, University of Torino, Via Valperga Caluso 35, I-10125 Torino, ITALY

³ Department of Mineralogy and Petrology, University of Padova, c.so Garibaldi 37 35122 Padova, ITALY

* For correspondence, email: carosi@dst.unipi.it

In the Arun and Barun valleys the upper portion of the Lesser Himalayan section is made up by the Num orthogneiss. It is a 3–4 km thick unit of granitic augen gneiss with bands of kyanite-flogopite schists (Lombardo et al. 1993). It records a non-coaxial deformation related to its involvement within the Main Central Thrust zone that produced an heterogeneous mylonitic deformation with rotated feldspar porphyroclasts, bookshelf structures and localized shear bands with a prominent top-to-the SW sense of shear. The base of the Num orthogneiss is the Main Central Thrust I (MCT I, sensu Arita 1983).

Micaschists and/or micaceous levels are often intercalated within the Num orthogneiss, being parallel to the mylonitic foliation. Two different kinds of micaceous levels have been recognized:

- Type a: derived from sedimentary levels deformed and transposed within the orthogneiss. They often contain garnet and could be referred to Kushma and/or Seti Formations (Goscombe and Hand 2006);
- Type b: decimetric- to metric-thick micaceous levels with the same mineral assemblage as in the orthogneiss but showing a strong grain size reduction and mica enrichment along the main foliation.

In Type b levels strain increases from the mylonitic orthogneiss toward the micaceous levels as highlighted by strong grain size reduction of feldspar crystals and development of polycrystalline quartz ribbons; small-size tourmaline crystals are still present.

A conspicuous enrichment in muscovite and biotite has been observed along the shear planes and sometimes gneiss is transformed into phyllonites.

Microstructural studies revealed that many of the micaceous intercalations within Num orthogneiss are the product of the localization of non-coaxial deformation during the evolution of deformation in the MCT zone.

References

- Arita K. 1983. Origin of the inverted metamorphism of the Lower Himalayas, Central Nepal. *Tectonophysics* 93: 43–60
- Goscombe B and M Hand. 2006. *Gondwana Research* 10: 232–255
- Lombardo B, P Pertusati and A Borghi. 1993. Geology and tectono-magmatic evolution of the eastern Himalaya along the Chomolungma-Makalu transect. In: Treloar P J and Searle M P: (eds.) *Himalayan Tectonics Geological Society, London Special Publication* 74: 341–355

Ductile-brittle deformation in the hanging-wall of the South Tibetan Detachment System (Southern Tibet)

R Carosi^{1*}, C Montomoli¹, E Appel², I Dunkl³ and Lin Ding⁴

¹ University of Pisa, ITALY

² University of Tübingen, GERMANY

³ University of Göttingen, GERMANY

⁴ Institute of Tibetan Plateau Research, CAS, Beijing, CHINA

* For correspondence, email: montomoli@dst.unipi.it, carosi@dst.unipi.it

The South Tibetan Detachment System (Burg et al. 1984, Burchfiel et al. 1998) is characterized by a lower ductile shear zone, an upper low-angle normal fault and high-angle normal faults (Carosi et al. 1998, Searle 2003). The low-angle normal fault puts in contact the base of the Tibetan Sedimentary Sequence with the high-grade sillimanite-bearing schists and mylonitic leucogranites of the Greater Himalayan Sequence and, in several places, the intervening North Col Formation. In the Rongbuk valley, Sa'er and Nyalam areas (southern Tibet) a sharp contact of the low-angle normal fault is associated to breccias and cataclasites.

Samples collected from the Ordovician rocks up to Triassic rocks reveal that temperature increases toward the bottom of the Ordovician limestone. Localized high-strain zones have been recognized in the Ordovician limestone where it is transformed in calcmylonites. Calcite crystals show a shape preferred orientation and grain size reduction in cm-size bands and show mechanical twins mainly of Type II with lesser amount of Types I and III (Passchier and Trouw 2006) suggesting a temperature of deformation in the range of 200–300°C.

Ductile deformation at the base of the limestone is heterogeneous and gives rise to mylonitic bands post-dating D1 folds. Quartz and calcite displacement-controlled fibres around pyrite crystals, asymmetric tails around polycrystalline calcite or calcite/dolomite aggregates, foliation boudinage and asymmetric boudinage of calcite veins confirm a top-to-the NE sense of shear, in agreement with the movement of the South Tibetan Detachment System.

Moving to the Silurian, Devonian and Carboniferous sequences primary structures are well-preserved and deformation mechanisms show a sharp transition to low-temperature mechanisms, being pressure-solution dominant both in limestone, sandstones and conglomerates. In limestone pressure solution is linked to the development of calcite veins nearly perpendicular to

pressure solution seams showing cross-cutting relationships.

The ductile shear zones recognized at the base of the Tibetan Sedimentary Sequence cannot be attributed to the thickening stage (with south verging deformation and lithostatic load of the overlying Tibetan Sedimentary Sequence) but it is related to the earlier ductile activity of the South Tibetan Detachment.

Further brittle deformation of the South Tibetan Detachment System localized mainly at the base of the Ordovician limestone giving rise to breccias, cataclasites and ultracataclasites. However, “ghosts” of recrystallized pseudotachilites, preserving the geometry of injection veins, have been detected even in the underlying mylonitic granites in the Nyalam section, testifying their involvement in brittle deformation.

References

- Burg JP, M Brunel, D Gapais, GM Chen and Liu GH. 1984. Deformation of leucogranites of the crystalline main central thrust sheet in southern Tibet (China). *Journal of Structural Geology* 6: 535–542
- Burchfiel BC, Z Chen, KV Hodges, Y Liu, LH Royden, R Carosi, B Lombardo, G Molli, G Musumeci and PC Pertusati. 1998. The South Tibetan Detachment System in the Rongbuk valley, Everest region. Deformation features and geological implications. *Journal of Asian Earth Science* 16: 299–311
- Changrong D and L Xu. 1992. The South Tibetan Detachment System, Himalayan Orogen: extension contemporaneous with and parallel to shortening in a collisional mountain belt. *Geological Society of America Special Paper* 269: 41 p
- Passchier CW and RJ Trouw. 2006. *Microtectonics*, Springer Verlag, Berlin, Heidelberg. 366 p
- Searle MP, RL Simpson, RD Law, RR Parrish and DJ Waters. 2003. The structural geometry, metamorphic and magmatic evolution of the Everest massif, High Himalaya of Nepal–South Tibet. *Geological Society [London] Journal* 160: 345–366

Three-Dimensional Strain Variation across the Kathmandu Nappes: Insight to Nappe Emplacement Mechanism

Deepak Chamlagain

Department of Environment Science, Amrit Science College, Tribhuvan University, Kathmandu, NEPAL

* For correspondence, email: dchamlagain@hotmail.com

Introduction

The Main Central Thrust (Mahabharat Thrust of Stöcklin 1980) is one of the key thrusts in central Nepal Himalaya to understand the nappe tectonics because it is considered that MCT acted as a glide plane for the thrust sheets, which traveled more than 100 km towards south over the LHS forming a large folded-thrust sheet called Kathmandu Nappe. Much of the research has been focused on structural and kinematic analysis of the MCT zone, a root zone of the Kathmandu Nappe. These studies have confirmed a top-to-the south directed sense of shear in the MCT zone, which is associated with the emplacement of Kathmandu Nappe. Although large-scale geometry of the Himalayan thrust sheets and nappes are relatively understood, features of the internal deformation are not well understood in terms of strain geometry. Several studies have shown that the pattern of the internal deformation varies between thrust sheets because it depends on pressure, temperature, and complex tectonic boundary condition. Although strain analysis bears important clues to understand internal deformation, there

is still lack of studies across the Himalaya nappes. It is, therefore, necessary to address several problems like (1) three-dimensional strain geometry, (2) relation between inverted metamorphism and strain pattern, (3) precise kinematic model to reveal nature of internal deformation and emplacement mechanism. These issues are certainly useful to decipher tectonics of the Himalayan nappes and thrust sheets. This study, therefore, mainly attempts to discuss above-mentioned issues using structural data, three-dimensional strain geometries, and metamorphism across the MCT and basal part of the Kathmandu Nappe in central Nepal Himalaya (Figure 1).

Structural Geology

In the study area, the MCT is only a major thrust that served as a glide plane along which Kathmandu Nappe has been emplaced towards south from its root zone. It carried Precambrian to Devonian rocks over the Lesser Himalaya. Although displacement magnitudes are difficult to determine for the MCT, 100 km was estimated at least (Johnson et al. 2001). The entire thrust sheet has

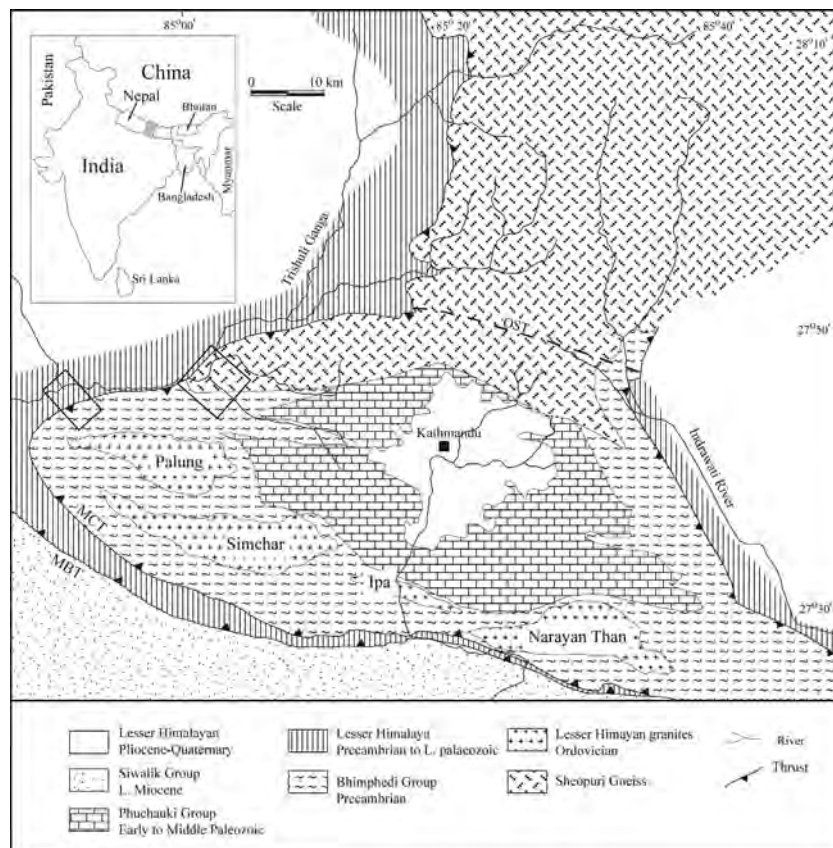


FIGURE 1. Geological map of central Nepal (modified after Stöcklin 1980). MCT: Main Central Thrust, MBT: Main Boundary Thrust, OST: Out of sequence thrust. Rectangles show studied areas.

an oval shape structure and convex towards the foreland, which is folded giving rise to large synclinorium. Along the Malekhu Khola section, complete sequences of both footwall and hanging wall are well exposed. About 100 m thick mylonite, and phyllonite zones characterize MT zone, where thrust related structures are abundant. In the study area, the NE-SW trending MCT represents thin ductile zone with the highest degree of finite deformation. It is distinctly marked by a penetrative foliation, and stretching and mineral lineation. Deformation fabric intensities are generally homogeneous at the outcrop scale. Foliation within the quartzites and schists is defined by aligned biotite and muscovite, and the mineral lineation is defined by streaking of mica domain in foliation surfaces in schists and in quartzites by quartz grain-shape alignment. In the footwall, platy phyllites display lineation with south-southwest plunge and the foliation planes in the footwall block show steep dipping towards south. Near to MCT, mylonitic quartzite is characterized by the strong stretching lineation with southwest plunge. The S-C fabrics at the MT zone show top-to-the-south directed shear sense (Johnson et al. 2001). At the central part of thrust zone, quartz veins are often folded asymmetrically and the axial plane is sub-parallel to the foliation plane. Garnet grains of centimeter scale are normally present in the MT zone. At the base of the hanging wall, the garnetiferous schist (Raduwa Formation) is well foliated with poorly developed linear structures. Foliation plane is dominantly dipping towards south excluding area at the proximity of MCT. At least three phases of deformation can be documented: first (D1) development of S1 parallel to So. Second (D2) phase is mostly observed along the Mahesh Khola and is characterized by the tight folds and lineations, which moderately plunge toward southwest. The axial planes of these folds are slightly oblique to the S1 foliation and, S2, a new schistosity is incipiently developed along the axial plane of the F2 folds. F2 fold is considered as a refolding of the F1 folds. The D3 deformation phase is characterized by the F3 and consists of crenulation cleavages with easterly or southeasterly plunges and steeply dipping axial plane trending east-west or northwest-southeast. The linear structure associated with the D3 deformation is roughly considered parallel to the axis of the Mahabharat synclinorium which trends east southeast. Structural data support a single nappe model considering Mahabharat Thrust as a southern continuation of the MCT, which acted as a glide plane for Kathmandu Nappe.

Three-Dimensional Strain Geometry

Three-dimensional strain data show heterogeneous strain field both in footwall Lesser Himalayan sequence (LHS) and hanging wall (Kathmandu Nappe). In the footwall Nadai amount of strain intensity (ϵ_s) varies from 0.396 at the base to 0.575 adjacent to the MCT whereas in the Kathmandu Nappe, it varies from 0.345 to 0.946. In general, the footwall block shows increasing trend of ϵ_s value towards MCT whereas in the Kathmandu Nappe increases away from the MCT (Figure 2). Lower value of ϵ_s at the base of the Kathmandu Nappe is due to thermal relaxation that led to a low temperature dynamic metamorphism and plastic deformation after the emplacement of hot Kathmandu Nappe. The complex patterns of orientation of the strain ellipsoids are due to superposition of strain partitioning mechanisms on different scales, which have also created a complex regional strain variation in terms of magnitude. The shape, orientation of strain ellipsoids, and mesoscale structural data indicate transpressional strain

field in the MCT zone. The dominance of prolate type strain ellipsoids suggest simple shear model for the footwall LHS. In the hanging wall, however, strain field is dominantly oblate type with few prolate types suggesting pure shear with a thrust parallel shortening model (Figure 2). For the both walls computed k-values have revealed non-plane strain deformation for the MCT, which is apparently consistent with several fold-and-thrust belts on the earth.

Emplacement Mechanism

Various models have been designed to explain the exhumation of the HHCS e.g. (a) rigid extrusion (b) ductile channel extrusion or channel flow (c) Ductile extrusion by general shear. None of the models are able to show complete scenario of the exhumation mechanism of the HHCS. Recently, Channel flow model is widely used but also a matter of strong debate. This model for the Himalaya-Tibet orogenic system are particularly intriguing because of the proposed link between channel flow and ductile extrusion driven by focused precipitation/denudation at the Himalayan topographic front (Beaumont et al. 2001). The primary drivers for channel flow in the Himalayan-Tibetan Orogen are (1) unusually weak zones that exist in the crust at different depths throughout

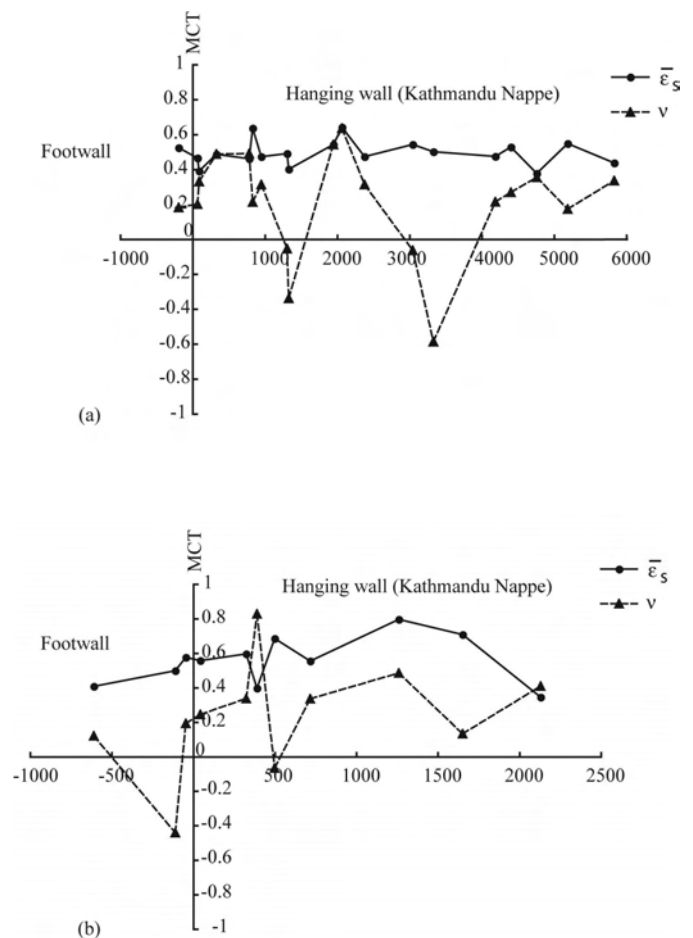


FIGURE 2. Variation of strain parameters across the MCT (a) Galchhi area (b) Malekhu area. Note that measured distance (in meter) is normal to the MCT.

the modern Tibetan Plateau, and (2) that gravitational/pressure-driven flow. Based upon results from the INDEPTH studies, Nelson et al. (1996) proposed that crust on the leading edge of the subducting Indian plate partially melts below the Lhasa terrane, and flows southward toward the Himalayan orogenic front, where it is denudationally extruded between the coeval MCT and STDS as Higher Himalayan rocks. Harrison (2006) opposed this concept because their 'bright spots' restricted to a single rift and evidence that they represent aqueous fluids rather than molten silicate; the seismogenic nature of Moho in southern Tibetan and $^3\text{He}/^4\text{He}$ data indicates the presence of mantle heat and mass in the rift valley. Therefore, any melt present is due to late Neogene calc-alkaline magmatism and is supported by the lack of Tertiary migmatites in the crustal section exposed in the uplifted rift flank of the Yangbajain graben. The absence of Gangdese zircon xenocrysts in the Higher Himalayan rocks and the broadly coherent stratigraphy further put question on validity of channel flow model. Further, the model must explain observed geological relationships in the nappes composed of rocks of HHCS. For example in central Nepal the MCT juxtaposes hanging wall rock that consists of the Higher Himalayan rocks (Bhimpheedi Group of Stöcklin 1980) against LHS rocks. However, there is no evidence of normal fault equivalent to STDS that serves as an upper bounding fault for the extruding channel. Therefore, the lack of an upper bounding shear zone clearly suggests that existing channel flow models that describe the emplacement of HHCS rocks in the High Himalaya may not apply to the Kathmandu Nappe. Gross stratigraphic relationships within the well-bedded Bhimpheedi Group appear to be intact and in the

more quartz-rich lithologies, primary sedimentary structures such as cross-beds and ripple marks can be observed (Stöcklin 1980). If rocks of the Bhimpheedi Group flowed within a channel, it is highly likely that original stratigraphic relationships and sedimentary structures would have been obscured. Further, central Nepal Himalaya doesn't show the coupling between the climate and tectonics, posing question on validity of the channel flow model. Rather, structural and three-dimensional strain data support the general shear extrusion model proposed by Vannay and Grasemann (2001).

References

- Beaumont C, RA Jamieson, MH Nguyen and B Lee. 2001. Himalayan tectonics explained by extrusion of a low-viscosity crustal channel coupled to focused surface denudation. *Nature* 414: 738-742
- Harrison TM. 2006. Did the Himalayan Crystallines extrude partially molten from beneath the Tibetan Plateau? In Law RD, MP Searle and L Godin (eds.) Channel Flow, Ductile Extrusion and Exhumation in Continental Collision Zones. *Geological Society, London, Special Publications* 268: 237-254
- Nelson KD and others. 1996. Partially molten middle crust beneath southern Tibet; synthesis of Project INDEPTH results. *Science* 274: 1684-1688
- Stöcklin J. 1980. Geology of the Nepal and its regional frame. *Journal of the Geological Society of London* 137: 1-34
- Vannay J-C and B Grasemann. 2001. Himalayan inverted metamorphism and syn-convergence extension as a consequence of a general shear extrusion. *Geological Magazine* 138: 253-276

Crustal configuration of NW Himalaya based on modeling of gravity data

Ashutosh Chamoli^{*}, AK Pandey¹, VP Dimri¹ and P Banerjee²

¹ National Geophysical Research Institute, Hyderabad- 500 007, INDIA

² Wadia Institute of Himalayan Geology, Dehradun- 248 001, INDIA

^{*} For correspondence, email: chamoli.a@gmail.com

The crustal structure of the Himalayan fold-thrust belt in NW Himalaya is constrained using spectral analysis, wavelet transform (WT) and forward modeling of the Bouguer gravity anomaly. The data covers the Himalayan range from the Sub Himalayan zone in the hanging wall of Himalayan Frontal Thrust (HFT) to the Karakoram fault across the Indus Tsangpo Suture Zone (ITSZ), along about 450 km long (projected distance), the Kiratpur-Manali-Leh-Panamik transect. The spectral analysis of power spectrum of the gravity data yielded three layer interfaces. The short wavelength data is modeled on the basis of density contrast across the litho-tectonic boundaries and regional structural geometries along the profile section. The average depth and location obtained using the wavelet

transform (WT), which shows good correlation with the major mapped tectonic boundaries including intracrustal/subcrustal faults in space scale domain. The long wavelength gravity data is analysed using coherence method for isostatic compensation to obtain the average depth of effective elastic thickness. The Moho configuration and the locus of flexure of Indian crust is constrained using forward modeling incorporating information from other studies. The Moho depth increases from 40 to 75 km towards north with the locus of flexure of Indian crust beneath the Lesser Himalayan zone. The combination of forward modeling and WT analysis of the data gives insight into the subsurface extent and geometry of regional structures for the first time from the NW Himalaya.

Tectonometamorphic evolution of collisional orogenic belts in the Korean Peninsula: Implications for East Asian tectonics

Moonsup Cho

School of Earth and Environmental Sciences, Seoul National University, Seoul, 151-747, KOREA

E-mail: moonsup@snu.ac.kr

The Korean Peninsula consists of three Precambrian massifs (Nangrim, Gyeonggi and Yeongnam massifs from north to south), bisected by two Phanerozoic fold-thrust belts (Imjingang and Ogcheon belts). Tectonometamorphic evolution of these terranes is of prime importance for understanding the continental growth of East Asia. In particular, the eastward extension of the Dabie-Sulu collisional belt between North and South China cratons, across the Korean Peninsula towards Japan, has been discussed by many workers but still contentious. In this study I review the Permo-Triassic collisional orogeny recorded in the Korean Peninsula.

The Ogcheon fold-thrust belt consists of the Taebaeksan basin and the Ogcheon metamorphic belt, which are in fault contact. The Paleozoic formations in the Taebaeksan basin are well correlated with those of the North China craton. On the other hand, the Ogcheon metamorphic belt comprises Neoproterozoic (ca. 750 Ma) to Paleozoic meta-sedimentary and -volcanic sequences which may belong to the South China craton. Regional metamorphism has produced the Barrovian-type assemblage at peak metamorphic conditions estimated to be 4.2–9.4 kbar and 490–630°C. This syn-tectonic metamorphism in association with the Ogcheon orogeny was dated at ca. 280 Ma. During the subsequent Indosinian (Songrim) orogeny at ca. 250–220 Ma, the Ogcheon metamorphic belt experienced the greenschist-facies metamorphism and was thrust over the Taebaeksan basin along brittle-ductile shear zones.

The Imjingang belt, commonly known as an extension of the Dabie-Sulu belt, consists primarily of Barrovian-type metapelites, calc-silicate rocks and garnet amphibolites. Biotite poikiloblasts of the metapelites initially grew between two contractional events (Dn-1 and Dn), and was subsequently overgrown during Dn by crack-filling mechanism. On the other hand, the growth of poikiloblastic garnet started after Dn-1, and predominated during Dn. The garnet porphyroblast partly replaced biotite at the post-Dn stage. Peak temperatures were estimated at 450–700°C, and metamorphic pressures apparently increase from ca. 8 kbar in the garnet zone to ca. 11 kbar in the kyanite zone. The matrix of the kyanite-zone schist, however, records much lower pressure of 5–7 kbar, suggesting a clockwise P–T path. The timing for high-P peak metamorphism was dated at ca. 250 Ma, whereas relatively rapid cooling through ca. 500–300°C took place at 230–220 Ma. The latter was associated with Dn+1 responsible for rapid exhumation along a ca. 20 km-wide ductile shear zone. The clockwise P–T–t history is similar to that documented in not only the basement gneisses of the Gyeonggi massif but also high-P schists in the Alps. It is thus likely that the whole peninsula, including Phanerozoic fold-thrust belts and Precambrian basement massif, has experienced a crust thickening during the Permo-Triassic orogeny, and that the Dabie-Sulu collisional belt continues towards the Korean Peninsula.

The Sedimentary Record of Deglaciation in the Western Himalaya recorded in the Indus Delta, Pakistan

PD Clift^{*}, L Giosan², IH Campbell³, J Blusztajn², M Pringle⁴,
AR Tabrez⁵, A Alizai¹, MM Rabbani⁵ and S Vanlaningham¹

¹ School of Geosciences, University of Aberdeen, UK

² Woods Hole Oceanographic Institution, USA

³ Australian National University, Canberra, AUSTRALIA

⁴ Massachusetts Institute of Technology, Cambridge, MA, USA

⁵ National Institute of Oceanography, Clifton, Karachi, PAKISTAN

* For correspondence, email: pclift@abdn.ac.uk

The retreat of icesheets following the end of the Last Glacial Maximum (LGM) might be expected to have caused a significant change in the nature of erosion in the Western Himalaya. We investigated the nature of this changing erosion and the stratigraphic record of the transition by drilling in the Indus delta of Pakistan. A section dating back to ~14 ka was recovered and dated by ¹⁴C AMS methods. The delta appears to have been built in two prograding stages, separated by a transgressive surface dated at around 8 ka. Curiously the delta and shoreline migrate oceanwards during the fastest stages of eustatic sealevel rise prior to 9 ka (Giosan et al. 2006). This requires strongly accelerated sediment delivery at this time, much as seen in the Bengal delta. Provenance analysis shows that this sediment is newly eroded in the Early Holocene and is not simply glacial sediments that are transported to the ocean at that time. Nd isotope analysis provides an overview of how erosion patterns change. The greatest isotopic shift is seen before ~10 ka, coincident with summer monsoon intensification (Clift et al. 2008). The direction of isotopic change is towards more continental, radiogenic values. A combination of Ar-Ar mica and single grain zircon dating indicates that the proportion of Lesser Himalayan material increases sharply at this time, largely at the expense of the Karakoram and Trans Himalaya. These more northerly ranges are still heavily glaciated and appear to have dominated the erosional flux to the delta prior to the Holocene. Glaciation was not so important in driving erosion in the western Himalaya, but may have more important in the wetter East. At the LGM glaciers did not extend much further than presently seen, largely because the climate was very arid at this time. Glaciers never covered the Lesser Himalaya, so that the pulse in erosion after 14 ka from these ranges is not due to

glacial retreat. Instead we suggest that it is the intensified summer monsoon that caused both the faster overall rate and the change in the patterns of erosion. The Lesser Himalaya and the southern flanks of the Greater Himalaya are the recipients of the greatest amounts of summer rain. The fact that the Lower Holocene sediment is isotopically distinct from LGM sediment shows that reworking of older sediment is minimal. Transport times from source to the delta sink are short, at least less than the resolution of the age control (~1000 yr), as provenance and climate appear to change in parallel. However, sediment now on the seafloor of the Indus Canyon has a glacial Nd isotope character and confirms that sediment flux to the deep ocean ceased no later than the Bølling-Allerød. As a result the sediment record of Himalayan erosion preserved in the Indus Fan is buffered and lags the erosion events by at least ~10 k.y. Marine data suggest that much of the sediment now found in the delta and on the Pakistan Shelf is eroded during sealevel fall and has low preservation potential over long periods of geologic time, largely because tectonic subsidence in the delta region is now slow.

References

- Clift PD, L Giosan, J Blusztajn, IH Campbell, C Allen, AR Tabrez, M Danish, MM Rabbani, A Alizai, A Carter and A Lückge. 2008. Holocene erosion of the Lesser Himalaya triggered by intensified summer monsoon. *Geology* 36 (1): 79-82
- Giosan L, PD Clift, J Blusztajn, A Tabrez, S Constantinescu and F Filip. 2006. On the control of climate- and human-modulated fluvial sediment delivery on river delta development: The Indus. *Eos, Transaction of American Geophysical Union* 87(52): OS14A-04

Seismic reflection evidence for a Dangerous Grounds mini-plate in the South China Sea and implications for extrusion tectonics in SE Asia

Peter Clift^{1,2*}, Gwang H Lee³, Nguyen Anh Duc⁴, Udo Barckhausen⁵, Hoang Van Long¹ and Sun Zhen²

¹ School of Geosciences, University of Aberdeen, Aberdeen, AB24 3UE, UNITED KINGDOM

² Key Laboratory of the Marginal Sea Geology, South China Sea Institute of Oceanology, Chinese Academy of Sciences, 164# Xingangxi Road, Guangzhou, 510301, CHINA

³ Department of Environmental Exploration Engineering, Pukyong National University, Busan 608-737, KOREA

⁴ Vietnam Petroleum Institute, Yên Hoa, Cau Giay, Hanoi, VIETNAM

⁵ BGR, Federal Institute for Geosciences and Natural Resources, Stilleweg 2, 30655 Hannover, GERMANY

* For correspondence, email: pclift@abdn.ac.uk

The collision of India and Asia has caused large strike-slip faults to form in East Asia, resulting in the “extrusion” of crustal blocks towards the southeast since the Eocene as a result of the indentation of rigid India into Asia (Peltzer and Tapponnier 1988, Tapponnier et al. 1982). It has been suggested that the South China Sea opened as a result of relative motion between a rigid Indochina (Sundaland) block and China (Briais et al. 1993). Alternative models propose that rifting and seafloor spreading were driven by trench forces to the south (Morley 2002, Taylor and Hayes 1980). We test these competing models by analysis of seismic reflection profiles across the boundary between Sundaland and the southern rifted margin, known as the Dangerous Grounds. We show that the southern boundary of the Dangerous Grounds is a subduction zone that jammed in the Middle Miocene (Hutchison et al. 2000). To the west the Dangerous Grounds is bounded by a strike-slip zone, also active until ~16 Ma, that becomes diffuse south of the now inactive South China Sea seafloor spreading centre. We place the western edge of the Dangerous Grounds just to the east of the Natuna Arch (Lupar Line). The West Baram Line is confirmed as originating as a major strike-slip fault within the Dangerous Grounds and continuous with Red River Fault Zone. Because the Dangerous Grounds were independent of Sundaland until ~16 Ma its motion cannot have been constrained by motion of this block, making extrusion impossible as a mechanism to rift the South China Sea. SE motion by both the Dangerous Grounds and Sundaland suggests subduction forces were the primary trigger for plate motions. Our reconstruction places a ~280 km upper limit on the motion on the Red River Fault, and a ~1400 km width to the paleo-South China Sea. This value is intermediate

between the low estimates of Searle (2006) and the higher values of > 1000 km (Tapponnier et al. 1990).

References

- Briais A, P Patriat and P Tapponnier. 1993. Updated interpretation of magnetic anomalies and seafloor spreading stages in the South China Sea: implications for the Tertiary tectonics of Southeast Asia. *Journal of Geophysical Research* 98: 6299-6328
- Hutchison CS, SC Bergman, DA Swaiger and JE Graves. 2000. A Miocene collisional belt in north Borneo: uplift mechanism and isostatic adjustment quantified by thermochronology. *Journal of the Geological Society* 157: 783-793
- Morley CK. 2002. A tectonic model for the Tertiary evolution of strike-slip faults and rift basins in SE Asia. *Tectonophysics* 347(4): 189-215
- Peltzer G and P Tapponnier. 1988. Formation and evolution of strike-slip faults, rifts, and basins during the India-Asia Collision: an experimental approach. *Journal of Geophysical Research* 93: 15085-15117
- Searle MP. 2006. Role of the Red River Shear zone, Yunnan and Vietnam, in the continental extrusion of SE Asia. *Journal of the Geological Society* 163: 1025-1036
- Tapponnier P. et al. 1990. The Ailao Shan/Red River metamorphic belt; Tertiary left-lateral shear between Indochina and South China. *Nature* 343(6257): 431-437
- Tapponnier P, G Peltzer, GAY Le Dain, R Armijo and PR Cobbold. 1982. Propagating extrusion tectonics in Asia: New insights from simple experiments with plasticine. *Geology* 10: 611-616
- Taylor B and DE Hayes. 1980. The tectonic evolution of the South China Basin. In: D Hayes (ed), *The Tectonic and Geologic Evolution of Southeast Asian Seas and Islands*. Geophysical Monograph. American Geophysical Union, Washington DC, p89-104

Examination of relocated earthquake hypocenters in the Pamir-Hindu Kush seismic zone using 3-D plots

S Das

*Department of Earth Sciences, University of Oxford, Oxford OX1 3PR, UK
E-mail: das@earth.ox.ac.uk*

Reliably relocated earthquake hypocenters in the Pamir-Hindu Kush region for about 1700 earthquakes deeper than 50 km, are examined using 3-D color plots. The hypocenters define an single contorted "S" shaped seismic zone, 700 km long and no more than 30 km wide and with most activity concentrated in the 100-300 km depth range. The main features observed are:

- a) the continuous steepening of the north dipping Hindu Kush seismic zone as we move eastwards towards the Pamirs;
- b) the southeast dipping Pamir seismic zone;
- c) the curvature and forking of the subducting slab at depths greater than 200 km within the eastern part of the Hindu Kush seismic zone;
- d) the very abrupt cutoff in intermediate depth seismicity at 90-110 km depth with no extension to shallower depths, under the Pamirs, suggesting that the slab has

- become decoupled from the surface deformation;
- e) the unusual horizontal T-axes for intermediate depth earthquakes of the Pamir seismic zone, which align with its curvature, suggesting that this region is under horizontal compression. The study shows that the seismic zone under the Hindu Kush has stress axes which follow the classical pattern for subducting slabs controlled by gravity, whereas the Pamir region has horizontal T-axes that follow the trend of the contorted seismic zone. We suggest that the Pamir seismic zone is a remnant slab has been completely overturned and torn away from the Hindu Kush slab, to be in the current south dipping geometry, as a result of flow in the upper mantle. The 3-D plots will be shown as computer animations at the conference.

Unzipping Lemuria from its Himalaya suture to understand mammalian origins

Maarten J de Wit^{1*} and Judith Masters²

¹ *AEON – Africa Earth Observatory Network and Department of Geological Sciences, University of Cape Town, Rondebosch 7700, SOUTH AFRICA*

² *Department of Zoology, University of Fort Hare, Private Bag X1314, Alice 5700, SOUTH AFRICA*

* *For correspondence, email: maarten.dewit@uct.ac.za*

Information relating to the suturing history between India and Asia is crucial to understanding the historical biogeography of living mammals. It is particularly relevant to understanding the origins of Madagascar's mammal fauna that contributes to the island's standing as one of the world's biodiversity hotspots. Evolutionary biologists are strongly divided as to the timing and place of the origins of extant mammalian orders. Most palaeontologists stand by the opinion that living mammal orders arose after the K/T boundary (66 Ma) in the northern hemisphere, while molecular phylogeneticists push these divergences back into the Cretaceous (≥ 100 Ma) and favour a southern hemisphere origin. Recent discovery of an ungulate fossil at about 65 Ma in peninsular India supports the molecular argument. Within the circa 40 Ma period that separates the two estimates, the global palaeobiogeography of the Indian Ocean changed dramatically as continents moved and oceans evolved rapidly during the final break-up of Gondwana and the suturing between India and Asia. A detailed understanding of the movement and suturing history of India will allow biologists to formulate more robust scenarios of early mammalian dispersal, and perhaps identify, finally, the places of origin of major mammal clades.

The precise extent of palaeo-continental lithosphere north of India that vanished following the sub-continent's collision with

Asia is poorly quantified. Argand, in 1922, assumed it stretched all the way from northern India, then in the southern hemisphere as part of Gondwana, to Asia. He called this landmass Lemuria and predicted that during continental drift away from Gondwana, much of Lemuria was thrust beneath Asia. We know this to be incorrect in detail today, but the concept is still with us. Yet facts about the chemical and physical composition of this continental shelf to the north of paleo-India are few. There is also a lack of consensus on the precise timing (and possible along-strike diachronous events) of docking and final suturing between Lemuria and Asia. The fragmentation history of Gondwana and the evolution of the Indian Ocean are now well-enough understood to re-evaluate evidence for transient land bridges, given the unlikelihood of cross-water dispersals of early mammals between different fragments of Gondwana, and especially between Africa, Madagascar and India. Resolution of the uncertainties associated with India's accretion to Asia by geologists and geophysicists will enable biologists to unravel one of the great long-standing debates in natural history that dates back to the heydays of AR Wallace and C Darwin, i.e. the colonization of Madagascar. In this presentation we outline the major controversies relating to this problem, and show how a detailed analysis of the events that occurred along the length of the suture will contribute to resolving this debate.

Addressing Tectonic and Metamorphic Controversy in the Pakistan Himalaya

Joseph A Dipietro

University of Southern Indiana, Dept. of Geology, 8600 University Blvd., Evansville, IN 47712, USA

E-mail: dipietro@usi.edu

Some of the more controversial or less agreed upon aspects of the Pakistan Himalaya include the absolute age (or ages) of metamorphism, the cause of metamorphism, the location (or existence) of the MCT, the existence of the STDS or STDS-equivalent extensional faulting, the correlation of stratigraphy and tectonostratigraphic zones, and transport direction. In this paper I address some of these in an attempt to summarize the geology of the Pakistan Himalaya.

It must first be pointed out that the geology is not perfectly continuous across Pakistan. There is a discontinuity located along the western margin of the Hazara syntaxis. It was shown as a major fault by Wadia (1931) who bent it northeastward and extended it all the way to the Kohistan arc. Part of this fault was mapped by Bossart et al. (1986) as the 'mylonite zone.' Later workers ignored Wadia's interpretation and, within about 5 km of the Kohistan arc, bent the fault eastward to connect with the Batal thrust, referring to its entire trace as the MCT. DiPietro and Pogue (2004) argued in support of Wadia's interpretation and referred to it as the Jhelum-Balakot fault. This fault effectively divides the Pakistan Himalaya into an eastern half (the Naran region), and a western half (the Western Hinterland) (Figure 1).

All known occurrences of eclogite are in the Naran region on the upper plate of the Batal thrust. According to DiPietro and Pogue (2004), the Batal thrust is truncated at the Jhelum-Balakot fault, offset southward, and reappears in the Western Hinterland as the Banna thrust which, itself, terminates against the Indus suture zone on the east side of the Indus Syntaxis. Irregardless of whether the Batal and Banna faults correlate, the relationships indicate that nearly the entire Western Hinterland is structurally below the Batal thrust. In the Naran region, the Batal thrust is interpreted as extending eastward into the mountains and metamorphic rocks south of Nanga Parbat. This is not the MCT.

An important distinction must also be made between thrust faults that underlie the Indus Suture Zone, and the Kohistan fault which underlies the Kohistan arc. Foliation in graphic schists at the top of the Indian plate are continuous with chlorite and talc schists that form the matrix rock in the Indus Suture Zone. Additionally, the suture zone is folded about late-metamorphic F3 folds. This implies that Indian plate rocks were underthrust beneath the suture zone prior to and/or during regional foliation-forming metamorphism. The Kohistan fault, by contrast, truncates foliation in both the suture zone and Indian plate and truncates the late-metamorphic F3 folds that deform the suture zone. The fault cuts across strike such that suture zone rock is absent in the Indus Syntaxis region and in the area north of the Malakand fault slice. The assumption that there was simultaneous transport and emplacement of the Indus Suture Zone and the Kohistan arc is incorrect. Thrusting of Kohistan played no role in the prograde metamorphism of the Western Hinterland.

The only major thrust faults in the Western Hinterland are the Banna thrust in the east, and the Malakand thrust in the west. Both are syn-metamorphic and both are folded by late-metamorphic F3 folds. They appear to have been active during activity in the suture zone. Significant shortening may have been accommodated along these thrust faults but neither extend across the hinterland. Both truncate against the suture zone or Kohistan fault. The remainder of the Western Hinterland appears to have acted as a single coherent block throughout metamorphism that remained largely autochthonous prior to middle Miocene displacement along the Panjal-Khairabad thrust. This is indicated by Permian and Mesozoic stratigraphic rock units that can be traced continuously across the hinterland. Wadia (1934) mapped what he referred to as a Paleozoic unconformity below Permian Panjal Volcanics in the region surrounding the Kashmir Basin. He showed that the age of rocks directly below the unconformity vary considerably from middle Paleozoic to what are probably Lower Proterozoic. Wadia implicitly showed that the Kashmir region contains a coherent stratigraphy of (probable) Early Proterozoic age to Mesozoic age that would later correlate with parts of the Lesser Himalayan, Greater Himalayan, and Tethyan Himalayan sequence. This stratigraphy is likely present in the Naran and Nanga Parbat regions and is unquestionably present in the Western Hinterland. Intrusive rock, such as Lesser Himalayan, Ulleri-equivalent, Kotla orthogneiss, and Greater Himalayan 500 Ma orthogneiss, are also present. The Panjal-Khairabad thrust forms the southern boundary of the Western Hinterland and is considered to be the western continuation of the MCT. Greater Himalayan stratigraphy, and 500 Ma orthogneiss, are both absent south of the thrust. This fault, however, is post-metamorphic, appears to have initiated later than the Central Himalayan MCT and does not show nearly the displacement.

It has been assumed that transport of both the Indus Suture Zone and the Kohistan arc was in a southward direction presumably because both are oriented roughly east-west, faulting in the Pakistan foreland is toward the south, and the most obvious lineations within the western Hinterland are oriented generally north-south. Detailed analysis does not support this conclusion. The most widespread lineation is a north-south crenulation of the regional foliation associated with late-metamorphic F3 folds. These folds deform the suture zone and are truncated by the Kohistan fault. They are not valid indicators of transport direction for either tectonic terrane. South-directed thrusting in the foreland also is not relevant because it is younger than displacement on the Kohistan fault. Syn-metamorphic transport of the Indus Suture zone and Banna thrust zone is inferred to be toward the SW or WSW based on westward vergence of large-scale syn-metamorphic F1/F2 folds and on stretching lineations which, although variable, are dominantly oriented NNE-SSW. The Kohistan arc was transported in a different

direction. Kinematic indicators along the fault consistently show thrust and dextral strike-slip displacement with ESE to E-directed transport. This is consistent with the Naran region where early SW-transport and then SE-transport is also reported (Greco et al. 1989). The southern termination of the Kohistan fault in the western part of the hinterland is interpreted to be a right-slip sidewall ramp such that the Kohistan arc never advanced much farther south on the Indian plate than its present position. This fault likely remained active until late Oligocene or early Miocene when south vergence first began in the hinterland. Although active in the foreland since middle Miocene, south vergence presently is not active in the hinterland. The 2005 Kashmir earthquake revealed the Bagh blind fault with southward transport that cuts across all earlier structures.

The Kohistan fault has been interpreted as a major extensional fault equivalent with the STDS even though it is located north of the Indus Suture Zone (not within the Indian plate). The evidence, however, is not convincing. Detailed analysis of the fault zone at three locations in the Western Hinterland provides evidence that long-term and final displacement was in the form of thrusting or dextral strike-slip faulting. The Kohistan fault in the Naran and Nanga Parbat regions has been overprinted by the Balakot, Diamir, and Raikot fault zones. All three faults are north to northwest-striking with southeast or east-side-up reverse displacement that places Indian plate rocks structurally above the Kohistan arc. None appear to be extensional.

The age of metamorphism in the Western Hinterland is poorly constrained. Flat hornblende Ar-Ar spectra vary from 67 to 31 Ma with additional dates circa 175 Ma and 1900 Ma (Treloar and Rex 1990). Zircons from the post-metamorphic Malakand granite recently gave a well defined LA-ICPMS age of 32.7 ± 0.5 Ma (unpublished data). Smith et al. (1994) reported a zircon rim SHRIMP age of 47 ± 3 Ma from the same granite. The disparate ages, and the description that their rock is deformed, suggests that Smith et al. (1994) may have dated a metamorphic overgrowth from the nearby Chakdarra orthogneiss. Zircons from another post-metamorphic intrusion, the Khar Diorite, gave a well defined LA-ICPMS age of 48.1 ± 0.8 Ma (unpublished data). This rock intrudes the suture zone (not the Indian plate) near Afghanistan at the structural top of the metamorphic pile. Collectively, the Western Hinterland has yielded detrital zircons from circa 2200 to 2930 Ma; igneous zircons circa 1850, 825, 500, 270, 48 (within the suture zone), and 33 Ma; metamorphic

zircons circa 2175, 262, and 89 Ma; and possible metamorphic zircon overgrowths circa 47 and 40 Ma (DiPietro and Isachsen 2001). These data suggest only that metamorphism was active during middle Eocene (49–37 Ma) and that there may have been multiple metamorphic episodes during late Mesozoic/Cenozoic and earlier. This is broadly consistent with ages obtained in the Naran region. More work is required to constrain the timing of metamorphism relative to fabric development.

In summary, the cause of metamorphism in the Western Hinterland is underthrusting beneath the Indus Suture Zone prior to, and/or during, the middle Eocene. The Kohistan arc arrived post-metamorphic, after development of F3 folds that deform the suture zone. Neither produced south-verging structures in the Western Hinterland. The Western Hinterland consists of conformable Lesser, Greater, and Tethyan stratigraphy that, with the exception of the Banna and Malakand thrusts, remained coherent throughout deformation.

References

Bossart P, D Dietrich, A Greco, R Ottiger and JG Ramsay. 1988. The tectonic structure of the Hazara-Kashmir syntaxis, Southern Himalayas, Pakistan. *Tectonics* 7: 273-297

DiPietro JA and CE Isachsen. 2001. U-Pb zircon ages from the Indian Plate in northwest Pakistan and their significance to Himalayan and pre-Himalayan geologic history. *Tectonics* 20: 510-525

DiPietro JA and KR Pogue. 2004. Tectonostratigraphic subdivisions of the Himalaya: A view from the west. *Tectonics* 23: TC5001 doi:10.1029/2003TC001554 20

Greco A, G Martinotti, K Papritz, JG Ramsay and R Rey. 1989. The crystalline rocks of the Kaghan Valley (NE-Pakistan). *Eclogae Geologicae Helveticae* 82: 629-653

Smith HA, CP Chamberlain and PK Zeitler. 1994. Timing and duration of Himalayan metamorphism within the Indian plate, northwest Himalaya, Pakistan. *Journal of Geology* 102: 493-508

Treloar PJ and DC Rex. 1990. Cooling and uplift histories of the crystalline thrust stack of the Indian plate internal zones west of Nanga Parbat, Pakistan Himalaya. *Tectonophysics* 180: 323-349

Wadia DN. 1931. The syntaxis of the northwest Himalaya: Its rocks, tectonics and orogeny. *Records of the Geological Survey of India* 65: 189-220

Wadia DN. 1934. The Cambrian-Trias sequence of northwest Kashmir (parts of the Mazaffarabad and Baramula District). *Records of the Geological Survey of India* 68: 121-146

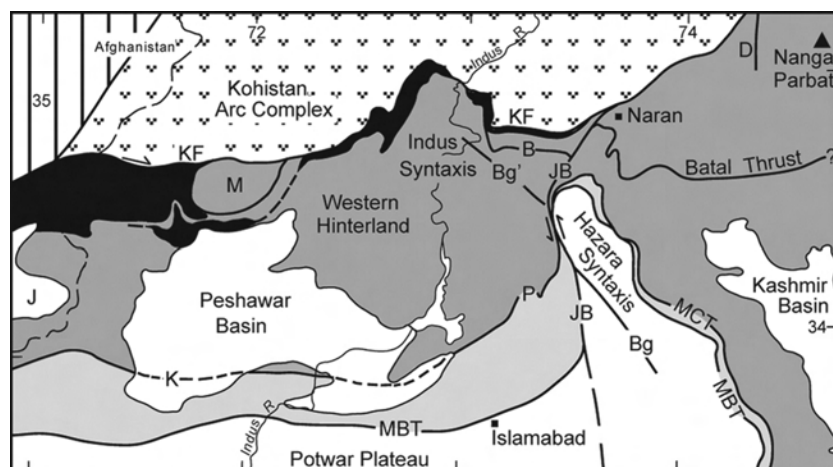


FIGURE 1. Simplified map of the Pakistan Himalaya. Black areas are lenses of suture zone rock. B-Banna Thrust; Bg-Bagh Fault; Bg'-Bagh Blind Fault; D-Diamir Fault; J-Jalalabad Basin; JB-Jhelum-Balakot Fault; K-Khairabad thrust; KF-Kohistan Fault; M-Malakand Fault Slice; MBT-Main Boundary Thrust; MCT-Main Central Thrust; P-Panjal thrust.

Active tectonics and origin of Tso Moriri Lake observed by Remote sensing and GIS techniques

Chandra Shekhar Dubey and Dericks Praise Shukla

University of Delhi, Delhi-1100 07, INDIA

Large-scale landscaping processes become strongly influenced by tectonic and geomorphological changes caused to a great degree, by the vertical morphotectonic and climatic zoning which gradually took place on the slopes of the rising mountain ranges. The development of the relief in the northern and central parts of these mountain ranges and near Tso-Moriri area the Tibet displays strong exhumation evidences of deep crustal material as well as the features of horizontal movements of the nappe type followed by tectono-geomorphic features of faulting with pronounced differential uplifts on faults, during the Quaternary.

The Tso Moriri lake is located between latitude $32^{\circ} 40' - 33^{\circ} 15' N$ and longitude $78^{\circ} 15' - 78^{\circ} 25' E$, which is about 220 km southeast of Leh in the northwestern Himalaya at an altitude of 4900 m and close to the ISZ (Figure 1).

In the present study, we have attempted to identify active faults, tilting of deposits and Neotectonic origin of Tso Moriri lake having a dimension of $3 \text{ km} \times 8 \text{ km}$ with the help of Remote sensing and GIS. The study also demonstrates that

geomorphological and structural inferences are possible using high resolution TERRA Satellite (ASTER) as well as 30 meter Landsat 7 ETM+ and pseudo Landsat covers of 1990 TM and 2000 ETM data for the arid, often inaccessible and complex terrain of the northwestern Himalaya (Figure 2).

The north-south transect passing near Tso Moriri Lake suggest that the SW-directed North Himalayan nappe stack (comprising the Mata, Tetraogal and Tso Moriri nappes) was emplaced and metamorphosed by c. 50–45 Ma, and exhumed to moderately shallow depths (c.10 km) by c. 45–40 Ma. From the mid-Eocene to the present, exhumation continued at a steady and slow rate except for the root zone of the Tso Moriri nappe, which cooled faster than the rest of the nappe stack (Schlup et al. 2003).

The Ladakh region of the northwestern Indian Himalaya is rich in quaternary deposits but it has not received much attention. The region was under the influence of tectonic activity and cold climate during the late Quaternary times. Tectonic activity at 50,000 years BP, 35,000 years BP and 25,000 years BP has been recorded (Phartiyal et al. 2005).

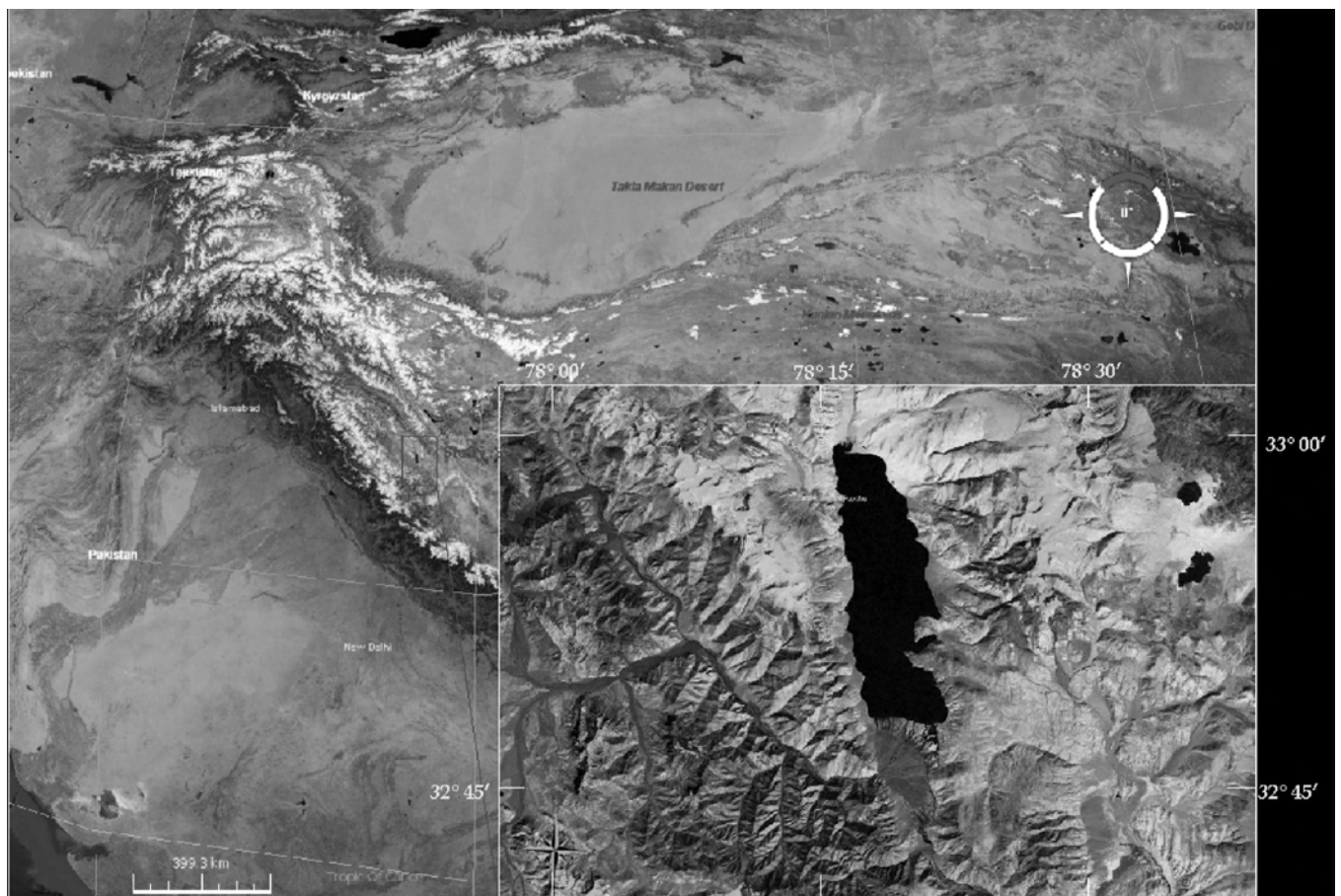


FIGURE 1. Location of the Area



FIGURE 2. Geology and Tectono-Geomorphology of the Area

This fact is corroborated by Aspect at 1° and Grain classification map derived from SRTM Digital Elevation Model (DEM) using MICRODEM software. Also medium sized recent earthquake activity lie linearly on the fault (source USGS database). It is important to note that most of the recent seismic activity is limited to south of the direction of flow of NW-SE trending river also changed from NNW-SSE to almost NE-SW feeding the Lake. This fault seems to be younger and active and hence has displaced the N-S trending Tso Morari fault (Figure 3).

The LANDSAT ETM 2000 and TM 1990 alongwith the Google earth and NASA world wind pseudo landsat covers depict the damming of the NW-SE trending River on N-S to NNW-SSE trending fault passing upto Kaurik, Leo and Sangla valley (Singh et al. 2007 and this study) and its tributaries by debris avalanches /deposits initiated mainly by tilting of fan due to tectonic

Activity along the WNW-ESE fault lineament. Another prominent feature of this fault is that it cuts the fan at the mouth of Tso Morari lake in such a way that the northern portion takes a concave shape while the southern portion takes a convex shape. The aspect and grain size classification marks the extent of the fault which is well corroborated by the microseismic events draped from google earth over the fault depicting neotectonic activity (Figure 4).

The Tso Morari lake in this region is formed in the late Quaternary due to the damming of the NW-SE trending River and its tributaries by debris avalanches/deposits initiated mainly by tilting of fan due to tectonic activity along the WNW-ESE fault lineament. The seismic activity on this fault is related to neotectonism.

References

Phartiyal B, A Anupam Sharma, R Upadhyay, Ram-Awatar and AK Sinha. 2005 Quaternary geology, tectonics and distribution of palaeo- and present fluvio/glacio lacustrine deposits in Ladakh, NW Indian Himalaya—a study based on field observations. *Geomorphology* 65 (3-4): 241-256

Schlup M, A Carter, M Cosca and A Steck. 2003. Exhumation history of eastern Ladakh revealed by 40Ar/39Ar and fission-track ages: the Indus River–Tso Morari transect, NW Himalaya. *Journal of the Geological Society of London* 160(1): 385-399

Singh S and AK Jain. 2007. Liquefaction and fluidization of lacustrine deposits from Lahaul-Spiti and Ladakh Himalaya: Geological evidences of palaeoseismicity along active fault zone *Sedimentary Geology* 196: 47-57

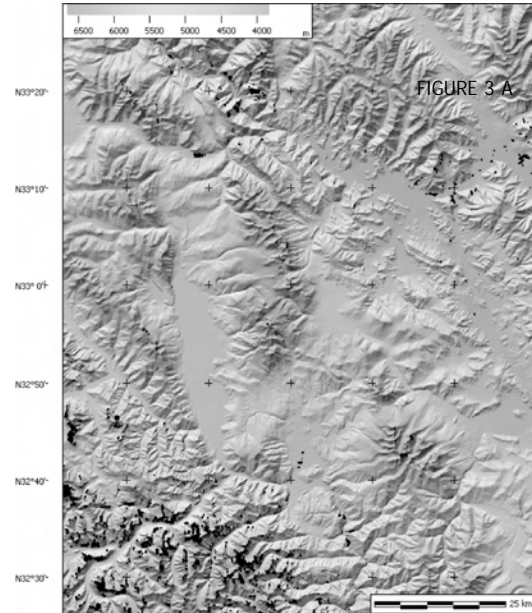


FIGURE 3. A) DEM of the Area B) Aspect at 10 of the area showing tilted Fan

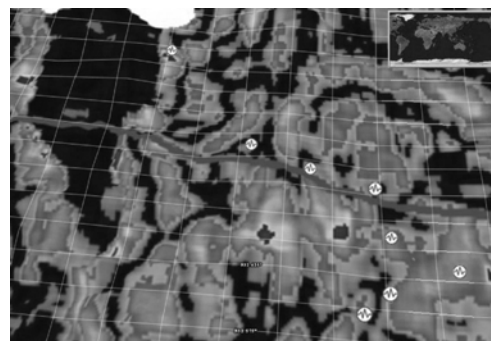


FIGURE 4. Grain size classification map and fault draped on Google showing microseismicity on the identified fault by remote sensed and GIS dataset.

Diagenetic and metamorphic overprint and deformation history of Permo-Triassic Tethyan sediments, SE Tibet

István Dunkl¹, Ding Lin², Chiara Montomoli³, Klaus Wemmer¹, Gerd Rantitsch⁴, Borja Antolin⁵, Rachida El Bay⁵ and Erwin Appel^{5*}

¹ University of Göttingen, GERMANY

² Institute of Tibetan Plateau Research, CAS, Beijing, CHINA

³ University of Pisa, ITALY

⁴ University of Leoben, AUSTRIA

⁵ University of Tübingen, GERMANY

* For correspondence, email: erwin.appel@uni-tuebingen.de

We have studied the deformation history and the grade and age of metamorphic overprint of the folded and imbricated Permo-Triassic limestone and flysch sequences of the Tethyan Himalaya in several strike-perpendicular profiles in SE Tibet in order to supply time and temperature constraints for a running paleomagnetic study and to describe the behaviour of the hanging wall of STDS.

The longest profile (ca. 40 km) runs from Tsetang to the SW and exposes mainly Triassic flysch. The deformation at the southern part is weak, big-scale, south-vergent isoclinal folds are characteristic foliation associated to folds is mainly a stilolitic surface with dominant pressure solution. At the northern part of the profile a second, top-to-north folding event generated a complex deformation pattern and locally intense neo-crystallization of illite-sericite, gives rise to a fine continuous foliation parallel to axial planes of folds. The applied methods were "illite crystallinity" (results are expressed as Kübler Index: KI), vitrinite reflectance (VR), K/Ar geochronology and microtectonic analyses. The appearance of the Tethyan sedimentary formations suggests a very wide range of overprint: in some sites fossils and sedimentary micromorphological elements are well preserved, while in other

tectonic blocks the formations experienced metamorphism in greenschist facies. The analytical results reflect well the variable overprint: VR ranges from 1.8% to the graphite stage, and KI ranges from 0.38 to 0.17°. The majority of K/Ar results is interpreted as mixed age, because the shift of apparent ages between 106 Ma and 24 Ma shows good correlation with decreasing KI. The most re-crystallized samples (KI ca. 0.17°) show no reaction after ethylen-glycol treatment and they have uniform K/Ar ages in the <2 μm and <0.2 μm grain size fractions around ca. 24 Ma. We suppose that these ages are close to the climax of the second, top-to-north folding event. Probably the structural block in the middle of the Tsetang profile showing the highest degree of metamorphism is structurally related to the Yalar Xiangbo dome.

Late orogenic large-scale deformations have been recorded in many areas of the Tethyan Himalaya by stable secondary magnetizations residing in pyrrhotite and postdating main Himalayan folding. In SE Tibet, however, a complex magnetic behaviour (noisy demagnetization, scattering remanence directions, very variable pyrrhotite content) is observed and paleomagnetic data have to be analyzed and interpreted with thorough selection criteria based on the thermal history and deformation style.

Impact of coeval tectonic and sedimentary-driven tectonics on the development of overpressure cells, on the sealing, and fluid migration –Petroleum potential and environmental risks of the Makran Accretionary Prism in Pakistan

N Ellouz-Zimmermann, A Battani, E Deville, A Prinzhofer and J Ferrand

IFP, Dir of Geology, 1-4 av de Bois-Préau, 92856 Rueil-Malmaison, cedex FRANCE

The tectonic evolution of the Makran accretionary prism is resulting from the continuous subduction to the North of the Arabian/Indian plates below the Eurasian blocks. Subduction processes started during Cretaceous time, and the tectonic accretionary prism developed progressively southeastward. The 3D evolution of the prism is not only controlled by tectonic processes (architecture of the slab, changes in orientation & speed of convergence), but also by the strong impact of the sedimentary parameters on the deformation style. Structural architecture results from the N-S shortening of the sediment deposited in the migrating trench, which are scrapped over an oceanic (to the west) and a stretched continental crust (to the East close to transform fault system). To understand the present-day 3D architecture and the localization of overpressure zones it is obvious that sedimentary origin and rates as well as the place where sediment deposited is a first order parameter.

Sedimentary supply

History of the sedimentation in the Pakistani Makran can be described in two large periods:

(1) Since Eocene times, the Makran trench was progressively filled by erosion products, which have been conveyed by the paleo-Indus River (from Himalayan erosion). The deltaic to deep-slope sediment progressively involved in the deformation, were coming successively from the deposition of the Himalayan detritics forming the Katawaz delta (Paleogene times), and the paleo-Indus delta (up to Middle-Miocene times).

(2) During Middle Miocene times, due to the re-organisation of the relief along the transform fault system, a drastic change occurred inducing the transfer of the Indus River East of the Kirthar-Sulaiman Ranges. From this time, the sedimentary detritics were produced by the erosion of the prism itself.

From this time, the deposition of the Himalayan-derived sediment has been transferred south of the Murray Ridge to the present-day position Indus delta.

Structural evolution

The complex tectonic style of the prism is characterized by: (1) a basal décollement level located within Paleogene or Cretaceous series, which deepens progressively from 6-8 km at the deformation front down to 11-12 km depth onshore; (2) an internal structure depending on several parameters: the lithology which is controlled by the regional and/or local depositional environment (determining the extension of secondary “décollement levels”); and the sedimentary loading which control the dynamics of the pressure conditions.

We infer that the deformation propagation is directly linked to the origin, rate and location of the sediment deposits, which has changed through times:

* during the 1st period, all the sedimentary input arrived from the Eastern back-side of the growing prism, and were deposited laterally along the trench.

* during the 2nd period, a large part of the sedimentation was directly transferred all along the Makran, from the northern Inner units (backside) to the south. Sediment series were, either trapped in small or large “piggy-back basins” (developed as a platform) on the frontal units, or supplied by a diffuse hydrographic net, through small rivers and canyons across the frontal units up to the abyssal plain.

Mud volcanoes and overpressure generation

Based on field data, re-processed seismic data, and new bathymetric and seismic data acquired in 2004 during the CHAMAK oceanographic survey, regional sections have been analyzed (Ellouz-Zimmermann *et al* 2007). A couple of local detachments have been observed above the late Cretaceous-Early Paleogene basal one. Close to the shelf area, the disharmonic late Miocene slope series can be considered as the uppermost detachment level, along with the compressive but also extensive deformation propagated, introducing a disconnection between surface and Middle Miocene structures.

The huge sedimentary loading superimposed to the regional shortening conditions, contributed to develop overpressure conditions within Late Miocene (Parkini fm) at depth. Linked with these deep pressure cells, fluid and mud mobilization have been recognized at surface. Onshore in the Coastal Range, a spectacular “belt” of active mud volcanoes outlined the episodic decompression processes, and expelled products, mud and fluids (i.e. water and gas) represent a “window” for the deep processes. Mud, and fluids (waters and gas) have been sampled and analyzed on several of these mud volcanoes, as well as in the core samples from the CHAMAK survey.

Analytical results

The origin of the mineral fraction of the mud expelled in the mud volcanoes has been attributed to the late Miocene series (from nannoplankton datings).

Geochemical analyses (including noble gas isotopes) of the gas sampled from three mud volcanoes and one gas seepage indicate a thermogenic signature, showing that source-rocks have generated gas at depth. Meanwhile, the other samples from coastal mud volcanoes show a bacterial signature, as well as offshore from

long cores (sampled with the Calypso of Marion Dufresne II on BSR). Spatial organization of the “thermogenic signature” mud volcanoes implies a connection with deeper levels than Parkini Fm, probably linked with fluid migration along major faults.

Thermal variation of the heat flow have been calculated over the frontal Makran zone, on the base of 1) of the geothermic gradient calculated on thermal T°C measurements sampled on the Chamak cores, 2) then calibrated on the present-day heat flow values with conductivity parameters from BGR measurements

and 3) finally along seismic profiles, interpolated with the largely recognizable BSR (Bottom-simulating-reflectors) modeling using the previously determined conductivity parameters.

Conclusion

Integrating the structural, sedimentological and geochemical new results, we propose a conceptual model of the architecture of the structural traps-reservoirs system and of the fluid migration mechanisms in the Pakistani Makran accretionary prism.

The Tso Morari Nappe of the Ladakh Himalaya: formation and exhumation

Jean-Luc Epard^{1*} and Albrecht Steck²

¹ *Institut of Geology and Paleontology, University of Lausanne, Anthropole, CH-1015 Lausanne, SWITZERLAND*

² *Institut of Mineralogy and Geochemistry, University of Lausanne, Anthropole, CH-1015 Lausanne, SWITZERLAND*

* *For correspondence, email: jean-luc.epard@unil.ch*

The Tso Morari Nappe is one of the North Himalayan nappes and is characterized by ultra-high pressure metamorphic rocks. It is composed of graywackes, slates, sandstones and dolomites of the Upper Haimantas and Karsha formations (Vendian-Cambrian). It includes also metabasites. The Tso Morari anatectic granite is dated at 479 Ma (Ordovician, Girard and Bussy 1999) and is intrusive in the Haimantas and Karsha formations. It contains basic dikes, perhaps in part cogenetic. The Tso Morari Nappe is characterized by high to ultra-high pressure metamorphic paragenesis (de Sigoyer et al. 1997, Mukherjee and Sachan 2001) dated at 53 Ma (Leech et al. 2005). Eclogites are absent of the surrounding units. Static eclogite facies crystallization preserves folded boudins of metabasites in the Tso Morari granite. These structures predate the HP metamorphism and can be interpreted as deformation of cogenetic dikes in relation with the Tso Morari granite intrusion. Only sparse deformational structures can be attributed to the ultra-high pressure event.

The main schistosity S1 is associated to an E-directed stretching lineation L1 with top-E shear indicators. In general, this is a strong deformation dominated by mylonitic structures. Strain is however heterogeneous and relatively large area of massive, non-deformed granite can be observed. This deformation is related to mineral assemblages of the amphibolite facies attesting a pressure drop and a temperature increase. It is interpreted as associated to the nappe extrusion. A younger deformation D2 is characterized by a N-S trending stretching lineation L2 with top-S shear indicators. This deformation is developed at the upper part of the Tso Morari nappe and can be found in the higher Tertaogal and Mata nappes. It has been observed also at the front of the North Himalayan nappes in the Lingti Valley (Epard and Steck 2004). It is interpreted as related to an early phase of north-directed underthrusting of the Tso Morari Nappe below the Tetraogal and Mata nappes. This is coherent with the early N movement of India below Asia (Patriat and Achache 1982). The D2 deformation is superimposed by the D3, L3 deformation with top-SW shear indicators. It is associated to the main phase of North Himalayan nappes emplacement and is a shared structure in the North Himalayan nappe stack. Barrovian regional metamorphism is coeval to the extrusion of the Tso Morari Nappe and its incorporation into the North Himalayan nappe stack. It reaches amphibolite facies in most area of the Tso Nappe except the eastern part, close to the colder rocks of the Indus Suture Zone where it reaches only higher greenschist facies. This is due to a more rapid extrusion of this part of the nappe and is responsible

for the first warping of the Tso Morari Nappe (Schlup et al. 2003). This first warping has been emphasized by NE verging backfolding already described by Steck et al. (1998) and also by structures related to neotectonics. The superposition of these structures leads to the present day dome structure. These tectonic structures are compatible with a late, NW-SE striking dextral shear zone, parallel to the Indus Suture Zone. They consist in large E-W trending, en-echelon, open folds as well as N-S striking normal faults. Additional new structural and metamorphic data, as well as a compilation of the published data on the Tso Morari nappe can be found in Epard and Steck (2008).

References

- de Sigoyer J, S Guillot, J-M Lardeaux and G Mascle. 1997. Glaucofane-bearing eclogites in the Tso Morari dome (eastern Ladakh, NW Himalaya). *European Journal of Mineralogy* 9: 1073-1083
- Epard J-L and A Steck. 2004. The eastern prolongation of the Zaskar Shear Zone (Western Himalaya). *Eclogae Geologicae Helvetiae* 97: 193-212
- Epard J-L and A Steck. 2008. Structural development of the Tso Morari ultra-high pressure nappe of the Ladakh Himalaya. *Tectonophysics* : doi:10.1016/j.tecto.2007.11.050
- Girard M and F Bussy. 1999. Late Pan-African magmatism in the Himalaya: new geochronological and geochemical data from the Ordovician Tso Morari metagranites (Ladakh, NW India). *Schweizerische Mineralogische und Petrographische Mitteilungen* 79: 399-417
- Leech ML, S Singh, AK Jain, SL Klemperer and RM Manickavasagam. 2005. The onset of India-Asia continental collision: Early, steep subduction required by the timing of UHP metamorphism in the western Himalaya. *Earth and Planetary Science Letters* 234: 83-97
- Mukherjee BK and HK Sachan. 2001. Discovery of coesite from Indian Himalaya: A record of ultra-high pressure metamorphism in Indian Continental Crust. *Current Science* 81: 1358-1361
- Patriat P and J Achache. 1984. India-Eurasia collision chronology has implications for crustal shortening and driving mechanism of plates. *Nature* 311: 615-621
- Schlup M, A Carter, M Cosca and A Steck. 2003. Exhumation history of eastern Ladakh revealed by ⁴⁰Ar/³⁹Ar and fission track ages: The Indus river-Tso Morari transect, NW Himalaya. *Journal of the geological Society of London* 160: 385-399
- Steck A, J-L Epard, J-C Vannay, J Hunziker, M Girard, A Morard and M Robyr. 1998. Geological transect across the Tso Morari and Spiti areas: The nappe structures of the Tethys Himalaya. *Eclogae Geologicae Helvetiae* 91: 103-121

Implications of geochemical signatures in the Trans-Himalayan Lohit batholith, Arunachal Pradesh, India

TK Goswami

Department of Geology, JB College, Jorhat, Assam, INDIA

Email: taposgoswami@yahoo.com

The Trans Himalayan Lohit batholith studied both in the Lohit and Dibang valley gives an insight as far as the source characteristics of magma and the possible evolutionary trend. The batholith represents at least four phases of intrusion representing changing sources of magma generation. The early gabbro-quartz diorites are followed by trondhjemite and followed by intrusions of leucogranites towards the end phase. The aplite and the pegmatite dykes finally intruded all the earlier intrusive. The rocks are metaluminous and mostly calc-alkaline and a few early gabbros also show tholeiitic parentage. Gabbro-quartz diorites form a single group with the SiO_2 range from 40.34 to 59.64 %. Leucogranites show high values of Rb, Ba

and K_2O . Four samples of diorites and granodiorites have $^{87}\text{Sr}/^{86}\text{Sr}$ initial ratios from 0.7039 to 0.7061, suggesting the upper mantle could be the source of the granitoids. Two samples of leucogranite with high and very high $^{87}\text{Sr}/^{86}\text{Sr}$ initial ratios 0.7079 and 0.7144 indicate that they are the products of the melting of the crustal rocks. In the Walong area dextral shearing might be synchronous with the intrusion of the copious volume of the leucogranites into the earlier rocks. In the Dibang valley, leucogranites near Dumbuen invariably follow the right lateral shearing in the earlier intrusives. Leucogranite intrusion might be associated with the collision induced shearing towards the later stages in the thick continental crust.

Cretaceous - Tertiary carbonate platform evolution and the age of India – Asia collision along the Ladakh Himalaya (NW India)

Owen R Green^{1*}, Michael P Searle¹, Richard I Corfield² and Richard M Corfield^{1,3}

¹ Department of Earth Sciences, University of Oxford, Oxford OX1 3PR, UK

² BP Amoco Exploration, Farburn Industrial Estate, Dyce, Aberdeen AB21 7PB, UK

³ Department of Earth and Environmental Sciences, The Open University, Walton Hall, Milton Keynes, MK7 6AA, UK

* For correspondence, email: oweng@earth.ox.ac.uk

The India – Asia collision resulted in the formation and uplift of the Himalaya and enhanced uplift of the Tibetan plateau. The transition from marine to continental facies within the Indus – Yarlung Tsangpo suture zone and along the northern margin of the Indian plate provides the most accurate method of dating the closure of Tethys Ocean separating the Indian and Asian plates. The use of shallow water, carbonate platform-dwelling larger benthic foraminifera provides the means for defining 20 shallow benthic zones (SBZ) ranging from the base of the Paleocene up to the Eocene-Oligocene boundary (Serra-Kiel, et al. 1998), and is applied to Cretaceous-Tertiary rocks of the Ladakh Himalaya. Indirect methods of dating the collision such as palaeomagnetism (Zhu et al. 2005), dating the UHP metamorphism along the north margin of India (Leech et al. 2005), dating the youngest subduction-related granites along the southern margin of Asia (Weinberg and Dunlap 2000) or dating the post-orogenic Indus Molasse Group deposits within the suture zone (Aitchison et al. 2007), cannot provide such a precise or reliable age of collision. Ophiolite obduction onto the Indian passive margin occurred during the latest Cretaceous and pre-dated initial collision of the two continental plates (Corfield et al. 1999). Unconformities occur beneath the Late Maastrichtian Marpo Formation, and beneath the Danian Stumpata Formation on the shelf and beneath the Upper Paleocene Sumda Formation in the suture zone. Stratigraphic and structural data from the Indian plate continental margin in the Ladakh and Zaskar Himalaya, NW India, suggest that the final marine sediments were shallow marine limestones containing a diverse assemblage of larger benthic foraminifera (Figure 1) deposited during the planktonic zone P8/shallow benthic zone SBZ10, corresponding to the Cusian stage of the late Lower Eocene (Ypresian), 50.5 Ma. A regional unconformity across shelf and suture zone above these rocks marks the beginning of continental red-bed deposition (Chulungla and Nurla Formations). The age of the final marine sediments is similar in Waziristan (NW Pakistan) to the west, and the south Tibet region to the east, suggesting that there was no significant diachroneity along the Indus – Yarlung Tsangpo suture zone. South of the Himalaya in the Hazara syntaxis, Pakistan, the youngest marine sediments correspond to Nummulite bearing limestones of the shallow benthic zone SBZ10, and planktonic foraminifera P7 zone (52–51 Ma). The timing of closure of Neo-Tethys between India and Asia corresponds closely to the ending of subduction-related granodiorite - granite magmatism along the Ladakh – Gangdese batholith (southern, Andean-type margin of the Asian plate) and precedes the drastic slowing of the northward drift of India. Continental fluvial – deltaic red-beds unconformably overlie all marine sediments, both in the suture zone and along the north Indian plate margin.

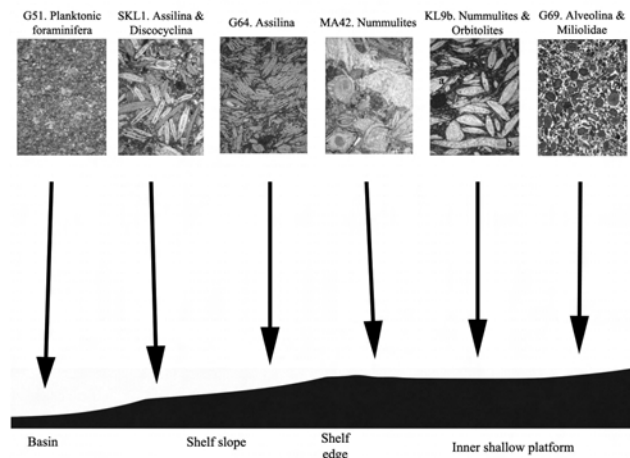


FIGURE 1. Diagrammatic reconstruction of the carbonate platform of the Cusian stage of the late Lower Eocene (Ypresian) illustrating the relative positions of the foraminiferal biofacies present along the Indian plate margin (Samples from exposures at: G = Gongma, KL = Kesi La, MA = Marling, SKL = Stumpata).

References

- Aitchison JC, JR Ali and AM Davis. 2007. When and where did India and Asia collide? *Journal of Geophysical Research* 112: doi: 10.1029/2006JB004706
- Corfield RI, MP Searle and OR Green. 1999. Photang thrust sheet: an accretionary complex structurally below the Spontang ophiolite constraining timing and tectonic environment of ophiolite obduction, Ladakh Himalaya, NW India. *Journal of the Geological Society, London* 156: 1031-1044
- Leech ML, S Singh, AK Jain, SL Klemperer and RM Manickavasagam. 2005. The onset of India-Asia continental collision: Early, steep subduction required by the timing of UHP metamorphism in the western Himalaya. *Earth and Planetary Science Letters* 234: 83-97
- Serra-Kiel J, L Hottinger, E. Caus, K Drobnec, C Ferrández, AK Jauhari, G Less, R Pavlovec, J Pignatti, JM Samso, H Schaub, E Sirel, A Strougo, Y Tambareau, J Tosquella and E Zakrevskaya. 1998. Larger foraminiferal biostratigraphy of the Tethyan Paleocene and Eocene. *Bulletin de la Societe géologique de France* 169: 281-299
- Weinberg RF and WJ Dunlap. 2000. Growth and deformation of the Ladakh Batholith, Northwest Himalayas; implications for timing of continental collision and origin of calc-alkaline batholiths. *Journal of Geology* 108: 303-320
- Zhu B, SF Kidd, DB Rowley, BS Currie and N Shafique. 2005. Age of initiation of the India-Asia collision in the East-Central Himalayas. *Journal of Geology* 113: 265-285

P-T evolution across the Main Central Thrust zone (Eastern Nepal): hidden discontinuities revealed by petrology

Chiara Groppo^{1*}, Franco Rolfo^{1,2} and Bruno Lombardo²

¹ Dipartimento di Scienze Mineralogiche e Petrologiche, University of Torino, ITALY

² Istituto di Geoscienze e Georisorse, CNR – Section of Torino, ITALY

* For correspondence, email: chiara.groppo@unito.it; franco.rolfo@unito.it

Identifying the location and nature of the Main Central Thrust Zone (MCTZ) is a major challenge in most of the Himalayan chain. As a contribution to clarifying this geopuzzle, a number of metapelite samples were selected for petrologic studies along a transect on the eastern flank of the “Arun Tectonic Window” (Bordet 1961) in eastern Nepal. The results provide information on the distribution of the Lesser Himalaya and MCTZ in a relatively poorly known area.

Both to the west and east of the study area, the classical Makalu and Kangchendzonga transects (Brunel and Kienast 1986, Lombardo et al. 1993, Meier and Hiltner 1993, Pognante and Benna 1993, Goscombe and Hand 2000, Goscombe et al. 2006) show metamorphic units characterized by a well-documented inverted metamorphism, with a general increase of metamorphic grade northward from lower (Lesser Himalaya) to higher (Higher Himalaya Crystallines – HHC) structural levels across the MCTZ (e.g. Le Fort 1975, Arita 1983, Valdiya 1983, Hodges et al. 1998, Inger and Harris 1992, Vannay and Hodges 1996).

Metamorphic assemblages in the studied metapelites range from the low-grade chlorite zone (Chl+Wm+Qtz+Pl±Ctd±Mn-rich Grt), to the medium-grade staurolite (Wm+Bt+Grt+St) and kyanite (Wm+Bt+Grt+St+Ky) zones, up to the sillimanite zone (Wm+Bt+Grt+Sil+Pl±St±Ky) and a further zone of partial melting with the appearance of K-feldspar and the breakdown of white mica. The P-T evolution of 5 metapelite samples collected at different structural levels has been reconstructed in detail using the modern petrological approach of P-T pseudosections, and considering the possible chemical fractionation of the bulk rock composition due to the presence of zoned porphyroblasts (e.g., garnet).

The resulting P-T paths may be grouped in three different families:

(i) the structurally lower Lesser Himalayan samples show a prograde P-T path characterized by an increase in both P and T, up to peak metamorphic conditions of 550°C and 0.65 GPa;

(ii) two structurally intermediate samples preserve relics of a prograde history characterized by heating and decompression from 550°C, 1.0 GPa to 620°C, 0.8 GPa and from 570°C, 1.1 GPa to 650°C, 0.9 GPa, respectively, showing a similar exhumation history characterized by cooling and decompression along the same metamorphic gradient;

(iii) the structurally higher samples consist of mostly unzoned minerals and well equilibrated assemblages that do not preserve relics of their prograde metamorphic history. Peak metamorphic T and P of these two samples are higher than the structurally lower MCTZ samples: 650°C, 0.7 GPa, but still inside the white mica stability field, and ~ 780°C, 1.0 GPa, beyond the stability limit of white mica and in the melt-bearing field.

The different P-T paths inferred for the studied metapelites suggest the presence of important metamorphic discontinuities that are not structurally evident in the field because the regional metamorphic fabric mainly developed

during late deformation events. The first discontinuity found may correspond to the MCT in the classical sense of Heim and Gansser (1939) as it juxtaposes the medium-grade metamorphic units of the MCTZ, characterized by a clockwise P-T path with heating during decompression followed by cooling and decompression, over the Lesser Himalaya sequence, which only preserves prograde metamorphism characterised by an increase in both P and T. A second discontinuity, at a higher structural level, separates units of the MCTZ from overlying metapelites that were metamorphosed at higher T and relatively lower P.

References

- Arita K. 1983. Origin of the inverted metamorphism of the Lower Himalayas, Central Nepal. *Tectonophysics* 93: 43–60
- Bordet P. 1961. *Recherches géologiques dans l'Himalaya du Népal, région du Makalu*. Paris: Editions du Centre National de la Recherche Scientifique. 275 p
- Brunel M and JR Kienast. 1986. Etude pétro-structurale des chevauchements ductiles himalayens sur la transversale de l'Everest-Makalu (Népal oriental). *Canadian Journal of Earth Sciences* 23: 1117–1137
- Goscombe B and M Hand. 2000. Contrasting P-T paths in the Eastern Himalaya, Nepal: inverted isograds in a paired metamorphic mountain belt. *Journal of Petrology* 41: 1673–1719
- Goscombe B, D Gray and M Hand. 2006. Crustal architecture of the Himalayan metamorphic front in eastern Nepal. *Gondwana Research* 10: 232–255
- Heim A and A Gansser. 1939. Central Himalaya: geological observations of the Swiss expedition 1936. *Memoir Society Helvetica Science Nature* 73: 1–245
- Hodges KV, S Bowering, K Davidek, D Hawkins and M Krol. 1998. Evidence for rapid displacement on Himalayan normal faults and the importance of tectonic denudation in the evolution of mountain ranges. *Geology* 26: 483–486
- Inger S and NBW Harris. 1992. Tectonothermal evolution of the High Himalaya: geochemical and sedimentological evidence. *Geology* 10: 439–452
- Le Fort P. 1975. Himalayas: the collided range. Present knowledge of the continental arc. *American Journal of Science* 275: 1–44
- Lombardo B, P Pertusati and A Borghi. 1993. Geology and tectono-magmatic evolution of the eastern Himalaya along the Chomolungma-Makalu transect. *Geological Society of London, Special Publication* 74: 341–355
- Meier K and E Hiltner. 1993. Deformation and metamorphism within the Main Central Thrust zone, Arun tectonic Window, eastern Nepal. *Geological Society of London, Special Publication* 74: 511–523
- Pognante U and P Benna. 1993. Metamorphic zonation, migmatization, and leucogranites along the Everest transect (Eastern Nepal and Tibet): record of an exhumation history. *Geological Society of London, Special Publication* 74: 323–340
- Valdiya KS. 1983. Tectonic setting of Himalayan granites. In: Shams FA (ed), *Granites of Himalayas Karakorum and Hindu Kush*, Lahore Punjab University, 39–53
- Vannay JC and KV Hodges. 1996. Tectonometamorphic evolution of the Himalayan metamorphic core between the Annapurna and Dhaulagiri, central Nepal. *Journal of Metamorphic Geology* 14: 635–656

Kyanite-bearing anatectic metapelites from the Eastern Himalayan Syntaxis, Eastern Tibet, China : textural evidence for partial melting and phase equilibria modeling

Carl Guilmette^{1*}, Indares Aphrodite², Hébert Réjean¹ and CS Wang³

¹ Département de Géologie et de Génie Géologique de l'Université Laval, Québec, QC, CANADA, G1K7P4

² Earth Sciences Department, Memorial University of Newfoundland, St-John's, NL, CANADA, A1C5S7

³ School of Earth Sciences and Mineral Resources, China University of Geosciences, Xueyuan Road #29, Beijing, PEOPLE'S REPUBLIC OF CHINA

* For correspondence, email: carl.guilmette.1@ulaval.ca

The Eastern Himalayan Syntaxis (EHS), or Namche Barwa antiform, Tibet, China, marks the eastern termination of the Himalayan Range. In the EHS, the overall E-W trending India-derived Higher Himalayan Crystallines are bent in a N-S orientation and are actively indenting and exhuming into and from underneath the Asian-derived rocks of the Lhasa terrane, strongly altering the otherwise linear trend of the Yarlung Zangbo Suture Zone (YZSZ). As reflected by its tormented landscape, the EHS is characterized by extreme denudation and exhumation rates. Up to now, no consensus has been made on the metamorphic history of the metamorphic core of the EHS, and the mechanisms that drove its burial and exhumation are still strongly debated.

In the core of the EHS, rare kyanite-bearing anatectic paragneisses locally occur as boudins within sillimanite-bearing paragneisses. Worldwide, kyanite-bearing anatectic rocks are seldom found and such an occurrence within a young and active orogenic belt provides both an excellent opportunity to study partial-melting of aluminous paragneisses in the kyanite stability-field and a unique insight into the evolution of the Himalayan range and Tibetan Plateau.

Previous studies described kyanite-bearing boudins found at the foot of the Namche Barwa massif, near the locality of Zhibai (Liu and Jhong 1997 and references therein, Burg et al. 1998), in the core of the EHS. These rocks consist of an early HP-granulite assemblage (garnet-kyanite-biotite-quartz-plagioclase-K-feldspar-rutile) variably overprinted by a late high temperature but lower pressure assemblage including sillimanite pseudomorphs after kyanite cordierite-spinel coronas after sillimanite and orthopyroxene coronas after garnet. These studies outlined the unique character of these rocks and tentatively estimated P-T conditions for peak and retrograde metamorphism. However, partial melting was not taken into account, leading to much controversy on the peak conditions (amphibolite vs HP-granulite facies) and therefore on the maximum depth of burial.

In the present study, we describe kyanite-bearing anatectic paragneisses from the NW side of the Yarlung Zangbo River, in the western rim of the EHS. These rocks were found at the eastern end of an E-W cross-section that in an eastward direction crosses granitic batholiths of the Lhasa terrane, metamorphosed and deformed units of the YZSZ and a metasedimentary sequence. This sequence is characterized by an eastward increasing metamorphic grade going from 2-micas garnet schists through garnet-kyanite-staurolite gneisses and sillimanite-bearing gneisses to kyanite-bearing anatectic gneisses. At the outcrop scale, the kyanite-bearing rocks occur in the same setting as the boudins described in the inner core. However, they lack the late lower-P

high-T overprint, being devoid of corona assemblages.

In this contribution, we present textural evidences for partial-melting of these rocks in the kyanite stability field supported by phase equilibria modelling with THERMOCALC. The studied rocks have broadly pelitic to semi-pelitic compositions and are characterised by the assemblage garnet-kyanite (\pm sillimanite)-biotite-quartz-plagioclase-K-feldspar \pm rutile/ilmenite with sillimanite locally occurring as pseudomorphs after kyanite. Although the rocks are strongly deformed, melt related textures are locally preserved in the matrix as (1) fine grained feldspar-rich domains corroding relict coarser grained quartz ribbons and (2) films and pockets of randomly oriented fine grained biotite and feldspars surrounding corroded kyanite. However, melt related textures are best preserved in polymineralic inclusions within garnet porphyroblasts, consisting of rounded quartz and/or skeletal biotite surrounded by optically continuous pools of feldspar, with crystalline garnet faces towards the inclusions. All the above textures are consistent with the continuous reaction biotite + kyanite + quartz \pm plagioclase = garnet + melt \pm K-feldspar (R1) which marks the entrance to the HP-granulite facies. In addition retrograde textures related to melt crystallization are observed in form of biotite-fibrolite aggregates locally corroding garnet rims and suggesting that the melt solidified in the sillimanite stability field.

Phase equilibria modelling in the NCKFMASHO system with THERMOCALC is in progress. Preliminary pseudosections built with the bulk compositions of one pelitic and one semi-pelitic sample show that for these rocks the biotite-kyanite-garnet-quartz-plagioclase-K-feldspar-liquid-rutile \pm ilmenite field in which reaction R1 operates, occurs within the P-T range of \sim 800-875°C and \sim 10-17 kbar. In addition these pseudosections show topologies that are consistent with substantial melt loss during prograde metamorphism. Preliminary minimum P-T estimates of \sim 13.5-14.5 kbar and \sim 830°C are inferred for the metamorphic peak based upon the the intersection of composition isopleths reflecting the grossular contents and XFe of homogeneous cores of garnet in the metapelitic sample. Subsequent solidification of melt in the sillimanite stability field implies strong post-peak decompression at high temperatures.

References

- Burg J-P, P Nievergelt, F Oberli, D Seward, P Davy, J-C Maurin, Z Diao and M Meier. 1998. The Namche Barwa syntaxis: Evidence for exhumation related to compressional crustal folding. *Journal of Asian Earth Sciences* 16: 239-252
- Liu Y and D Zhong. 1997. Petrology of high-pressure granulites from the eastern Himalayan syntaxis. *Journal of Metamorphic Geology* 15: 451-466

New occurrence of eclogitic continental rocks in NW Himalaya: The Stak massif in northern Pakistan

Stéphane Guillot,^{*1} Nicolas Riel¹, Kéiko Hattori², Serge Desgreniers³, Yann Rolland⁴, Jérémie Van Melle¹, Mohamad Latif⁵, Allah B Kausar⁵ and Arnaud Pêcher¹

¹ University of Grenoble, OSUG - CNRS, BP 53, 38041 Grenoble cedex 9, FRANCE

² University of Ottawa, Dept of Earth Sciences, Ottawa, Ontario, CANADA K1N 6N5

³ University of Ottawa, Dept of Physics, Ottawa, Ontario, CANADA K1N 6N5

⁴ University of Nice, Geosciences Azur – CNRS, 06108 Nice Cedex 02, FRANCE

⁵ Geological Survey of Pakistan– Northern Area, Plot N°. 84, H-8/1, Islamabad, PAKISTAN

* For correspondence, email: sguillot@ujf-grenoble.fr

Three occurrences of ultrahigh pressure (UHP) rocks have been recognized along the Himalayan belt. In southern Tibet, Yang et al. (2007) documented diamond- and coesite-bearing chromitites from the Loboosa ophiolite in the Indus-Tsangpo Suture zone (ITSZ). Coesite-bearing eclogites are reported in the Tso Morari and Kaghan massifs in NW Himalaya (O'Brien et al. 2001, Mukherjee et al. 2003 2005) in the ITSZ of the Main Mantle Thrust (MMT). The latter occurrences are the products of the subduction of the margin of the Indian continent between 57 and 44 Ma (Leech et al. 2005, Parrish et al. 2006, Guillot et al. 2008). We report a new occurrence of eclogitic rocks from the Stak area where pyroxenite boudins with a retrogressed eclogitic assemblage were described by Le Fort et al. in 1997. This massif east of the Nanga Parbat-Haramosh anticline consists of garnet-bearing orthogneisses, metasediments, and marbles intruded by dykes of boudinaged garnet-bearing metabasites. The metabasites have similar chemical composition as the basalts of the Panjal Traps and this association of the metabasites with metasediments suggest that the rocks represent the western margin of the Indian continent, similar to the UHP massifs at Kaghan (Chaudhry and Ghazanfar 1987) and Tso Morari (Guillot et al. 1997). The rocks in the Stak area have undergone at least two phases of folding. The youngest event is defined by NE oriented steep folds (up to 100m in size) with axial plane dipping $\sim 60^\circ$ towards the NW. Asymmetrical folds indicate the top verging to the SE, which is likely related to the exhumation of the Nanga Parbat-Haramosh block (Argles and Edwards 2002). The deformation of the MMT also affected the area, which resulted in alternating layers of weakly metamorphosed rocks of the Ladakh arc and strongly metamorphosed Indian continental rocks.

The Stak massif contains well preserved eclogitic assemblage; garnet (Pyr34), omphacite (Jd46), phengite, Ca carbonate (most likely aragonite). The presence of coesite is suspected because the peak metamorphic condition is in the stability field of coesite, greater than 2.7 GPa, based on the bulk and garnet compositions. Rims of garnet contain inclusions of phengite and dolomite, clinopyroxene (Jd24) and plagioclase (Ab80). Omphacite in the matrix is altered to a symplectitic mixture of Na-Ca clinopyroxene (Jd18) and albite, indicating that the retrogression under eclogitic conditions at

$\sim 1.8 \pm 0.1$ GPa and 650–700°C. The late folding developed under amphibolitic facies conditions as marked by pargasitic amphibole, biotite and ilmenite and later the crystallization of hornblende. The assemblages indicate that the folding took place during a pressure decrease from 11 to 8 kbar and a temperature decrease from 700 to 600°C. Finally late localized millimetric shear bands defined by calcite and chlorite developed at the ductile-brittle transition under greenschist facies conditions.

A few Ar-Ar biotite ages have been obtained in this study, and the data suggest that the Stak massif was cooled below 350°C before 20–10 Ma, which corresponds to the exhumation of the Nanga Parbat Haramosh anticline (Zeitler et al. 2001). The Stak massif shares many features with the Kaghan massif including lithologies, location in the MMT and the mineral chemistry. The similarities suggest that the Stak-Kaghan massifs were possibly once a continuous UHP unit and later separated by the Plio-Miocene uplift of the Nanga Parbat Haramosh block. If this hypothesis is correct, the size of the Kaghan-Stak UHP massif (> 500 km²) is comparable to those of the Western Gneiss region of Norway and the Dabie-Sulu region in China. This will be tested by the data of our on-going studies including new micro-Raman spectrometry, SHRIMP ages of zircon and Ar-Ar ages of amphibole, biotite and white micas.

References

- Argles TW and MA Edwards. 2002. *Journal of Structural Geology* 24: 1327-1344
- Chaudhry MN and M Ghazanfar. 1987. *Geological Bulletin University of Punjab* 22: 13-57
- Guillot S et al. 1997. *Contribution to Mineralogy and Petrology* 128: 197-212
- Guillot S et al. 2008. *Tectonophysics*: doi:10.1016/j.tecto.2007.11.059
- Kaneko Y et al. 2003. *Journal of Metamorphic Geology* 21: 589-599
- Le Fort P et al. 1997. *Compte Rendus de l'Académie des Sciences, Paris* 325: 773-778
- Leech ML et al. 2005. *Earth and Planet Science Letters* 234: 83-97
- Mukherjee B et al. 2005. *Géologie Alpine* 44: 136
- Mukherjee B et al. 2003. *International Geology Review* 45: 49-69
- O'Brien P et al. 2001. *Geology* 29: 435-438
- Parrish R et al. 2006. *Geology* 34: 989-992
- Yang JS et al. 2007. *Geology* 35: 875-878
- Zeitler PK et al. 2001. *Tectonics* 20: 712-728

Evolution of the Indian Monsoon System and Himalayan-Tibetan Plateau uplift during the Neogene

Anil K Gupta

Department of Geology and Geophysics, Indian Institute of Technology
Kharagpur – 721 302, INDIA
E-mail: anilg@gg.iitkgp.ernet.in

The Indian monsoon also known as the South Asian monsoon is an important feature of the climate system, marked by seasonal reversals in the wind direction with southwesterly winds in summer and northeasterly winds in winter. The summer monsoon plays an important role in global hydrological and carbon cycles, and affects climate and societies over a large part of Asia between 35°N and 10°S. The monsoon is the lifeline to the people of Asia as region's food production and water supply are largely dependent on the summer monsoon rains. Thus the Indian monsoon constitutes a critical resource for the region's largely agrarian economies.

Considerable efforts have been made toward high resolution (high density sampling of the marine cores) reconstruction of proxy records of monsoon that have helped in the understanding of monsoon evolution, its variability over various time scales, and forcing factors that drive the monsoon on orbital and sub-orbital time scales. However, there are still unresolved questions as to the timing of the advent of the modern monsoon and driving mechanisms of monsoon variability. The elevated heat source of the Himalayas and the Tibetan Plateau is of vital importance for the establishment and maintenance of the Indian summer monsoon circulation through mechanical and thermal factors.

But there are different propositions about the attainment of the critical elevation by the Himalayas and the Tibetan Plateau to drive the Indian monsoon, ranging from 35 to 7.5 Ma (Table 1). While the marine records indicate a major shift in the monsoon system between 9 and 8 Ma, the continental records suggest a range from 22 to 7.5 Ma during which time the monsoon may have evolved. The model studies, on the other hand, put the origin farther back in time at ~ 35 Ma. Recent study from China suggests a wet phase in the early Miocene and beginning of an arid phase (weakening of the summer monsoon) across 13-11 Ma (Hanchao et al. 2008). Thus to resolve these issues, a coordinated effort is required to analyze and compare high resolution records from marine cores from high sedimentation areas of the Arabian Sea and the Bay of Bengal as well as continental records of continuity.

References

- Gupta AK, RK Singh, E Thomas and S Joseph. 2004. Indian Ocean high-productivity Event (10-8 Ma): Linked to Global Cooling or to the Initiation of the Indian Monsoons? *Geology* 32: 753-756
- Hanchao J, J Ji and Z Ding. 2008. Cooling-driven climate change at 12-11 Ma: multiproxy records from a long fluviolacustrine sequence at Guyuan, Ningxia, China. *Palaeo3* In press

TABLE 1. Evidence and timing of the Himalayan Uplift and Monsoon Intensification (Modified from Gupta et al. 2004)

SOURCE	TYPE OF EVIDENCE	EVENT	TIMING (MA)
Rowley and Currie 2006	Oxygen isotope	Tibetan Plateau	35
Ramstein et al. 1997	Modeling	Monsoons and Paratethys retreat	~30
Guo et al. 2002	China loess deposits	Monsoon climate	22
Wang 1990	Sediments in China	Monsoons	20
Clift and Gaedicke 2002	Indus Fan sediments	Erosion and weathering	~16
Clift et al. 2002	South China Sea smectite mineral	Precipitation and monsoons	~15.5
Spicer et al. 2003	Fossil flora	Himalayan elevation and monsoons	>15
Coleman and Hodges 1995	Tectonics	Himalayan elevation	>14
Blisniuk et al. 2001	Tectonics	Himalayan uplift and monsoons	>14
Chen et al. 2003	Oceanic microfossils	Monsoons and upwelling	12-11
Dettman et al. 2001	Isotopes and land	Monsoons	~10.7
An et al. 2001	Land and marine sediments	Uplift and onset of monsoons	9-8
Kroon et al. 1991	Oceanic microfossils	Monsoons and upwelling	8.6
Filipelli 1997	Weathering and sediments	Monsoons	~8
Quade et al. 1989	Isotopes and flora	Monsoons	8-7.6

Structural and metamorphic equivalence across the LHS-HHCS contact, Sikkim Himalaya – indicator of post-deformation metamorphism or the wrong MCT?

Saibal Gupta* and Suman Mondal

*Department of Geology and Geophysics,
Indian Institute of Technology Kharagpur, Kharagpur – 721 302, INDIA*

* For correspondence, email: saiblgupta@yahoo.co.in

In the Sikkim Himalaya, the contact between the base of the Lingtse Gneiss (an augen gneiss body at the base of the Higher Himalayan Crystalline Sequence, HHCS) and the metapelitic schists of the Lesser Himalayan Sequence (LHS) has been considered to be the Main Central Thrust (MCT). The region is characterized by an inverted metamorphic sequence, with the index minerals chlorite to sillimanite appearing at progressively higher structural levels across the sequence. The study has been conducted along the North-Sikkim Highway (NH -31A), and focuses along the contact zone between HHCS and LHS. Structural studies reveal that the contact zone is a ductile shear zone (the MCT zone) dominated by a single penetrative fabric (S2) trending NW-SE and dipping northeast. This corresponds to a second deformation event that affected lithounits on either side of the contact. Since the intersection lineation between the earlier fabric in both units (S1) and S2 is identical, it is inferred that the earlier fabrics in the HHCS and LHS had similar disposition prior to D2 deformation. A third deformation event (D3) is recorded in the mica schists of the LHS, but this is confined to lower structural levels. The late S3 foliation related to this event cuts across the earlier S1 and S2 fabrics in the LHS. Microstructural relationships between the mineral

phases and deformation fabrics, and zoning characteristics of garnet indicate a progressive metamorphic history from the syn-D1 to post-D2 period. Peak metamorphic conditions in both the HHCS and the LHS were attained after D2 deformation, and there appears to be no significant difference in the estimated peak P-T (~ 7 Kb, 650°C) across the MCT zone. The pressures and temperatures have been estimated through both conventional thermobarometric techniques and THERMOCALC, and the interpretations cannot be attributed to flaws in the applied methodology, as suggested by some workers. Thus, the estimated conditions are considered to be realistic. The lack of any detectable difference in peak metamorphic conditions that followed D2 deformation in both units may indicate that the entire metamorphic development is independent of and unconnected to, movement along the MCT. Alternatively, it is possible that the observed shear zone does not correspond to the MCT at all, and that the MCT in this sector needs to be relocated. The latter possibility appears to be supported on structural grounds, since the structural orientation of pre-D2 fabrics in the HHCS and LHS are interpreted to be similar. A more comprehensive study is being undertaken across the sequence to confirm one or the other possibility.

Continental Relamination Drives Compositional and Physical-Property Changes in the Lower Crust

Bradley Hacker,* Peter B Kelemen and Mark D Behn

University of California, Santa Barbara, CA, 93109-9630, USA

* *For correspondence, email: hacker@geol.ucsb.edu*

A long-standing paradigm for the genesis and evolution of Earth's continental crust holds that the crust is andesitic and reached this composition in the 'subduction factory' by delamination or foundering of a dense, mafic or ultramafic component into the mantle from the base of initially basaltic arc crust. However, the range of suggested compositions for the lower crust and our incomplete understanding of subduction-zone processes render this paradigm non-unique. Recent discoveries from (ultra)high-pressure xenoliths and terranes, combined with re-evaluation of methods for inferring lower crustal compositions from seismic velocity data, show that "relamination" of buoyant, subducting continental crust may be an efficient means of altering the composition of the lower crust.

Ultrahigh-pressure terranes show that large areas (>60,000 km²) of continental crust are subducted to depths >100

km where they undergo heating to temperatures of 600–1000°C for periods of up to 20 Myr. Xenoliths from the Pamir show that subduction erosion can drag continental rocks to depths >90 km and temperatures of ~1200°C. In both settings, devolatilization and melting transform cold, hydrous, low-density crust into hot, less hydrous residues. Felsic and intermediate rocks attain densities similar to the middle–lower continental crust; buoyancy may drive such rocks to rise through the mantle to pond at the Moho or higher crust levels. The calculated seismic wavespeeds of such material are indistinguishable from the bulk lower crust. Both ultrahigh-pressure continental subduction and subduction erosion operate at rates of 1–1.5 km³/yr, such that over the lifetime of Earth either could have led to large-scale 'continental relamination', refining the composition and physical properties of the continental lower crust.

Comparison of regional geoelectric structure of Himalayan region

T Harinarayana and RS Sastry*

National Geophysical Research Institute, Hyderabad – 500007, INDIA

** For correspondence, email: sastry_r@rediffmail.com*

In order to understand the regional tectonics of the Himalayan region, a few geotranssects have been carried out along different transects in India and also in Nepal. The prominent among them are wide band magnetotelluric soundings along Panamik-Leh-Bara-la-chala, Una-Mandi, Siliguri-Gangtok-Lachung, Joshimath-Gaucher in India and also in Central Nepal.

These studies are carried out as a part of deep crustal investigations for better understanding of the seismotectonics of the region. Additionally, several other deep geoelectric studies are

carried out using wide band digital magnetotelluric investigations for geothermal exploration in Puga, Ladakh region, Tapovan-Vishnugad and Lohari-Nag-Pala regions in Uttaranchal, Kullu-Manali-Manikaran, Sutlej Spiti valley regions in Himachal Pradesh. The major geological features in the study region are Munciari, vaikrita thrust and other expressions of main central thrust. These geotrasects have shown anomalous conductive features at mid-lower crustal depths. This feature in relation to the regional tectonics and seismo tectonics of the regions is discussed.

Pre-collisional Crustal Structure Adjacent the Indus-Yalu Suture

T Mark Harrison^{1*}, Donald J Depaolo² and Amos B Aikman³

¹ *Institute of Geophysics and Planetary Physics, UCLA, Los Angeles, CA 90095, USA*

² *Earth and Space Science & LBL, University of California, Berkeley, CA 94720, USA*

³ *Research School of Earth Sciences, Australian National University, Canberra, ACT 0200, AUSTRALIA*

* *For correspondence, email: director@igpp.ucla.edu*

Understanding the evolution of the Indus-Yalu Suture (IYS) has significance well beyond its key role in recording events of the Indo-Asian collision. Although this continent-continent collision is likely just reaching middle age, the IYS is already largely bereft of ophiolitic rocks and the adjacent subduction complex is completely absent. This serves as a powerful cautionary example to those who see the apparent absence of ophiolites in Archean terranes as counterevidence of plate tectonics. Knowledge of the pre-collisional geometries of India and Asia is vital to assessing when collision began and how much convergence was accommodated by thickening, extrusion, or delamination. However, post-collisional thrusting and strike-slip faulting have transmogrified the suture zone to such an extent that little can be learned about syn-collisional crustal structure from its direct study. In light of these limitations, we have investigated rocks adjacent the IYS isotopically with a view to inferring crustal thickness through time. Nd isotopic data from K-T granitoids in a N-S traverse near Lhasa show a pronounced gradient in ϵ_{Nd} , with mantle-like values adjacent to the IYS ($+5$) and $\epsilon_{Nd} \approx -12$ at ~ 120 km north of the suture. This type of spatial gradient in ϵ_{Nd} is interpreted as reflecting decreasing mantle input/increasing crustal

assimilation due to progressively thickened crust (i.e., higher lower crustal temperatures enhance crustal assimilation). Using a calibrated crustal thermal model, we can then relate ϵ_{Nd} to crustal thickness. A test of this model may be possible using the recently calibrated zircon thermometer as crystallization temperature spectra and inheritance patterns are characteristic of specific assimilation scenarios. Our preliminary results suggest that the strong continentward gradient in assimilation is due to a gradually decreasing mantle magma flux and increasing crustal thickness; from ≤ 20 km adjacent the IYS to ≥ 50 km in the northern portion of the Gangdese Batholith where the granitoids are essentially 100% crustal melts. South of the suture, emplacement of the 44 ± 1 Ma Dala granites into highly deformed Tethyan Himalaya units indicates that significant crustal thickening had occurred there prior to 'hard collision'. However, no current model for evolution of the IYS yet explains why such magmas should appear south of the suture. The similarity of ϵ_{Nd} in the Dala granites and Lhasa terrane crustal melts is consistent with lower crustal flow southward across the IYS, but more likely reflects the origin of the Lhasa terrane and Tethyan Himalaya as adjacent blocks in the northern Gondwana Supercontinent.

Discovery of crustal xenolith-bearing Miocene post-collisional igneous rocks within the Yarlung Zangbo Suture Zone southern Tibet: Geodynamic implications

Réjean Hébert^{1*}, Lesage Guillaume¹, Bezard Rachel¹, Carl Guilmette¹, Émilie Bédard¹, Chengshan Wang², Thomas David Ullrich³ and Jaroslav Dostal⁴

¹ Département de géologie et de génie géologique, Université Laval, Québec, QC, G1K 7P4, CANADA

² Research Center for Tibetan Plateau Geology, China University of Geosciences, 29 Xueyuan Road, Haidian District, 100083 Beijing, CHINA

³ Department of Earth and Ocean Sciences, The University of British Columbia, Vancouver, BC, V6T 1Z4, CANADA

⁴ Department of Geology, Saint Mary's University, Halifax, NS, B3H 3C3, CANADA

* For correspondence, email: rejean.hebert@ggl.ulaval.ca

The Neo-Tethys Ocean has been consumed into north-dipping intra-oceanic and active margin subduction zones. Post-collisional potassic to ultrapotassic magmatism occurred between 11.8 and 17 Ma. No such magmatism was reported within the YZSZ. The purpose of this presentation is to document, for the first time, the 2006-2007 discovery of Miocene magmatic rocks within the YZSZ. A 12.9 Ma ultrapotassic dyke cutting through the Xigaze flysch and containing crustal xenoliths have been reported by Chan et al. (2007, HKTW22). The igneous rocks crop out in the Saga and Sangsang areas about 600 and 450 km west of Lhasa respectively. They consist of intrusions cutting through the ophiolitic upper mantle at Sangsang and the ophiolitic mélange and ophiolitic crust at Saga. The phenocrysts are made of amphibole and F-bearing biotite (Mg# 0.3-0.6; F up to 2.56 wt. %), phlogopite, K-feldspar (Or₈₅₋₆₁), plagioclase (An₇₇₋₄₀), garnet (Al₇₉₋₅₉Gr₅₋₂₆Sp₅₋₁₂Py₁₁₋₃), and pleonaste set in quartz-rich albite-oligoclase, apatite, and zircon fine-grained matrix. Partly resorbed xenocrysts of garnet (Al₆₇₋₇₄Gr₃₋₇Sp_{0.4-2}Py₂₈₋₁₉). The xenoliths contain various amounts of K-feldspar (Or₅₅₋₆₀), plagioclase An₅₋₅₇), brown and green biotite (Mg# 0.42-0.85), rare phlogopite, kyanite, garnet (Al₃₆₋₇₇Gr₂₁₋₉Sp₅₋₆Py₃₁₋₆), quartz, muscovite, corundum, rutile, pleonaste, ilmenite, magnetite, hematite, magnesiohastingsite, epidote. Plagioclase grains contain up to 0.2 wt. % BaO and 0.47 wt. % SrO. The mineral chemistry of the xenoliths suggest that the high-Al content could be related to partial melting extraction of migmatitic liquids and the ferromagnesian assemblage correspond to basaltic protolith.

The geochemical data reveal that the host rocks are trachyandesites and trachydacites. The range in composition is: 44,5-64,7 wt. % SiO₂, 15,3-18 wt. % Al₂O₃, 1,5-5,2 wt. %, MgO, 1,4-11,7 wt. %, CaO, 2,5-4,9 wt. % K₂O, and 3,1-5,6 wt. % Na₂O. The intrusive rocks belong to the shoshonitic clan in terms of K₂O vs Na₂O and K₂O vs SiO₂ relationships and to ultrapotassic in the CaO vs Al₂O₃ space but have K₂O/Na₂O < 2 (0.5-1.7). Trace elements show high contents in Ba (703-1288 ppm), Ce (48-137 ppm), La (up to 73 ppm), Rb (up to 201 ppm), Sr (262-1498 ppm), and Zr (148-230 ppm). The rocks show large variations in Ba/Nb (34-117), Rb/Ba (5-15), Sr/Y (20-105) but uniform Rb/Sr (0.14-0.18) and La/Ce (0.5-0.6). 143Nd/144Nd ratios vary from 0,512167 to 0,512439 and time corrected -9,01 to -3,71. Strongly fractionated Zr/Y ratios (11-18), high concentrations of LaPM (42-117), Cc_{PM} (21-75), Ti and other incompatible elements negative ϵ Nd, and their similarities to the average of the upper continental crust, suggest these rocks were largely derived from a continental source with possible lower crustal and lithospheric mantle components. They are likely derived from post-collisional partial melting of lower to middle crustal material underlying the YZSZ. 40Ar-39Ar geochronology on magmatic amphibole and biotite points to a Middle Miocene age, making them the youngest igneous rocks reported within the YZSZ. The presence of magma at depth south of the Gangdese belt by Miocene time could have an impact on further modeling of crustal thermal behaviour. The trachyandesites and trachydacites provide a unique window allowing a probe into the deep Indian crust underlying Tibet Plateau.

Constraints to the timing of India-Eurasia collision determined from the Indus Group: a reassessment

Alexandra L Henderson^{1*}, Yani Najman¹, Randall R Parrish², Andrew Carter³, Marcelle Boudagher-Fadel³, Gavin Foster⁴, Eduardo Garzanti⁵ and Sergio Andò⁵

¹ Department of Environmental Science, Lancaster University, Lancashire, UK

² NERC Isotope Geosciences Laboratory, British Geological Survey, Nottingham, UK

³ Department of Earth Sciences, University College London, University of London, UK

⁴ Department of Earth Sciences, Wills Memorial Building, University of Bristol, UK

⁵ Dipartimento di Scienze Geologiche e Geotecnologie, Università Milano-Bicocca, Milano, ITALY

* For correspondence, email: a.henderson@lancaster.ac.uk

The Indus Group is a Tertiary aged sequence composed of marine and terrestrial sedimentary rocks which were deposited in an evolving late-forearc to intermontane basin setting during the initial phases of Indian-Asian continental collision (Brookfield and Andrews-Speed 1984, Van Haver 1984, Searle et al. 1990, Sinclair and Jaffey 2001, Clift et al. 2002). For this reason, the Indus Group provides the earliest record of erosion from the Himalayas. Clift et al. (2002) have constrained the age of collision by determining the lowermost stratigraphic point in the Indus Group that contains detritus from both Indian and Asian plates, and also by identifying where the Asian plate derived Indus Group unconformably overlies Indian plate margin sediments. The Chogdo Formation, dated by an overlying limestone at older than 54.9 Ma (O. Green, unpublished data cited in Sinclair and Jaffey 2001) is identified by Clift et al. (2001), to be the oldest unit of the Indus Group to contain detritus from both the Indian and Asian plates, and to stratigraphically overlie Lamayuru Group Indian slope turbidites and Jurutze forearc basin rocks, thereby pinpointing the timing of continental collision to the Late Paleocene. However, despite its importance, these previous evaluations of the Indus Group have been hampered by poor stratigraphic knowledge and uncertain lateral correlations, largely due to the relatively complex deformation of the rocks and poor biostratigraphic control.

We use a combination of geological mapping, biostratigraphy, facies analysis, petrography, bulk rock geochemistry, and isotopic characterisation of single detrital grains to 1) create an accurate and more widely representative stratigraphy for the Indus Group, 2) determine the nature of the contacts which separate the overlying Indus Group from underlying Indian and Asian Plate formations and 3) determine the provenance of the Group, in particular the stratigraphic level within the Indus Group at which both Indian and Asian plate detrital minerals occur together, in order to constrain the time of collision and discover which geological terranes were exhumed and actively eroded during the early stages of the Himalayan orogeny. Our initial analyses indicate that the Chogdo Formation may not be as

widely occurring as previous interpretations have led to believe; partly due to obscured tectonic contacts and problems with lateral correlations along strike. Therefore certain formations which are currently identified as belonging to the Chogdo Formation may well be younger (<48.6 Ma; Wu et al. 2007) Indus Group formations. Reassessment of constraints to the timing of India-Asia collision as determined from the Chogdo Formation is required.

References

- Brookfield ME and CP Andrews-Speed. 1984. Sedimentology, petrography and tectonic significance of the shelf, flysch and molasse clastic deposits across the Indus suture zone, Ladakh, NW India. *Sedimentary Geology* 40: 249–286
- Clift PD, N Shimizu, GD Layne and J Blusztajn. 2001. Tracing patterns of erosion and drainage in the Paleogene Himalaya through ion probe Pb isotope analysis of detrital K-feldspars in the Indus Molasse, India. *Earth and Planetary Science Letters* 188: 475–491
- Clift PD, A Carter, M Krol and E Kirby. 2002 Constraints on India-Eurasia collision in the Arabian sea region taken from the Indus Group, Ladakh Himalaya, India. In: Clift PD, D Kroon, C Geadicke and J Craig (eds), *The Tectonic and Climatic Evolution of the Arabian Sea Region. Geological Society Special Publication* 195: 97–116
- Searle MP, KT Pickering and DJW Cooper. 1990. Restoration and evolution of the intermontane molasse basin, Ladakh Himalaya, India. *Tectonophysics* 174: 301–314
- Sinclair HD, and N Jaffey. 2001. Sedimentology of the Indus Group, Ladakh, northern India; implications for the timing of the initiation of the palaeo-Indus River. *Journal of the Geological Society of London* 158: 151–162
- Van Haver T. 1984. *Etude stratigraphique, sedimentologique et structurale d'un bassin d'avant arc: Exemple du bassin de l'Indus, Ladakh, Himalaya* [Ph.D dissertation]. Grenoble, France: Université de Grenoble:204 p
- Wu FU, PD Clift and JH Yang. 2007. Zircon Hf isotopic constraints on the sources of the Indus Molasse, Ladakh Himalaya, India. *Tectonics* 26: TC2014

Structure of the crust and the lithosphere in the Himalaya-Tibet region and implications on the rheology and eclogitization of the India plate

György Hetényi^{1+*}, Jérôme Vergne^{1x}, John L. Nábělek², Rodolphe Cattin¹, Fabrice Brunet¹, Laurent Bollinger³ and Michel Diament⁴

¹ *Laboratoire de Géologie, Ecole Normale Supérieure, CNRS – UMR 8538, 24 rue Lhomond, 5005 Paris, FRANCE*

² *College of Oceanic and Atmospheric Sciences, Oregon State University, Corvallis OR 97331, USA*

³ *Laboratoire de Détection et de Géophysique, CEA, BP12, 91680 Bruyères-le-Châtel, FRANCE*

⁴ *Institut de Physique du Globe de Paris, 4 place Jussieu, 75252 Paris, FRANCE*

⁺ *Present address: Institute of Geophysics and Tectonics, School of Earth and Environment, University of Leeds, Leeds, UK*

^x *Present address: Ecole et Observatoire des Sciences de la Terre, Strasbourg, FRANCE*

^{*} *For correspondence, email: hetenyi@geologie.ens.fr*

The Himalayas and the Tibetan Plateau are considered as the classical case of continental collision. The geophysical, geological and geochemical observations in this region as well as numerical modelling studies have been interpreted in the frame of different models of plateau formation, including continental subduction (Tapponnier et al. 2001, Haines et al. 2003), crustal thickening (England and Houseman 1986), and underplating (Argand 1924, Barazangi and Ni 1982, Owens and Zandt 1997). In the meantime, due to the uneven coverage and resolution of the data over the plateau, some fundamental questions concerning the evolution of the region's lithosphere are still pending. What are the main structural features of the collision zone? How do new constraints on structure influence our understanding of rheology? What are the physical processes which play a major role in the evolution of this system?

The “Himalayan-Tibetan Continental Lithosphere in Mountain Building” (Hi-CLIMB) project provides new data to bring answers to the questions on structure. This passive seismological experiment deployed a large number of broadband stations at 255 sites during three years. More than 150 closely spaced (4–9 km) stations form the main profile, spanning on 800 km along 85°E, across the Himalayas and the southern half of the Tibetan Plateau. The remaining sites were deployed more sparsely and allow to map lateral structural variations. The large amount of data (1.5 terabyte), the high-frequency receiver functions and the use of multiply converted waves result in a detailed image of lithospheric structures at all scales. Two of the main results are as follows:

(1) We observe shallow and localized low-velocity layers in the Tibetan crust. These features, previously referred to as “bright spots”, have a limited size both horizontally (~50 km) and vertically (~10 km). This, together with estimates of average crustal VP/VS-ratios between 1.7 and 1.8, does not support the presence of widespread partial melt. Moreover, the position of these low-velocity zones is strongly correlated to extensional grabens, which supports their localized occurrence, and suggests a rifting mechanism for their presence.

(2) Our images show underthrusting of the Indian lower crust beneath most of Lhasa block. The high resolution of the

images allow to clearly follow the Moho of the India plate: its geometry descends smoothly beneath the Himalayas, reaching a maximum depth of ~73 km b.s.l. at the Yarlung-Tsangpo suture, and then continues sub-horizontally for further ~200 km to the North. The underthrusting is identified by the appearance of a second interface ~15 km above the Moho, which is related to the top of the lower crust undergoing eclogite facies transformation (see below).

The conducted receiver function analyses also allow to:

(3) map faults at shallow (~3–4 km) depth in Nepal;

(4) follow the Main Himalayan Thrust from its shallow part to its deep and ductile continuation;

(5) trace the main lithospheric boundary between India and Eurasia at about the centre of the plateau (south of and beneath the Banggong-Nujiang suture);

(6) conclude that the main sutures at the surface have no pronounced signature at depth;

(7) show that the upper mantle discontinuities at 410 and 670 km do not seem to be affected by the ongoing orogeny

The obtained information on the geometry of the structures are then used to bring answers to the questions on rheology and major physical processes.

The improved image on the flexural shape beneath the foreland basin allows to re-assess the rheology of the India plate using thermo-mechanical modelling. This reveals that flexural and thermal weakening causes decoupling of the lithospheric layers, which results in a south-to-north decrease of the effective elastic thickness. To explain the support of the Tibetan Plateau's topography as well as regional isostasy in the Himalayas, a strong upper mantle is required (Hetényi et al. 2006).

The geometry of underplating is combined with density models to reproduce observed Bouguer anomaly data. These models shows that localized densification of the Indian lower crust is occurs where it reaches its maximal depth. This effect is associated to eclogitization. Using thermo-kinematic and petrological models, we investigate the thermal field and pressure-temperature-density relations assuming different hydration levels, respectively. The results suggest partial hydration of the Indian lower crust, and kinetical hindrance of its eclogitization compared

to phase equilibria. This overstepping is explained by the absence of free water in the system, and subsists until dehydration reactions occur at higher P-T conditions (Hetényi et al. 2007).

References

- Argand E. 1924. La tectonique de l'Asie. In: Congrès Géologique Internationale, Bruxelles, Compte rendus de la XIIIe session 1: 171–372
- Barazangi M and J Ni. 1982. Velocities and propagation characteristics of Pn and Sn beneath the Himalayan Arc and Tibetan plateau: possible evidence for underthrusting of Indian continental lithosphere beneath Tibet. *Geology* 10(4): 179–185
- England P and G Houseman. 1986. Finite strain calculations of continental deformation. 2: Comparison with the India-Asia collision zone. *Journal of Geophysical Research* 91(B3): 3664–3676
- Haines SS, SL Klemperer, L Brown, GR Jingru, J Mechie, R Meissner, A Ross and WJ Zhao. 2003. INDEPTH III seismic data: from surface observations to deep crustal processes in Tibet. *Tectonics* 22(1): 1001
- Hetényi G, R Cattin, J Vergne and JL Nábělek. 2006. The effective elastic thickness of the India Plate from receiver function imaging, gravity anomalies and thermomechanical modelling. *Geophysical Journal International* 167(3): 1106–1118
- Hetényi G, R Cattin, F Brunet, L Bollinger, J Vergne, JL Nábělek and M Diament. 2007. Density distribution of the India plate beneath the Tibetan Plateau: geophysical and petrological constraints on the kinetics of lower-crustal eclogitization. *Earth and Planetary Science Letters* 264(1-2): 226–244
- Owens TJ and G Zandt. 1997. Implications of crustal property variations for models of Tibetan plateau evolution. *Nature* 387(6628): 37–43
- Tapponnier P, ZQ Xu, F Roger, B Meyer, N Arnaud, G Wittlinger and JS Yang. 2001. Oblique stepwise rise and growth of the Tibet plateau. *Science* 294: 671–1677

Present-day E-W extension in the NW Himalaya (Himachal Pradesh, India)

Esther Hintersberger^{1*}, Rasmus Thiede², Manfred Strecker¹ and Frank Krüger¹

¹ Department of Geosciences, University of Potsdam, GERMANY

² Department of Geology, ETH Zurich, SWITZERLAND

* For correspondence, email: estherh@geo.uni-potsdam.de

During the evolution of most major orogens, both contemporaneously developed compressional and extensional structures have been documented. Thus, localized extension within an overall compressional setting seems to be a fundamental process for the evolution of orogens, however, their kinematic linkage is still debated. Since the Indian-Eurasian collision, the Himalayan mountain belt has formed as the southern termination of the Tibetan Plateau. While at present day, thrusting at lower elevations within the Lesser Himalaya is observed (Billham et al. 1997, Lavé and Avouac 2000), several generations of extensional structures have been detected in the high-elevation regions of the Higher Himalaya, both parallel and perpendicular to the strike of the orogen, which are the following: (1) The Southern Tibetan Detachment System (STDS), the most prominent example for orogen-perpendicular extension, was active during the Miocene (around 25 to 19 Ma, Burchfield et al. 1992) and potentially locally reactivated during the Quaternary (Hogdes et al. 2001, Hurtado et al. 2001). (2) Orogen-parallel extension is observed along roughly N-S striking normal faults and graben systems whose onset is mainly constraint to 15-12 Ma (e.g., Fort et al. 1982, Burchfield et al. 1991, Wu et al. 1998, Murphy et al. 2000, Hogdes et al., 2001, Garzzone et al. 2003, Thiede et al. 2006). Earthquake information (e.g., Pandey et al. 1999) and fault-plane solutions (Harvard catalog, Molnar and Lyon-Caen 1989) infer that they are recently active. To explain the kinematic linkage between extensional structures in an overall compressional setting, several models have been developed, the most important ones are: (a) radial extension (Molnar and Lyon-Caen 1989), (b) gravitational collapse (Molnar and Chen 1983, Royden and Burchfield 1987), (c) the partitioning of oblique convergence (McCaffrey 1996, McCaffrey and Nabelek 1998), and (d) arc-shaped, convex-southward propagation (Ratschbacher et al. 1994). Alternatively, local extension due to metamorphic dome formation has also been invoked (Aoya et al. 2005). However, the interpolated deformation patterns of these models are not consistent to focal mechanisms of larger earthquakes (Harvard Catalogs) and regional GPS measurements (Banerjee and Bürgmann 2002) in the Sutlej-Spiti River Valleys and the Garhwal in the NW Himalaya (India). These data sets reveal ongoing E-W extension in this area. In contrast to model predictions, however, this direction is neither parallel nor perpendicular to the NW-SE regional shortening direction. Therefore, currently available models of extensional faulting within the Himalaya apparently do not reconcile the observations in this part of the mountain range and alternative, less ambiguous mechanisms have to be involved.

Here we present new geological and geophysical data sets such as newly calculated earthquake fault-plane solutions, new structural geological mapping, fault kinematic analysis of hundreds of brittle faults, and satellite imagery analysis covering

the area between the Tso Morari Lake in the Tibetan Himalaya in the north and the mountain front in the Garhwal Himalaya in the south. The data sets that we obtained allow us to get a detailed overview of the extensional deformation history in this area and to try to reveal the underlying driving mechanism. In the following, we describe the data sets in detail.

We observed that globally recorded seismicity data is arranged in a narrow N-S striking swath ranging from the Tso Morari Lake in the Tibetan Himalaya almost to the mountain front in the Garhwal Himalaya (NEIC Catalog). Earthquake fault-plane solutions, however, are only available for the northern part of our study area extending between the Tso Morari Lake and the Spiti River Valley. Therefore, we used several medium-size earthquakes recorded during the last 20 years to determine new earthquake fault-plane solutions using a moment tensor inversion technique. All together, we now have an extended and detailed data set available reaching from the Lesser Himalaya in the south to the suture zone in the north and are able to provide much more detailed view into the recent deformation of the Himalayan wedge. All the new data suggest consistently recently ongoing E-W extension.

Furthermore, in the northern part of the study area, between the Spiti River Valley and the Tso Morari, we found new undescribed large N-S striking normal faults up to 10 km length separating basement rocks from sedimentary deposits. By analyzing high-resolution satellite imagery (LandSat, ASTER, GoogleEarth) we reveal that normal faults have played an integral role during the development of local sedimentary basins. In addition, we have observed structures such as steeply dipping, mainly N-S striking normal faults with displacements in the range of mm deforming fluvial fans and lake deposits in the Spiti River Valley. Inferring the age of these deposits to Quaternary, the normal faults document E-W extension during this time span. By compiling earlier published data (Anand and Jain 1987, Singh and Jain 2006), we were able to extend the record of sedimentary deposits affected by normal faulting further south into the thrust belts in the Garhwal Himalaya.

We have mapped extensional structures in the Garhwal Himalaya and the Sutlej River Valley and compiled them with structures already shown in geological maps (e.g., Steck et al. 1998, Neumayer et al. 2004, Thiede et al. 2006). We found large N-S striking normal faults with gouge zones up to 3 m in width which are observed mainly in a narrow band between 78° and 78.5° E. They are generally associated with steep slickensides indicating dip-slip faulting and E-W extension with limited offset. New-grown micas on the fault plane and within the fault gouge indicate that these faults have their origin in the brittle-ductile transition zone. However, we cannot be absolutely sure whether this limitation on such a small swath is really related to focused concentration of

deformation or this is only an artifact due the restricted accessibility in the field area. In addition, small brittle normal fault planes on outcrop scale with displacements up to several cm cover the whole region from Tibetan Himalaya down to the mountain front. These densely spaced, steeply to the W and E dipping structures crosscut all older structures related to the shortening in the mountain belt. To analyze fault kinematic data (strike and dip of the fault, slip direction and sense of slip) for these small fault planes, we determined approx. 30 pseudo fault-plane solutions using the program TectonicsFP (Ortner et al. 2002). The results indicate a regional E-W oriented extension arranged in a diffuse N-S trending swath, overlaying other deformation patterns, e.g., orogen-parallel and orogen-perpendicular extension along the lower-elevation parts of the study area. The consistency with fault-plane solutions derived from seismicity data shows that E-W extension in the area between the Tso Morari and the Garhwal Himalaya seems to be a long-lasting and consistent phenomenon.

Combining all these data sets reveals that there is ongoing extension in the Sutlej-Spiti River Valleys and the Garhwal Himalaya, which is aligned in an overall N-S striking zone. Our compilation of geological and geophysical data sets suggest that E-W extension spreads almost over the entire mountain range from the Tibetan Himalaya in the north to the thrust belt in the south and seems to be a long-lasting phenomenon rather than a localized disturbance in the regional deformation pattern. Crosscutting relationships indicate that this extensional deformation phase here is younger than the extensional deformation phases described at the beginning. Furthermore, this extensional direction is neither parallel nor perpendicular to the regional shortening direction. Therefore, models explaining orogen-parallel or orogen-perpendicular extension are not able to explain the observed extension. We derive a model that proposes a southward propagation of the E-W extension from the Tibetan Plateau into the Himalayan mountain range. In this model, the Karakorum fault, a large strike-slip fault separating the Himalaya and the Tibetan Plateau, would not be able to accommodate the whole E-W extensional deformation in the Tibetan Plateau. Therefore, a part of this extension would be compensated in N-S striking normal faulting in the NW Himalaya, where our study area is located.

References

- Anand A and AK Jain. 1987. Earthquakes and deformational structures (seismites) in Holocene sediments from the Himalayan-Andaman Arc, India. *Tectonophysics* 133: 105-120
- Aoya M, S Wallis, K Terada, J Lee, T Kawakami, Y Wang, and M Heizler. 2005. North-South extension in the Tibetan crust triggered by granite emplacement. *Geology* 33(11): 853-856
- Banerjee P and R Bürgmann. 2002. Convergence across the Northwest Himalaya from GPS Measurements. *Geophysical Research Letters* 29(13): doi: 10.1029/2002GL015184.
- Bilham R, K Larson, J Freymueller and Project Idylhim Members. 1997. GPS measurements of present-day convergence across the Nepal Himalaya. *Nature* 386: 61-64
- Burchfiel BC, Z Chen, LH Royden, Y Liu and C Deng. 1991. Extensional development of Gabo Valley, Southern Tibet. *Tectonophysics* 194: 187-193
- Burchfiel BC, Z Chen, K Hodges, Y Liu, LH Royden, C Deng and J Xu. 1992. The South Tibetan Detachment System, Himalayan Orogen: Extension contemporaneous with and parallel to Shortening in a Collisional Mountain Belt. *Geological Society of America Special Paper* 269.
- Fort M, P Freydet and M Colchen. 1982. Structural and Sedimentological Evolution of the Thakkhola-Mustang Graben (Nepal Himalayas). *Zeitschrift für Geomorphologie* 42: 75-98
- Garzzone CN, PG DeCelles, D Hodkinson, R Ojha and B Upreti. 2003. E-W Extension and Miocene Environmental Change in the Southern Tibetan Plateau: Thakkhola graben, Central Nepal. *Geological Society of America Bulletin* 115(1): 3-20
- Hodges KV, Hurtado JM and KX Whipple. 2001. Southward Extrusion of Tibetan Crust and its effect on Himalayan Tectonics. *Tectonics* 20(6): 799-809
- Hurtado JM, KV Hodges and KX Whipple. 2001. Neotectonics of the Thakkhola Graben and implications for Recent activity on the South Tibetan Fault System in the central Nepal Himalaya. *Geological Society of America Bulletin* 113(2): 222-240
- Lave J and JP Avouac. 2000. Active folding of fluvial terraces across the Siwalik Hills, Himalayas of central Nepal. *Journal of Geophysical Research* 105: 5735-5770
- McCaffrey R. 1996. Estimates of modern arc-parallel strain rates in fore-arcs. *Geology* 24(1): 27-30
- McCaffrey R and J. Nabelek. 1998. Role of oblique convergence in the active deformation of the Himalayas and Southern Tibet Plateau. *Geology* 26: 691-694
- Molnar P and WP Chen. 1983. Focal depths and fault-plane solutions of earthquakes under the Tibetan plateau. *Journal of Geophysical Research* 88: 1180-1196
- Molnar P and H Lyon-Caen. 1989. Fault-plane solutions of earthquakes and active tectonics of the Tibetan Plateau and its margins. *Geophysical Journal International* 99: 123-153
- Murphy M, A Yin, P Kapp, TM Harrison, D Lin and G Jinghui. 2000. Southward Propagation of the Karakoram Fault System, Southwest Tibet: Timing and Magnitude of Slip. *Geology* 28(5): 451-454
- Neumayer J, G Wiesmayr, C Janda, B Grasemann and E Draganits. 2004. Eohimalayan fold and thrust belt in the NW-Himalaya (Lingti-Pin Valleys): Shortening and depth to detachment calculation. *Austrian Journal of Earth Sciences* 95/96: 28-36
- Ortner H, F Reiter and P Acs. 2002. Easy handling of tectonic data: the programs TectonicVB for Mac and TectonicsFP for Windows. *Computers and Geosciences* 28: 1193-1200
- Pandey MR, RP Tandukar, JP Avouac, J Vergne and Th Héritier. 1999. Seismotectonics of the Nepal Himalaya from a local seismic network. *Journal of Asian Earth Sciences* 17(5-6): 703-712
- Ratschbacher L, W Frisch, GH Liu and CS Chen. 1994. Distributed deformation in Southern and Western Tibet during and after the India-Asia Collision. *Journal of Geophysical Research (Solid Earth)* 99(B10): 19917-19945
- Royden L and BC Burchfield. 1987. Thin-skinned N-S extension within the convergent Himalayan Region: Gravitational collapse of a Miocene topographic front. In: *Continental Extensional Tectonics, Blackwell Scientific Publications*: 611-619
- Singh S and AK Jain. 2006. Liquefaction and fluidization of lacustrine deposits from Lahaul- Spiti and Ladakh Himalaya: Geological evidences of paleoseismicity along active fault zone. *Sedimentary Geology* 196(1-4): 47-57
- Steck A, JL Epard, JC Vannay, J Hunziker, M Girard, A Morard and M Robyr. 1998. Geological transect across the Tso Morari and Spiti areas: the nappe structures of the Tethys Himalaya. *Eclogae geologicae Helveticae* 91: 103-122
- Thiede R, J Arrowsmith, B Bookhagen, M McWilliams, E Sobel and M Strecker. 2006. Dome formation and extension in the Tethyan Himalaya, Leo Pargil, northwest India. *Bulletin of Geological Society of America* 118: 635-650
- Wu C, K Nelson, G Wortman, S Samson, Y Yue, J Li, W Kidd and M Edwards. 1998. Yadong Cross Structure and South Tibetan Detachment in the East Central Himalaya (89° - 90° E). *Tectonics* 17: 28-45
- Zhang P, Z Shen, M Wang, W Gan, R Bürgmann, P Molnar, Q Wang, Z Niu, J Sun, J Wu, S Hanrong and Y Xinzhaoh. 2004. Continuous deformation of the Tibetan Plateau from Global Positioning System data. *Geology* 32(9): 809-812

3-D Velocity Structure of the Crust and upper Mantle in Tibet and its Geodynamic Effect

Zheng Hongwei^{1*}, He Rizheng², Zhao Dapeng³, Li Tingdong² and Rui Gao²

¹ Department of Geophysics, Peking University, Beijing 100871, CHINA

² Institute of Geology, Chinese Academy of Geological Science, Beijing 100037, CHINA

³ Research Center for Prediction of Earthquake & Volcanic Eruptions, Graduate School of Science, Tohoku University, Sendai 980-8578, JAPAN

* For correspondence, email: zhenghongwei004@sina.com

The crust and upper mantle structure under Tibet is the direct result of the India plate subducting and colliding with the Eurasian plate. 3-D seismic velocity structure of the crust and upper mantle under Tibet was determined by using the Tomo3D tomography program developed by Prof. Dapeng Zhao (Zhao et al. 1992, 1994). In the tomographic inversion we used 139,021 P-wave arrival times from 9649 teleseismic events recorded by 305 seismic stations. The major results of this study (Zheng 2006) are summarized as follows:

1) The Tibetan crust velocity structure is generally consistent with the surface tectonic features which are oriented nearly east-west. But the main trend of the velocity anomalies in the upper mantle is generally oriented in the north-south direction. The location of the NNE strike low-velocity zone is consistent with the N-S strike negative aeromagnetic data.

2) Low-velocity anomalies in the crust are clearly visible under the Himalaya Mountain.

3) Our tomographic images show that the Indian lithospheric mantle subducting angles are different under different areas, but their front locations are all beneath the Qiangtang terrain. The tomographic images (Figure 1) along 88°E show that the Indian lithospheric mantle is underthrusting northwards with a dip angle of about 22° beneath the center of Qiangtang terrane at about 34°N latitude, and its frontier has reached to the deep part of the upper mantle. The tomographic images along North-East profile show that the Indian mantle has nearly horizontally underthrust under the Tibet from Ganges plain to 33°N. Then, the Indian mantle broke off down to the asthenosphere and caused the asthenosphere upwelling. The top shows the surface topography. The tectonic lines are the same as those in Figure 1. The middle panel shows tomography. White circles show local earthquake hypocenters. The dash lines indicate the estimated upper and lower boundaries of the subducting Indian lithospheric mantle. The low-left panel shows the P-wave velocity perturbation scale. The low-right panel shows the location of profile AB along 88° E.

4) There is a huge low-velocity body (Wittlinger et al., 1996) which looks like a mantle plume beneath the Qiangtang terrain. Such a prominent low-velocity body is impossible to be the partial melting products. It is speculated to be either the subducted delamination of the Indian lithospheric mantle according to its location and extending depth with Qaidam block holding back the thermal disturbance in the area, and so resulting in higher temperature which begets falling velocity or be the mantle upwelling materials along the surface of Indian lithospheric mantle.

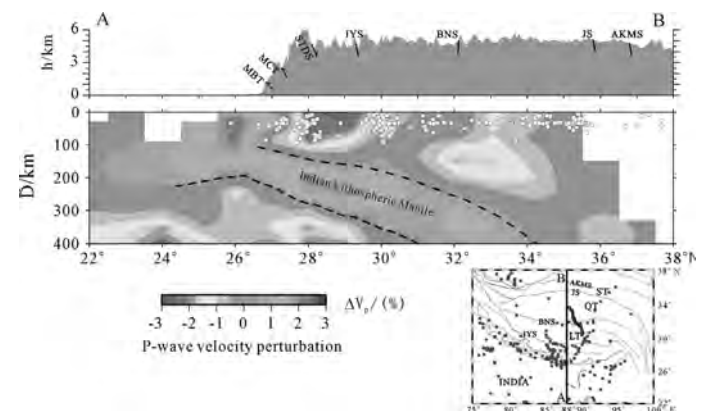


FIGURE 1. P-wave tomographic image of the subducting Indian lithospheric mantle along profile AB.

Acknowledgements

This work was supported by grants from National Natural Science Foundations of China (No. 40404011-40774051), 2007 Year of the Basic outlay of scientific research work from Ministry of Science and Technology of the People's Republic of China, International Cooperative Project from Ministry of Science and Technology of the People's Republic of China-No.2006DFA21340, Open Fund (No. GDL0602) of Geo-detection Laboratory, Ministry of Education of China, China University of Geosciences.

References

- Zhao DP, A Hasegawa and S Horiuchi. 1992. Tomographic Imaging of P and S wave velocity structure beneath Northeastern Japan. *Journal of Geophysical Research* 97(B13): 19909-19928
- Zhao DP, A Hasegawa and H Kanamori. 1994. Deep structure of Japan subduction zone as derived from local, regional, and teleseismic events. *Journal of Geophysical Research* 99 (B11): 2313-2329.
- Wittlinger G, F Masson and G Poupinet. 1996. Seismic tomography of northern Tibet and Kunlun; evidence for crustal blocks and mantle velocity contrasts. *Earth and Planetary Science Letters* 139: 263-279.
- Zheng HW. 2006. 3-D velocity structure of the crust and upper mantle in Tibet and its geodynamic effect. Ph. D. thesis in Chinese, Beijing: Chinese Academy Geological Sciences.

Electrical Structure of Garhwal Himalayan region, India, inferred from Magnetotelluric

M Israil*, DK Tyagi, PK Gupta and Sri Niwas

Department of Earth Sciences, Indian Institute of Technology Roorkee, Roorkee- 247667, INDIA

*For correspondence, email: mohdfes@iitr.ernet.in

Magnetotelluric investigations have been carried out in the Garhwal Himalayan corridor to delineate electrical structure of the crust along a profile extending from Indo-Gangetic Plane to Higher Himalayan region in Uttarakhand, India. The profile passing through major Himalayan thrusts: Himalayan Frontal Thrust (HFF), Main Boundary Thrust (MBT) and Main Central Thrust (MCT), and is nearly perpendicular to the regional geological strike. These Himalayan thrusts are broadly parallel to each other, steeper near surface and become shallow with the depth until they merge with the detachment surface. The main tectonic elements of Garhwal Himalayan region have an average strike of NW-SE (Khattri 1992). Magneto-variation (MV) studies (Arora et al 1982), were carried out over a rectangular array of 24 stations in the Siwalik Himalayan region, indicated the presence of a conductive anomaly, which they interpreted as an extension of the Aravallis and referred to as Trans Himalayan conductor. Subsequently, MT investigations were carried out by Gupta et al (1994) in the Siwalik region over 150 km long Mohand - Ramnagar profile to determine the thickness of Siwalik sediments. They recorded MT data in the frequency range 0.01–100 Hz using short period MT system and estimated geoelectric strike of N 800 W on the basis of

simple rotation of impedance tensor

We have conducted a Broadband MT survey in the Garhwal Himalayan corridor during 2004-06, data were recorded in the frequency band 1000 - .001 Hz. The locations of the 44 stations are shown in figure 1. The paper presents the electrical structure of the crust along the profile inferred from the 2D smooth inversion of MT data.

The recorded time domain data were transformed to the frequency domain impedance tensor and subsequently used to determine intrinsic dimensionality and directionality of the geological structure with respect to the geographical coordinate system. We have used Groom and Bailey (1989) tensor decomposition as implemented by McNeice and Jones, 2001 in strike code provided by Alan G. Jones. The decomposition analysis suggests an average strike direction of N 700 W for entire profile. The measured responses are rotated in the estimated strike direction to obtain TE and TM response for inversion.

Smooth inversion of only TE mode, TM mode and joint TE and TM responses have been done so as the final model incorporates the important features of both TE and TM responses. The main results are given in figure 2 which presents (i) 2D

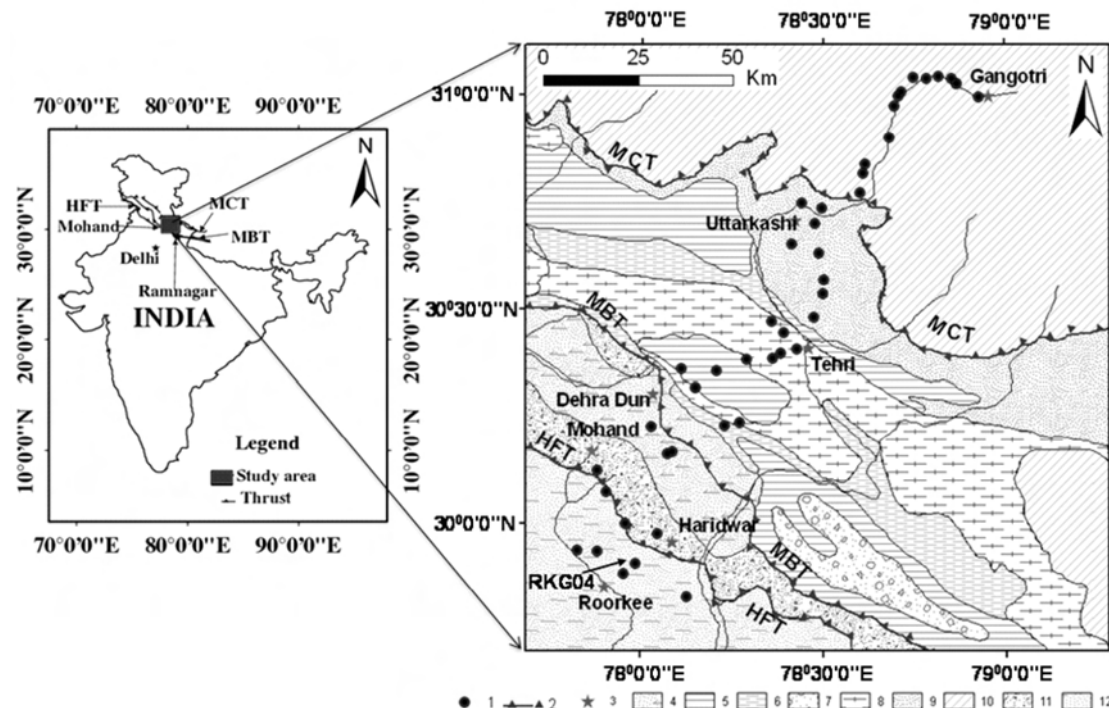


FIGURE 1. Location the study area (geological map compiled from Viridi, 1988, Sorkhabi et al. 1999, Kumar et al. 2002). 1- MT Sites; 2- Thrust; 3- Cities; 4- Dehra Dun Reentrant; 5- Blaini-Infrakrol-Krol; 6- DaMTha; 7- Garhwal Nappe; 8- Jaunsar-Simla (Undifferentiated); 9- Sunder Nagar-Berinig Groups; 10- Undifferentiated Metamorphics; 11- Undifferentiated Tertiaries; 12- Piedmont zone. MT data collected in the Indo-Gangetic Plains, Siwalik, Lesser and Higher Himalayan region in Garhwal Himalaya.

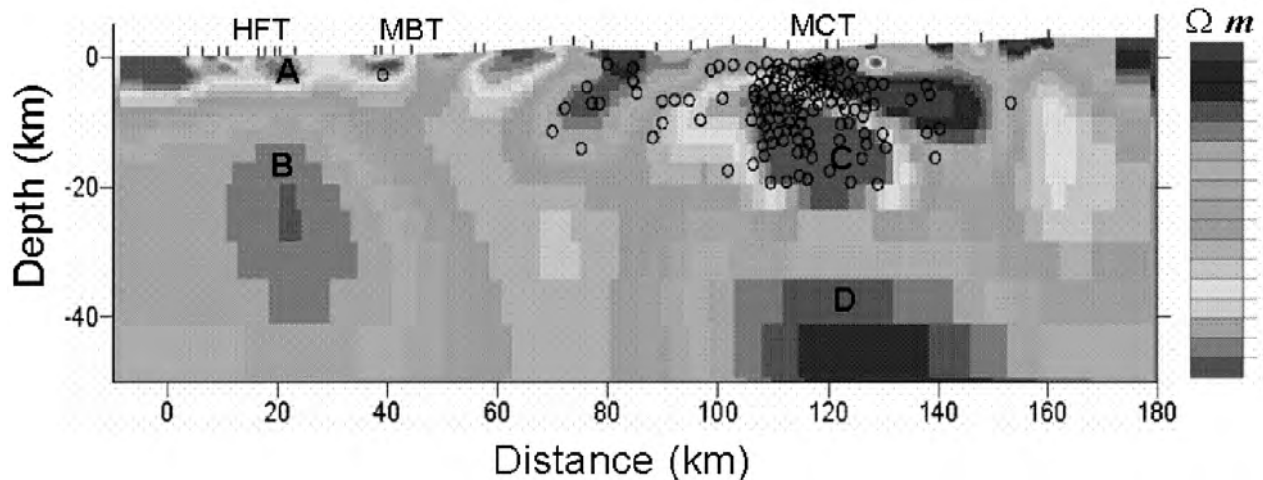


FIGURE 2. 2D resistivity models of Roorkee-Gangotri profile in Garhwal Himalaya corridor with (i) elevation profile on the top, (ii) 2D smooth geoelectric model obtained from the joint inversion of TE, TM responses (iii) the local seismicity (hypocenters) locations plotted as circles in the model, (iv) locations of 27 MT sites indicated by vertical bar, (v) the major Himalayan thrusts (HFT, MBT, MCT).

smooth geoelectric model obtained from the joint inversion of TE and TM responses (ii) the local seismicity (hypocenters) plotted as circle in the electrical model, (iii) elevation profile, (iv) locations of 27 MT sites, used for 2D inversion, indicated by vertical bar, (v) the major Himalayan thrusts.

The electrical model shows a shallow conductive structure ($< 50 \Omega m$) mainly confined in the southern part of the profile located in Indo-Gangetic Plane (IGP) and Lesser Himalayan (LH) region. The conductive structure is extended to a depth of 6 km. Geologically, the zone corresponds to the loose sediments, mollasse of the Miocene and younger age, transported from Higher Himalayan region. Resistive structure ($1000 \Omega m$) underneath the near surface conductive sediments is interpreted as electrical image of the Indian crust. Low resistivity ($< 5 \Omega m$) zone present below MCT. This zone is a typical example of low resistivity zone in mid crustal region invariably observed in Himalayan region. This zone also appears to coincide with the location of hypocenter of local earthquake. The conducting zone appears to be related with the strain accumulation zone in Himalayan region for future earthquakes. This conductive zone is analogous to the similar conductive zone reported in the central Nepal – Himalaya profile (Lemonnier et al. 1999). The MCT zone falls in high heat flow area, majority of hot spring are concentrated around this zone, might be associated to this low resistivity zone. Resistive feature underlying the low resistivity zone in mid crustal depth is interpreted as the electrical image of north dipping Indian Plate.

References

- Arora BR, F E M Lilley, M N Sloane, B P Singh, B J Srivastava and S N. Prasad 1982. Geomagnetic induction and conductive structures in northwest India; *Geophysical Journal of Royal Astronomical Society* 69: 459-475
- Groom RW and RC Bailey. 1989. Decomposition of Magnetotelluric impedance tensors in the presence of local three-dimensional galvanic distortion; *Journal of Geophysical Research* 94: 1913-1925
- Gupta G, SG Gokarn and BP Singh 1994. Thickness of the Siwalik Sediments in the Mohand-Ramnagar region using magnetotelluric studies; *Physics of the Earth and Planetary Interiors* 83: 217-224
- Khattari K N. 1992. Local seismic investigations in the Garhwal-Kumaun Himalaya. *Mem. Geol. Soc. India*, 23, pp. 45-66
- Kumar R, S K Ghosh, S J Sangode and V C Thakur. 2002. Manifestation of Intra – Foreland thrusting in the Neogene Himalaya foreland basin fill; *Journal of Geological Society of India* 59: 547-560
- Lemonnier C, Marquis G, Perrier F, Avouac J P, Chitrakar G, Kafle B, Sapkota S, Gautam U, Tiwari D and Bano M 1999 Electrical structure of the Himalaya of central Nepal: high conductivity around the mid-crustal ramp along the MHT; *Geophysical Research Letters* 26: 3261-3264
- McNeice G W and A G Jones. 2001. Multisite, multifrequency tensor decomposition of magnetotelluric data. *Geophysics* 66: 158-173
- Sorkhabi R B, E Stump, K Foland and A K Jain. 1999. Tectonic and cooling history of the Garhwal Higher Himalaya (Bhagirathi Valley): constraints from thermochronological data; *Gondwana Research Group Memoir* 6: 217-235
- Virdi N S. 1988. Pre – Tertiary geotectonic events in the Himalaya; *Z. geol. Wiss, Berlin* 16: 571-585

Heterogeneous Himalayan crust using shear wave attenuation in the Pithoragarh region of Kumaon

A Joshi^{1*}, M Mohanty², AR Bansal³, VP Dimri³ and RK Chadha³

¹ Indian Institute of Technology, Roorkee, Roorkee 247 667, Uttarakhand, INDIA

² Department of Science and Technology, Government of India, New Delhi, INDIA

³ National Geophysical Research Institute, Uppal Road, Hyderabad, INDIA

* For correspondence, email: anushijos@yahoo.co.in

Pithoragarh district of Uttarakhand Himalaya, which lies in the border region of India and Nepal, falls in the seismically active zone of the seismic zoning map of India. Under a major DST sponsored project a network of eight strong motion stations has been installed in this region since March 2006. This paper presents a method of finding shear wave quality factor ' $Q_{\beta}(f)$ ' from strong motion data recorded by this network. The method used for this study is based on modified technique, given by Joshi (2006). Data of local noise recorded at various stations have been utilized for the purpose of site survey and average value at each station is used for correcting the accelerograms for site amplifications. Based on availability of data, hypocentral parameters and clear S phases from horizontal component of 37 strong motion records from six stations have been used for in this work. The output of this inversion gives $Q_{\beta}(f)$ relation and corner frequencies of earthquake at different stations. Low value of coefficient (< 200)

and high frequency dependence ($>.8$) in the $Q_{\beta}(f)$ relationships obtained at different stations suggest that the region is seismically and tectonically active and is characterized by large number of heterogeneities. Obtained $Q_{\beta}(f)$ are used to compute source spectrum of S wave from the accelerogram and are compared with theoretical Brune's source spectrum of corner frequency obtained from inversion. Comparison of source spectrum obtained from the corrected accelerograms with the theoretical Brune spectrum shows that this technique has potential to give reliable $Q_{\beta}(f)$ and source parameters of the studied earthquakes using records from single station. Using the obtained $Q_{\beta}(f)$ values at different stations at different frequencies an average $Q_{\beta}(f)$ relation of $50f^{1.08}$ has been obtained for Pithoragarh region of Kumaon Himalaya. Obtained relations not only explain the complexities and heterogeneities of earth crust in Himalaya, it can be used as an input for simulation of strong ground motion in this region.

Lithostratigraphy of the Naga-Manipur Hills (Indo-Burma Range) Ophiolite Belt from Ukhrul District, Manipur, India

A Joshi^{1*} and KT Vidyadharan²

¹ Geological Survey of India, NH-5P, NIT Faridabad-121001, Haryana, INDIA

² 310, Block "B", Maharaja Residency, Balmatta Road, Hampankatta, Mangalore-575001, INDIA

* For correspondence, email: joanil@rediffmail.com

Two late Mesozoic ophiolite belts occur along the eastern margin of the Indian plate. The eastern or Sumatra belt is poorly exposed whereas the western or the Indo-Burma Range (Naga-Manipur Hills) ophiolite belt is well preserved particularly in the Myanmar bordering terrain of Manipur. The NE-SW trending western belt extends in the states of Nagaland and Manipur and is about 200 km wide in north before splitting into thin slices towards south. This study delineates the lithostratigraphic ensemble of the ophiolite belt in the northernmost part of Manipur in Ukhrul district while discussing its petrology and tectonic implications.

Three major lithopackages have been mapped in this area. From west to east these comprise a thick, folded pile of Paleogene sediments, which are tectonically juxtaposed with an ophiolite suite followed by feebly metamorphosed pelagic cover sediments (Figure 1). The sedimentary rocks in the west include shale-siltstone rhythmities with minor sandstone (Disang Group) representing distal shelf facies that grades upward to a conglomerate-grit-sandstone-coal streaks-bearing shallow marine to fluviatile sequence (Barail Group). The upper part of Disang Group depicts an olistostromal zone with olistoliths of mainly fossiliferous limestone, varying in dimensions from a few meters to more than 0.5 km. The foraminiferal assemblage of limestone suggests a wide, upper Cretaceous (Maastrichtian) to Oligocene age range supporting their exotic nature in the mélange zone (Vidyadharan and Joshi 1984, Vidyadharan et al. 1989).

The ophiolite suite exhibits a dismembered sequence with alternating slices of variable dimensions including ultramafics, mafic differentiates and volcanics. Harzburgite is the dominant lithology of the ultramafic clan followed by volumetrically insignificant dunite, and pyroxenite. All ultramafic variants depict various stages of serpentinization with development of magnetite, talc and a typical ribbon and mesh texture. Chromite occurs as massive chromitite bands (metallurgical to refractory grade), nodular pods and disseminations. A significant feature of the peridotite association is the occurrence of thin, discontinuous lenses of coarse, dark coloured garnet bearing ultramafic segregations, with diopside, grossular-almandine garnet, magnesio-hastingsite and rutile as the other major minerals, in the northeastern part of this area. These rocks show strong enrichment of CaO and severe depletion of MgO from the host peridotites besides higher values for Al₂O₃, TiO₂, Na₂O, K₂O and resemble the metarodinite formed by extensive Ca metasomatism during serpentinization of the host rocks followed by high pressure recrystallization (Evans et al. 1979). Mafic differentiates are represented mainly by gabbros and plagiogranite. Prolonged rodingitization of these rocks is displayed by the presence of chlorite, epidote, zoisite and calcite. Massive to amygdaloidal, low MgO basalts showing

intersertal and glomeroporphyritic textures represent the volcanic rocks besides a few occurrences of volcanic agglomerates.

The easternmost unit of this area exposes oceanic pelagic cover sediments comprising mainly phyllite, quartzite, bedded radiolarian chert and limestone. These have undergone low grade metamorphism and also incorporate tectonic slices of the ophiolite suite.

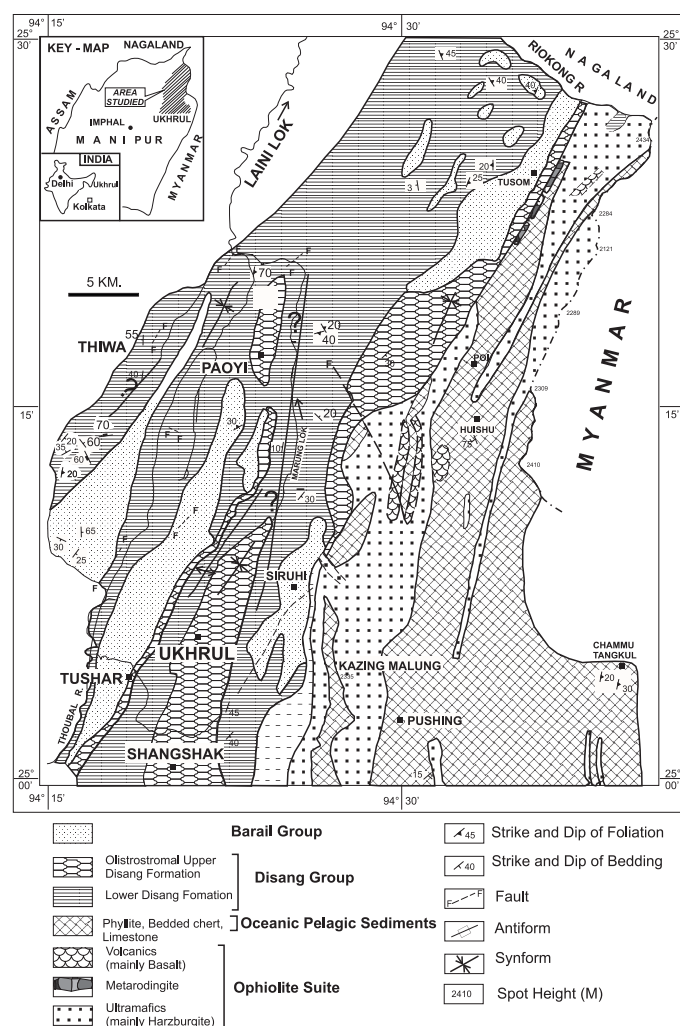


FIGURE 1. Geological map of the area around Ukhrul, Naga-Manipur Hills, Manipur (Modified after Vidyadharan et al. 1989).

Absence of dyke swarms and the chemistry of the volcanic rocks indicates an ocean island or seamount type of setting for this belt, whereas presence of metarodingite and glaucophane-bearing schists further north in Nagaland suggests a complex subduction process. Linear zone of negative gravity anomalies over the western ophiolite belt has been explained by shallow nature of these nappes, while linear gravity high over the eastern belt makes it the site of the of the root zone of the eastern suture of Indian plate (Acharyya et al. 1990, Acharyya 2007, Sengupta, 1990).

References

- Acharyya SK, KK Ray and DK Roy. 1990. Tectono stratigraphy and emplacement history of the ophiolite assemblage from the Naga Hills and Andaman Island Arc, India. *Journal of the Geological Society of India* 33: 4-18
- Acharyya SK. 2007. Collisional emplacement history of the Naga-Andaman ophiolites and the position of the eastern Indian suture. *Journal of the Asian Earth Sciences* 29: 229-242
- Evans BW, V Trommsdorff and W Richter. 1979. Petrology of an eclogite-metarodingite suite at Cima di Gagnone, Ticino, Switzerland. *American Mineralogist* 64: 15-31
- Vidyadharan KT and A Joshi. 1984. *Unpublished Geological Survey of India Report*. 42p
- Vidyadharan KT, A Joshi, S Ghosh, MP Gaur and R Shukla. 1989. Manipur ophiolites: Its geology, tectonic setting and metallogeny. In: Ghose NC (ed.) *Phanerozoic ophiolites of India*. Patna: Sumna Publication. p197-212

Pre-Himalayan tectonometamorphic signatures from the Kumaun Himalaya

Mallickarjun Joshi

Department of Geology, Banaras Hindu University-221005, INDIA

E-mail: m_joshi@sify.com

It is necessary to resolve the relative contributions of the Himalayan and Pre-Himalayan tectonometamorphic signatures for refinement of the existing models for the evolution of the Himalaya. An attempt has been made for the Lesser Himalayan metamorphics exposed in the Kumaun Himalaya to identify the Pre-Himalayan deformations and metamorphisms. The isoclinal F1 folds and the tight to isoclinal F2 folds in the Lesser Himalayan metamorphics of the Kumaun Himalaya can be safely inferred to be distinctly Pre-Himalayan as the 560 ± 20 Ma old Champawat Granitoides and its equivalent Almora Granite (Rb-Sr dating, Trivedi et al. 1984) intrude the F2 folds.

The metamorphics comprising the Almora Group of rocks have been subjected to green schist facies to upper amphibolite facies metamorphism (M1) reaching temperatures of $\geq 700^\circ\text{C}$ and pressures of 7.4 ± 0.5 kbar (Joshi and Tiwari 2004). Four metamorphic zones, viz. chlorite-biotite, garnet-biotite, kyanite-biotite and sillimanite K-feldspar zone have been identified in the Almora Group of rocks. These metamorphics can be demonstrated in the field to gradually increase in metamorphic grade from the chlorite zone of the green schist facies to the K-feldspar sillimanite zone of the upper amphibolite facies comprising gneisses through a migmatite zone in the Champawat, Almora, Dwarahat and Dudatoli regions. Thus, these sillimanite K-feldspar gneisses are evidently a product of the culmination of metamorphism and have been dated at 1860 ± 50 Ma by Trivedi et al. (1984) by Rb-Sr dating. The metamorphic sequence both in the southern flank, viz. Champawat and Almora areas and in the northern flank, viz. south of Someshwar and Dwarahat areas have been affected by F1 and F2 folding which has led to a repetition of isograd surfaces across north-south transects.

This folded sequence in the southern flank of the Almora Nappe has been intruded by 560 ± 20 Ma granitoids. This hot

intrusion of granitoids has left a well preserved contact aureole in the Champawat area (Joshi et al. 1994) and the Almora area (Joshi and Tiwari 2007). The well preserved randomly oriented chloritoids and andalusites overprinting the regional schistosity (S2) clearly show that the regional metamorphism is older than the 560 ± 20 Ma contact metamorphism (M2). This fact is further corroborated by the age of the gneisses around 1860 Ma, which have formed as an end product at the culmination of regional metamorphism. Thus it is highly likely that the age of the dominant regional metamorphism is also close to 1860 Ma.

The two stage garnet growth in these metamorphics is suggestive of a polymetamorphic history of the area and it is likely that the outer rim of the garnet formed during the Tertiary (Himalayan) metamorphism (M3). It can be safely inferred that the dominant regional metamorphism in the Almora Group of rocks is of Pre-Himalayan (Pre-Cambrian) age and the Himalayan metamorphic imprint in the Almora Nappe was of lower grade and in all likelihood did not exceed the garnet grade.

References

- Joshi M, BN Singh and OP Goel. 1994. Metamorphic conditions from the aureole rock from the Dhunaghat area, Kumaun Lesser Himalaya. *Current Science* 67(3): 185-88
- Joshi M and AN Tiwari. 2004. Quartz c-axes and metastable phases in the metamorphic rocks of the Almora Nappe: evidence of Pre-Himalayan signatures. *Current Science* 87(7): 995-999
- Joshi M and AN Tiwari. 2007. Folded metamorphic reaction isograds in the Almora Nappe, Kumaun Lesser Himalaya: Field evidence and tectonic implications. *N. Jb. Geol. Palaont. Abh.* 244: 215-225.
- Trivedi JR, K Gopalan and KS Valdiya. 1984. Rb-Sr ages of granites within Lesser Himalayan Nappes, *Kumaun Himalaya, Journal of the Geological Society of India* 25: 641-654

Northeast Tibetan Crustal Structure from INDEPTH IV Controlled-Source Seismic Data

Marianne Karplus¹, Simon Klempner^{1,*}, Zhao Wenjin², Wu Zhenhan², Shi Danian², Su Heping², Larry Brown³, Chen Chen³, Jim Mechie⁴, Rainer Kind⁴, Fred Tilmann⁵, Yizhaq Makovsky⁶, Rolf Meissner⁷ and INDEPTH Team

¹ Department of Geophysics, Stanford University, CA 94305-2215, USA

² Chinese Academy of Geological Sciences (CAGS), Beijing 100037, CHINA

³ Department of Earth and Atmospheric Sciences, Cornell University, NY 14853, USA

⁴ GeoForschungsZentrum (GFZ), Telegrafenberg, 14473 Potsdam, GERMANY

⁵ Department of Earth Sciences, Cambridge University, Cambridge CB3 0EZ, ENGLAND

⁶ School of Marine Sciences, University of Haifa, Haifa 31905, ISRAEL

⁷ Institute of Geosciences, Christian Albrechts University, Kiel, GERMANY

* For correspondence, email: sklemp@stanford.edu

Since 1992, project INDEPTH (International Deep Profiling of Tibet and the Himalaya) geoscientists from Chinese, American, British, German, and Canadian institutions have collaborated to collect high-quality seismic, MT, and geologic data along a roughly north-south transect from the Himalaya to northern Tibet. The current field effort from 2007–2009, INDEPTH IV, targets the NE margin of the plateau, with goals of testing models of subduction (relict and current) near the Kunlun and Jinsha sutures and probing the deep geometry of key features such as the Kunlun and Altyn Tagh Faults. Our new datasets are intended to shed light on the possible existence of a lower-crustal flow channel beneath northern Tibet, analogous to the weak (and flowing?) lower crust evidenced by INDEPTH observations of mid-crustal low seismic velocities, seismic bright spots and high electrical conductivities (Nelson et al. 1996) in southern Tibet. INDEPTH IV further aims to evaluate the possible subduction of Asian crust from the north beneath the Kunlun suture (Kind et al. 2002) and to probe whether the Kunlun and Jinsha sutures act as crustal-scale faults.

Active seismic experiment, summer 2007

The INDEPTH IV active-source seismic experiment spans 270 km from the Qaidam Basin (Figure 1), across the North Kunlun Thrusts, the Kunlun Mountains, the North and South Kunlun Faults onto the Tibetan Plateau. The recording spread consists of four elements: 1) a wide-angle deployment of 295 IRIS PASSCAL Texan seismometers at 650 m spacing, 2) a near-vertical deployment of 655 Texans at 100 m spacing, 3) an adjacent deployment of a 1000-channel Sercel cabled spread with 50 m geophone spacing, and 4) an overlapping three-component array (48 Geophysical Instrument Pool Potsdam and SEIS-UK short-period and broadband instruments at 5–6 km spacing). Sources included five large shots (each 1000–2000 kg explosives) roughly evenly spaced along the profile, augmented by ~110 small shots (each ~60–80 kg) nominally spaced at 1 km in the central part of the profile.

We are using two-dimensional ray-tracing to model basin and basement refractions, and lower-crustal and Moho reflections to determine the crustal velocity structure. The preliminary model compiled incorporates a southward-thinning low-velocity Qaidam

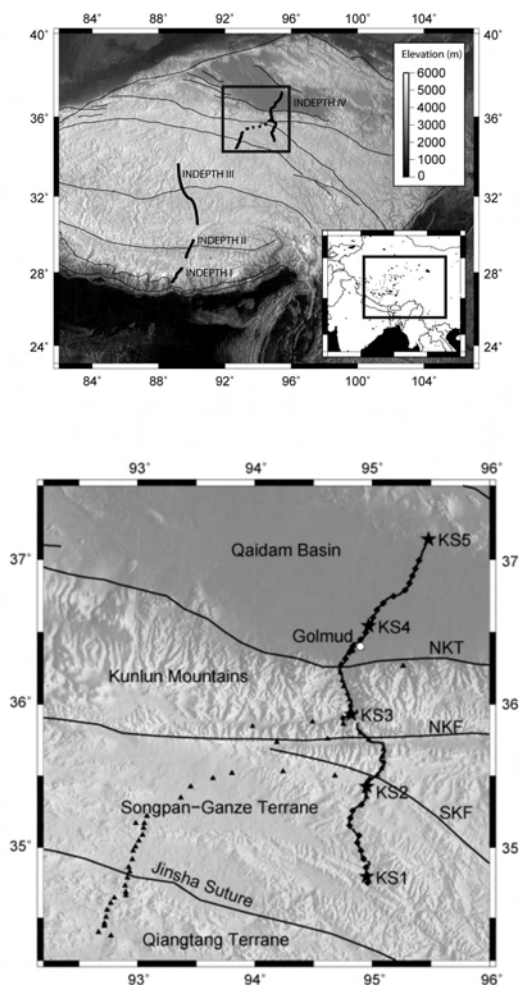


FIGURE 1. (a) Locations of INDEPTH I-IV transects spanning Tibetan Plateau. (b) Topographic map of northeast Tibet showing the locations of INDEPTH IV Texan and Sercel (continuous line of black dots) receivers, three-component short-period (diamonds) and broadband instruments (triangles), and small (circles) and large shots (stars).

basin, unusually low crustal velocities of 6 km/s compatible with older controlled-source observations further south and east in Tibet (e.g. Klemperer 2006), lower-crustal reflectors beneath the Plateau, and Moho depths of 50-55 km beneath the Qaidam Basin in the north. Near-vertical data from the small shots contains unusually strong s-wave arrivals as well as fault-plane reflections: reflectors at about 6 seconds beneath the Kunlun front range that we interpret as décollement horizons of the North Kunlun Thrusts.

Passive seismic experiment, 2007-2009

The passive seismic effort is cored by dense, linear broadband seismic arrays (59 stations at ~5 km spacing) deployed across the Jinsha and Kunlun sutures. Depth-domain teleseismic receiver-function processing from these arrays should allow detailed mapping of the Moho, the base of the lithosphere, and possibly subducted elements of Asia. This high-resolution passive profiling is complemented by a large areal array simultaneously deployed across NE Tibet by the ASCENT (Array Seismology Collaborative Experiments in Northeastern Tibet) consortium. Data from these passive deployments is scheduled for retrieval in summer 2008.

Other studies: Geology, thermochronology & magnetotellurics

INDEPTH Sino-US field parties will investigate shortening and strike-slip deformation near the seismic transects in 2008, using thermochronologic and stratigraphic studies to investigate timing of shortening and total offset on different strands of the Kunlun fault. MT surveys are planned for 2009 across the Kunlun and Altyn Tagh Faults. These new data will augment the INDEPTH III profile, which showed that the middle crust is conductive as far north as the Kunlun Fault, although with less extreme conductivity values than in southern Tibet (Wei et al. 2001).

References

- Kind R and 10 others. 2002. Seismic images of crust and upper mantle beneath Tibet: Evidence for Eurasian plate subduction. *Science* 298: 1219-1221
- Klemperer SL. 2006. Crustal flow in Tibet: geophysical evidence for the physical state of Tibetan lithosphere, and inferred patterns of active flow. In: RD Law, MP Searle and L Godin, eds., *Channel flow, ductile extrusion and exhumation in continental collision zones*, Geological Society London Special Publication 268: 39-70
- Nelson KD and 28 others. 1996. Partially molten middle crust beneath southern Tibet; synthesis of Project INDEPTH results. *Science* 274: 1684-1688
- Wei W and 14 others. 2001. Widespread fluids in the Tibetan crust. *Science* 292: 716-718

Geochronologic, structural and metamorphic constraints on the evolution of the South Tibetan detachment system, Bhutan Himalaya

Dawn A Kellett^{1*}, Djordje Grujic¹, Isabelle Coutand² and Clare Warren^{1,3}

¹ Department of Earth Sciences, Dalhousie University, Halifax, Nova Scotia, B3H 4J1, CANADA

² Université des Sciences et Technologies de Lille 1, UFR Sciences Terre (SN5), UMR 8157 du C.N.R.S., 59655 Villeneuve d'Ascq Cedex, FRANCE

³ Department of Earth and Environmental Sciences, The Open University, Walton Hall, Milton Keynes MK7 6AA, ENGLAND

* For correspondence, email: dawn.kellett@dal.ca

Geodynamic models of collisional orogenesis provide predictions about the provenance and pressure-temperature-time-deformation (PTtD) history of material within exposed crustal-scale structures. Focused field studies across relevant natural analogues provide the requisite data against which these models must be tested. Here we present structural, geochronologic, thermochronologic, thermometric and thermo-barometric data from transects across the

South Tibetan detachment system (STDS) in Bhutan (Figure 1) and compare them to model predictions for the equivalent structures in numerical geodynamic models (e.g., Jamieson et al. 2006).

The STDS in Bhutan occurs as two discrete detachments (Hollister and Grujic 2006) similar to the STDS in eastern Nepal (Searle et al. 2003). The upper detachment appears to be a brittle-ductile normal fault, which juxtaposes the poly-deformed

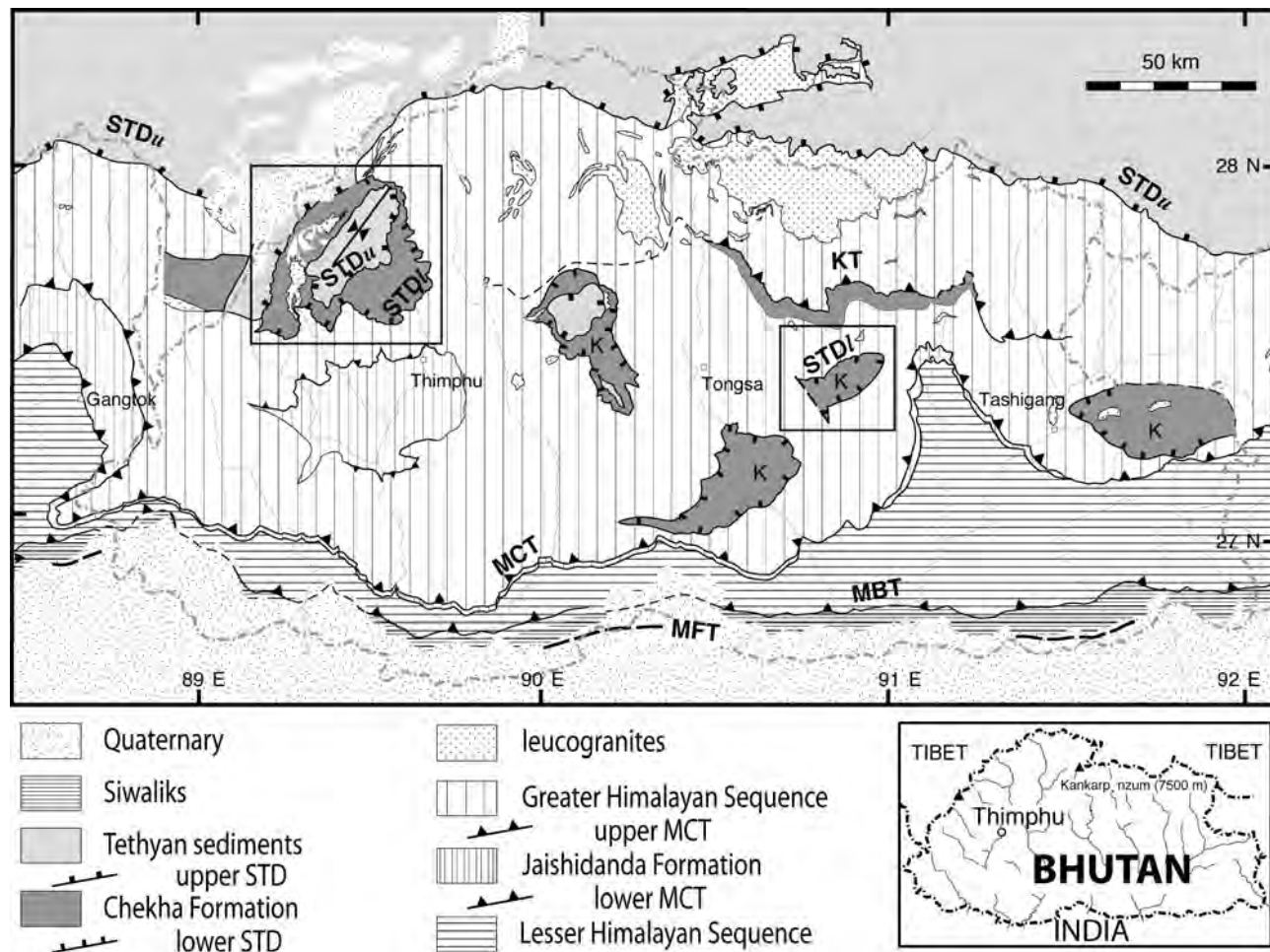


FIGURE 1. Geological map of Bhutan, with field areas enclosed in boxes. K, klippen of Chekha Formation; STDu, upper South Tibetan detachment; STDl, lower South Tibetan detachment; MCT, Main Central thrust; MBT, Main Boundary thrust; MFT, Main Frontal thrust. From Hollister and Grujic 2006 and unpublished data.

metasedimentary Chekha Group against unmetamorphosed Tethyan sedimentary rocks. The timing of motion along the upper detachment has been constrained to <12-11 Ma in northern Bhutan by U-Pb zircon dating of cross-cutting leucogranites (Edwards and Harrison 1997, Wu et al. 1998).

The lower detachment is a ductile, top-to-the-north shear zone separating high-grade metamorphic rocks of the Greater Himalayan sequence (GHS) in the footwall from the Chekha Group in the hangingwall. It is characterized by pervasive intrusion of multi-generational Tertiary leucogranite dikes and sills. These granite bodies have been variably boudinaged and folded by the detachment. SHRIMP-RG U-Pb dating combined with trace element geochemical analysis of concentrically-zoned magmatic zircon rims indicates pre- to syn-deformational emplacement and crystallization of the leucogranite dikes into Chekha Group rocks during ~23-16 Ma, reflecting ductile motion along the lower South Tibetan detachment since at least 16 Ma. Porous, inclusion-rich, U-rich zircon cores may indicate early magmatic crystallization of zircon within a highly-fractionated partial melt between 30 and 20 Ma.

Ti-in-zircon thermometry of dated zircon rims suggests slow cooling during zircon crystallization from ~650°C to ~500°C between 23 and 16 Ma. Crystallization temperatures are well below the closure temperature for Pb diffusion in zircon, suggesting that the spread of ages reflects protracted crystallization during the Early Miocene. ⁴⁰Ar/³⁹Ar step-heat ages from bulk separate igneous muscovite from the leucogranite dikes (same samples) indicate rapid cooling to below ~350°C, and hence cessation of ductile shearing by ~13-11 Ma. Apatite fission track data indicate that the lower detachment reached 110-120°C at 5-8 Ma, thus the cooling rate slowed slightly into the Late Miocene.

The peak temperature gradient across both strands of the STDS in NW Bhutan has been determined by Raman spectroscopy of carbonaceous material and conventional thermobarometry in low- and high-grade metamorphic rocks, respectively. Peak temperatures in the Tethyan sequence increase down-section from ~200°C in the core of a map-scale syncline (Figure 1) to ~400°C in the hanging wall of the upper STDS. Temperatures in the structurally-highest Chekha Group rocks are >400°C, but not substantially higher than Tethyan sedimentary rocks, suggesting throw on the upper STDS is not significant.

Peak temperatures continue to increase down-section across the lower STD to 600-750°C in the structurally lowest CG and highest GHS rocks respectively. These are higher temperatures than the Ti-in-zircon rim temperatures suggest, indicating that the leucogranites intruded during cooling and exhumation.

The metamorphic sequence across both strands of the STDS is right-way-up, from granulite-facies rocks in the uppermost Greater Himalaya sequence through amphibolite facies in the Chekha Group and into structurally-highest, unmetamorphosed Tethyan sedimentary rocks, confirming the normal sense of shearing observed through the sequence. The lower detachment was most likely active during the Early to Mid-Miocene, and marks the protolith and rheological boundary between the upper (Chekha Group) and middle (GHS) crust. The upper detachment was most likely active since Late Miocene and has contributed to the tectonic denudation of the rocks beneath, as reflected by the rapid cooling of the lower detachment during Late Miocene. These PTtD data provide crucial constraints on the choice of an appropriate geodynamic model for the evolution of the Tibetan-Himalayan orogen.

References

- Jamieson RA, C Beaumont, MH Nguyen and D Grujic. 2006. Provenance of the Greater Himalayan Sequence and associated rocks: Predictions of channel flow models. In: Law R, MP Searle and L Godin (eds), Channel flow, ductile extrusion, and exhumation in continental collision zones, *Geological Society, London, Special Publications* 268: 165-182
- Edwards MA and TM Harrison. 1997. When did the roof collapse? Late Miocene north-south extension in the high Himalaya revealed by Th-Pb monazite dating of the Khula Kangri Granite. *Geology* 25(6): 543-546
- Hollister LS and D Grujic. 2006. Pulsed channel flow in Bhutan. In: Law R, MP Searle and L Godin (eds), Channel flow, ductile extrusion, and exhumation in continental collision zones, *Geological Society, London, Special Publications* 268: 415-423
- Searle M, RL Simpson, RD Law, RR Parrish and DJ Waters. 2003. The structural geometry, metamorphic and magmatic evolution of the Everest massif, High Himalaya of Nepal-South Tibet. *Journal of the Geological Society, London* 160: 345-366
- Wu C, KD Nelson, G Wortman, SD Samson, Y Yue, J Li, WSF Kidd and MA Edwards. 1998. Yadong cross structure and South Tibetan Detachment in the east central Himalaya (89°-90°E). *Tectonics* 17(1): 28-45

Paired terraces of the Seuti Khola, Dharan, eastern Nepal

Matrika Prasad Koirala^{1,2,3*}, Sunil Kumar Dwivedi^{1,2,3}, Prakash Dhakal³, Ghanashyam Neupane³, Yadav Prasad Dhakal³, Suresh Prasad Khanal³, Niraj Kumar Regmi³, Gobinda Ojha³, Suchita Shrestha³ and Ranjan Kumar Dahal^{1,3}

¹ Department of Geology, Tri-Chandara Campus, Tribhuvan University, Kathmandu, NEPAL

² Simulation Tectonics Laboratory, Faculty of Sciences, University of the Ryukyus, Nishihara, Okiwana, 901-0213, JAPAN

³ Central Department of Geology Tribhuvan University, Kathmandu, NEPAL

* For correspondence, email: matrikakoiraal@hotmail.com

Terraces are the geomorphic units once occupied by the rivers. When a river cuts down into its flood plain, the former alluvial surface is no longer flooded and is left as a more or less flat terrace above the new level of the river. If the downcutting resumes, a second pair of terrace may then be left on the valley side. Terrace mapping on the riverside is important in evaluating the environmental impact of the river to the adjacent area. The suitability of area to a particular landuse, and the possible action of river on the adjacent area of the river can also be understood from the terrace mapping. About 4 km stretches of the Seuti Khola, east of the Dharan Bazar has been mapped to illustrate the terrace patterns associated to this stream. The Seuti Khola is a hilly stream, characterized by low discharge during dry season, but tremendously high flow during rainy time. The river valley is wide (> 150 m) consisting of boulder-cobble beds. The stream valley has gradient of about 2°. Within the mapped area the river channels drops from 480 m elevation at upper reaches to 340 m elevation at the lower reaches. This provides high energy to the river during high discharge level that is capable of transporting boulder-sized clasts.

Four levels of terraces on each side has been identified and mapped on either side. The terraces are of paired type, thus can be individually recognized on either side. These terraces are well developed, and can easily be recognized as being successive step-like geomorphic units. Lower Terrace (T₁) is about 5 to 10 m above the present river channels. This terrace is distributed within elevation range of 350 – 400 m. The Lower Middle Terrace (T₂) is distributed within 370 – 440 m level. Upper Middle Terrace (T₃) is situated between 390 – 460 m levels. Similarly, the Upper Terrace (T₄) is identified above 410 – 550 m level.

The terraces of the Seuti Khola might be the evidence of the neo-tectonic activity in the Himalayan realm. The terraces along this stream are resulted due to the recent upliftment of the area. The terrace forming material is characterized by the north-tilting loose boulder-beds exposed on the steep riverbank scarps. This may be due to the rapid upward and southward movement associated with the Himalayan Frontal Thrust (HFT) that carries the Sub-Himalaya as hanging wall, onto the footwall of the Terai sediments. The continuous upliftment provides the extra elevation to be undercut by the stream.

Late Quaternary climatic changes in the eastern Kumaun Himalaya, India as deduced from multi-proxy studies

Bahadur Singh Kotlia^{1*}, Jaishri Sanwal¹, Binita Phartiyal², Lalit Mohan Joshi¹, Anjali Trivedi³ and Chhaya Sharma³

¹ Department of Geology, Kumaun University, Nainital, 263002, Uttarakhand, INDIA

² Birbal Sahni Institute of Palaeobotany, University Road, Lucknow, 226007, INDIA

³ Department of Geology, Lucknow University, Lucknow, 226 007, INDIA

* For correspondence, email: bahadur.kotlia@gmail.com

.....

An event of neotectonic activity on an NE-SW trending subsidiary fault in the zone of E-W running intracrustal boundary thrust (South Almora Thrust) in the Champawat district of eastern Kumaun Himalaya resulted in creation of a lake at ca. 21.5 BP. The lake was drained out in the late Holocene leaving behind a 5.0 m thick sedimentary sequence of mostly black and carbonaceous mud indicating at the base a minor magnetic reversal between 20.5-19.7 ka BP. The profile, studied by using multi-proxies (e.g., carbon isotopes, pollen

analysis, palaeo and mineral magnetism and clay minerals) has recorded globally well established abrupt climatic events in the last 20,000 years, such as, LGM, Older Dryas (OD), Younger Dryas (YD), Holocene warming, 8.2 ka and 4.2 ka events. Most events, estimated assuming the invariable rate of sediment accumulation for similar lithologies, may be related to the rapid changes in the local climate and albedo structure. We suggest that the ITCZ may have played a key role to control the behavior of south-west monsoon from LGM onwards.

Palaeozoic granites and their younger components - A study of Mandi and Rakcham granites from the Himachal Himalaya

A Kundu*, NC Pant and Sonalika Joshi

Geological Survey of India, NH-5P, NIT Faridabad-121001, Haryana, INDIA

* For correspondence, email: akundu62@rediffmail.com

Several occurrences of Palaeozoic granites are recorded from the Lesser Himalayas as well as from the Higher Himalayas (Miller et al. 2001). From Himachal many such bodies have been dated (Bhanot et al. 1979, Frank et al. 1977, Jager et al. 1971, Kwatra et al. 1986, Pognante et al. 1990, Kwatra et al. 1999, Kundu et al. 2006). All of these bodies are deformed and several occur in the vicinity of Main Central Thrust (MCT). Studies have indicated presence of more than one granite type in most of these occurrences (e.g. Gupta 1974, Chatterjee 1976) but definitive reference to the Himalayan orogeny has generally been lacking. The present work supplements the earlier field and petrographic classification with rigorous mineralogical including rare earth element (REE) bearing mineral data for the two Palaeozoic granites of Mandi and Rakcham and show association of younger granites with these occurrences.

Four petrographic variants of Mandi granites can be identified (Chatterjee 1976). These are as follows.

1. *Porphyritic granite*: With two mica and two feldspar. The ratio of the micas number to feldspar phenocryst vary. The other mineral phases are quartz, ilmenite, sphene, epidote, zircon, secondary muscovite, chlorite, monazite, allanite, zircon, apatite and fluorite.

2. *Fine grained porphyritic granite*: Two mica two feldspar granite and mineralogy similar to the porphyritic granite but has distinctly finer ground mass size and less phenocrysts.

3. *Trondjemite/albite granite*: Leucocratic rock with one feldspar (albite) and one mica (muscovite). Other minerals are quartz, rare biotite, chlorite, wolframite, iron oxides, monazite, fluorite, apatite and tourmaline.

4. *Leucogranite/tourmaline granite*: Two feldspar and one mica (muscovite) granite, some outcrops have significant amount of tourmaline (more than 1%). Quartz, k-feldspar, albite, tourmaline, muscovite, fluorite, monazite etc. In Rakcham occurrence three variants are identifiable namely 1. porphyritic granite: two feldspar biotite granite, 2. granodiorite and 3. trondjemite. The latter two variants are subordinate and the major constituent is the porphyritic granite. Magma mingling is indicated by the presence of mafic pillows in the Mandi occurrence (Miller et al. 2001).

Mandi Occurrence: In porphyritic granite plagioclase has a range of composition. The larger grains of plagioclase are zoned with core composition (An29) being more calcic than the rim (An23). Finer grained matrix grains are less calcic (An12) and inclusion of plagioclase within K-feldspar is nearly pure albite. Biotite has a high Fe content (Fe/Fe+Mg~ 0.73). The fine grained porphyritic granite has nearly albitic plagioclase and the biotite is more Fe rich (Fe/Fe+Mg~ 0.780). In trondjemite granite the

albite is the main feldspar and muscovite is the only mica present. The iron content of the muscovite in this variant is over 3 times that of the same mineral in other variants of Mandi occurrence. Enclaves present in the Mandi occurrence include enclaves of host rock (schist) engulfed by the granite during ascent, mica-rich coarse grained small rounded to oval lumps of restite material, fine grained, melanocratic commonly angular small sized dioritic rocks and oval to elongated, pillow shaped, melanocratic, up to 5 m in size mafic rocks (basalts). In diorite biotite as phenocrysts are more magnesium (Fe/Fe+Mg~ 38) than those in the groundmass (Fe/Fe+Mg~ 48). Anorthite content of plagioclase is ~ An37. In contrast the mafic rock has higher Ca in plagioclase (An70) and lower Fe in biotite (Fe/Fe+Mg~ 18). Most Fe rich composition of biotite in enclaves is observed in restite (Fe/Fe+Mg~72), while the plagioclase in this is most albitic (An18).

Rakcham Occurrence: In porphyritic granite perthitic K-feldspar is the dominant mineral while plagioclase is relatively finer grained and subordinate. Biotite is the main mafic mineral. Muscovite is of two generations. Composition of the host in perthitic K-Feldspar has significant Na content (Ab~8%). Anorthite content of plagioclase varies from oligoclase to andesine. Plagioclase is locally zoned in granodiorite and has higher calcium (An44), biotite is the main mafic and the muscovite content is very low. Garnet and allanite is present occasionally. Trondjemite is relatively finer grained variant and is made up dominantly of quartz, plagioclase and muscovite with rare biotite. Plagioclase is Ca-poor (albite to oligoclase). Monazite in the porphyritic granite from Rakcham is a Ce-monazite.

Chemical dating of both Mandi and Rakcham granite bodies has been carried out. In a euhedral monazite enclosed within quartz, chemical age determination yielded an age of 462 Ma with a standard deviation of 44 Ma (Kundu et al. 2006). This compares well with the reported Rb/Sr age of 453 ± 9 Ma for the Akpa, a granite body possibly part of Rakcham granite and 477 ± 29 Ma for Rakcham (Kwatra et al. 1999). Indications of Tertiary ages is obtained from two samples in the Rakcham area thus describing coexistence of Himalayan granite in this Pan-African age granite complex. In Mandi, the dominant granite (porphyritic granite) gives Pan-African age (514 Ma with a standard deviation of 49 Ma), which compares well with the reported age data for this occurrence (Jager et al. 1971, Mehta, 1977, Miller et al. 2001). However, effects of resetting of ages of monazite and commensurate mineralogical transformations record imprints of Tertiary geological events. It is possible that besides the presence of Tertiary granite, formation of trondjemite may also be linked to the Himalayan mountain building processes in Mandi and Rakcham occurrences.

References

- Bhanot VB, AK Bhandari, VP Singh and AK Kansal. 1979. Geochronological and geological studies of granites of Higher Himalaya, NE of Manikaran, H. P. *Journal of the Geological Society of India* 20: 90-94
- Chatterjee BC. 1976. Petrology and structural geology of the Mandi granite, Mandi district, Himachal Pradesh. *Geological Survey of India Miscellaneous Publications* 24: 302-315
- Frank W, A Gansser and V Trommsdorff. 1977. Geological observations in the Ladakh area (Himalaya): a preliminary report. *Schweizerische Mineralogische und Petrographische Mitteilungen* 57: 89-113
- Gupta LN. 1974. Petrology of Mandi granites and associated rocks. *Center of Advanced Studies, Punjab University, Chandigarh* 10: 95-108
- Jager E, AK Bhandari and VB Bhanot. 1971. Rb-Sr age determinations on Biotites and whole rock samples from the Mandi and Chor granites, Himachal Pradesh, India. *Eclogae Geologicae Helvetica* 64(3): 521-527
- Kwatra SK, VB Bhanot, RK Kakar and AK Kansal. 1986. Rb-Sr radiometric ages of the Wangtu Gneissic complex, Kinnaur District, Higher Himachal Himalayas. *Bulletin Indian Geological Association* 19(2): 127-130
- Kwatra SK, S Singh, VP Singh, RK Sharma, B Rai and N Kishore. 1999. Geochemical and geochronological characteristics of the early Palaeozoic granitoids from Sutlej-Baspa Valleys, Himachal Himalayas. In: Jain AK and RM Manickavasagam(eds). *Geodynamics of the N-W Himalaya. Gondwana Research Group Memoir No.6*: 145-158
- Kundu A, S Joshi, NC Pant and D Bhatnagar. 2006. Electron microprobe dating technique- critical evaluation and application for a Pan-African granite from the Himachal Himalayas. *Indian Journal of Geochemistry* 21(1): 211-230
- Mehta PK. 1977. Rb-Sr geochronology of the Kulu-Mandi belt: its implication for the Himalayan tectonogenesis. *Geologische Rundschau* 66(1): 156-175
- Miller C, M Thoni, W Frank, B Graseman, T Klotzli, D Guntli and E Draganits. 2001. The early Palaeozoic magmatic event in the Northwest Himalaya, India: Source, tectonic setting and age of emplacement. *Geological Magazine* 138(3): 237-251
- Pognante U, D Castelli, P Benna, G Genovese, F Oberali, M Meier and Tonarini S. 1990. The crystalline units of the high Himalayas in the Lahaul-Zaskar region (northwest India): Metamorphic-tectonic history and geochronology of the collided and imbricated Indian plate. *Geological Magazine* 127: 101-116

Out-of-sequence deformation and expansion of the Himalayan orogenic wedge: insight from the Changgo culmination, south-central Tibet

Kyle P Larson* and Laurent Godin

Department of Geological Sciences and Geological Engineering, Queen's University, CANADA

* For correspondence, email: larsen@students.geol.queensu.ca

The Changgo culmination, one of a series of granitic and/or metamorphic domal structures that crop out along the North Himalayan antiform, comprises a multi-phase, foliated granitic core surrounded by a polydeformed metasedimentary carapace. The carapace of the Changgo culmination consists of two structural domains. The upper domain is characterized by vertical thickening recorded as large-scale, close-to tight overturned, south-verging folds while the lower domain is characterized by a dominant transposition foliation. The contact between the meta-sedimentary cover and the granitic core is marked by a >300 m thick top-to-the north sense shear zone. The shear zone predominantly consists of mylonitized pelitic schist, but also contains 30–50 m thick lenses of sheared leucogranite. One of these leucogranite lenses has been dated as 35.35 ± 0.37 Ma based on U–Pb SHRIMP analyses. The main phase of the igneous core of the Changgo culmination is a foliated alkali-feldspar porphyritic granite, which has been dated using spot U–Pb SHRIMP analyses as 22.78 ± 0.91 Ma. Quartz c-axis petrofabrics measured in specimens of this foliated granite yield a top-to-the south shear sense. Undeformed aplite dykes that cut the foliated porphyritic granite yield a U–Pb TIMS monazite age of 22.08 ± 0.19 Ma. $40\text{Ar}/39\text{Ar}$ cooling ages of specimens sampled from both the meta-sedimentary carapace and igneous core of the Changgo culmination range between ca. 20 Ma and 16 Ma. The cooling ages young with increasing structural depth towards the center of the culmination.

The tectonic evolution of the Changgo culmination is interpreted to comprise three main episodes.

1) Crustal thickening through folding of the carapace: This episode is equivalent to Eohimalayan events described elsewhere along the orogen and, as in those events, it is interpreted to result in prograde metamorphism and melt formation. The sheared leucogranite lenses dated at ca. 35 Ma are interpreted to have formed during this episode.

2) Horizontal stretching and extrusion of the mid-crust: Subsequent to initial crustal thickening, or perhaps as a response to crustal weakening associated with earlier deformation, the mid-crustal core of the Himalayan-Tibetan orogen was extruded southward. The transposition foliation developed in the Changgo area, which is associated with a top-to-the-south shear sense in the granite core, is thought to reflect deformation during extrusion. In many areas along the Himalaya this extrusion is coincident with significant anatexis and formation of plutons. The Changgo granite is interpreted to have formed during the later stage of this episode at 22.78 ± 0.91 Ma. Top-to-the-south shear ended prior to the intrusion of aplite dykes at 22.08 ± 0.19 Ma. These dykes are nonetheless deformed adjacent to the top-to-the north shear zone

at the core/carapace interface. This shear zone, therefore, must have been active after the intrusion of the dykes. Deformation in the shear zone took place at $520 \pm 50^\circ\text{C}$ according to quartz petrofabric analysis and likely ceased prior to cooling through a calculated muscovite closure temperature of $414 \pm 21^\circ\text{C}$ at 18.43 ± 0.25 Ma. Based on shear sense, structural position and chronology, the shear zone at the core/carapace contact is interpreted to be a branch of the South Tibetan detachment system (STDS).

3) Out-of-sequence exhumation: The late-stage evolution of the Changgo culmination is interpreted to reflect out-of-sequence deformation within the Himalayan system. In central Nepal, southward extrusion of mid-crustal material between the STDS and the Main Central thrust ceased by ca. 19 Ma as a result of insufficient gravitational potential to drive the southward expansion of the orogenic wedge. The exhumation of the Changgo culmination, shortly thereafter, is interpreted to reflect the out-of-sequence rebuilding of the Himalayan wedge. Subsequent to the exhumation of the Changgo area, in-sequence deformation began to propagate southward as reflected in the ca. 16 Ma exhumation of the Chako antiform, and then the cooling of the central Nepalese frontal Himalaya (in the Annapurna region) at ca. 14–15 Ma (Figure 1). The orogenic wedge continued its lateral growth with the development of the Lesser Himalayan duplex and the succeeding activation of the Main Boundary thrust, thereby completing the transfer of slip from the kinematically unfavorable Main Central thrust.

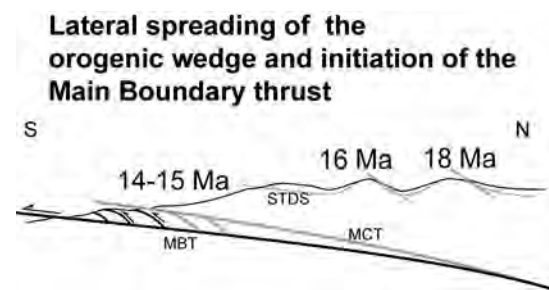


FIGURE 1. Diagram depicting the southward progression of cooling ages in the central Nepalese Himalaya. Assuming a constant rate of erosion cooling ages are interpreted to reflect the lateral spreading of the orogenic wedge after out-of-sequence rebuilding. Grey represents past structures, black represents active structures. MBT, Main Boundary thrust; MCT, Main Central thrust; STDS, South Tibetan detachment system.

Is the Ramgarh thrust equivalent to the Main Central thrust in central Nepal?

Kyle P Larson* and Laurent Godin

Geological Sciences & Geological Engineering, Queen's University, Kingston, CANADA

* For correspondence, email: larsen@students.geol.queensu.ca

Recent studies of the Main Central thrust (MCT), as exposed in the Nepalese Himalaya, have attempted to elucidate its character, contentious definition and locality (e.g. Searle et al. 2008, Imayama and Arita 2008). Examination of vertical exposures in the Budhi Gandaki and Darondi rivers, which drain the Manaslu-Himal Chuli massif, supported by detailed thermobarometry and microstructural analyses provide the means to critically evaluate the applicability of such studies.

The Ramgarh thrust is defined in western Nepal as the fault that juxtaposes green-schist facies rocks on top of lower-grade Lesser Himalayan series rocks. The Ramgarh thrust has not been mapped previously in the Budhi Gandaki or Darondi valleys; however, it has been inferred in the adjacent Annapurna and Langtang Himalaya. The geology of the Budhi Gandaki and Darondi valleys is dominated by a >30 km thick package of transposed medium-to high grade metamorphic rock of the Greater Himalayan series. The upper boundary of the highly strained section is the base of the top-to-the-north sense shears zone of the South Tibetan detachment system, while the lower boundary of the highly strained package is interpreted to be the MCT using the definition of Searle et al. (2008). In the Budhi Gandaki, rocks in the hanging wall of the MCT show evidence of Tertiary metamorphism, display abundant C/S/C' fabrics, yield quartz c-axis crystallographic preferred orientations that suggest horizontal stretching, and contain partial melt at higher structural levels. Rocks below the MCT often preserve primary sedimentary features such as bedding, contain abundant detrital porphyroclasts,

and are characterized by large-scale folding indicative of vertical thickening. Mapping the MCT at the base of the transposed, pervasively deformed rock package exposed in the Budhi Gandaki and Darondi valleys positions the fault more than 20 km farther south than previous studies.

In the Budhi Gandaki and Darondi valleys, the MCT separates greenschist or higher-grade metamorphic rocks over unmetamorphosed-to low-grade rocks of the Lesser Himalayan series, similar to the Ramgarh thrust in western Nepal. There is nowhere in the Budhi Gandaki or Darondi valleys direct evidence for the large-scale structural repetition of lithologic units or a localization of strain along a discrete fault above the MCT; analysis of quartz petrofabrics further indicates that the entire meta-sedimentary package was likely deformed at temperatures exceeding 500°C. Furthermore, thermobarometric and ⁴⁰Ar/³⁹Ar cooling profiles across the study area do not contain any disturbances that would necessitate mapping a thrust fault above the MCT. We therefore suggest that the Ramgarh thrust mapped in other areas may actually be equal to the MCT in the Budhi Gandaki and Darondi valleys.

References

- Searle MP, RD Law, L Godin, KP Larson, MP Streule, JM Cottle and MJ Jessup. 2008. Defining the Main Central thrust in Nepal. *Journal of the Geological Society* 165: 523-534
- Imayama T and K Arita. 2008. Nd isotopic data reveal the material and tectonic nature of the Main Central Thrust zone in Nepal Himalaya. *Tectonophysics* doi:10.1016/j.tecto.2007.11.051

Telescoping of isotherms beneath the South Tibetan Detachment, Mount Everest Massif: implications for magnitude of internal flow during extrusion of the Greater Himalayan Slab

Richard D Law^{1*}, Micah J Jessup², Michael P Searle³, John M Cottle³ and David Waters²

¹ Department of Geosciences, Virginia Tech, Blacksburg, VA24061, USA

² Department of Earth & Planetary Sciences, University of Tennessee, Knoxville, TN 37969, USA

³ Department of Earth Sciences, University of Oxford, Oxford OX1 3PR, UK

* For correspondence, email: rdlaw@vt.edu

Both petrologic and microstructural/crystal fabric data indicate that isotherms recorded in the schists and gneisses of the Greater Himalayan Slab (GHS) and located in the footwall to the South Tibetan Detachment System (STDS) have undergone extreme telescoping during penetrative flow associated with southward extrusion of the GHS from beneath the Tibetan Plateau. Within the Rongbuk Valley located to the north of Mount Everest we have made vertical sampling traverses working downward from the STDS into the GHS at Hermit's Gorge, Rongbuk Monastery

and the northern entrance to Rongbuk Valley. Adopting the calibration of Kruhl (1998) and Law et al. (2004), deformation temperatures were estimated using the opening angle of cross girdle c-axis fabrics measured by optical microscopy in plastically deformed and dynamically recrystallized quartz grains in each sample. Traced from south to north, linear regression of the deformation temperature data indicates apparent thermal gradients of 420, 385 and 369 °C per km for the Hermit's Gorge, Rongbuk Monastery and northern sampling transects respectively (Figure

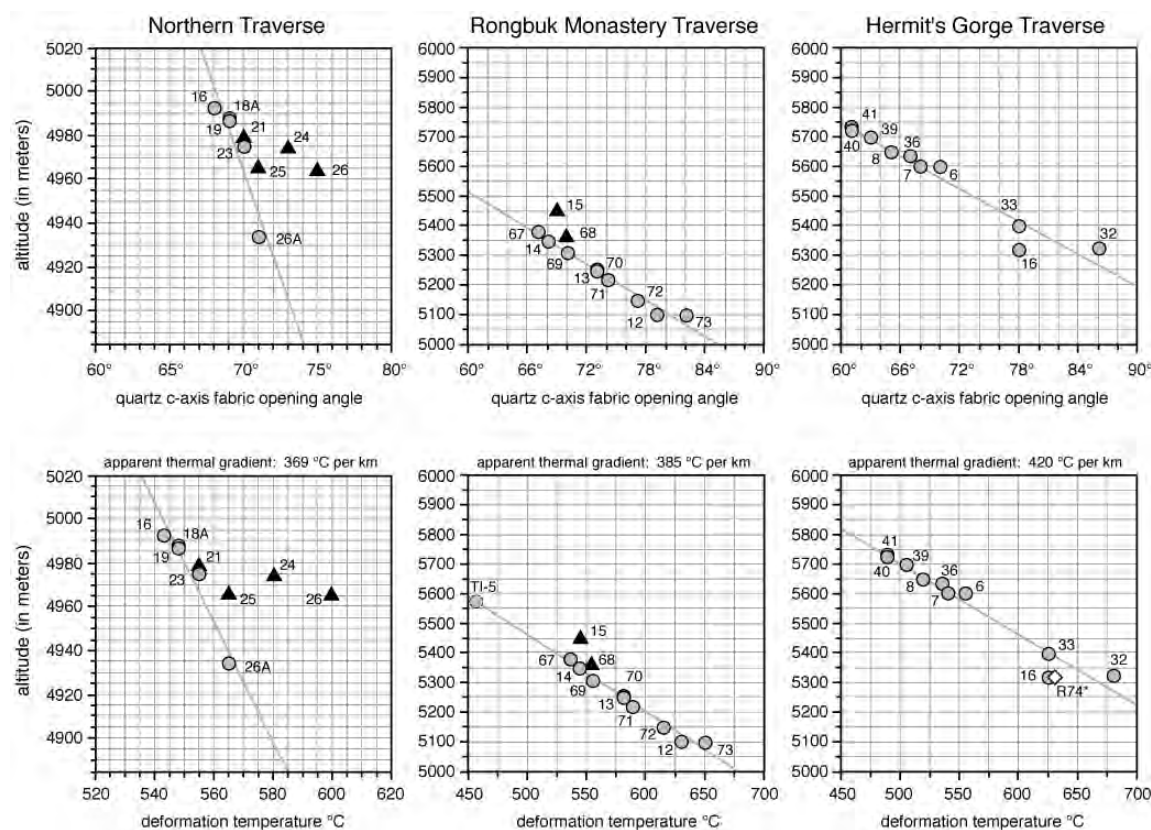


FIGURE 1. Upper row: opening angle of cross-girdle c-axis fabrics versus sampling altitude in (from north to south) the Northern, Rongbuk Monastery and Hermit's Gorge traverses. Gray circles and black triangles indicate data from metasedimentary rocks and leucogranite sills respectively. Linear regression lines for opening angle versus altitude (metasedimentary rocks only) are shown. Lower row: deformation temperatures (using the calibration of Kruhl 1998 and Law et al. 2004) versus sampling altitude. Linear regression lines (metasedimentary rocks only) used to estimate apparent thermal gradients are shown. Note deformation temperatures estimated for leucogranites at a given altitude are always greater than those for metasedimentary rocks suggesting that leucogranites cooled during deformation. Open diamond symbol (sample R74) in Hermit's Gorge traverse indicates phase-equilibria based temperature data of Hodges et al. (1992) from same outcrop as our sample 16.

1). Isothermal surfaces projected between these three traverses have an apparent dip of c. 2° towards the NNE, parallel to the apparent sheet dip of foliation.

The observed telescoping of isotherms could be due to: a) penetrative strain associated with extreme vertical thinning, b) chilling from juxtaposition against cooler hanging wall rocks, or c) downward increasing transport of material during penetrative flow associated with southward extrusion of the GHS as assumed, for example, in channel flow models. Vertical penetrative thinning requires strain ratios of between 100:1 and 250:1 measured in XZ sections for which there is no supporting field or microstructural evidence - assuming geothermal gradients of 40-25 °C per km during plane strain deformation (as indicated by the cross girdle fabrics) at constant volume. Chilling against cold hanging wall rocks is a possibility requiring further analysis, but in itself implies significant (at least tens of kilometers) transport in order to place hot GHS footwall rocks against cooler Tethyan hanging wall rocks.

Adopting the differential transport model, simple geometric analysis using cross sections drawn parallel to the local 030° transport direction indicated by stretching lineations in the GHS suggests that detachment-parallel transport magnitudes of 25-85 km are needed to place rocks originally deforming at 675°C at no more than 0.5 km beneath stationary rocks at 475°C, assuming geothermal gradients of 40 to 25°C and particle paths parallel to an overlying planar STDS dipping at between 10 and 5° to the north. Perhaps more realistically, if both the reference rock particles at

475 and 675°C are moving during extrusion, and do not become coupled at a vertical spacing of 0.5 km until they pass through the brittle-ductile transition zone (c. 300°C), then detachment parallel transport magnitudes of 85-170 and 45-85 km are indicated for the 675 and 475°C reference particles respectively, with differential transport on the order of 45-85 km between these reference particles. These particle transport estimates are similar to those previously calculated from petrologically determined barometry data of GHS rocks in the Everest region (Searle et al. 2003) and are at least compatible with recently published channel flow models for extrusion and exhumation of the GHS.

References

- Hodges KV, RR Parrish, TB Housch, DR Lux, BC Burchfiel, LH Royden and Z Chen. 1992. Simultaneous Miocene extension and shortening in the Himalayan orogen. *Science* 258: 1466-1470
- Kruhl JH. 1998. Reply: Prism- and basal-plane parallel subgrain boundaries in quartz: a microstructural geothermobarometer. *Journal Metamorphic Petrology* 16: 142-146
- Law RD, MP Searle and RL Simpson. 2004. Strain, deformation temperatures and vorticity of flow at the top of the Greater Himalayan Slab, Everest Massif, Tibet. *Journal of Geological Society of London* 161: 305-320
- Searle MP, RL Simpson, RD Law, RR Parrish and DJ Waters. 2003. The structural geometry, metamorphic and magmatic evolution of the Everest massif, High Himalaya of Nepal - South Tibet. *Journal of Geological Society of London* 160: 345-366

Does the Karakoram fault interrupt mid-crustal channel flow in the western Himalaya?

Mary L Leech

Department of Geosciences, San Francisco State University, San Francisco, CA 94132, USA
E-mail: leech@sfsu.edu

Variations in the volume and age of Miocene granites and in mid-crustal conductance from the northwest Himalaya to southeastern Tibet imply lateral differences in late orogenic processes. The east-west change occurs near Gurla Mandhata dome, where the Karakoram fault terminates and merges with the Indus-Yarlung suture zone. The 'channel flow' model, developed in southeastern Tibet, predicts anatectic partial melts beneath the Tibetan plateau are gravitationally-driven south to a topographic erosional front and are exposed as leucogranites in the Greater Himalaya Sequence; upwellings of these channel granites occur as gneiss domes in the Tethyan Himalaya Sequence. Magnetotelluric profiles show high conductivity 30-40 km deep beneath Tibet from c. 400 km north of the Main Frontal thrust south across

the suture zone, beneath the Himalayan gneiss domes, and to the topographic front; this conductive middle crust implies 2-4% partial melt in the northwest Himalaya and 5-12% melt in southeastern Tibet, sufficient in the latter case to weaken rock for flow. East of the Karakoram termination channel granites are abundant and are as young as 7 Ma; west of the termination, channel granites are less abundant and no younger than 18 Ma. Middle Miocene (16-14 Ma) leucogranites are found in the Karakoram shear zone located north of the suture zone and south of the proposed anatectic melt source. The initiation of motion on the crustal-penetrating Karakoram fault at 25-21 Ma may have created a barrier to southward flow of mid-crustal melts and acted as a vertical conduit for these same melts.

Miocene exhumation of the granulite-eclogite of the Ama Drime range (high Himalayas) through polyphased syn-convergence normal faulting

Philippe Hervé Leloup^{1*}, Elise Kali², Nicolas Arnaud², Gweltaz Mahéo¹ and Emmanuelle Boutonnet^{1,2}

¹ *Laboratoire des Sciences de la Terre, CNRS UMR 5570, Université Claude Bernard Lyon 1-ENS Lyon, 69622 Villeurbanne Cedex, FRANCE*

² *Géosciences Montpellier (UMR CNRS 5243), Groupe GEODE, CC 060, Université de Montpellier 2, Place Eugène Bataillon, 34095 Montpellier Cedex 5, FRANCE*

* *For correspondence, email: herve.leloup@univ-lyon1.fr*

E-W extension in southern Tibet, and related N-S normal faults, are generally interpreted as resulting from the ongoing post-orogenic thinning of a hot and thick crust. It however appears that some of these faults are quite old and may result from other mechanisms.

High grade rocks have been exhumed in the core of the Ama Drime range in South Tibet. This range is bounded to the east (DingYe) and the west (Karta) by two major presently active normal faults, that also offset the STDS. The footwall of the DingYe fault consists of migmatitic, sillimanite-garnet bearing gneisses with kyanite relics intruded by deformed and undeformed leucogranites. C/S relations show top to the east ductile normal shearing prior to the presently active brittle normal faulting. Microprobe measurements and pseudosections analysis show minimum pressures of equilibration of 13.5 kbar and temperature < 650°C. The gneisses first record an episode of isobaric heating up to ~750°C leading to partial melting. This was followed by the main phase of decompression to 6kbar and 700°C during ongoing partial melting. Migmatitic gneisses SHRIMP U/Pb dating of monazite give middle Miocene ages (~14 Ma) for partial melting, while SIMS U/Pb dating of zircons from orthogneisses of the same unit reveal ages of more than 2 Ga. P-T conditions and inherited Proterozoic ages indicate that the core of the AmaDrime belongs to the Lesser Himalayan Crystalline Series (LHCS as in Groppo et al., 2007, *J Metam. Geol.*). 40Ar/39Ar dating suggest that the main exhumation took place prior to ~13 Ma on the eastern side of the AmaDrime.

To the east, in the hanging-wall of the DingYe fault, garnet-sillimanite micaschists with staurolite relics, intercalated with deformed tourmaline-bearing leucogranites and locally intruded by un-deformed ones, are sheared top to North in relation with the overlying STDS. Paleozoic inheritance in zircons shows that the unit belong to the High Himalayan Crystalline series. P-T paths constrained by garnet isopleths show decompression and reheating from 6 to 4 kbar and 600 to 660°C implying ~6kb of differential unroofing with respect to the core of the AmaDrime. U/Pb SIMS dating of monazite on un-deformed and deformed leucogranites suggest a middle Miocene age (~17 Ma) for the end of the deformation associated with the STDS. 40Ar/39Ar dating suggests that the rocks cooled below 350°C at ~14.5 Ma.

A ductile normal fault, whose age will be constrained by ongoing 40Ar/39Ar dating, also exist on the western flank of the range. The Ama Drime thus appears to be a fault-bounded anticlinorium in the prolongation of the N-S Arun fold. Uncertainties on the dating of the deformation phases leave open two main possibilities. 1) Fast exhumation of deep (~35 km) partially molten crustal rocks took place in less than 1 Myr, just after the end of motion on the STDS. 2) Exhumation along the N-S Ama Drime shear zones occurred at the same time than normal faulting along the E-W STDS. In any case, N-S ductile normal faults of the Ama Drime are not related to the onset of the ongoing generalized E-W extension in southern Tibet.

Lateral heterogeneity in lithospheric structure in SE Tibet

Anne Meltzer*, Brian Zurek, Stephane Sol and Lucy Brown

Department of Earth and Environmental Sciences, Lehigh University, Bethlehem, PA 18015, USA

** For correspondence, email: ameltzer@lehigh.edu*

Southeastern Tibet hosts the termination of the Himalayan orogen in the Eastern Himalayan Syntaxis and a transition between the geodynamic setting of the main Plateau, its eastern margin, and the lithosphere of southeast Asia. The Eastern Himalayan Syntaxis occupies a substantial portion of the diffuse India-Asia collision zone, and because it serves as the watershed for the largest rivers in Asia, its highly active tectonic and surface processes have a direct impact on over one billion people. The syntaxis is a crustal manifestation of the complex lithospheric dynamics associated with the Indian "indenter corner." Steep lateral surface velocity gradients and a laterally heterogeneous lithospheric structure mark the northeastern margin of the Indian plate. Such corners are also sites of significant accommodation of crustal convergence by erosion and fluvial evacuation. Within the core of the syntaxis, the Yarlung-Tsangpo River exits the Tibetan Plateau dropping ~ 2 km in elevation along an ~ 100 km section of the river cross cutting the Namche Barwa-Gyala Peri massif. This metamorphic massif is the site of high relief, high topography, and rapid recent ongoing exhumation exposing mid to lower crustal rocks of the Indian plate at the surface. Analysis of data recorded by a temporary seismic array document substantial lateral heterogeneity in lithospheric structure and rheology across southeastern Tibet. To first order, observed heterogeneity correlates to surface topography indicating that tectonic and surficial processes interact to shape the evolution of the orogen.

In southeastern Tibet, the fast directions of seismic anisotropy in the lithospheric mantle correlate with surficial geology including major sutures and shear zones, extensional rifts, and with the surface strain derived from the GPS velocity field. These observations are consistent with a clockwise rotation of material around the eastern Himalayan syntaxis and suggest coherent and distributed lithospheric deformation beneath much of southeastern Tibet. The presence of small-scale and regional lateral variations in seismic anisotropy is observed within individual tectonic domains such as the Lhasa terrane and across major sutures and tectonic blocks. In the Lhasa terrane, we observe a change in the orientation of the fast axis of shear-wave polarization suggesting a change in the mode of deformation from orogen perpendicular extension in central Tibet to orogen parallel strike-slip in the eastern syntaxis. Shear-wave splitting measurements also show lateral variations in seismic anisotropy across the Tsangpo and the Bangong sutures indicating that these sutures separate lithospheric domains with distinct rheological properties or deformation regimes.

Detailed 3-d receiver function analysis documents a dramatic change in crustal thickness, Poisson's ratio, and lower

crustal reflectivity across the transition from the central Tibetan plateau to the eastern syntaxis. Crustal thickness beneath the southeastern Tibetan plateau varies between 65 to 75 km but thins eastward beneath the eastern margin of the plateau to 42-50 km. Regionally Poisson's ratio is low (0.24-0.25) where the crust is thick and tends to increase (0.26-0.29) where the crust is thinner. Inversion for velocity structure and geometry using finite difference wave-form inversion indicates a high velocity (7.5 to 7.8 km/s) layer near the base of the crust extends north of the Tsangpo suture beneath the southern Lhasa block and terminates just west of the Namche Barwa - Gyala Peri massif. Modeled P-wave velocities for this layer are consistent with eclogite. Further east, an asymmetric anticlinal fold on the crust-mantle boundary is associated with the Namche-Barwa/Gyala Peri metamorphic massif. The asymmetric fold trends north south and is ~ 50 km wide with an ~ 10 km near vertical step in the Moho on its eastern side. The fold on the crust-mantle interface correlates with a region of high topography and rapid recent exhumation on the surface. Locally higher values of Poisson's ratio (0.26-0.29) exist in this region suggesting a change in average crustal composition, and/or areas with some partial melt.

The eastern syntaxis is seismically active with over 3800 regional and local events ($M > 1.4$) located during a 15-month window. Seismicity is unevenly distributed. A significant number of events locate within the northern margin of the Namche Barwa - Gyala Peri massif. While these events locate at a range of depths in the upper 20 km of the crust, a significant number of events locate above sea level. These events tend to have extensional focal mechanisms consistent with the release of topographic stress where the Tsangpo and Po-Tsangpo rivers generate dramatic relief. Seismicity is also associated with portions of the Himalayan front, linear river valleys, the Gulu rift, the Nari Yun Chu (or Cona-Qusum) rift, and the Burmese arc. Seismicity is more evenly distributed in the Qiangtang terrane in contrast to the Lhasa terrane which contains several relatively aseismic regions. A portion of the Himalayan front in this region is also relatively aseismic. Most of the seismicity within the plateau appears to be concentrated in the upper 20 km of the crust but a modest number of events locate in the lower crust and upper mantle.

To first order, lateral heterogeneities in structure and rheology at depth correlate with the transition from the high elevation low relief plateau in central Tibet to deeply incised linear valleys in southeastern Tibet. Our observations suggest that lateral heterogeneities play an important role in the geodynamic evolution of the region.

Polyphase deformation history of the “Tibetan Sedimentary Sequence” in the Himalayan chain (South-East Tibet)

Chiara Montomoli^{1*}, Erwin Appel², Antolin Borja², István Dunkl³, Rachida El Bay², Lin Ding⁴ and R Gloaguen⁵

¹ University of Pisa, ITALY

² University of Tübingen, GERMANY

³ University of Göttingen, GERMANY

⁴ Institute of Tibetan Plateau Research, CAS, Beijing, CHINA

⁵ University of Freiberg, Freiberg, GERMANY

* For correspondence, email: montomoli@dst.unipi.it

Meso and microstructural analyses performed on the Triassic flysch belonging to the Tibetan Sedimentary Sequence cropping out in SE Tibet led to recognize a polyphase deformation history linked to the evolution of continental collision. The study area is located SE of Lhasa, from Tsedong and Gyatsa to the southern Yala Xiangbo dome.

In the southern analyzed sectors the main deformation event is a D1 tectonic phase. During D1 metric to chilometric asymmetric F1 folds developed. The folds, facing to the South and striking ENE-WSW are associated to an axial plane foliation (S1). S1 is a low grade foliation and varies from a disjunctive spaced stylolitic cleavage with no dynamic recrystallization to a fine continuous foliation. In the first case pressure solution is the dominant deformation mechanism while dynamic recrystallization of illite, quartz, calcite, oxides is associated to the continuous foliation.

Object lineations, trending NW-SE, are well represented by strain fringes, mainly composed by quartz, around pyrite crystals.

A later D2 deformation phase is superimposed to D1 structures. The D2 is represented by a faible crenulation cleavage in the southern portions, but moving towards the northernmost sectors, it becomes the predominant tectonic phase. Moving towards the Yarlung Tsampo Suture zone (YTSZ) we detected

the development of E-W trending F2 folds, from decimetric to decametric in size, verging to the North.

A synkinematic recrystallization of illite-sericite has been observed along S2 foliation that, in more strained areas, becomes a fine continuous foliation

The further tectonic evolution is characterized by the development of brittle-ductile shear zones. The shear zones are often localized on the inverted limbs of F2 folds.

Kinematic indicators are mainly represented by S-C structures and point to a top-to-the-north sense of movement.

D1 tectonic phase is linked to continental collision; the continuation of shortening gave rise to the back-verging D2 tectonic phase with a strain increase in the more internal areas (moving towards the YTSZ) related also to the development of Renbu-Zedong Thrust (Yin et al. 2000), bringing the TSS over the mélange complex (Harrison et al. 2000).

References

- Harrison TM, AYin, M Grove and OM Lovera. 2000. The Zedong Window: A record of superposed Tertiary convergence in southeastern Tibet. *Journal of Geophysical Research* 105 (B8): 19,311-19,320
- Yin, A and TM Harrison. 2000. Geologic evolution of the Himalayan-Tibetan orogen. *Annual Reviews in Earth and Planetary Sciences* 28: 211-280

How significant is erosion in extrusion- insights from analogue and analytical models

Soumyajit Mukherjee^{1*}, Hemin A Koyi², Christopher J Talbot² and AK Jain³

¹ *Engineering Mechanics Unit, Jawaharlal Nehru Centre for Advanced Scientific Research, Jakkur, Bangalore-560064, INDIA*

² *Hans Ramberg Tectonic Laboratory, Uppsala University, 752 36 Uppsala, SWEDEN*

³ *Department of Earth Sciences, Indian Institute of Technology Roorkee, INDIA*

* *For correspondence, email: soumyajitm@gmail.com*

The absolute role of climate/erosion in extrusion of mountains has been debated for a long time. Field-studies, micro-structural observations and few analytical trials confirm that the extrusion of the Higher Himalayan Shear Zone, Sutlej section took place initially by simple shearing and was followed by combined simple shear and channel flow in a shifting mode (Mukherjee 2007). The extrusion mechanism of the HHSZ is studied with 10 analogue models of channel flow initiating from a horizontal channel and extrusion through a linked inclined channel. The inclined channel is the model HHSZ and is of parallel, gently diverging-up and strongly diverging-up geometries in different considerations. In these experiments, Polydimethylsiloxane (PDMS), a transparent Newtonian viscous polymer is used as the model material and geometric- and dynamic similarities are maintained with the prototype. Six flow zones are deciphered in the two channels in the mature stage of extrusion of the PDMS. Parabolic profiles are produced at the middle of both the inclined- and the horizontal channel during a Poiseuille and Jeffery Hamel flows. The part of the PDMS originally inside the horizontal channel starts moving through the inclined channel at a faster rate than the part of the PDMS initially residing in the inclined channel. This in effect gives rise to thrust movement of the former part of the PDMS. The thrust plane originates at the corner joining the inclined and the horizontal channel and rotates while coming closer to the free surface. The tectonic insights gained from these experiments are (i) secondary ductile thrusting took place in the HHSZ as a delayed response to its channel flow mode of extrusion, (ii) the genesis of the thrust seems to be related to the change in the direction of extrusive flow- from horizontal to inclined up; (iii) as these models were performed without any erosion of the extruded PDMS, erosion induced by climate did not trigger nor was a deciding factor in the genesis of the secondary thrust and concomitant extrusion of the HHSZ. However, erosion induced by a disparity in precipitation on the HHSZ might have augmented the extrusion process i.e. it had a passive role. In Sutlej section of the HHSZ, the simulated thrust can be correlated with the Chaura Thrust with the recorded activation at least 13 Ma after the ongoing extrusion of the HHSZ by channel flow mechanism around 18 Ma.

Salt diapirs are spectacular natural structures and are products of an interaction between the extrusive force that build and erosion that tends to degrade them. While in humid climate, their erosion rate can reach few mm per year, in arid climates it goes down to one tenth to that of the former rate (Bruthans et al. 2008). Salt diapirism has been modeled as a product of the density difference between the salt and the surrounding limestone country rock in the islands of Hormuz and Namakdan in the Persian Gulf (Mukherjee et al. 2007). Most of the 200 or so diapirs of Hormuz salt in the Zagros mountains of Iran extrude majestic mountains of salt that rise 400 m above their strong vents in limestones. Even if a difference in density between the salt and the country rocks are in the order of 10^{-1} gm.cm⁻³, such a low magnitude persistent over tens of thousands of years can give rise to extrusion of the salt for kilometers that can have dynamic viscosity as high as 1021 Pa s (Mukherjee et al. 2007). Without taking into account their erosion rates, diapirism was modeled as being triggered and maintained by the density contrast. This indicates that erosion is not a crucial controlling factor for the extrusion. Erosion is one out of many components that can, however, modify the pressure gradient controlling the extrusion process. The other components are (i) the up-building extruded mass of salt that imparts temporally increasing weight downwards, and (ii) gravitational spreading that allows the extruded salt to flow away (Weinberger et al. 2006).

References

- Bruthans J, N Asadi, M Filippi, Z Vilhelm. and M Zare. 2008. A study of erosion rates on salt diapir surfaces in the Zagros Mountains, SE Iran. *Environmental Geology* 53: DOI 10.1007/s00254-007-0734-6
- Mukherjee S. 2007. *Geodynamics, Deformation and Mathematical Analysis of Metamorphic Belts, NW Himalaya*. Unpublished Ph.D. thesis. Indian Institute of Technology Roorkee: 267p
- Mukherjee S, CJ Talbot, HA Koyi. 2007. Estimation of viscosity of natural salts of the Hormuz and Namakdan salt diapirs in the Persian Gulf. *Annual Transaction of Nordic Rheology Society* 15: 189-196
- Weinberger R, V Lyakhovskiy, G Baer and ZB Begin. 2006. Mechanical modeling and InSAR measurements of Mount Sedom uplift, Dead Sea basin: Implications for effective viscosity of rock salt. *Geochemistry Geophysics and Geosystems* 14: DOI: 10.1029/2005GC001185

Flexural-slip folding and fold-accommodation faulting in the Tethyan Sedimentary Zone, NW Himalayas

Dilip K Mukhopadhyay

*Department of Earth Sciences, Indian Institute of Technology Roorkee, Roorkee 247667, INDIA
E-mail: dilipfes@iitr.ernet.in*

In the northwestern Himalayan orogenic segment, a highly metamorphosed and deformed lithotectonic zone (Central Crystallines) separates two sedimentary belts. The southern sedimentary belt consists of largely upper Proterozoic Lesser Himalaya Zone (LHZ), and Tertiary Sub-Himalaya Zone (SHZ). In recent years, detailed structural studies including application of cross-section balancing techniques by many workers show that the LHZ and SHZ constitute a typical frontal fold-thrust belt. Thrust faulting and fault-related folding over a gentle northerly-dipping detachment are the main structural elements in this belt.

The Tethyan Sedimentary Zone (TSZ) occurring north of the Central Crystallines, contains a continuous sequence of sedimentary rocks ranging in age from Proterozoic through Palaeozoic to Cretaceous. The basal part of TSZ contains very low-grade metamorphic rocks at places. These rocks were deposited on the leading edge of the northerly moving Indian plate. The contact between the Central Crystallines and the TSZ is marked by a system of low northerly dipping normal faults collectively known as South Tibet Detachment System (STDS). The stratigraphy and paleontology of this zone have been studied for more than a hundred years and they are very well known. However, the deformation history in this belt is still not very well understood.

The TSZ in the Himachal Himalayas consists primarily of limestones with subordinate amount of sandstones and shales. The

rocks are thinly bedded with thickness of individual beds ranging in scale from a few mm through few cm to tens of cm. The well-bedded rocks trace spectacular folds in outcrop to intermediate scales. Folds, tens of meters in amplitude, are seen on subvertical valley surfaces cut at high angles to strike. Tightness of folds varies from very open to very tight. The folds have straighter limbs and sharp hinges of limited areal extent giving rise to chevron or kink fold geometry. Axial planes are usually steeply dipping to subvertical and hinges are horizontal or gently plunging. Thus the folds usually have horizontal upright geometry. Evidence of layer-parallel slip is very common with the slip direction towards the hinges of mesoscopic folds. The folds have developed through buckling of thinly-bedded multilayer with high viscosity contrast and moderate to low packing distance. The folding is not related to faulting. Consideration of map pattern, stratigraphic relations and analysis of structural data show that the large-scale structure can be best described as a horizontal upright synclinalorium. There are innumerable faults present in outcrop to intermediate scales. These faults are fold-accommodation faults and are accommodation structures developed during folding. Therefore faulting is a consequence of folding. This interpretation is in contrast to a few recent works that suggest the deformation pattern in the TSZ is somewhat akin to frontal fold-thrust belt seen in the Lesser and Sub-Himalaya zones.

The Paleogene record of Himalayan erosion; Burma and Bangladesh

Yani Najman^{1*}, Ruth Allen¹, Mike Bickle², Marcelle BouDagher-Fadel³, Andy Carter³, Eduardo Garzanti⁴, Maxence Paul⁵, Jan Wijbrans⁶, Ed Willett⁷, Grahame Oliver⁸, Randy Parrish⁹, S Humayun Akhter¹⁰, Sergio Ando⁴, Dan Barfod¹¹, Emdad Chisty¹², Laurie Reisberg⁵, Giovanni Vezzoli⁴ and Jasim Uddin¹³

¹ Department of Environmental Science, Lancaster University, UK

² Dept of Earth Sciences, Cambridge University, UK; ³ Dept of Geological Sciences, UCL-Birkbeck, UK

⁴ Dipartimento di Scienze Geologiche e Geotecnologie, Universita Milano-Bicocca, ITALY

⁵ Centre de Recherches Pétrographiques et Géochimiques-CNRS, Vandoeuvre-Les-Nancy Cedex, FRANCE

⁶ Dept Isotope Geology, Vrije Universiteit, Amsterdam, NETHERLANDS

⁷ Cairn Energy plc, Edinburgh, UK. Now at: Bowleven plc, Edinburgh, UK

⁸ School of Geography and Geosciences, St-Andrews University, UK

⁹ NIGL, BGS Keyworth, UK and Dept of Geology, Leicester University, UK

¹⁰ Dept of Geology, University of Dhaka, BANGLADESH

¹¹ SUERC, East Kilbride, UK; ¹² Cairn Energy Bangladesh, Dhaka, BANGLADESH

¹³ Tullowoil, Dhaka, BANGLADESH

* For correspondence, email: y.najman@lancs.ac.uk

The record of sediment eroded from a mountain belt provides a valuable archive of an orogen's early evolution. Yet identification of an archive which records the Palaeogene erosion of the Himalaya's southern flanks remains enigmatic. In the western Himalaya, orogenic-derived material has been identified in the Indus Fan as far back as Mid Eocene, although the precision of dating is poor, and the proportion of material derived from north of the suture zone rather than the Himalaya's southern flanks is likely high (Clift et al. GSA Bulletin 2001). For the eastern-central Himalaya, no significant Palaeogene sediments eroded from the orogen's southern flanks have been documented. In the foreland basin, a disconformity represents much of the Paleogene (Najman Earth Science Reviews 2006). In the Bengal Basin, the Oligocene deposits are of disputed provenance (Johnson and Nur Alam GSA Bulletin 1991; Uddin and Lundberg GSA Bulletin 1998). In the Bengal Fan, the onset of turbidite sedimentation can be dated no more precisely than approximately the Eocene-Oligocene boundary based on extrapolation of accumulation rates at ODP Site 116, and "post Paleocene" by seismic correlation of a dated unconformity on the Ninetyeast Ridge into the adjacent basin (Curry et al. Marine and Petroleum Geology 2003 and references therein). It has also been proposed that the Palaeogene Indo-Burman Ranges represent Palaeogene Bengal Fan material offscraped into an accretionary prism (Curry et al. AAPG Memoir 1979) but this provenance is disputed (Mitchell J. Geol Soc London 1993).

We undertook a detailed provenance analysis of the Indo-Burman Ranges in Burma and Bangladesh, and identified a major difference in composition between Palaeogene and Neogene rocks. Whilst the Neogene Indo-Burman Ranges (west of the Kaladan Fault, in both Bangladesh and Burma) are clearly Himalayan-derived (Allen et al. in review, Allen et al. in press), the Paleogene rocks contain a much higher proportion of arc-derived material, most probably derived from the Burman arc to the east (Allen et al. in press).

In the Bengal Basin we have identified earliest evidence of Himalayan detritus at 38 Ma (Najman et al., in press), determined using an integrated provenance approach utilising seismic data and a number of isotopic and geochemical techniques. Detrital mineral lag

times show that exhumation of the orogen was rapid by 38 Ma. The identification of sediments shed from the rapidly exhuming southern flanks of the eastern-central Himalaya at 38 Ma, provides a well dated accessible sediment record 17 Myrs older than the previously described 21 Ma sediments in the foreland basin in Nepal (DeCelles et al. Tectonics 2001). Discovery of Himalayan detritus in the Bengal Basin from 38 Ma: 1) resolves the puzzling discrepancy between the lack of erosional evidence for Paleogene crustal thickening that is recorded in the hinterland; 2) invalidates those previously proposed evidences of diachronous collision which were based on the tenet that Himalayan-derived sediments were deposited earlier in the west than the east; 3) requires that models of Himalayan exhumation (e.g. by mid crustal channel flow) be revised to reflect vigorous erosion and rapid exhumation by 38 Ma, and 4) provides evidence that rapid erosion in the Himalaya was coincident with the marked rise in marine ⁸⁷Sr/⁸⁶Sr values since ~40 Ma. Whether 38 Ma represents the actual initial onset of vigorous erosion from the southern flanks of the east-central Himalaya, or whether older material was deposited elsewhere, perhaps now buried beneath the thrust stack, remains an open question.

References

- Allen R, Y Najman, A Carter, D Barfod, M Bickle, H Chapman, E Garzanti, G Vezzoli, S Ando and Parrish R. In press. Provenance of the Tertiary sedimentary rocks of the Indo-Burman Ranges, Burma (Myanmar): Burman arc or Himalayan-derived? *Journal of the Geological Society of London*, [In press]
- Allen R, Y Najman, E Willett, A Carter, D Barfod, E Garzanti, J Wijbrans, M Bickle, G Vezzoli, S Ando, G Oliver and J Uddin. New seismic, biostratigraphic and isotopic constraints to the geological evolution and sedimentary provenance of the SE Bengal Basin, Bangladesh. *Basin Research*, [in review]
- Najman Y, M Bickle, M BouDagher-Fadel, A Carter, E Garzanti, M Paul, J Wijbrans, E Willett, G Oliver, R Parrish, H Akhter, A Allen, S Ando, E Chisty, L Reisberg and G Vezzoli. In press. The Paleogene record of Himalayan erosion, Bengal Basin, Bangladesh. *Earth and Planetary Science Letters*, [In press]

The Main Central Thrust Revisited: New Insights from Sikkim Himalaya

Sudipta Neogi^{1*} and V Ravikant²

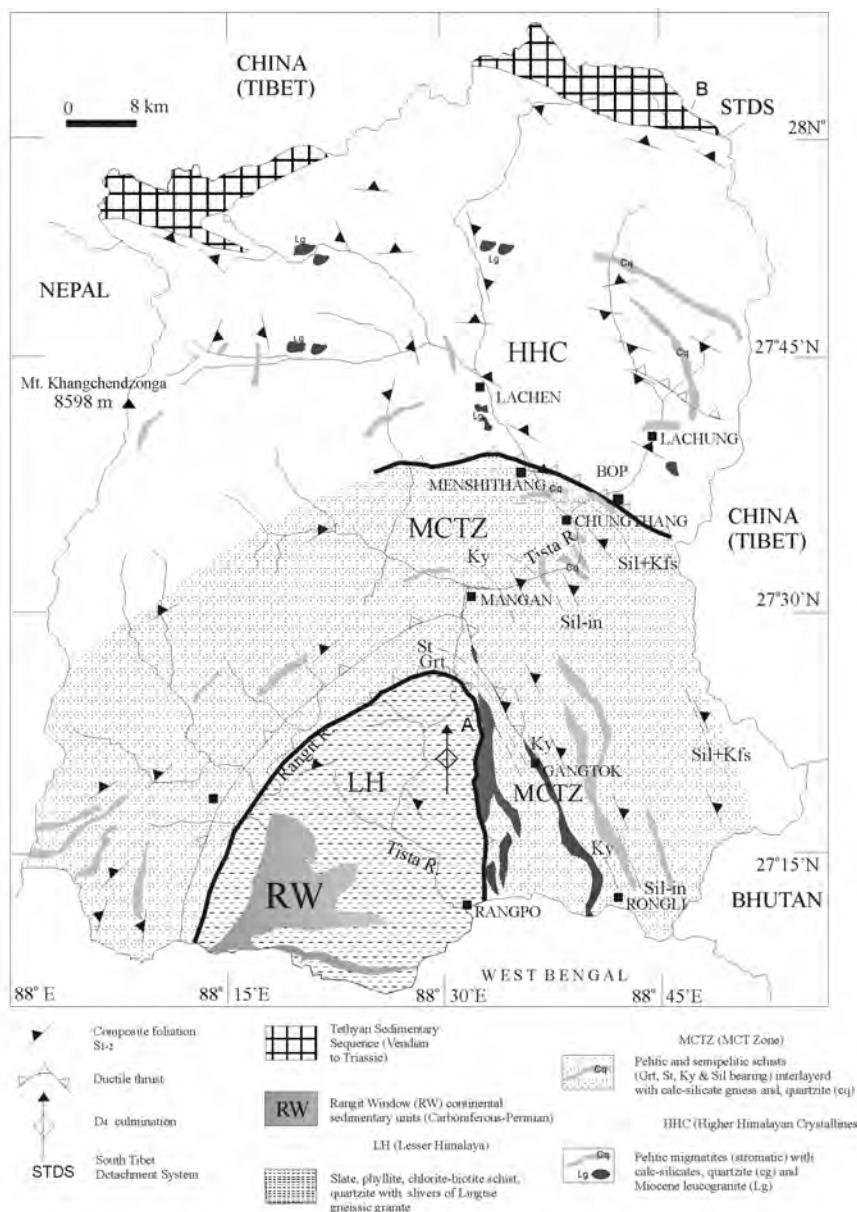
¹ Geological Survey of India, 27 J.L. Nehru Road, Kolkata – 700 016, INDIA

² Indian Institute of Technology, Roorkee-247667, INDIA

* For correspondence, email: sudiptaneogi@hotmail.com

One of the most coherent crustal sections in the entire Himalaya, from the point of view of lack of disruption or repetitions of key beds due to thrusting, is exposed in Sikkim. Structural studies across this unique section in Sikkim, covering the so-called Lesser Himalaya, the Higher Himalaya and the intervening Main Central

Thrust zone (MCT zone) reveals a remarkable continuity in structures and metamorphic history. Due to lack of clear evidences for pervasive ductile shearing and thrusting, the position of the MCT in Sikkim and therefore, the exact demarcation of the Lesser and Higher Himalayan Belts has remained controversial with the



MCT being placed at different positions by various workers.

Rocks from the entire studied section in Sikkim preserve imprints of four deformational episodes (D1-D4), with broad similarity in their deformation patterns and structural elements. A single penetrative regional planar structure (S2), associated with F2 folds and sub-parallel to narrow ductile shears, formed during the dominant D2 deformation episode. A complete and systematic sequence of inverted progressive Barrovian metamorphic zones is exposed, showing a regular pattern of variation of P and T (increasing P and T upsection; Neogi et al. 1998, Dasgupta et al. 2004). Metamorphism was broadly coeval with the progressive deformation that produced the regional pervasive S2 fabric in all the domains, and continuing into the D2-D3 interkinematic period. The consistent relation of the porphyroblastic phases with the marker fabric in all the domains suggests a common growth history for the “index minerals” defining the Barrovian metamorphic zones.

In Sikkim, it has not been possible to map the MCT following its original definition as a thrust fault or as a lithostratigraphic boundary between the two distinct geological units, Lesser and Higher Himalaya, based on structural criteria. What is now seen is a broad zone of distributed ductile shearing with few localised discrete zones of ductile deformation, which have accommodated a major part of the shearing strain (Figure 1). This comes closest to the definition of the MCT zone, as identified from other parts of the Himalaya. The confusion in the definition of the MCT as a significant lithostratigraphic boundary between the Lesser and Higher Himalaya and the ~15-25 km wide MCT zone as observed now, can be largely reconciled if it is considered that these two had formed separately in time. We do not rule out the possibility that the lithostratigraphic boundary may be a relatively older surface that has been largely modified by a wide ductile shear zone during the main phase of Himalayan shortening. This is consistent with the work of DeCelles et al. (2000), Robinson et al. (2001) and Gehrels et al. (2003), who suggested that the Higher Himalaya may represent

an exotic terrane that was accreted to the Indian margin at some time during the Palaeozoic. Without discounting the possibility that parallel fabrics in the Lesser Himalaya, MCT zone and Higher Himalaya could be time-transgressive and in spite of the fact that direct correlation of the deformation events in these domains is not possible based on structural data alone, the simplest explanation seems to be that at least a part of the deformation and metamorphic history experienced by these domains was common and that the inverted metamorphic sequence was established during a single tectonothermal episode. This is consistent with the observed structural integrity, coupled with a smooth P-T profile of increasing P and T upsection, established through rigorous thermobarometry in earlier studies in Sikkim. Available age data from included monazite are not in conflict with such an interpretation and do not rule out a common event affecting the entire section.

A workable model on the Himalayan inverted metamorphic sequence would have to account for mechanisms in terms of combinations of heat sources and tectonic processes by which mineral growth could occur syntectonically with the second deformation event in each domain but at different times and in addition yield a profile which shows smooth increase in both P and T with structural height. The results of the present studies are evaluated in the light of available monazite age data.

References

- Dasgupta S., J Ganguly, and S Neogi. 2004. *Journal of Metamorphic Geology* 22: 395-412
- DeCelles, P.G., Gehrels, G.E., Quade, J., Lareau, B., and Spurlin, M., 2000. *Science* 288, 497-499
- Gehrels, G.E., DeCelles, P.G., Martin, A., Ohja, T.P., Pinhassi, G. and Upreti, B.N. 2003. *Geological Society of America Today* 13 (9): 4-9
- Neogi, S., Dasgupta, S., Fukuoka, M., 1998. *Journal of Petrology* 39: 61-99
- Robinson, D.M., DeCelles, P.G., Patchett, P.J., Garzzone, C.N., 2001. *Earth and Planetary Science Letters* 192: 507-521

Deformation partitioning at the rupture front in NW Himalaya: evidence from tectono-geomorphic and paleoseismic investigations

Anand K Pandey^{1*}, Prabha Pandey¹, Guru Dayal Singh¹, GV Ravi Prasad², K Dutta² and DK Ray²

¹ National Geophysical Research Institute, Uppal Road, Hyderabad - 500 007, INDIA

² AMS Radiocarbon Laboratory, Institute of Physics, Bhubaneswar - 751005, INDIA

* For correspondence, email: akpandey@ngri.res.in

The southernmost terrain defining intracrustal fault in Himalaya, Himalayan Frontal Thrust (HFT), is recognized as an abrupt topographic break separating the Sub-Himalayan Siwalik range from the Piedmont/alluvial plain. The relative relief of Sub-Himalaya, from Gangetic alluvium, was attained during Late-Quaternary due to episodic seismic slip on HFT. Recent active tectonic studies and paleoseismic investigations have documented the surface ruptures of past earthquakes in the HFT zone, which is recognized as the locus of primary earthquake rupture front in the Himalaya. The same is responsible for the growth of various levels of strath terraces and fold growth in the mountain front.

We explored the mountain front and HFT zone to explore the deformation partitioning in the mountain front in parts of NW Himalaya. Three levels of strath terraces and shear zones in the growing Dhanaura anticline have been mapped along transverse stream sections in Himachal Sub-Himalaya. The active faults and scarp are identified and paleoseismic trench across one of the surface rupture scarp (5-7 m high), with considerable lateral extension in the T1 terrace, is carried out. The trench was excavated close to another previously explored trench (Kumar et al. 2006) on a different fault scarp. In the trench section, two imbricate splays of surface rupture fault are observed, thrusting the Middle Siwalik

mudstone/sandstone over the T1 terrace deposits. The terrace deposits are folded by fault-propagation mechanism with thinning and truncation of the overturned limb in the footwall. The charcoal samples in the pre-earthquake surface, marked by soil development, have yielded calibrated ¹⁴C ages older than AD 1335±85 (2σ) suggesting that the event postdates this period. Similar timing was obtained for the adjoining trench by Kumar et al. (2006).

Analyzing the deformation characteristics of rupture in the present trench and previous trenches by Kumar et al. (2006) show distinctly contrasting structural expression. The variability in structural expressions on different fault scarps of the same age suggests that the rupture is partitioned on different splays laterally as it emerge and the front behaves more like an en echelon fault system in the Himalayan front rather than a single discrete fault. The terrace growth and fault also suggests that the strain is partitioned onto various splay faults which aid the fold growth of HFT zone.

Reference

Kumar S, S G Wesnousky, T K Rockwell, R W Briggs, V C Thakur and R Jayangondaperumal. 2006. Paleoseismic evidence of great surface rupture earthquakes along the Indian Himalaya. *Journal of Geophysical Research*. 111: B03304, doi:10.1029/2004JB003309

Geochemical characters of muscovite from the Pan African Mandi Granite, and its emplacement and evolution

NC Pant* and A Kundu

Geological Survey of India, NH-5P, N.I.T., Faridabad- 121001, INDIA

* For correspondence, email: pantnc@rediffmail.com

The Mandi granite, a well known Palaeozoic granite of the Himachal Himalaya, is emplaced in the medium grade metamorphic rocks of Vaikrita Group. The development of andalusite in the contact aureole of Mandi granite indicates its emplacement depth to less than 12-14 km. Several petrological variants such as porphyritic granite, fine-grained porphyritic granite and trondjemitic granite within the Mandi pluton have been recognized (Chatterjee 1976, Gupta 1994, Kundu et al. in press). Muscovite is a ubiquitous mineral in all of these variants. Muscovite is an indicator of crystallization history of granite. Thus, it is important to assess the magmatic or metamorphic nature of this mica.

Muscovite is present in variable amounts in the Mandi granite. They vary from being nearly absent to greater than 10 mode %. Textural features such as subhedral nature, sharp grain boundaries and high modal proportion indicate at least some of these to be a magmatic mineral. Igneous nature of muscovite is also indicated by their chemistry (Higher Ti in porphyritic and trondjemitic granite in TiO_2 - Fe_2O_3 - MgO plot; Monier et al., 1984; higher Al and Na and lower Mg and Si; Miller et al. 1981). The metamorphic/late muscovites are clearly distinguishable on chemical criteria. The magmatic muscovites are associated with

apatite, monazite and zircon. In deformed granites such coarse grains are commonly present as mica fish. Many of such coarse muscovite grains have a brighter rim which commonly has a trail of small grains of sphene. The rim portion of such grains have higher phengite component (FeO- 4 to 4.5 wt%, MgO = 0.55 to 1.5 wt %) and lower paragonite component ($Na/Na+K = 0.03$ to 0.04) than the core of the grains. Another textural variety of muscovite is present as fine grained flakes in foliated granites as part of the matrix. It defines the foliation plane in these granites. Such grains have compositions similar to the rim portions of large grains.

A cursory examination of the mineral chemistry of muscovite presented above indicate that significant percentage of the muscovites are of primary origin based on their Na/Na+K ratio an observation opposed to that of Nag et al. (2005). The upper stability of muscovite has been considered as 4 kbar and in view of the emplacement of Mandi granite at equivalent depth, as inferred from the development of andalusite in the contact zone, the emplacement conditions are well constrained. Micas of the Mandi granite and associated rocks have been used to decipher the emplacement conditions and evolutionary history of Mandi granite.

Segmented Nature of the Himalaya and Gangetic Plain

B Parkash*, Rajat S Rathor, AK Awasthi, Pitambar Pati, Balaji Bhosle, Rajendra P Jakhmola, Seema Singh and Vivekanand Acharya

Department of Earth Sciences, Indian Institute of Technology Roorkee, Roorkee -247 667, INDIA

* *For correspondence, email: bparkfes@iiyr.ernet.in*

The Ganga River terraces near Hardwar, in eastern part of the Dehradun Valley, northwestern Himalaya, close to the Himalayan Frontal Thrust (HFT), formed due to movements along this thrust. These terraces give overall uplift rate, slip rate and convergence rates 8.26 ± 1.67 mm/yr, 16.57 ± 3.35 mm/yr and 14.31 ± 2.90 mm/yr, respectively. These rates are similar to those reported from the western part of the valley and are significantly less than those published from Eastern Nepal Himalaya. The Eastern Nepal Himalaya is also marked by the many high peaks (>8000 m), resulting in high sediment loads of rivers originating therein. The Middle and Lower Gangetic Plains adjoining to this segment of the Himalaya show high rates of subsidence, a narrow width and major sedimentation by large rivers

in the form of megafans of rivers like the Gandak, Kosi and Teesta. The reverse is true of the northwestern Himalaya including the western Nepal, which has a lower relief (<7000 m), low sediment load of the rivers originating in this segment and low convergence rates along the HFT. The adjoining (Upper) Gangetic Plain is wide, mainly uplifted in nature (forming interfluvies with moderately to well-developed soils) and incised by large rivers. These plains also show signatures of extensional tectonics. Thus, the Himalaya and adjoining Gangetic Plain are both segmented in nature and these are due to different quasi-equilibriums prevailing in the two segments, in terms of rates of convergence and underthrusting, and uplift of ranges and width of the adjoining plains.

Significance of the clay mineral distribution in the fluvial sediments of the Neogene Himalayan Foreland Basin (central Nepal)

Pascale Huyghe^{1*}, Romain Guilbaud¹, Matthias Bernet¹ and Ananta Prasad Gajurel²

¹ LGCA, Maison des Géosciences, Université de Grenoble, BP53, 38041 Grenoble, FRANCE

² Department of Geology, Tribhuvan University, Kathmandu, NEPAL

* For correspondence, email: huyghe@ujf-grenoble.fr

Sandstones and mudstones of Siwalik fluvial formations (Surai Khola and the Tinau Khola sections, western-central Nepal) and sand and clay of the modern Ganga drainage system were analysed for clay mineralogy. The clayey assemblage is composed of illite, chlorite, smectite and kaolinite. Illite and chlorite mineral are mainly of detrital origin, provided by Lower Himalayan and High Himalayan sources. From depth of about 2500m, diagenetic processes have affected the original clay signature and illitization of smectites occurs from 2500 m depth (~70-95°C). Dickitisation of kaolinite occurs from 3000 m depth (~110°C). Illite particles therefore consist of a mixture of inherited illites and illitized smectites, as suggested by illite crystallinity. Kaolinites and smectites have essentially authigenic forms although some detrital particles may also be observed. They mainly occur within the porosity and as coating of detrital particles.

Despite essentially felsic rock sources and dominant physical erosion processes in the Himalayan belt, smectites are abundant in the <7 Ma Siwalik deposits. Their great occurrence can not be explained by source changes and they seem to be essentially of authigenic origin. Detailed analysis of an individual fluvial Siwalik sequence, and comparison with the clay mineralogy of the modern drainage system suggest that smectites preferentially form in plain and low topographic areas preserved from erosion such as intra-mountainous valleys. Downward percolating cations released during soil formation concentrate (and may evaporate) and may precipitate smectites clay minerals along their pathways during eodiagenesis. The increasing seasonality and aridity linked to intensification of monsoon from 8 Ma has enhanced clay authigenesis in these areas.

Deformation and exhumation of the Higher and Lesser Himalayan Crystalline sequences in the Kumaon region, NW-Himalaya based on structural and fission-track analysis

RC Patel*, Nand Lal and Yogesh Kumar

Department of Geophysics, Kurukshetra University, Kurukshetra-136119, INDIA

* For correspondence, email: patelramesh_chandra@rediffmail.com

The crystalline rocks of the Himalayan orogen, exposed in the Kumaon Himalaya, consist of two distinct high-grade metamorphic units separated by a sequence of meta-sedimentary rocks of the Lesser Himalayan Zone (Figure 1). The northern unit corresponds to the Higher Himalayan Crystalline (HHC) sequence composed mainly of amphibolite facies to migmatitic para-gneiss. At the base, the Main Central Thrust (MCT) (locally named as Munsiri Thrust: MT) bounds the HHC, which is separated from the overlying low-grade meta-sediments of the Tethyan Sedimentary Zone (TSZ) by a gradational contact. A normal fault, equivalent to the South Tibetan Detachment System (STDS), is demarcated within the upper part of the HHC due to the presence of several normal faults. The southern unit i.e. the Chiplakot Crystalline Belt (CCB) is located within the Lesser Himalayan meta-sedimentary sequence (LHMS) of rocks to the south of the MCT. The North Chiplakot Thrust (NCT) in the north and South Chiplakot Thrust (SCT) in the south separate the CCB from the Lesser Himalayan meta-sedimentary rocks. Both the thrusts dip due NE and join to each other in the west along the Goriganga valley. The LHMS is overriding the CCB along the NCT while the CCB is overriding the LHMS along the SCT. A major NE-dipping thrust zone i.e. Central Chiplakot Thrust (CCT) breaks the CCB into two blocks along which the northern block is thrust over the southern block (Kumar and Patel 2004, Patel and Kumar 2006). The CCB mainly consists of greenschist facies rock derived from an early Proterozoic basement.

Structural results indicate that both the CCB and the HHC have undergone deformation history of pre-Himalayan (D1) to Himalayan deformations (D2/D3/D4). The prominent penetrative fabric in the CCB and the HHC, developed during the D2 reflect the ductile stage of deformation. It resulted in crustal thickening during Himalayan orogeny and became zone of rapid exhumation. The whole HHC moved along a broad ductile top-to-SW shear zone and the MCT/MT over the LHMS, while the CCB has undergone intense horizontal shortening in a NE-SW direction. It gave rise to the evolution of the CCB by emplacement over the LHMS zone along a broad shear zone developed within the duplex structure that formed south of the MCT (Patel and Kumar 2006).

Apatite and zircon fission-track data along the Darma and the Kaliganga valleys along with other published data from the CCB (Patel et al. 2007) and communicated data along the Goriganga valley (Patel and Carter, Communicated to *Tectonics*) from NW-Himalaya document bedrock cooling histories of the HHC and the CCB units exposed in the Kumaon region. Apatite FT ages range from 0.7 ± 0.2 Ma to 2.9 ± 0.6 Ma along the Goriganga Valley, from 1.0 ± 0.1 Ma to 2.8 ± 0.3 Ma along the Darma valley and from 1.4 ± 0.2 Ma to 2.4 ± 0.3 Ma along the Kaliganga valley within the HHC. These show no relationship to either structural position or elevation. The uniform

apatite cooling ages in the hanging wall of Vaikrita Thrust (VT) cluster around 0.8 Ma along the Goriganga valley, 1.5 Ma along Darma valley and 2 Ma along Kaliganga valley. In the footwall side ages are older and cluster around 1.6 Ma along Goriganga valley. Only one sample has been dated as 2.8 Ma along the Darma valley and no data is obtained in the Kaliganga valley in the footwall side of the VT. It is older than the ages obtained from the hanging wall side. Zircon FT ages range from 1.7 ± 0.1 Ma to 4.4 ± 0.4 Ma along Goriganga valley, from 4.0 ± 0.2 Ma to 4.5 ± 0.3 Ma along Darma valley and from 4.5 ± 0.2 Ma to 5.2 ± 0.2 Ma along the Kaliganga valley. Taking into account the sample locations with respect to MCT/MT, the data sets from all valleys in the Kumaon region show a uniform exhumation history of the HHC; and there is

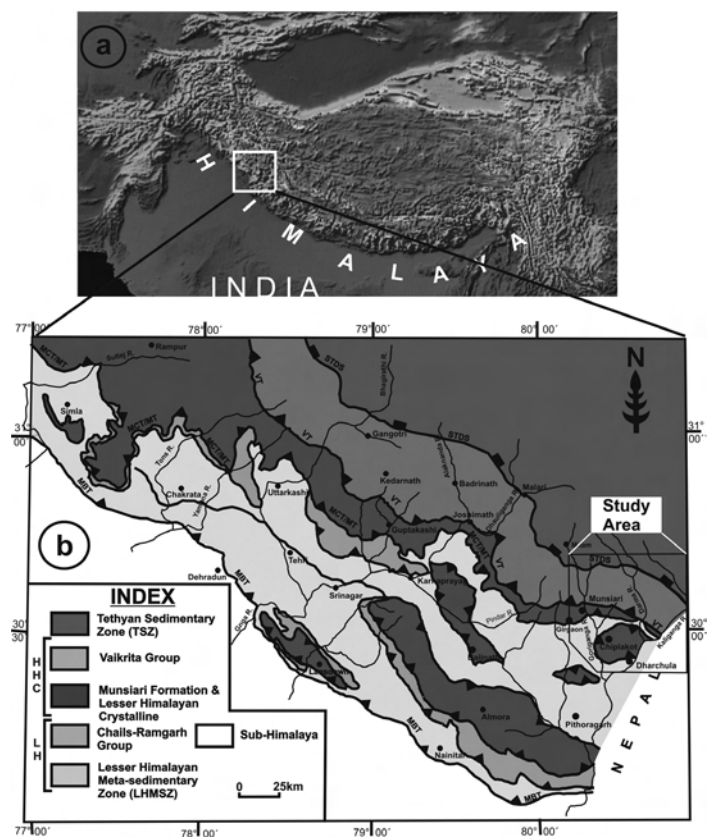


Fig. 1 (a) Geological setting of the studied area in the Himalaya (topography based on the GTOPO30 digital elevation model, U.S., Geological Survey), (b) Geological map of the Garhwal and Kumaon Himalayan region of India showing the tectonic setting of the Higher Himalayan Crystalline (HHC) and Chiplakot Crystalline Belt (CCB) in the overall lithostratigraphic framework of the region (modified after Valdiya, 1980). The study area is shown in the square box. STDS: South Tibetan Detachment System, VT: Vaikrita Thrust, MCT: Main Central Thrust, MT: Munsiri Thrust, MBT: Main Boundary Thrust, HHC: Higher Himalayan Crystalline and LH: Lesser Himalaya

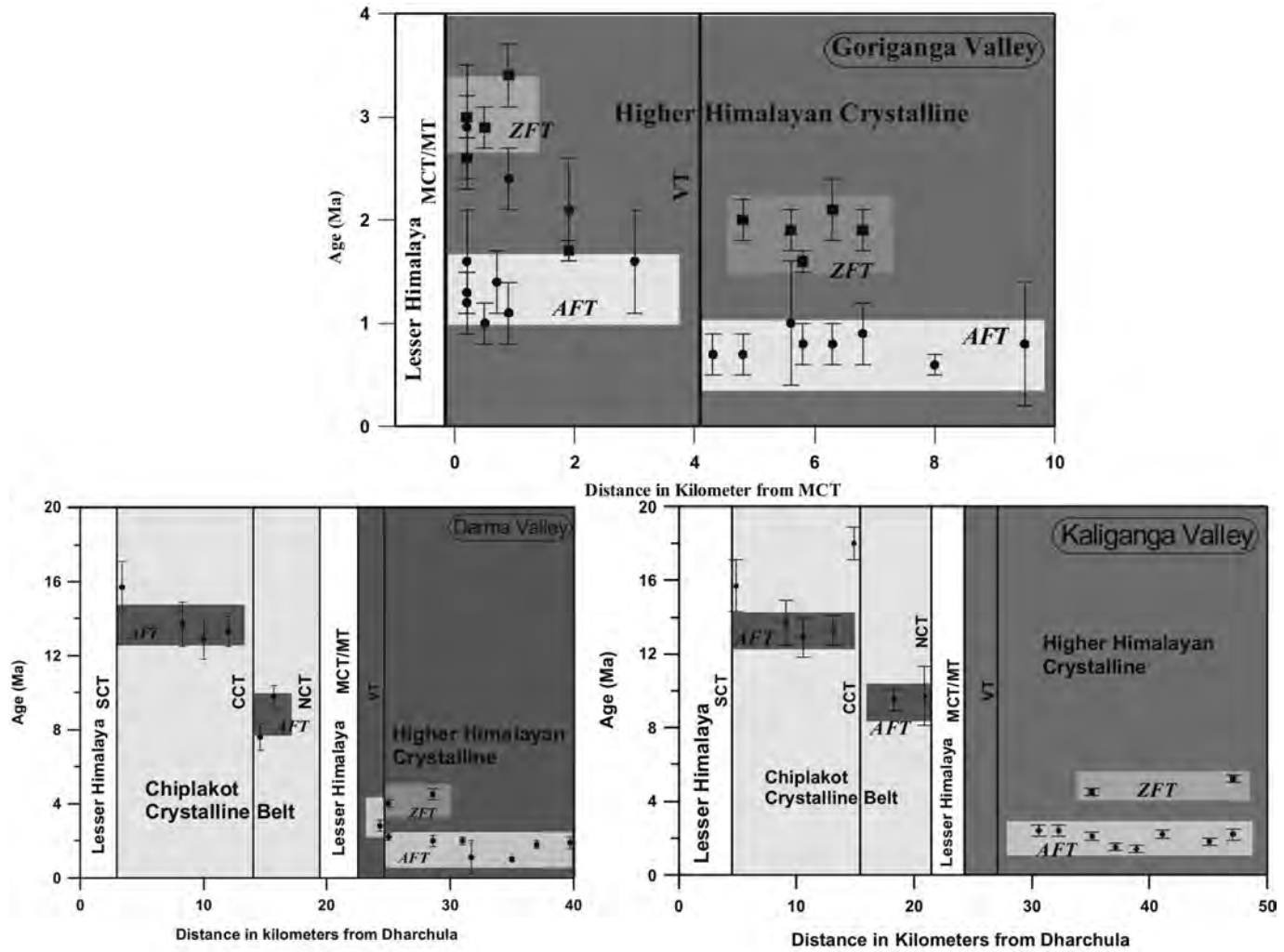


FIGURE 2. FT age Vs distance plots along the Goriganga, Darma and Kaliganga valleys in the Kumaon region, NW-Himalaya. Solid circles represent apatite FT ages and squares represent zircon FT ages

no change in the FT ages with distance from the MCT/MT (Figure 2). It indicates a constant parallelism between the surface and closure temperature implying a steady-state condition between topographic and exhumation since Pliocene. The distribution of the FT ages in all valleys suggests active movements along the VT that is almost synchronous along strike in the Kumaon region.

On the other hand, the AFT ages from the CCB (Lesser Himalayan Crystalline) are much older than the HHC. The ages range from 7.6 ± 0.6 Ma to 17.9 ± 0.9 Ma. Within the CCB, the AFT data statistically fall in two distinct groups: for southern block the ages range from 12.9 ± 1.1 Ma to 17.9 ± 0.9 Ma, while for northern block it ranges from 7.6 ± 0.6 Ma to 9.8 ± 0.6 Ma (Patel et al., 2007). It implies differential exhumation history in the hanging wall and footwall blocks of the CCT within the CCB. It appears to be possibly due to structural-controlled erosive exhumation since middle Miocene.

References

Kumar Y and RC Patel. 2004. Deformation mechanisms in the Chiplakot Crystalline Belt (CCB) along Kali-Gori valleys (Kumaon), NW-Himalaya. *Journal of Geological Society of India* 64: 76-91

Patel RC and Y Kumar. 2006. Late-to-post collisional brittle-ductile deformation in the Himalayan orogen: Evidences from structural studies in the Lesser Himalayan Crystallines., Kumaon Himalaya, India. *Journal of Asian Earth Sciences* 27: 735-750

Patel RC, Y Kumar, N Lal and A Kumar. 2007. Thermotectonic history of the Chiplakot Crystalline Belt in the Lesser Himalaya, Kumaon, India: Constraints from apatite fission-track thermochronology. *Journal of Asian Earth Sciences* 29/2-3, 430-439

Patel RC and A Carter. Deformation and exhumation of the Higher Himalayan Crystalline along Dhauliganga-Goriganga valleys, NW-Himalaya, India: New constraints from fission-track analysis. *Tectonics* (Communicated)

Valdiya KS. 1980. *Geology of Kumaon Lesser Himalaya*, Wadia Institute of Himalayan Geology, Dehradun, India, 291p.

Tectonics vs. erosion: evidences from apatite fission track and Rb-Sr (Biotite and Muscovite) thermochronology, Arunachal Himalaya

James Pebam^{1*}, AK Jain¹, R Kumar¹, Sandeep Singh¹ and Nand Lal²

¹ Department of Earth Sciences, Indian Institute of Technology Roorkee, Roorkee– 247667, INDIA

² Department of Geophysics, Kurukshetra University, Kurukshetra-136119, INDIA

* For correspondence, email: james_pebam@yahoo.com

Thermochronology has been extensively used to study the interplay between tectonics and erosion in recent years. Numerous works have been carried out in the Himalaya to explain this phenomenon with one school of thought giving more emphasis on tectonic exhumation (Burbank et al. 2003, Jain et al. 2000, Kumar et al. 1995), while other emphasizing on climatic control (Huntington et al. 2006, Thiede et al. 2004). Most of the earlier works made their conclusion based on a limited corridor study selected from this 2500 km long mountain range. In our present attempt, we give a comparative overview of different sector with similar tectonic setting and diverse climatic condition. So, in order to give a clearer picture we have taken up Apatite Fission Track (AFT) thermochronology and Rb-Sr thermochronology of bedrock samples of Arunachal Himalaya, which is one of the rainiest places on earth so as to compare with climatically stable western sector of this orogen.

Regional geology

The Himalayas represents the classical example of continent collision tectonics between Indian and Eurasian plates. In this orogen, the Arunachal Himalaya occupies the easternmost sector between longitude 91° 31' and 96° 0' E including the Eastern

Himalayan Syntaxis (Singh 1993, Yin et al. 2006). The syntaxis also includes the major Siang Antiform

In Subansiri valley (Figure 1) the Siwalik belt belonging to Cenozoic foreland basin rises abruptly over the Holocene Brahmaputra alluvium along the Main Frontal Thrust (MFT) (Figure 1) and is overridden by the pre-Cenozoic sedimentary sequence along the Main Boundary Thrust (MBT) in the north. The low grade metasediments of the Khetabari Group (Lesser Himalaya) are overridden by the medium to high grade Daporijo Gneiss of the Himalayan Metamorphic belt (HMB) along the folded Main Central Thrust (MCT); its southernmost exposure has been called as the Tamen Thrust. The contact is locally folded into an overturned fold as if the Lesser Himalayan quartzite-phyllite succession is overlying the gneiss. Along the strike, the thrust is intermittently exposed along road section from Tamen to Daporijo, where quartzite-phyllite succession of the Khetabari Group invariably underlies the Daporijo Gneiss. The quartzite and phyllite are intensely crushed and mylonitized all along the road section, where these dip towards NNW beneath the gneisses. Along the ENE-flowing Sipi River – a tributary of the Subansiri River, the Sipi Quartzite of the Menga Window is overridden by the Daporijo Gneiss at this confluence with a locally-folded

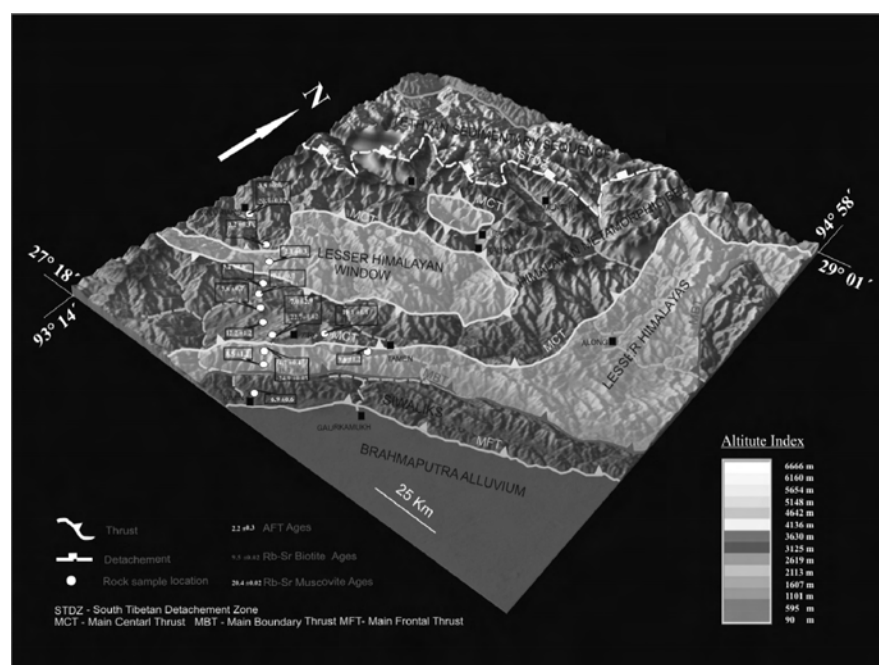


FIGURE 1. 3D perspective view of the Subansiri Valley, Arunachal Himalaya (90M SRTM from www.srtm.csi.cgiar.org) (Thakur and Jain 1974). From south to north this mountain belt is characterized by the Siwaliks, the Lesser Himalayas, the Himalayan Metamorphic belt (HMB), the Indus Tsangpo Suture Zone and the Trans-Himalayan units. The tectonic units trend E-W in the western parts and swing to NE-SW before bending abruptly to NNW-SSE along the Siang gorge.

contact. The Main Central Thrust (MCT) is exposed around Taliha, where low grade metamorphosed quartzite-phyllite alterations of the Sipi Quartzite are overridden by garnetiferous and kyanite-sillimanite schist/gneiss. The thrust is folded into a synform between Taliha and Baching and is again exposed around Nacho, where the underlying quartzite-phyllite sequence underlies the metamorphics of the HHC within a window.

AFT results and interpretation

AFT ages from bedrock samples in the Subansiri River catchment region from the Siwalik belt in the south to the Higher Himalaya, show spatial variation and have no positive correlation with elevation. Correlation the FT ages with the local tectonic setting highlights the overall thermotectonic evolution of this part of the orogen. The FT ages range from 2.1 ± 0.3 Ma to 12.2 ± 1.2 Ma, with youngest samples coming from the Lesser Himalayan window exposed within the HMB. The ages increase as the samples are analysed away from the core of the window (Figure 2), thus indicating that the folding has affected the cooling events in this part of the orogen. However, the ages vary relatively asymmetrically on the northern and southern limbs of the window. In the northern parts, the MCT hanging wall samples have young ages of 2.2 ± 0.3 and 3.5 ± 0.3 Ma. In the south, the Daporijo Gneiss yielded the AFT age of 5.2 ± 0.6 Ma in the immediate vicinity, while the ages become as old as 12.2 ± 1.2 Ma down south. Two Lesser Himalayan quartzite samples have AFT ages of 9.6 ± 1.8 and 8.5 ± 1.2 Ma, while a granite body intruding this unit has the AFT age of 4.7 ± 0.4 Ma. Therefore, the Daporijo Gneiss cooled much earlier than the HHC rocks. The entire cooling pattern of the HMB is affected by folding of the HHC and subsequent exposure of the Lesser Himalayan window. The samples in immediate vicinity of the Tamen Thrust, both from underlying and overlying package, show no significant variation in the AFT ages. These ages suggest resetting of the AFT clock at different geologic times and variable cooling rates across the lithounits of the Eastern Himalaya during the late Miocene.

The Rb-Sr biotite ages of the gneisses from the present section range from 9.2 to 18.7 Ma. The Lesser Himalayan granite (LHG) body around village Potin yields the maximum age with 18.7 ± 0.02 . In the Daporijo Gneiss, the ages vary from 11.1 ± 0.02 to 14.8 ± 0.02 Ma. But two samples from the HHC exhibit similar and younger ages of 9.2 ± 0.02 and 9.5 ± 0.02 Ma. Interestingly,

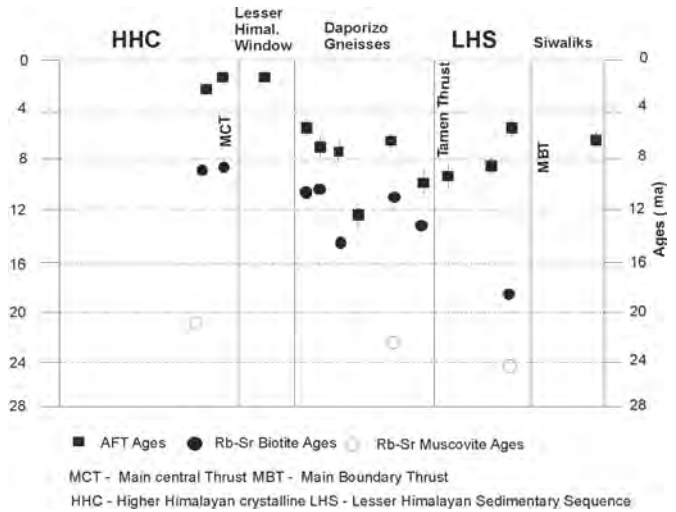


FIGURE 2. AFT, Rb-Sr biotite and muscovite)age profile along Kimin-Koloriang section.

the one sample each from the LHG, DG and HHC yields Rb-Sr muscovite age of 24.9 ± 0.02 , 22.7 ± 0.02 and 20.4 ± 0.02 respectively (Figure 2).

These ages suggest resetting of the AFT and Rb-Sr biotite and muscovite clock in different geologic times and exhibit variable cooling rate across the lithounits of the Eastern Himalaya. As indicated by the Rb-Sr muscovite ages, the lithounits in both the LH and HMB cooled uniformly during early Miocene. The pattern begins to differ slightly as it reach the Rb-Sr biotite closure temperature, in which the LH sequence cooled earlier than the package which constitute the present the DG and the HHC. But, as cooling approach the Apatite annealing zone, the different packages shows different cooling pattern, with maximum cooling rate in the LH window and the HHC, and a much slower cooling rate in the DG and LH sequences. The exhumation rates, calculated with simple assumption of geothermal gradient of $30^\circ\text{C}/\text{km}$, is fastest within the window zone with 1.9 ± 0.8 mm/yr during 2.1 Ma to Present, and that of the HHC is 1.56 ± 0.52 cm/yr during 20.4 ± 0.02 – 9.5 ± 0.02 Ma, 1.17 ± 0.29 cm/yr during 9.5 to 3.5 Ma

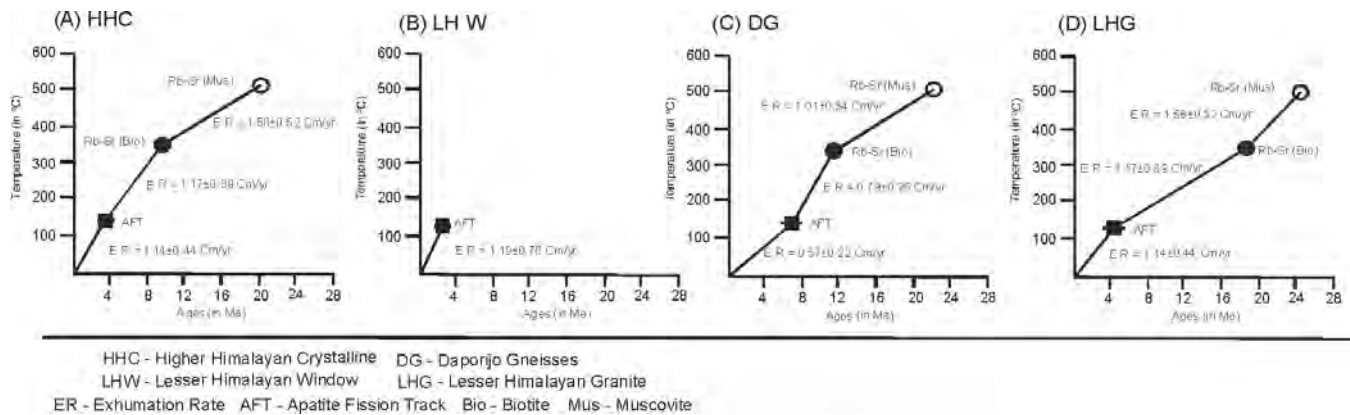


FIGURE 3. Exhumation pattern in different Lithounits of Kimin-Koloriang section

and 1.14 cm/yr thereafter (Figure 3). Within the DG, co-existing mineral pairs indicate exhumation rate of 1.01 ± 0.34 cm/yr during 22.7 Ma to 11.8 Ma, 0.8 ± 0.26 cm/yr during 11.8 to 7 Ma and 0.57 ± 0.32 cm/yr thereafter. The rate is much slower in the Lesser Himalayan metasediments with 0.5 cm/yr since 7.6 Ma. The LHG exhumed at a rate of 0.76 ± 0.25 cm/yr during 24.9 Ma and 11.8 Ma. The rate decreases to 0.4 ± 0.13 cm/yr 18.7 Ma and 4.7 Ma but increases again to 0.85 ± 0.35 cm/yr during 4.7 Ma to Present. The overall exhumation rate beginning in early Miocene is slower in the DG and LH sequence and fastest in the HHC and LH window. The AFT and Rb-Sr biotite and muscovite ages suggest the thrusting and crustal folding control the exhumation in Arunachal Himalaya.

References

- Burbank DW, AE Blythe, J Putkonen, B Pratt-Sittaula, E Gabet, M Oskin, A Barros and TP Ojha. 2003. Decoupling of erosion and precipitation in the Himalayas. *Nature* 426: 652–655
- Huntington KW, AE Blythe and KV Hodges. 2006. Climate change and Late Pliocene acceleration of erosion in the Himalaya. *Earth Planetary Science Letters* 252: 107–118
- Jain AK, D Kumar, S Singh, A Kumar and N Lal. 2000. Timing quantification and tectonic model of Pliocene-Quaternary movements in NW Himalaya: evidences from fission track dating. *Earth Planetary Science Letters* 179 (3-4): 437–451
- Kumar A, N Lal, AK Jain and RB Sorkhabi. 1995. Late-Cenozoic-Quaternary thermo-tectonic history of Higher Himalayan Crystalline (HHC) in Kishtwar-Padar-Zaskar region: Evidence from fission track ages. *Journal of Geological Society of India* 45: 375–391
- Singh S. 1993. Geology and tectonics of Eastern Syntaxial Bend, Arunachal Himalaya. *Himalayan Geology* 4(2): 149–163
- Thakur VC and AK Jain. 1974. Tectonics of the region of Eastern Himalayan syntaxis. *Current Science* 43 783–785
- Thiede RC, B Bookhagen, JR Arrowsmith, ER Sobel, and MR Strecker. 2004. Climatic control on rapid exhumation along the Southern Himalayan Front. *Earth and Planetary Science Letters* 222: 791–806
- Yin A, CS Dubey, TK Kelty, GE Gehrels, CY Chou, M Grove, and O Lovera. 2006. Structural evolution of the Arunachal Himalaya and implications for asymmetric development of the Himalayan orogen. *Current Science* 90(1-2): 195–206

Stress field evolution in the North West Himalayan syntaxis (Northern Pakistan)

A Pêcher^{1*}, S Guillot¹, F Jouanne², G Mahéo³, JL Mugnier², Y Rolland⁴, P Van der Beek¹ and J Van Melle¹

¹ LGCA, UMR 5025, CNRS - Université Joseph Fourier, FRANCE

² LGCA, UMR 5025, CNRS - Université de Chambéry, FRANCE

³ UMR5570, CNRS - Université Claude Bernard - ENS Lyon, FRANCE

⁴ Geosciences Azur, UMR 6526, CNRS - Université de Nice, FRANCE

* For correspondance, email: arnaud.pecher@ujf-grenoble.fr

In North-West Himalaya (Western Syntaxis) coexist both early stabilized parts of the belt, stable since Miocene (Kohistan, Deosai, for instance) and zone of active relief where deep parts of the crust have been very recently exhumed (late Miocene and Plio-Quaternary exhumation, in Karakorum and Nanga Parbat). This contrasted pattern was acquired in a context characterized by a strong partition of the deformation: from place to place, the structures can indicate shortening parallel to the bulk Himalayan convergence (Karakorum for instance), or at the opposite parallel to the belt strike (Nanga Parbat spur, Becham syntaxis, Murree syntaxis). A systematic study of the brittle deformation in those areas has been conducted (inversion of fault striations on fault planes to estimate the palaeostress state), in order to depict variations in time and space of the palaeostress field in this part of Himalaya.

At a regional scale, two main domains can be separated (Pecher et al., submitted), limited by the Raikhot fault, a reverse fault still active, bounding to the West the Nanga Parbat North-South pop-up anticlinal. West of this fault, in Kohistan and Karakorum, the predominant stress field is characterized by vertical σ_2 and close to N-S σ_1 (deformation field mainly

controlled by strike slip faults). It predates the Plio-Quaternary exhumation of the Nanga Parbat, and would correspond to the regional stress field inducted by the India-Asia convergence. East of the Raikhot fault, compression is parallel to the belt. It acts for the N-S structure of the Nanga Parbat, probably initiated around 5 Ma ago. Since 2 Ma, the stress field seems mainly extensive, the predominant extension being either perpendicular to the belt (NNE-SSW), or more often parallel to the belt strike (NW-SE).

Thus in North-West Himalaya, multidirectional extension is superimposed to shortening either parallel or perpendicular to the belt. Such a pattern implies a great instability of the stress field both in space (at a few tens km scale) and time (at one Ma scale or less). It could be a characteristic feature of crustal-scale strain partitioning in a oblate convergence context.

References

- Pêcher A, L Seeber, S Guillot, F Jouanne, A Kausar, M Latif, A. Madji, G Mahéo, JL Mugnier, Y Rolland, P van der Beek and J Van Melle. Stress field evolution in the Northwest Himalayan syntaxis, Northern Pakistan (submitted)

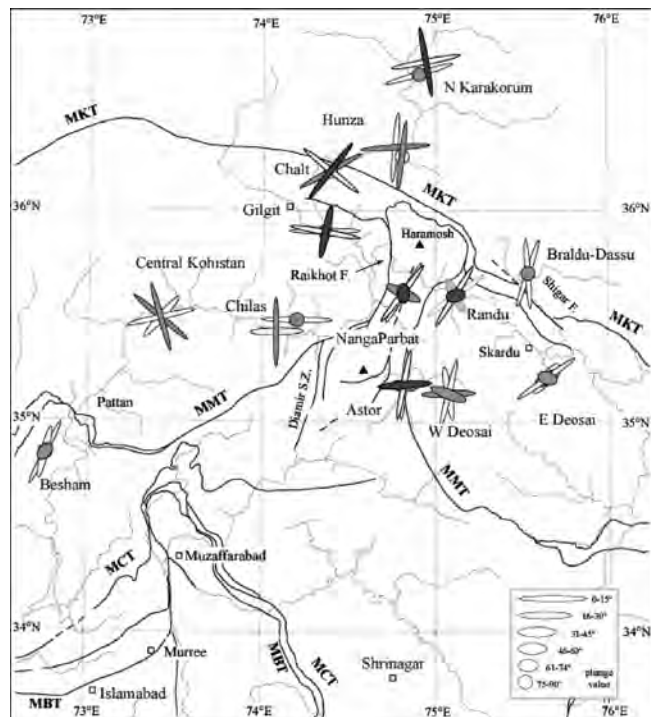


FIGURE 1. Regional stress orientations in Northern Pakistan. Regional tensors calculated by merging faults measured in 4 to 11 individual outcrop-scale sites. Each stress axis is indicated by an ellipse: the great axis of the ellipse gives the azimuth of the principal stress axis, the shape of the ellipse its plunge (classes of 15°). For each area, only the two best tensors are shown. T1: σ_1 in black, σ_3 thick plain symbol; T2: σ_1 in grey, σ_3 light plain symbol (in Pecher et al. submitted)

Soft sediment deformation structures in the Late Quaternary sediments of Ladakh: evidence of multiple phases of palaeoearthquakes in the North western Himalayan Region

Binita Phartiyal and Anupam Sharma

Birbal Sahni Institute of Palaeobotany, 53-University Road, Lucknow-226007, UP, INDIA

Ladakh, situated in the tectonically active terrain, in the vicinity of the Indus Suture Zone (ISZ), Shyok Suture Zone (SSZ) and Karakoram Fault (KF), is rich in Quaternary deposits and is truly a treasure trove for Quaternary researchers. This work presents the palaeoseismic signatures as recorded in the Quaternary sediments of the Spitik-Leh (along ISZ) and the Khalsar palaeolakes (along SSZ and KF). These two palaeolakes were a result of a regional tectonic activity at 35,000-40,000 yrs BP. 9 levels of soft-sediment deformation structures (seismites) are recorded from a >27 m thick, clay, sand sequence of the Spitik-Leh palaeolake. The deformation levels are confined to the lower 13 m of the sequence (0.5, 2.7, 3.2, 3.6, 5.5, 8.1, 9.8, 12.2 and 13.1 m). The upper part of the paleolakes seems to have stable tectonic conditions. About 90 km north of this section

and separated by the Ladakh batholith, in the ~11 m thick section of Khalsar palaeolake shows 8 levels of soft-sediment deformation structures at 1.2, 1.5, 4.2, 4.5, 5.4, 8.8, 9.2 and 10.8 m levels. Deformation sediments are composed of alternations of clay, silts and sand and are restricted to single stratigraphic layers bounded by undeformed beds suggesting synsedimentary deformation. They are simple and complex convolutes, pinch and swell bedding, microfolds and microfaults, flame-like structures, pseudonodules or cycloids, clay diapirs, ball and pillow structures, pillar structures, sedimentary dykes, mud lenses, etc. Lying in the vicinity of the active faults the ISZ, SSZ and KF, these two palaeolake systems record multiple phases of seismic tremors of magnitude >5 due to release of stress along these fault systems during the late Quaternary times.

Complex Seismic Discontinuities in the Mantle Transition Zone beneath NW Himalaya and Ladakh- Karakoram

KS Prakasam¹, SS Rai^{1*}, Keith Priestley² and VK Gaur³

¹ National Geophysical Research Institute, Hyderabad-500007, INDIA

² Bullard Lab., Cambridge University, Cambridge, UK

³ Indian Institute of Astrophysics, Bangalore, INDIA

* For correspondence, email: shyamsrai@gmail.com

Analyses of mantle converted Ps phase in 957 teleseismic receiver functions calculated from broadband seismograms deployed at 19 sites along a 700 km long N-S profile from the exposed northern edge of the Indian shield near Delhi to the Ladakh-Karakoram reveal complex features in the underlying Mantle Transition Zone (MTZ). Beneath the Gangetic plain and the Himalaya south of the Indus Zangbo Suture (IZS), the 410-km discontinuity is shallow (~392 km) and the mantle transition zone is relatively thicker (~260 km). To the north of the IZS beneath the Ladakh the 410-km discontinuity lies near

its normal depth but the transition zone is thinner (~242 km) and includes an interface at ~475 km depth. The base of the transition zone is complex as revealed in dominant converted phase from 660 depth and a weaker one at ~715 km. These observations suggest the presence of a high velocity slab within the MTZ beneath the Ladakh region, most likely a broken off segment of the subducted Indian Lithosphere, and the other deeper one beneath Himalaya and Ladakh which is likely the sunken delaminated oceanic lithosphere that was rolled back across the mantle transition zone.

High Crustal Seismic Attenuation in Ladakh- Karakoram

SS Rai¹, Ashish¹, Amit Padhi^{2*} and P Rajgopala Sarma¹

¹ National Geophysical Research Institute, Hyderabad-500007, INDIA

² Indian Institute of Technology Kharagpur, Kharagpur – 721 302, INDIA

* For correspondence, email: shyamsrai@gmail.com

Analysis of the Lg wave has been attempted to study the seismic attenuation along a profile from southern edge of NW Himalaya to Ladakh and Karakoram using broadband waveform recordings of regional earthquakes. The lateral variability in seismic attenuation is derived from inversion of 23 two station measurements using a Differential Evolution global optimization scheme. The Q value decreases northwards from ~ 700 in Himalaya and ~ 400 beneath Indus Zangbo Suture (IZS) to ~ 70 in Ladakh- Karakoram. This suggests efficient

transmission of seismic waves beneath Himalaya and the IZS and high attenuation under Ladakh-Karakoram. The Values for NW Himalaya and IZS are significantly ($>50\%$) higher compared to their counterpart at 90°E , while the Ladakh-Karakoram and southern Tibet show comparable (~ 70). The high attenuation zone (low) is correlatable with increase in electrical conductivity and decrease in the mid- crustal S-velocity suggesting the possible presence of aqueous fluid in the Ladakh – Karakoram crust.

The Deep structure of Western Himalaya – Ladakh-Karakoram

SS Rai^{1*}, VK Gaur², Keith Priestley³ and Lev Vinnik⁴

¹ National Geophysical Research Institute, Hyderabad-500007, INDIA

² Indian Institute of astrophysics, Bangalore, INDIA

³ Bullard Labs, Cambridge University, Cambridge, UK

⁴ Institute of Physics of the Earth, Moscow, RUSSIA

* For correspondence, email: shyamsrai@gmail.com

To understand the deep structure of the western Himalaya, Ladakh and Karakoram, we analysed teleseismic body wave recordings on a ~700 km long profile of 17 broadband seismographs from Delhi through the Himalaya to the Karakoram. The database includes P and S receiver functions, teleseismic P and S residuals and observations of shear wave splitting in SKS. Modelling of P-receiver function suggests the depth of Indian Moho increasing from ~40 km beneath Delhi, south of the Indo- Gangetic plain, to ~75 km beneath the Karakoram fault. Further north, Wittlinger et al (2004) imaged the Moho at ~90 km beneath western Tibet before shallowing to ~60 km at the Altyn Tagh fault. These results indicate that in the western Himalaya-Tibet region Indian plate underthrusts as far as Bangong- suture and possible to the Altyn Tagh Fault.

The analysis reveals presence of a cold region beneath the Himalaya at a depth of several hundred kilometers. This anomaly can be caused by the remnants of Tethys subduction and, perhaps,

is unrelated to the ongoing process. The present day process is reflected in velocities beneath the lesser Himalaya, intermediate between those of the crust and the upper mantle. This observation can be explained by scraping off the ductile lower crust of the underthrusting Indian plate and accumulation of the high-velocity crustal material in the frontal region of the thrustal zone. Seismic waves in the upper 200 km of the mantle are faster than in the global IASP91 model, and the structure includes a low velocity layer sandwiched between two high velocity layers. We interpret the lower layers as an image of subducted mantle lithosphere of the Indian plate. Shear wave splitting, derived from SKS phase data, is different in the south and the north of Indus Suture Zone. In the south, the fast direction of anisotropy is normal to the trend of the Himalaya and can be interpreted as an effect of the NE motion of the Indian lithosphere. In the north the fast direction is oriented E-W and can be explained by the fabric left in the presently extinct subduction zones.

Deep seismic reflection profiling over the Siwalik fold belt of NW Himalaya

B Rajendra Prasad*, V Vijaya Rao and HC Tewari

National Geophysical Research Institute (CSIR), Uppal Road, Hyderabad-500606, INDIA

* For correspondence, email: rajbitragunta@yahoo.com

The Himalayan orogeny during the Cenozoic is a product of continent-continent collision between the Indian and Eurasian plates with the formation of a peripheral foreland basin in front of the underthrust Indian plate. The basin was subsequently folded and uplifted. The foreland basin, located between the Main Frontal Thrust and Main Boundary Thrust, mainly consists of the Siwalik, Dharmasala and Subathu formations deposited during the Cenozoic. It extends almost over the entire length of the Himalayan foothills. The uplifted Siwalik foreland basin rises abruptly by 500–2000 m above the foredeep of the Holocene Indo-Gangetic alluvial plains. To understand the crustal structure of this region a deep seismic reflection study is carried out along 35 km long Barsar-Bhota-Sandhera and 65 km long Farsi-Bhota-Nerchowk profiles across this fold belt. The seismic profiles traverse the Jawalamukhi, Barsar, Gambhar, Palampur and Main Boundary thrusts of the Sub-Himalayan fold belt. The seismic data are acquired with 150-channel RF telemetry system using explosives. Seismic images from the present study indicate a bright reflection band around 3.0–3.5 s and a gently dipping reflection band from 13 s in the western part deepening to 15 s to the east. The present paper discusses about the significance of various reflection bands observed in the region.

Introduction

The Himalayan mountain belt has evolved through the late Mesozoic subduction of the Indian plate beneath the Eurasian plate with closure of Tethys Ocean and subsequent collision of two plates during the Cenozoic. The NE part of Himalaya is relatively well studied using various geophysical methods by the INDEPTH and other research groups. But, the structure of the NW Himalayan region is mostly determined by the geological mapping and a very few geophysical studies were carried out using gravity and magnetic methods. Shallow seismic studies are being used by the oil industry for exploration of hydrocarbons in the foreland basin. Keeping in view of the geodynamics of the region, a deep crustal seismic reflection study is carried out along 35 km long Barsar-Bhota-Sandhera and 65 km long Nangal-Bhota-Nerchowk profiles (Figure 1) by the National Geophysical Research Institute for the first time covering the NW part of the Cenozoic sub-Himalayan foreland basin to understand the tectonic fabric of the region. The seismic image of the deep crust can unravel the history of basin formation and can provide important constraints to understand the shallow structure in a better way. The present deep crustal reflection study is an attempt to delineate the deep crustal structure and its correlation with the shallow as well as the surface features.

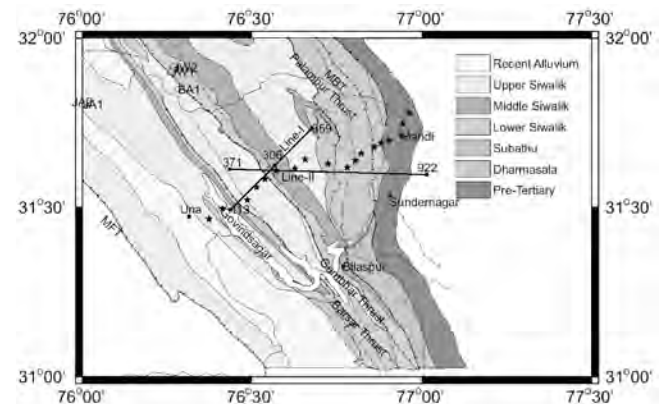


FIGURE 1. Simplified geology and tectonic map of the study region of the NW Himalaya along with seismic profiles and locations of oil wells. The numbers along the profile indicate locations of the pickets. MFT-Main Frontal Thrust; BT-Barsar Thrust; GT-Gambhar Thrust; PT-Palampur Thrust; DT-Drang Thrust, MBT-Main Boundary Thrust

Geology and tectonics

The Himalayan orogenic belt is classified into Sub-, Lesser, Higher and Tethyan Himalaya from south to north. The region south of the MBT consisting of the Tertiary sediments is referred as Sub-Himalaya. On the other hand, the region north of MBT consisting of pre-Tertiary (Mesozoic-Paleoproterozoic) is divided into Lesser, Higher and Tethyan Himalaya. The present study area is mostly located in the Sub-Himalayan Siwalik foreland basin. The basin consists of predominantly fluvial sediments derived from rising Himalayas during the Cenozoic. The Tertiary sediments mainly comprising of the Subathu, Dharmasala and Siwaliks cover the foreland basin. The litho-stratigraphy of the region derived from the well data shows that the Siwalik sequences are underlain by various older sedimentary formations of which the Dharmasala and Subathu are prominent. The foreland basin consists of a number of minor thrusts such as the Barsar, Gambhar, Palampur thrusts located between MFT and MBT. These thrusts separate different geological sequences of the region.

Deep Seismic Reflection Study

Deep seismic reflection study is carried out along 35 km and 65 km long profiles across the Siwalik ranges of the Sub-Himalaya.

Shot holes of 20-25 m depth loaded with 50-70 kg of explosives are used as seismic source. The seismic data are acquired on a 15-18 km long spreads using a high dynamic range Eagle-88, RF-Telemetry seismic equipment. The data are recorded with 4 ms sampling interval to include wide frequency bandwidth of 212 Hz. The data are recorded up to 24 s duration to observe deep crustal and sub-crustal reflections in the region. The topographic variations along the profiles are of the order of 550 to 1600 m (Figures 2 and 3).

The seismic reflection (CMP) data were processed using the ProMax software on a workstation. Bad traces and high amplitude noise bursts are removed and polarity reversals are corrected. Spherical divergence and static corrections are applied. Finally, a stack section is prepared after applying NMO correction using appropriate velocity model. Proper scaling, AGC and bandpass filtering are applied to enhance the data quality.

Seismic data reveal good reflectivity in the region. No prominent reflections are found upto 3.5 s twt, beyond which reflectivity increases. The strong reflection band observed at 3.5 s may represent Tertiary-Pretertiary boundary. Prominent reflectivity is observed from 3.5-12.0 s twt. A gently dipping reflection band observed at 13 s in the western part deepening to 15 s to the east. It may represent Moho.

Acknowledgements

We thank Dr. VP Dimri, Director NGRI for permission to publish this work and DST, Govt. of India, for financial assistance under the HIMPROBE project.



FIGURE 2. Topographic variations along seismic profile-I



FIGURE 3. Topographic variations along seismic profile-II

Occurrence of Permian palynofossils from the Saltoro Formation, Shyok-Suture-Zone, Ladakh Himalaya, India

Ram-Awatar

Birbal Sahni Institute of Palaeobotany, 53 University Road, Lucknow-226 007 (UP), INDIA
E-mail: rawatar_2003@yahoo.com

In India, the Shyok Suture Zone (SSZ) is tectonically intercalated between the rocks of the Indus Tsangpo Suture Zone (ITSZ) to the south and Karakoram Zone to north (Srimal 1986, Sinha 1992, Thakur 1992, Sinha and Upadhyay 1995). The major thrusts which make both boundaries are known as Shyok thrust and Karakoram thrust respectively. The Shyok Suture Zone is a complex association of Late Palaeozoic to Miocene rocks including turbidites and ophiolitic mélanges with volcanic, calcalkaline magmatic rocks, granite batholith and molasses-type sequence forming an accretionary complex. The following opinions exist regarding the tectonics of the Shyok Suture Zone: 1) It is a subduction zone older than the ITSZ (Frank et al. 1977). 2) It is a subduction zone younger than the ITSZ (Brookfield and Reynold 1981). 3) It is a tectonic repetition of the ITSZ (Rai 1982). 4) It is a back-arc complex related to the ITSZ (Thakur and Misra, 1984). 5) It is a the tectonic repetition of a marginal oceanic crust that existed between the ITSZ and the Asian land mass in the Middle Cretaceous (Srimal 1986, Upadhyay et al. 1999). 6) It is a back-arc basin (Thakur and Misra 1984, Sharma 1991).

The sedimentary, volcanic and plutonic rocks of the SSZ are highly deformed and occur as tectonic slices between Ladakh and Karakoram Batholith. The lowermost unit of the Saltoro Formation is well exposed to the south of Khalsar, where it consists of thinly and even bedded, highly fissile and cleaved slates, phyllites and siltstones. A diverse palynfloral assemblage has been recovered from the siltstone unit collected from the Khalsar-Sakti road section of the same formation. The palynoflora is represented by 14 genera and 20 species of the spores and pollen grains. The significant palynotaxa of the assemblage are: Leiotriletes, Verrucosiporites, Platysaccus, Primuspollenites, Alisporites, Gondisporites, Faunipollenites, Striatopodocarpites, Densipollenites, Caheniasaccites, Scheuringipollenites, Hemipollenites, Parasaccites, Crescentipollenites, Corisaccites, Vesicaspora and Tetraporina. Based on the qualitative and quantitative analysis, Early to Late Permian age has been assigned to the assemblage.

Although, on the basis of the gastropods, echinoids, foraminifera and bryozoans, age of the Saltoro Formation has

been assigned from Late Jurassic / Early to Middle Cretaceous (Upadhyay 2002). However, the palynomorphs recovered from the Saltoro formation are of Permian times. These palynomorphs could be found under two conditions: 1) Either the sediments (siltstone unit) containing palynofossils of Permian time remain intact in this highly tectonized region, or 2) These palynomorphs have been eroded, recycling and deposited into the tectonically active Cretaceous–trench-subduction complex that existed between the Indian and the Asian plates.

References

- Brookfield ME and PH Reynold. 1981. Late Cretaceous emplacement of the Indus Suture Zone ophiolitic melanges and an Eocene–Oligocene magmatic arc on the northern edge of the Indian plate. *Earth Planetary Science Letters* 55:157-162
- Frank W, A Gansser and V Trommsdorff. 1977. Geological observations in the Ladakh area (Himalaya): a preliminary report. *Schweiz. Miner. Petrogr Mitt* 57: 89-113
- Rai H. 1982. Geological evidence against the Shyok Palaeo-suture, *Ladakh Himalaya*. 297: 142-144
- Sharma KK. 1991. Tectonomagmatic and sedimentation history of Ladakh collision zone: a synthesis. *Physics and Chemistry of the Earth* 17: 173-194
- Sinha AK. 1992. Himalayan mountain building and tectonic processes involved in it. In: Sinha AK (ed) *Himalayan Orogen and Geological Tectonic*. Oxford and IBH Publ. Co., New Delhi/AA Balkema, Rotterdam, p1-18
- Sinha AK and R Upadhyay. 1995. Himalaya: geological aspect. *Palaeobotanist* 44: 9-28
- Srimal N. 1986. India-Asia collision: implication from the geology of the eastern Karakoram. *Geology* 14: 523-527
- Thakur VC. 1992. *Geology of Western Himalaya*. Pergamon Press, Oxford. 366 p
- Thakur VC and Misra DK. 1984. Tectonic framework of Indus and Shyok suture zones in eastern Ladakh, NW Himalaya. *Tectonophysics* 101: 207-220
- Upadhyay, R. 2002. Stratigraphy and tectonics of Ladakh, eastern Karakoram, western Tibet, and western Kun Lun. *Journal Geological Society of India* 59: 447-467
- Upadhyay R, AK Sinha, R Chandra and H Rai. 1999. Tectonic and magmatic evolution of the eastern Karakoram. *Geodinamica Acta* 12: 341-358

Central Crystallines as the Exclusive Source Terrain For The Sandstone-mudstone Suites Of Siwalik Group: Geochemical Evidence

Nikesh Ranjan and D M Banerjee

Department of Geology, University of Delhi, Delhi – 110007, INDIA

The major, trace and rare earth element composition of a sandstone – mudstone suite provide necessary information needed for interpreting the characteristic of its provenance. In the Siwalik sedimentary basin, compositional change is a function of stratigraphic height. Chemically this factor is demonstrated by an upward increase in the oxide concentrations of P, Na, Ca, Mg and Si, from Lower to the Upper Siwalik. At the same time, concentration of oxides of K, Fe, Ti and Al show marked fall with the increasing stratigraphic age. Such trends clearly reflect time-controlled changes in the rock type in the source terrain. Ratios of Eu/Eu^* (~ 0.65), $(La/Lu)_{cn}$ (~ 9.04), La/Sc (~ 3.79), Th/Sc (~ 1.54), La/Co (~ 3.59) and Cr/Th (~ 2.26) suggest prominence of felsic source area for the Siwalik mudstones and sandstones. Chondrite normalized REE pattern with LREE enrichment and moderately flat HREE pattern with sharp negative Eu anomaly can be clearly assigned to felsic rocks in the source area. Our analytical data set practically rules out any contribution by the mafic rocks of any kind as inferred in the previous workers. This is a significant departure from the general belief about the source area chemistry. Our analytical results highlight the compositional

similarities of Siwalik sediments with the crustal proxies like PAAS, NASC and UCC. Furthermore, large-scale Precambrian and early Paleozoic granitic activity in the Himalayan tectogene seems to have played much more significant role in shaping the composition of the foreland sediments. The variable CIA values (71-87) and marked depletion in Na, Mg and Ca exhibited by the Lower, Middle and Upper Siwalik sediments reflect the effect of variation in the climatic zones and in the rate of tectonic uplift of the source area. By the time Siwalik sedimentary prism was deposited, there seems to have existed sufficient orographic barriers to produce significant moisture to intensify weathering coupled with intense tectonic activity. Our results demonstrate that in the Lower Siwalik and a part of Middle Siwalik, Higher Himalayan crystalline sequences (HHCS) acted as the primary source area with minor contributions from the metasedimentary succession of the Lesser Himalaya. Later, during the deposition of the upper part of Middle Siwalik and the Upper Siwalik, the source terrain switched positions. These two prominent source terrains supplied sediments in steadily changing proportion through time.

Northern Margin of India in the Pre-Himalayan times

Vibhuti Rai* and Aradhana Singh

Centre of Advanced Study in Geology, University Of Lucknow, Lucknow 226007, UP, INDIA

* For correspondence, email: vibhutihrai@gmail.com

The Himalayan orogeny, during the post-Mesozoic times, has critically altered the continental framework of Indian sub-continent. In fact, there have been complete destruction of the northern leading edge of the Greater India as most of it is either underthrust below the massive chain of mountains or have been detached along several of the northern dipping regional faults/thrusts (MBF, MCT and many others). Overthrusting of several of these portions has further complicated the scenario. The detachment of sedimentary pile from the basement and its subsequent overthrusting, besides detachment of basement rocks themselves and their obduction/thrusting, has aggravated the situation.

Several efforts to perceive the nature of this enigmatic northern edge of Indian subcontinent prior to collision of Indian continental block with the Asian block have resulted in conflicting data and confusing results. The geophysical efforts have also failed to decipher the true nature of the leading edge due to inconsistencies in profiles and difficulties in the interpretation. Most of the data remain conjectural, which are erroneously projected in excellent cartographical sections and neat diagrams. In fact, in many of these figures, massive exaggeration in the vertical scale have been included to emphasize the structural nature of the cross-section without incorporating any factual data.

At the outset, we would like to clarify that the hidden configuration of the domain of northern edge needs multi-faceted data such as geophysical, structural, tectonic, sedimentary basinal, geochronological and palaeontological in order to have an overall perception of the terrain. Since the northern edge was also laden with sedimentary sequences ranging from Palaeoproterozoic to Mesozoic time spans over an Archaean basement, these sedimentary sequences can provide the geotectonic domain in configuring the northern extent of the basin. The present contribution focuses on this aspect using the late Proterozoic to early Cambrian data from several of these basins.

In the post-Rodinia times, the disintegration of several Rodinian blocks assembled in a framework, which constituted the basis of a regional terrain called as Proto-Eastern Gondwana.

Although, the geomagnetic signatures vividly support this new assembly, the regional geotectonic framework authenticates the assembly to a larger extent.

The culmination of various fragments of Rodinia-derived blocks (continents) into Afro-Asian region supports the idea that a regional assembly of India (including Pakistan), Madagascar, Oman, Arabia, Afghanistan (Lut) and Iran juxtaposed each other in such a way that during the later part of Neoproterozoic, a large depositional basin developed near the equator. The basin evolved for almost 100 million years up to the end of Early Cambrian (including the Precambrian-Cambrian Boundary) and in a few areas, the deposition further continued.

The occurrence of large carbonate deposits alongside evaporites, followed by phosphogenic events provided crucial inputs in deciphering the depositional realm in a geotectonic framework. An assessment of the basin using palaeobiological evidences suggests that Varanger equivalent glaciation marked by diamictite, followed by a cap-carbonate, occurs as the marker of Ediacaran period and later in the stratigraphic sequence we get the Ediacaran biota, microfossils of cyanobacterial affinity, other algal fossils, acritarchs, calcareous algae, sponges, typical bedding plane traces (grazing) and small shelly fossils heralding the beginning of the Early Cambrian period.

The occurrence of phosphorite deposits, evaporites and the Terminal Proterozoic oil from the strata (named differently in different parts of the region) suggests regional depositional system in which marine phytoplanktons got deposited, accumulated and later matured to generate hydrocarbons (Heavy Oil) triggering the development of Ediacaran play in the region. In addition to the Proterozoic oil occurrences, huge limestone deposit provides major input to cement industry, which is currently required for resource development.

We propose here a geotectonic model comprising the palaeogeography and evolution of the late Proterozoic to early Cambrian basins that extended from Peninsular India right across present day Himalayan region with a note on the nature of the northern margin of the Indian subcontinent during this time-span.

The petrogenesis of a crustal-derived Palaeoproterozoic Bomdila orthogneiss, Arunachal Pradesh, NE Lesser Himalaya

Shaik A Rashid

Department of Geology, Aligarh Muslim University, Aligarh – 202002, INDIA

E-mail: rashidamu@hotmail.com

The major and trace element geochemistry of the Paleoproterozoic Bomdila orthogneisses from the Arunachal Pradesh, NE Lesser Himalaya has been determined to understand their nature and petrogenetic processes. Rigorous field and mineralogical examinations have indicated that the Bomdila gneisses consists of two types of granitic phases; a coarse-grained porphyritic gneiss (CPG) comprising of biotite and muscovite with the spectacular absence of tourmaline (referred as two-mica granites or tourmaline-free granites) and a weakly to non-foliated leucogranite having abundant tourmaline (referred as tourmaline-bearing granite). All the Bomdila samples have high Al_2O_3 (>13wt.%), with molar A/CNK ($Al_2O_3/CaO+Na_2O+K_2O$) >1.1 and normative corundum indicating a high peraluminosity and S-type nature of these granites. They are enriched in incompatible elements such as Rb, Ba, K and Th and depleted in high field strength elements (HFSE) like Zr, Hf, Ta and Nb. The two-mica granites show higher Rare Earth Elements (REE) concentrations (sum up to 294 ppm) than the tourmaline granites (sum = 67 ppm). Both the phases reveal a LREE enriched and flat HREE patterns with

negative Eu anomalies. The enrichment of the Bomdila gneisses in the incompatible elements and depletion in the HFSE strongly supports their postulated crustal source. Both the granite suits are characterized by high incompatible elements/HFSE ratios, which is in agreement with many intracrustally derived granites. Tourmaline-bearing granites are clearly distinguished by their low Sr and Ba contents compared with the tourmaline-free facies and are generally depleted in Zr and Nb. The tourmaline granites of the Bomdila massif generally lie within the syn-collision field (as do other Himalayan leucogranites) in the discriminant Rb vs. (Nb + Y) diagram whereas the two-mica granites straddles the field boundary between collision granite and volcanic-arc granite. The peraluminous geochemistry and phase equilibria conditions of the tourmaline-free granites indicate that they have been derived from the biotite-limited, vapour-absent biotite dehydration melting of a pelitic source rock. The aluminous chemistry, low $Fe_2O_3 + MgO$ values (< 2) and the presence of tourmaline emphasize that the tourmaline granites may have been derived from dehydration melting of muscovite higher in the crustal levels.

The great 1950 Assam Earthquake revisited: field evidences of liquefaction and search for paleoseismic events

DV Reddy¹, Pasupuleti Nagabhushanam¹, Devender Kumar^{1*}, Balbir S Sukhija¹, PJ Thomas¹, Anand K Pandey¹, Radhendra Nath Sahoo^{1,2}, GV Ravi Prasad³ and Koushik Datta³

¹ National Geophysical Research Institute, Uppal Road, Hyderabad – 500 606, INDIA

² Present Address: Kishan Ganga Hydro Electric Project, National Hydroelectric Power Corporation, PDD Colony, Ghantamulla -193 101, INDIA

³ Institute of Physics, Sachivalaya Marg, Bhubaneswar -751 005, INDIA

* For correspondence, email: devngri@gmail.com

Extensive field investigations were carried out for the first time in the meizoseismal area of the Great 1950 Assam earthquake aimed at exploring the paleoseismic history of NE Indian region through documentation of liquefaction features. The precondition for any liquefaction like the presence of shallow water table, unconsolidated sand and shear wave as triggering agent prevail at the studied sites in the Brahmaputra valley. In such potential seismic zone a large number of liquefaction sites were expected to exist. Contrary to this, our extensive field investigations in this meizoseismal area could unravel only a few sites with liquefaction features. Non-availability of liquefaction sites within the flood plains of Brahmaputra River could be attributed to either sediment erosion or deep burial during seasonal floods. However, the sites located inland or close to low energy flood environment are quite suitable for preservation of liquefaction features. Owing to this, we could locate the liquefaction features mainly along and adjoining areas of Burhi Dihing river, a major tributary of Brahmaputra, and a few locations in distal part of the alluvial fans. The liquefaction features, like sand blows, dykes and sills, crater, and associated soft sediment deformation features were observed

in trenches at different depths from the ground surface. The liquefaction sites namely Haldibari, Khawang, Sapakhoaghat, Zinimari, Nagaon, Kalolwa, and Borbaligaon are distributed in lower reaches of Burhi Dihing River, while Jiya Nala, and Kaliya Nala fall in the distal part of alluvial fans of Dibang River near Sadiya. In order to constrain the formation timing of the different liquefaction features and causative earthquakes, associated organic material samples (e.g. charcoal, wood, peat) were collected. Out of 12 features, one feature at Haldibari site dates Modern (≤ 50 yr) for its lower, upper and pencontemporaneous bounds, thus exclusively constraining the 1950 earthquake. For some of the sand dykes, we obtained lower bound ages of about 500 yr, which infer the features might have formed any time after 1370 AD (Figure 1). We might have documented the signatures of historically reported 1548 AD and 1697 AD seismic events, but were devoid of organic material for 14C dating. Thus the paleoseismic history dating back to ~ 500 yr BP documented through 14C chronology of the organic material associated with these features indicates the absence of a comparable magnitude earthquake of that of 1950 in the studied area.

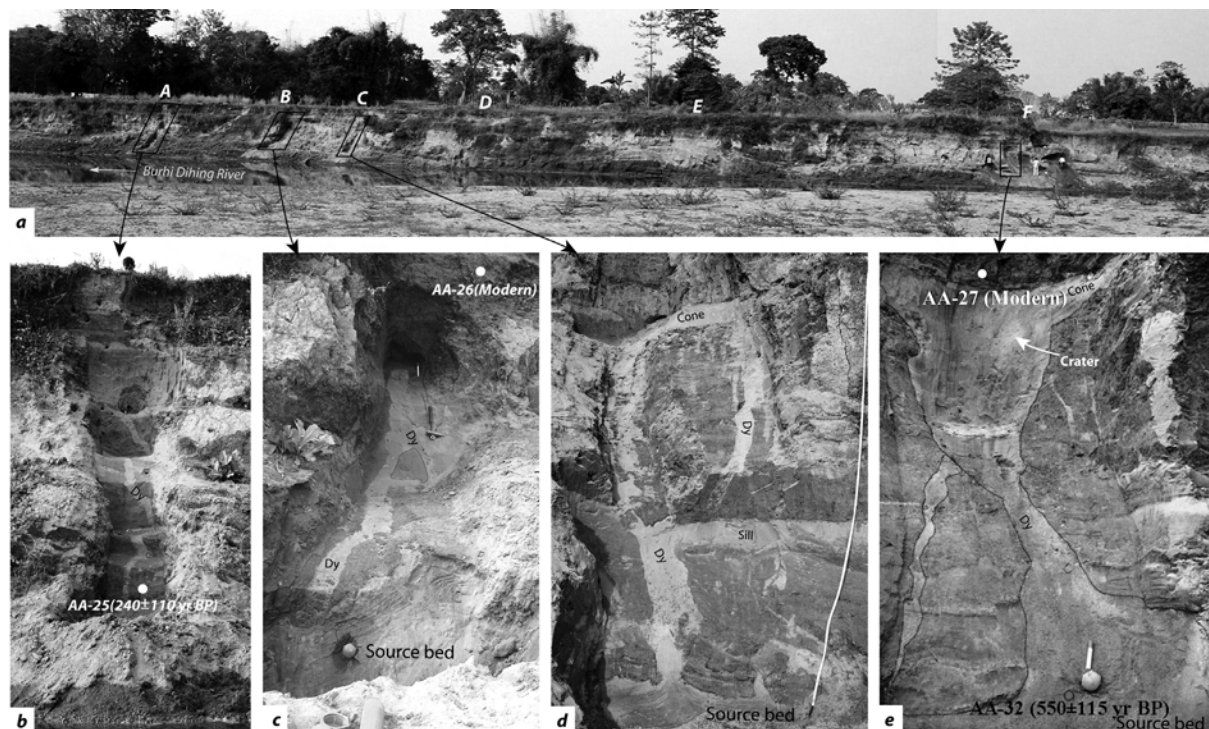


FIGURE 1. A series of dykes exposed in a 140 m long section in NW direction on the right bank of Burhi Dihing River at Nagaon. All the major dykes are numbered as A to F. Blow up of a few individual dykes along with the respective 14C ages are shown.

Occurrences of sulphide minerals in the Stak and Tso Morari eclogites: Implications for the behaviour of sulphur and chalcophile elements in subduction zones.

Nicolas Riel¹, Keiko Hattori^{2*}, Stephane Guillot¹, Mohamad Latif³ and Allah B Kausar³

¹ University of Grenoble, OSUG - CNRS, BP 53, 38041 Grenoble Cedex 9, FRANCE

² Department of Earth Sciences, University of Ottawa, Ottawa, Ontario, K1N 6N5, CANADA

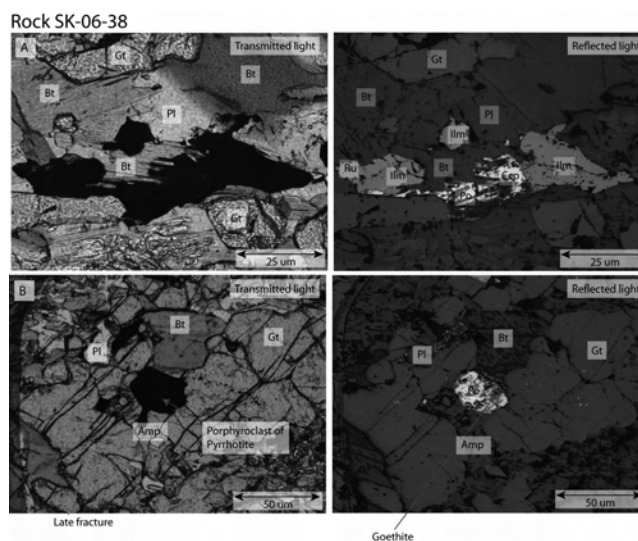
³ Geological Survey of Pakistan– Northern Area, Plot N. 84, H-8/1, Islamabad, PAKISTAN

* For correspondence, email: khattori@uottawa.ca

Exhumed rocks from subduction zones provide information relevant to element transfer from slabs to the overlying mantle wedges. Dehydration reaction of a slab during its subduction results in the hydration of the overlying mantle peridotites, forming a serpentinite layer at the base of the wedge margin. Eventual breakdown of the serpentinites releases water and contributes to partial melting of the interior of the mantle wedge for arc magmatism (Hattori and Guillot 2003). Fluid-mobile elements behave together with water and are transferred from slabs to the overlying mantle wedge. They are enriched in fore-arc mantle serpentinites and also arc magmas (Hattori and Guillot 2003). Most chalcophile elements (copper like elements) are soluble in aqueous fluids, but they may not be mobile in rocks with high sulphide sulphur because they are fixed in sulphide minerals. To evaluate the behaviour of sulphur and chalcophile elements in continental subduction zones, we examined the occurrence of sulphides in ultrahigh pressure rocks of the Stak and Tso Morari massifs in the western Himalayas. Both massifs represent the subducted margin of the Indian continent after its collision with Asian continent. The Stak rocks have the bulk composition of alkaline mafic igneous rocks and likely related to a hot spot magmatism. Our recent U/Pb ages of zircon using a SHRIMP suggest the protolith of ~ 60.4 Ma and the peak metamorphism (~ 23 kbar, 750 °C) at 51 Ma (Riel et al., this volume). These rocks were exhumed to 11 kbar under amphibolite facies condition. For the Tso Morari rocks, they underwent the peak metamorphism of 20-25 kbar and 580 ± 60°C (Guillot et al. 1997) at ~ 53 Ma (Leech et al. 2005) and exhumed with a similar P-T-t path as the Stak rocks.

Chalcopyrite (CuFeS₂) and pyrrhotite (FeS) are the two main sulphide minerals in the samples from the Stak massif. They form globular inclusions in garnet and angular grains outside garnet. Inclusions in garnet are predominantly pyrrhotite with minor chalcopyrite. The Tso Morari rocks contain minor pyrrhotite inclusions in garnet, with no chalcopyrite observed in the studied samples. The common occurrence of sulphide inclusions in garnet from both massifs indicates that sulphide sulphur is transferred deep into the mantle as garnet is stable in the upper mantle.

The lack of chalcopyrite in the Tso Morari rocks is explained by its protolith, and/or high oxidation condition during their subduction. The protoliths of the Stak massif are plume-related mafic igneous rocks. Copper contents are generally high in mafic igneous rocks, especially plume-related rocks. On the other hand, the protoliths of the Tso Morari rocks are shallow water sediments from granitic sources on the northern Indian continent. The protoliths of the studied rocks may have had low copper and sulphur contents, although their concentrations vary widely in such sedimentary rocks. It is also probable that both copper and sulphur may have been lost during the subduction of the Tso Morari rocks considering high oxidation state of the subduction zone (Hattori et al. 2005). Evaporite



beds of sulphate in the Tso Morari massif (e.g., Gaetani et al. 1986) likely maintained high oxidation state. Sulphide sulphur would have been destabilized to sulphate in the Tso Morari rocks.

During the exhumation of the Stak and Tso Morari massifs, they were retrogressed under amphibolite facies condition to form amphiboles. Sulphide grains associated with amphiboles are partially hydrated and oxidized to goethite (FeOOH). The evidence suggests that the retrogression is accompanied by the dissolution of sulphur and copper in aqueous fluids and their transfer into the overlying mantle or crust.

References

- Gaetani M, R Casnedi, E Fois, E Garzanti, F Jadoul, A Nicora and A Tintori, 1986. Stratigraphy of the Tethys Himalaya in Zaskar, Ladakh. *Riv. Ital. Paleont. Stratigr.* 91: 443-478
- Guillot S, J de Sigoyer, JM Lardeaux and G Mascle. 1997. Eclogitic metasediments from the Tso Morari area (Ladakh, Himalaya): Evidence for continental subduction during India-Asia convergence. *Contribution to Mineralogy and Petrology* 128: 197-212
- Hattori K and S Guillot. 2003. Volcanic fronts form as a consequence of serpentinite dehydration in the forearc mantle wedge. *Geology* 21: 525-528
- Hattori K, Y Takahashi, S Guillot and B Johanson. 2005. Occurrence of Arsenic (V) in fore-arc mantle serpentinites: X-ray absorption spectroscopy study. *Geochim. Cosmochim. Acta* 69: 5585-5596
- Leech ML, S Singh, AK Jain, SL Klempner and RM Manickavasagam. 2005. The onset of India-Asia continental collision: Early, steep subduction required by the timing of UHP metamorphism in the western Himalaya. *Earth and Planetary Science Letters* 234: 83-97
- Riel N, K Hattori, S Guillot, N Rayner, B Davis, M Latif and AB Kausar, 2008. SHRIMP zircon ages of eclogites in the Stak massif, northern Pakistan. *Himalayan Journal of Sciences* 5 (7): 119

SHRIMP zircon ages of eclogites in the Stak massif, northern Pakistan.

Nicolas Riel¹, Kéiko Hattori², Stéphane Guillot¹, Nicole Rayner³, Bill Davis³,
Mohamad Latif⁴ and Allah B Kausar⁴

¹ University of Grenoble, OSUG - CNRS, BP 53, 38041 Grenoble cedex 9, FRANCE

² University of Ottawa, Dept of Earth Sciences, Ottawa, Ontario, K1N 6N5, CANADA

³ Geological Survey of Canada, 601 Booth Street, Ottawa, Ontario, K1A 0E8, CANADA

⁴ Geological Survey of Pakistan– Northern Area, Plot N°. 84, H-8/1, Islamabad, PAKISTAN

* For correspondence, email: nicolas.riel@ujf-grenoble.fr, khattori@uottawa.ca

Retrogressed eclogites were reported by Le Fort et al. (1997) near the village of Stak from the Indus suture zone on the eastern side of the Nanga Parbat-Haramosh massif. The eclogite assemblage occurs in lenses and boudins in the matrix of phengite-bearing metasedimentary rocks and marbles. It is composed of pyrope rich garnet, omphacitic pyroxene, phengite, dolomite and rutile. New P-T estimates give a minimum pressure of ~ 2.3 GPa for 750°C (e.g. Guillot et al., this volume). The eclogites are distinctly mafic in mineralogy and compositions compared with UHP rocks at Tso Morari and Kaghan Valley both of them originated from the crustal material of the Indian continental margin (Guillot et al. 1997, O'Brien et al. 2001). The eclogites in the Stak massif contain high Mg (~ 9 wt%) and low Si (~ 48 wt%), yet high incompatible elements, including fluid-immobile elements. The bulk chemical compositions suggest that they are alkaline mafic igneous rocks most likely associated with a mantle plume.

Well-crystallized zircon grains are common within and adjacent to garnet in the eclogites. We hand-picked 34 grains, and mounted them into an Epoxy resin together with zircon grains with known ages from Fish Canyon Tuff, and Temara 2 for the CL-SEM examination and SHRIMP age determination at the Geological Survey of Canada in Ottawa. Zircon grains yielded 206Pb/238U ages varying from 80.0 to 48.1 ± 1.4 Ma with peaks at around 51.3 ± 0.7 Ma and 60.4 ± 0.6 Ma in the age distribution histogram. Outer rims of several grains are 51 Ma, suggesting that this likely represents the age of the eclogitization. The timing of the eclogitization at Stak is comparable to the 53.3 ± 0.7 Ma age for the Tso Morari massif (Leech et al. 2005) but older than the age of 46.2 ± 0.7 Ma for the Kaghan unit (Kaneko et al. 2003, Parrish et al. 2006). The protolith of the Stak eclogites is most likely between 70 and 80 Ma and younger ages are due to varying degrees of Pb-loss during the metamorphism because grains with

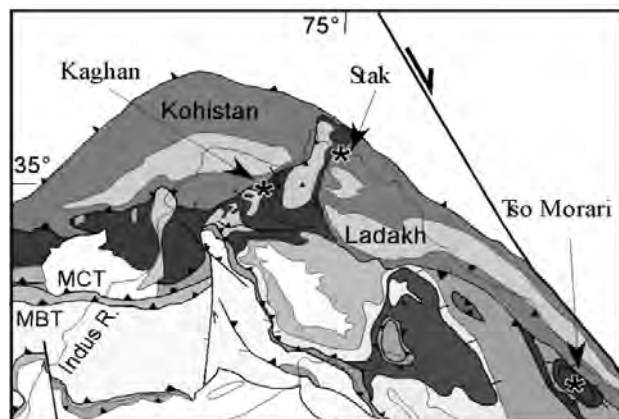


FIGURE 1. The location of the Stak eclogites

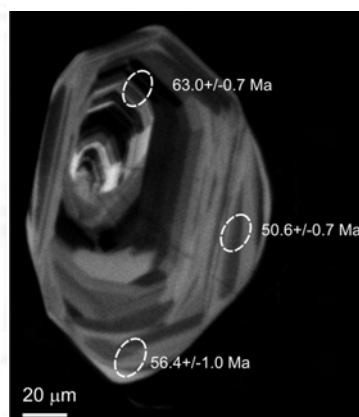


FIGURE 2. CL-SEM image of zircon grain 16 showing the areas for the SHRIMP age determination. The overgrowth yielded the age of the eclogitization, whereas the interior with oscillatory zoning shows two different ages. These ages are interpreted as reset ages by Pb loss during the metamorphism.

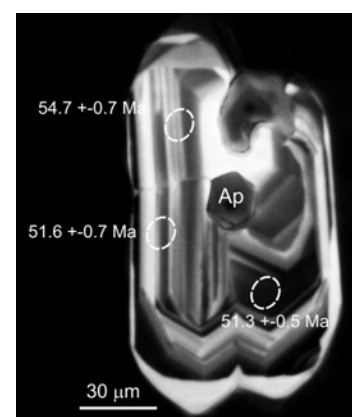


FIGURE 3. CL-SEM image of zircon grain 8 showing the areas for the SHRIMP age determination Ap= apatite

well-preserved igneous textures, such as oscillatory zoning and sector twinning, yielded different ages among different grains and even within individual grains. The data suggest either the protolith is igneous rocks associated with the Reunion hotspot on the distal part of the Indian continental margin (e.g. Mahoney et al. 2002) or a seamount/oceanic island formed on the Tethys Sea.

One small grain with low Th/U shows 31.3 ± 0.4 and 31.7 ± 0.5 Ma. This is interpreted as the secondary zircon formed in a late aplite-pegmatite dyke common in the area (Patterson and Windley 1985).

References

- O'Brien PJ, N Zotov, R Law, MA Khan and MQ Jan. 2001. Coesite in Himalayan eclogite and implications for models of India-Asia collision. *Geology* 29 (5): 435-438
- Guillot S, J de Sigoyer, JM Lardeaux and G Mascle. 1997. Eclogitic metasediments from the Tso Morari area (Ladakh, Himalaya): Evidence for continental subduction during India-Asia convergence. *Contribution to Mineralogy and Petrology* 128: 197-212
- Guillot S, N Riel, K Hattori, S Desgreniers, Y Rolland, J Van Melle, M Latif, AB Kausar and A Pêcher. 2008. New occurrence of eclogitic continental rocks in NW Himalaya: Tha Stak massif in north Pakistan. *Himalayan Journal of Sciences* 5(7): 57
- Kaneko Y, I Katayama, H Yamamoto, K Misawa, M Ishikawa, HU Rehman AB Kausar and K Shiraishi. 2003. Timing of Himalayan ultrahigh-pressure metamorphism: sinking rate and subduction angle of the Indian continental crust beneath Asia. *Journal Metamorphic Geology* 21: 589-599
- Le Fort P, S Guillot and A Pêcher. 1997. HP metamorphic belt along the Indus suture zone of NW Himalaya: new discoveries and significance. *Compte Rendus de l'Académie des Sciences* 325: 773-778.
- Leech, ML, S Singh, AK Jain, SL Klempner and RM Manickavasagam. 2005. The onset of India-Asia continental collision: Early, steep subduction required by the timing of UHP metamorphism in the western Himalaya. *Earth Planet Science Letters* 234: 83-97
- Mahoney JJ, RA Duncan, W Khan, E Gnos, GR McCormick. 2002. Cretaceous volcanic rocks of the South Tethyan suture zone, Pakistan: implications for the Réunion hotspot and Deccan Traps. *Earth Planet Science Letters* 203: 295-310
- Parrish RR, SJ Gough, MP Scarle, DJ Waters. 2006. Plate velocity exhumation of ultrahigh-pressure eclogite in the Pakistan Himalaya. *Geology* 34: 989-992
- Patterson MG and BF Windley. 1985. Rb-Sr dating of the Kohistan arc-batholith in the Trans-Himalaya of north Pakistan, and tectonic implications. *Earth Planet Science Letters* 74: 45-57

Structural, paleogeographic and topographic evolution of the northern Tibetan Plateau margin: Evidence from the southern Tarim basin, northern Hexi Corridor, and Qaidam basin

Bradley D Ritts^{1*}, Paul M Bovet², Malinda L Kent-Corson³, Brian J Darby⁴, Jeremy Hourigan⁵, Guangsheng Zhuang⁵, Stephan A Graham³ and Yongjun Yue⁶

¹ Chevron Energy Technology Company, San Ramon, CA, USA

² Chevron Energy Technology Company, Sugar Land, TX, USA

³ Stanford University, Stanford, CA, USA

⁴ ExxonMobil Upstream Research Center, Houston, TX, USA

⁵ University of California – Santa Cruz, Santa Cruz, CA, USA

⁶ Chevron North America Exploration and Production Company, Bakersfield, CA, USA

* For correspondence, email: bradleyritts@chevron.com

The sedimentary record on and adjacent to the northern Tibetan Plateau is providing new constraints on the absolute and relative timing of upper crustal deformation, exhumation, and topographic growth. Furthermore, these rocks record changing depositional environments through the Cenozoic and provide a recorder for isotopic, detrital thermochronologic and other measures of tectonic activity at Earth's surface.

The sequence of Cenozoic deformation on the northern margin of the plateau is poorly understood prior to the late Oligocene, resulting from a lack of extensive Paleocene-Eocene sedimentary deposits. However, the Oligocene-Pliocene sedimentary record is relatively complete in the Qaidam, Tarim and Hexi Corridor basins, as well as numerous smaller intermontane basins within the Altun Shan, Qilian Shan, and Kunlun Shan. These deposits are the focus of our studies.

Large-magnitude strike-slip faulting on the Altyn Tagh fault initiated in the Oligocene, as demonstrated by previous workers in the Tarim and Qaidam basins (Bally et al. 1986, Hanson 1999, Rumelhart 1999). Differential offsets on Late Oligocene – Early Miocene strike-slip basins along the Altyn Tagh fault also demonstrate progressive deformation on the Altyn Tagh fault, and suggest that most strike-slip (~310 km of 375±25 km in the central-eastern segment of the Altyn Tagh fault) occurred by the end of the early Miocene (Yue et al. 2001, 2004, Ritts et al. 2004). The older piercing points from the Oligocene-Early Miocene Xorkol basin that demonstrate this early phase of rapid, high-magnitude slip are age-correlative with fine-grained rocks in the footwall of the Northern Altyn Tagh reverse fault (Ritts et al. in press), fine-grained rocks in the footwall and hanging wall of the North Qilian thrust fault (Bovet et al., in review) and fine-grained rocks proximal to the Kunlun Shan and Qilian Shan in the Qaidam basin. These relationships are interpreted to indicate that significant crustal shortening and surface uplift in the Altun Shan, Kunlun Shan, and Qilian Shan did not accompany this Oligocene – earliest Miocene rapid slip on the Altyn Tagh fault.

Late Early to mid-Miocene strata throughout the region have a rapid transition to massive, boulder conglomerate sections; these lithologies continue to be dominant in the Miocene-Quaternary section. In all cases, these conglomeratic sections contain sediment derived locally from adjacent mountain ranges,

have paleocurrents directions that are strongly transverse to these ranges and display proximal to distal gradients moving away from these ranges. These characteristics indicate that these conglomeratic sections are coeval with shortening, surface uplift, and exhumation of the Altun Shan, Qilian Shan, and Kunlun Shan. The age of initiation of conglomeratic sedimentation is difficult to precisely define in some sections, but throughout the study region it can be bracketed to Miocene, and where more precise determinations are possible, it ranges from 18-11 Ma. In sections along the Altyn Tagh fault, this change to conglomeratic deposition overlies older strata that comprise large-offset piercing points on the Altyn Tagh fault. Furthermore, in the Xorkol, Aksay, Xorkol Pass, and Mangnai areas, these Neogene conglomerates have small or no offset from their source terranes on the opposite wall of the Altyn Tagh fault. Thus, piercing points in multiple post-Early Miocene basins along the Altyn Tagh fault demonstrate that the rate of strike-slip dramatically decreased after the Early Miocene, concomitant with initiation of shortening in the Qilian Shan, Kunlun Shan and Altun Shan.

Neogene conglomeratic deposition is dominated by waterlain facies, similar to the energetic river systems flowing from the Altun Shan, Kunlun Shan and Qilian Shan today. Furthermore, these conglomerates are interbedded with eolian deposits in some sections, particularly in the southern Tarim basin, suggesting that the modern depositional systems and climatic regime was fully established by mid-Miocene time.

We interpret this succession of depositional styles to reflect the evolving structural regimes on the northern margin of the Tibetan Plateau. Pre-Oligocene tectonic quiescence is suggested by the lack of Paleocene-Eocene strata in the region, and modeled slow-cooling from thermochronologic data (Sobel et al. 2001, Ritts et al. in press). Rapid, large-magnitude strike-slip faulting on the Altyn Tagh fault initiated in the Oligocene and continued into the Early Miocene, synchronous with shortening in the southern and central Tibetan Plateau (Cyr et al. 2005, Graham et al. 2005). Strike-slip faulting on the Altyn Tagh fault slowed dramatically with the mid-Miocene initiation of shortening in the fold-thrust belts of the northern Tibetan Plateau, the Qilian Shan, Kunlun Shan and Altun Shan. This mid-Miocene initiation of crustal shortening and slowing of strike-slip faulting, represents the timing of major

surface uplift and exhumation on the northern margin of the Tibetan Plateau and establishment of the present topographic front of the Plateau. We further suggest that this sequence of structural events indicates northward growth of the Tibetan Plateau through a process where strike-slip deformation accommodated plate-like lateral extrusion of the northern plateau in the Oligocene and Early Miocene, concomitant with crustal shortening and construction of topography in the southern and central Tibetan Plateau, followed by propagation of distributed crustal shortening, surface uplift into the northern Tibetan Plateau region in the mid-Miocene, and slowing of slip on the Altyn Tagh fault.

References

- Bovet PM, BD Ritts, G Gehrels, OA Abbink, BJ Darby and J Hourigan. Evidence of Miocene crustal shortening in the North Qilian Shan from Cenozoic stratigraphy of the western Hexi Corridor, Gansu Province, China. *American Journal of Science* (in review)
- Cyr AJ, BS Currie and DB Rowley. 2005. Geochemical evaluation of Fenghuoshan Group lacustrine carbonates, north-central Tibet: Implications for the paleoaltimetry of the Eocene Tibetan Plateau. *Journal of Geology* 113: 517-533
- Graham SA, P Chamberlain, Y Yue, BD Ritts, AD Hanson, TW Horton, JR Waldbauer, MA Poage and X Feng. 2005. Stable isotope records of Cenozoic climate and topography, Tibetan Plateau and Tarim basin. *American Journal of Science* 305:101-118
- Hanson. 1999. *Organic geochemistry and petroleum geology, tectonics and basin analysis of the southern Tarim and northern Qaidam basins, northwest China*. Ph.D. dissertation. Stanford University, Stanford, 388 p
- Ritts BD, YJ Yue and SA Graham. 2004. Oligocene-Miocene tectonics and sedimentation along the Altyn Tagh fault, northern Tibetan Plateau: Analysis of the Xorkol, Subei, and Aksay basins. *Journal of Geology* 114 (2)
- Ritts BD, YJ Yue, SA Graham, ER Sobel, OA Abbink and Stockli D. From Sea Level to High Elevation in 15 Million Years: Uplift History of the Northern Tibetan Plateau Margin in the Altun Shan, *American Journal of Science* (In press),
- Rumelhart PE. 1999. *Cenozoic basin evolution of southern Tarim, northwestern China: Implications for the uplift history of the Tibetan Plateau*. Ph.D. dissertation. Los Angeles, University of California. 268 p
- Yue, YJ, BD Ritts and SA Graham. 2001. Initiation and long-term slip history of the Altyn Tagh fault. *International Geological Review* 43 (12): 1087-1093
- Yue, YJ, BD Ritts, SA Graham, JL Wooden, GE Gehrels and Z Zhang 2004. Slowing extrusion tectonics: Lowered estimate of the post-Early Miocene slip rate along the Altyn Tagh fault. *Earth and Planetary Science Letters* 217: 111-122

New recognition of NNE-strike belt of negative aeromagnetic anomaly in Tibetan plateau

HE Ri-Zheng^{1,*}, GAO Rui¹ and ZHENG Hong-Wei²

¹ Institute of Geology, Chinese Academy of Geological Sciences, Beijing 100037, CHINA

² Geophysical Department, Peking University, Beijing 100871, CHINA

* For correspondence, email: herizheng@cags.net.cn

The aeromagnetic data (see Figure 1) used in this study came from the survey of scale 1:1000000 in mid-west Tibetan plateau conducted by the Center of Aerial Survey and Remote Sensing of the Land and Resources Department in 1998-2000 (Xiong et al. 2001). This study adopts the matched-filter technique to obtain regional anomaly fields (He et al., 2007; Figure 2). It has a good agreement with upward continuation (Xiong et al. 2001), which shows that there is a regional NNE-trending negative anomaly belt in the middle part of Tibetan plateau. Figure 2 indicates that the source depth responsible for generating this negative anomaly belt is greater than the average depth of Curie isothermal surface in Tibetan plateau (Alsdorf and Nelson 1999). Below the Curie surface, rock magnetism is mainly caused by inductive magnetization, which is related to the regional tectonic stress field. The regional tectonic stress field is in turn dictated by regional deep structures and tectonics.

Shapiro et al. (2004) studied the seismic waveform data crossing the mid-western part of Tibetan plateau and considered that there was a near-NS low-velocity zone from 20 km down to

the lower crust of Tibet, where the VSH is about 8% lower than the standard velocity. The result from Teleseismic P-wave tomography shows that the front of the subducting Indian lithospheric mantle reaches northward to the middle of Qiangtang terrane (He et al. 2006, Zheng 2006). Combining with the result of deep seismic profiling east-westerly crossing this low-velocity zone (Teng et al. 1994, Zhang et al. 2001), the synthesis indicates that the Indian lithospheric mantle beneath the plateau is deformed to a "spoon" shape, and the regional NNE-trending negative anomaly in the middle of the plateau is rightly in the center of the spoon. Beneath the northern part of Qiangtang terrane in middle Tibetan plateau, there is a mantle-originated low-velocity body (Zheng 2006, Zhou and Murphy 2005), whose position coincides with the region of low Pn velocity and insufficient Sn propagation (McNamara et al. 1997), on its top is the region of widespread potash volcanic rocks in northern Tibet (Deng et al. 1996 Hacker et al. 2000, Chung et al. 2005). This indicates that the front of Indian lithospheric mantle is not sutured together with that of Eurasian plate, resulting in a low-velocity anomaly body originated from the mantle (Zheng

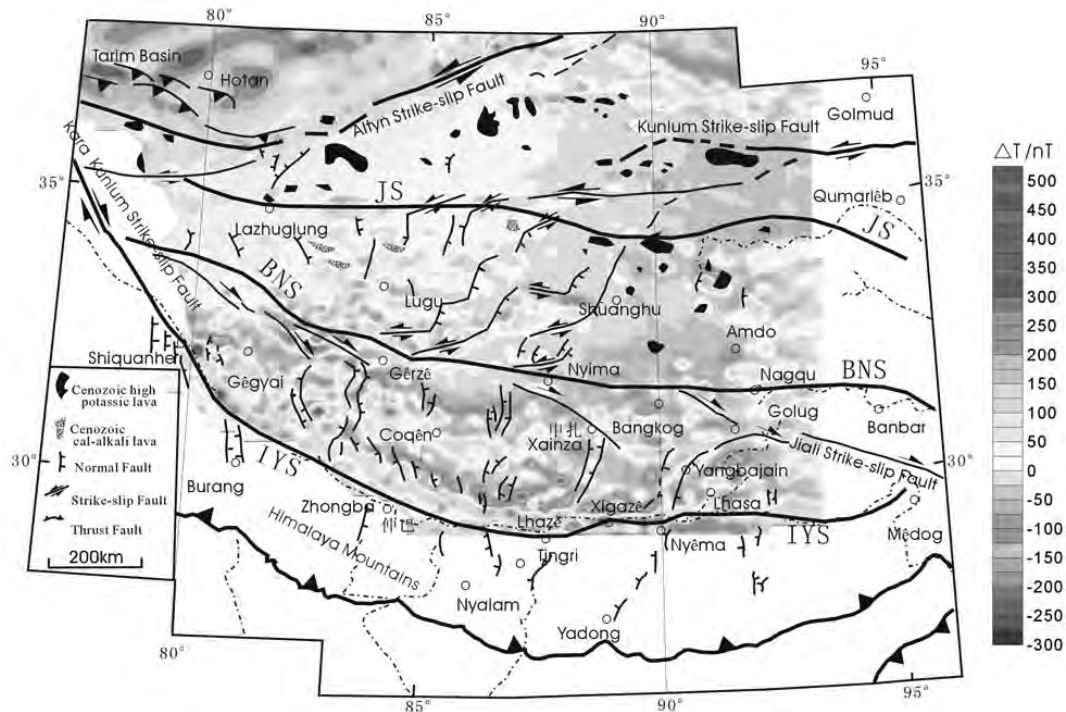


FIGURE 1. The map of aeromagnetic T anomaly reduced to the pole in mid-western Tibet Plateau. Tectonic base map from Yin et al. (2001). IYS: Indus-Yalung Zangbo Suture; BNS: Banggonghu-Nujiang Suture; JS: Jinshajiang Suture.

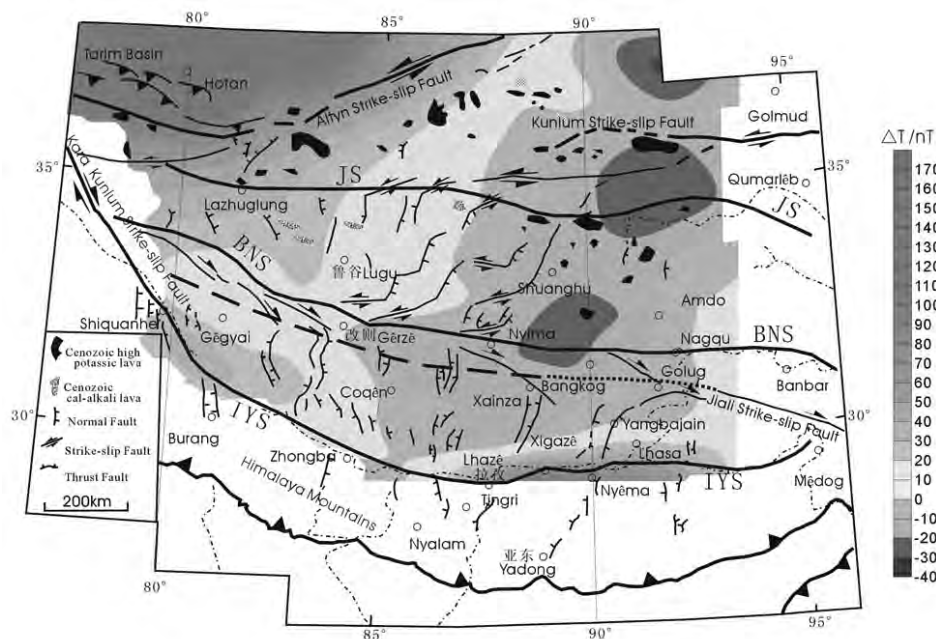


FIGURE 2. The regional magnetic anomaly field in mid-western Tibet Plateau (legends and tectonic basemap are the same as in Figure 1).

2006). The location of this low-velocity body is comparable to that of the NNE-trending negative aeromagnetic anomaly given in this paper. The anomalously hot material from deep mantle flows southward and upward along the NNE spoon-like Indian lithospheric mantle. This made the temperature of the primary lithosphere of midsouth Tibetan plateau on top of the spoon-like Indian lithospheric mantle to rise anomalously, resulting in an enclosed NNE-trending thermal anomaly zone, which caused thermal demagnetization of the magnetic minerals inside the lithosphere of middle Tibetan plateau. In this way the regional NNE-trending negative aeromagnetic anomaly belt was formed.

Acknowledgement

This work was supported by grants from Nation Science foundations Tian Shan project of US and National Natural Science Foundations of China (No. 40404011, 40774051), 2007 Year of the Basic outlay of scientific research work from Ministry of Science and Technology of the People’s Republic of China, International Cooperative Project from Ministry of Science and Technology of the People’s Republic of China No.2006DFA21340, Open Fund (No. GDL0602) of Geo-detection Laboratory, Ministry of Education of China, China University of Geosciences.

References

Alsdorf D and D Nelson. 1999. Tibetan satellite magnetic low: evidence for widespread melt in the Tibetan crust? *Geology* 27(10): 943-946
 Chung Sun-Lin, Chu Mei-Fei, and Zhang Yuquan. 2005. Tibetan tectonic evolution inferred from spatial and temporal variations in post-collisional magmatism. *Earth Science Reviews* 68: 173-196
 Deng W, X Zheng and Y. Matsumoto. 1996. Petrological characteristics and ages of Cenozoic volcanic rocks from the Hoh Xil Mountains, Qinghai. *Acta Petrologica et Mineralogica* (in Chinese with English abstract) 15 (4): 289-298
 Hacker BR, E Gnos and L Ratschbacher. 2000. Hot and dry deep crustal xenoliths from Tibet. *Science* 287: 2463-2466

He R, ZDP Zhao and R Gao. 2006. Teleseismic P-wave tomography under the central Tibet Plateau, *Eos Trans. AGU* 87(36) West. *Pacific Geophysics Meet, Supplementary, Abstract: T12B-04*
 He RZ, R Gao, HW Zheng and JS Zhang. 2007. Matched-filter analysis of aeromagnetic anomaly in mid-western Tibetan plateau and its tectonic implications. *Chinese Journal of Geophysics* (in Chinese) 50(4): 1131-1140
 McNamara DE, WR Walter and TJ Owens. 1997. Upper mantle velocity structure beneath the Tibetan plateau from Pn travel time tomography. *Journal of Geophysical Research* 102: 493-505
 Shapiro NM, MH Ritzwoller and P Molnar. 2004. Thinning and flow of Tibetan crust constrained by seismic anisotropy. *Science* 305: 233-236
 Teng JW, ZX Yin and HB Liu. 1994. 3-D and 2-D structure of Tibetan lithosphere and continental dynamics. *Chinese Journal of Geophysics (Acta Geophysica Sinica)* (in Chinese) 37 (Suppl. II): 117-130
 Xiong SQ, FH Zhou, ZX Yao, DJ Xue and SL Duan (Editors). 2001. *Aeromagnetic survey in Central and western Qinghai-Tibet plateau* (in Chinese with English abstract) Beijing: Geological Publish House.
 Yin A. 2001. Geologic evolution of the Himalayan-Tibetan orogen- Phanerozoic growth of Asia continental. *Acta Geoscientia Sinica* (in Chinese) 22(3): 193-230
 Zhang ZJ, Li YK, Wang GJ. 2001. E-W crustal structure of North Tibet and “Sunken” Moho – an implication from wide-angle reflection profile. *Science in China (Series D)* 31(11): 881-888
 Zheng HW. 2006. *3-D velocity structure of the crust and upper mantle in Tibet and its geodynamic effect*. (Ph. D. dissertation) Beijing, Chinese Academy Geological Sciences.
 Zhou FH, ZX Yao and ZJ Liu. 2002. The origin and implication of the NNE-trending deep negative magnetic anomaly zone in Central Qinghai-Tibet plateau. *Geophysical and Geochemical Exploration* (in Chinese with English abstract) 26(1): 12-16.
 Zhou HW and MA Murphy. 2005. Tomographic evidence for wholesale underthrusting of India beneath the entire Tibetan plateau. *Journal of Asian Earth Science* 25: 445-457

Identification of necessary conditions for supershear wave rupture speeds: Application to Californian and Asian Fault

David Robinson* and Shamita Das

Department of Earth Sciences, University of Oxford, Parks Road, Oxford, OX1 3PR, UK

* *For correspondence, email: davidr@earth.ox.ac.uk*

The Mw 7.8 2001 Kunlun, Tibet earthquake, with a 400 km long rupture, taught us that the portions of strike-slip faults most likely to propagate at supershear speed are long and straight. This is only a necessary (but not sufficient) condition, that is, of course all straight portions of faults will not reach super-shear speeds. Once a fault accelerates to the maximum permissible speed, it can continue at this speed provided it is straight and there are no obstacles along the way, and provided the fault friction is low. Laboratory experiments (Rosakis et al. *Science* 1999) show that such speeds can be attained in nature.

For the Tibet earthquake, the 100 km region of highest rupture speed not only exceeded the shear-wave speed, but actually approached the compressional wave speed of nearly 6 km/s (Robinson et al., *JGR*, 2006). This result has recently been confirmed in an independent study, using a very different technique (Vallée et al. *JGR* submitted 2008). Robinson et al. showed that this region of highest rupture speed also had the highest slip rate, the highest slip and the highest stress drop. Off-fault cracks, interpreted as due to the passage of the Mach front,

exists in only that portion of the fault identified as traveling at supershear speed and not in other places along the fault (Bhat et al. *JGR* 2007). Re-examination of earlier reports of super-shear rupture speeds on the North Anatolian fault show that such speeds did occur on very straight sections of the fault. Of course all straight portions of faults will not reach super-shear speeds.

So what can the Tibet earthquake teach us about other strike-slip faults worldwide? For the San Andreas fault, both the 1906 and the 1857 earthquakes have long, straight portions, the former having been identified by Song et al. (*EOS* 2005) as having attained a supershear speed to the north of San Francisco, the region of highest slip. If the repeat of the 1857 starts in the central valley, as it is believed to have done in 1857, it has the potential to propagate at supershear speeds through the long, straight portion of the San Andreas fault in the Carrizo Plain, the region believed to have had the largest displacement in 1857 based on paleoseismic studies. The resulting shock waves would strike the highly populated regions of Santa Barbara and the Los Angeles Basin (Das, *Science* 2007). Similar considerations will be discussed for Asian faults.

Discovery of granulitized eclogite in North Sikkim expands the Eastern Himalaya high-pressure province

Franco Rolfo^{1*}, Rodolfo Carosi², Chiara Montomoli² and Dario Visonà³

¹ *Dipartimento di Scienze Mineralogiche e Petrologiche, University of Torino, ITALY*

² *Dipartimento di Scienze della Terra, University of Pisa, ITALY*

³ *Dipartimento di Geoscienze, University of Padova, ITALY*

* *For correspondence, email: franco.rolfo@unito.it*

Eclogite occurrences are very few in the Himalayas and mainly consist of two types (Lombardo and Rolfo 2000): the coesite-bearing eclogites of the western Himalaya (Kaghan valley: O'Brien et al. 2001; Tso Moriri: Sachan et al. 2004) and the granulitized eclogites of the eastern Himalaya (Ama Drime range: Lombardo et al. 1998).

Unlike the "western type" eclogites, where post-peak decompression under constant to decreasing temperature suggests exhumation favoured by thrusting associated with accretion of the metamorphic pile onto the base of the over-riding plate, the "eastern type" Ama Drime eclogites were probably exhumed relatively slowly and were subjected to thermal relaxation in the thickened continental crust producing a strong granulite-facies overprint at intermediate crustal levels.

A new finding of granulitized eclogites in North Sikkim, east of Mount Kangchendzonga and some 120 km southeast of the Ama Drime, extends the eclogite province in eastern Himalaya.

Mount Kangchendzonga sits at the western flank of the Ranjit Tectonic Window (RTW), a regional structure cutting deeply through the Himalayan nappe pile. At low structural levels, the RTW exposes low grade Lesser Himalayan schists overlying unmetamorphosed Permo-Carboniferous sedimentary rocks of Gondwanian affinity. At higher structural levels, the northern end of the RTW shows an increase in metamorphic grade through the Main Central Thrust zone up to migmatites with garnet-bearing leucosomes in the Higher Himalayan Crystallines (HHC). In north Sikkim, along the Zemu Glacier east of Kangchendzonga, HHC main lithologies are granite to granodiorite orthogneiss with intercalations of biotite-rich paragneiss and very rare metabasites. Rolfo et al. (2006) gave a preliminary description of this geologic transect, where the main fabric is folded by two systems of later folds trending NNE-SSW and WNW-ESE with steeply dipping axial planes. The RTW can be the result of the interference pattern between these two later system of folds. Compressive and extensional shear zones with a top both to the SW and SE sense of shear respectively affect the main foliation. Top to the SE shear zones can be correlated with normal shear zones recognized in the nearest western Bhutan (Carosi et al. 2006), developed during the extrusion of the HHC.

The lithological associations of the HHC in the Zemu Glacier area are comparable to those described south of Mt. Kangchendzonga by Vezzoli et al. (2005). Among metabasites collected in the drainage of Zemu Glacier, a few samples are very similar to the granulitized eclogites first described in eastern

Himalaya by Lombardo et al. (1998) in the Ama Drime range, southern Tibet.

Microstructure of the North Sikkim granulitized eclogite is medium grained, granoblastic and little deformed. It is characterised by the occurrence of well preserved porphyroblastic garnet crystals several mm across, surrounded by a thick plagioclase + orthopyroxene corona, and a matrix mainly made of brown amphibole and plagioclase together with minor quartz, biotite and opaque minerals. Primary omphacite is not preserved, but is replaced by a distinctive symplectite of plagioclase + amphibole. Compared to the Ama Drime eclogite, the typical plagioclase-biotite intergrowths replacing pristine phengite occur very rarely and ilmenite aggregates and minor magnetite are locally abundant.

Though strongly re-equilibrated to granulite and amphibolite facies, the North Sikkim eclogite is clearly comparable to the Ama Drime eclogite. Bulk rock composition is analogous, showing a moderately high SiO₂ content (from 52 to 53 wt%), medium K₂O (0.54 wt%) and low MgO (5.47 wt%) contents. Ti content is relatively high (TiO₂ = 2.77 wt%) as well as the Fe content (FeOtot = 14.79 wt%), suggesting Fe-rich basalt as protolith. Most minerals of the high-pressure peak assemblage are not preserved, save for the eclogitic cores of garnet (Grs18-20, Alm55-56, Prp08-09, Sps08-09) very similar in composition to those of Ama Drime eclogite (Groppo et al. 2007). As a whole, chemical compositions of the North Sikkim eclogite main assemblage (garnet, pyroxene, amphibole) are strongly similar to those of Ama Drime eclogite, suggesting a comparable metamorphic evolution.

Mineral assemblages, reaction textures, geothermobarometry and isochemical phase diagram P-T sections suggest that at least three superposed metamorphic events have been recorded in the North Sikkim eclogite. The first event was eclogitic, with T > 600°C and P > 1.5 GPa, but is poorly constrained because of the nearly complete lack of eclogitic mineral relics. The second event was granulitic and is represented by the plagioclase + orthopyroxene corona around garnet, with medium P (> 0.4 GPa) and high T (ca. 750°C). The third event at comparable P and lower T (< 720°C) is marked by the growth of brown amphibole and plagioclase in the matrix.

The discovery of strongly overprinted eclogite in North Sikkim extends significantly the high-pressure province of the eastern Himalaya and confirms the duality in tectonic style of exhumation along the Himalayan chain.

References

- Carosi R, C Montomoli, D Rubatto and D Visonà. 2006. Normal-sense shear zones in the core of the Higher Himalayan Crystalline (Bhutan Himalayas): evidence for extrusion? *Geological Society of London, Special Publication* 268: 425-444
- Gropo C, B Lombardo, F Rolfo and P Pertusati. 2007. Clockwise exhumation path of granulitized eclogites from the Ama Drime Range (Eastern Himalayas). *Journal of Metamorphic Geology* 25: 51-75
- Lombardo B, P Pertusati, F Rolfo and D Visonà. 1998. First report of eclogites from the E Himalaya: implications for the Himalayan orogeny. *Memorie di Scienze Geologiche* 50: 67-68
- Lombardo B and F Rolfo. 2000. Two contrasting eclogite types in the Himalayas: implications for the Himalayan orogeny. *Journal of Geodynamics* 30: 37-60
- O'Brien PJ, N Zotov, R Law, M Ahmed Khan and M Qasim Jan. 2001. Coesite in Himalayan eclogite and implications for models of India-Asia collision. *Geology* 29: 435-438
- Rolfo F, R Carosi, C Montomoli, D Visonà and IM Villa. 2006. A geological transect east of Kangchendzonga (north Sikkim, India). *Journal of Asian Earth Sciences* 26: 158
- Sachan HK, MK Mukherjee, Y Ogasawara, S Maruyama, H Ishida, A Muko and N Yoshioka. 2004. Discovery of coesite from Indus Suture Zone (ISZ), Ladakh, India: Evidence for deep subduction. *European Journal of Mineralogy* 16: 235-240
- Vezzoli G., B Lombardo and F Rolfo. 2005. A geological reconnaissance to southern Kangchendzonga massif. *Géologie Alpine* 44: 192

Seismic Tomography of Garwhal-Kumaun Himalayas: Is the basal detachment a wistful thinking?

S Mukhopadhyay^{1*} J Sharma² and BR Arora²

¹ *Department of Earth Sciences, IIT Roorkee, Roorkee-247667*

² *Wadia Institute of Himalayan Geology, Dehradun*

* *For correspondence, email: sagarfes@iitr.ernet.in*

We carried out seismic tomography in the Garhwal-Kumaun Himalayas using P- and S-phase data of local earthquakes. We observe that the near surface low velocity zones generally coincide with sedimentary formations, such as, inner and outer sedimentary formations and Berinag formations. The metamorphic rocks like Vaikrita, Almora and Ramgarh Groups show up as bodies having higher velocity. Many workers have suggested the presence of a gentle northerly dipping detachment that decouples Lower Himalaya sedimentary formations from underlying metamorphic crystalline basement. This suggestion is based in part on seismicity pattern. The present seismic tomographic work does not show

a detachment surface but the interface is highly undulated. The nature of undulations varies strongly both across and parallel to the orogenic trend. Such strong undulations may indicate crustal-scale folding and thrusting whose geometries vary across and along the trend of the Himalayas. As a consequence, the structural trend inferred from the velocity models, along cross sections that are 50 km apart vary significantly. The velocity sections suggest that the rock formations below the sedimentary cover-basement interface are also significantly deformed. This would mean that the deformation in this part is basement involved and not basement detached.

Lake-level changes in the past 50 ka reconstructed from the lacustrine delta deposits in Kathmandu Valley, Nepal

Tetsuya Sakai^{1*}, Ananta P Gajurel², Hideo Tabata³, Nobuo Ooi⁴ and Bishal N Upreti²

¹ Department of Geoscience, Shimane University, Matsue 690-8504, JAPAN

² Department of Geology, Trichandra Collage, Tribhuvan University, Kathmandu, NEPAL

³ Applied Satoyama Study Laboratory, 1773-2 Yoshikawa-cho, Mino 501-3721, JAPAN

⁴ ONP Laboratory, 21-30 Tai-cho, Neyagawa 572-0021, JAPAN

* For correspondence, email: sake@riko.shimane-u.ac.jp

This study aims to elucidate lake-level changes in the past 50 ka from the deltaic succession exposed in the northern part of Kathmandu Valley, Nepal. The thick pile of the lacustrine delta succession (Gokarna, Thimi, Tokha and Patan Formations) exposed at 1,300–1,420 m above sea level (masl) allows reconstruction of the lake-level curve, based on estimation of paleolake levels within the deltaic succession and using 14C dating.

The paleolake levels were estimated based on facies analysis, which showed that the bulk of the sediments were deposited in the subaerial part of the lacustrine delta (fluvial, marsh and flood plain deposits). The levels of the sampling points for dating thus correspond to the lake level at the time of deposition. In addition, the following stratigraphic information was incorporated for delineating the curve: (1) sediments deposited during a rapid lake-level-fall event due to lake outburst were discovered in the Gokarna Formation. The event bed was dated as 39 ka, and the associated erosion surface was discovered in the succession at about 1,340 masl; the lake level reached 1,340 masl and then fell rapidly down to 1,300 masl, at which point the fluvial deposits after the event were deposited. (2) Because the top of the Gokarna Formation was truncated prior to the deposition of the Tokha Formation, the precise height of the top of the Gokarna Formation is unknown in the north Kathmandu Valley. In the eastern part of the basin, the top of the Gokarna Formation seems to have escaped the subsequent

erosion. The top of the formation at this site was 14C-dated at 35 ka. (3) The age of the lake draining is still uncertain. The youngest age formerly obtained from the lake sediments was 11 ka: ca. 10 ka is the most plausible age for the draining by another lake outburst. Just before the lake vanished, the lake-level reached 1,320 masl.

Two lake-level rise events around 34 ka and 19 ka are depicted in the curve; both were followed by rapid lake-level falls. These falls may also have been due to lake outbursts such as the 39 ka event, but do not represent climatic signals in Kathmandu Valley. However, the lake-level-rise events can be recognized as climate signals, because they occurred in an underfilled condition. The lake-level rises around 34 ka and 19 ka seem to reflect the humid climate. In particular, the lake-level rise around 34 ka is synchronized with the enhanced Indian monsoon recorded in the intermontane basins of the Himalayas (e.g. Kumaun Himalaya) and in the ice cores and lake-level records in Tibet. The 19 ka-rise event may have caused by reduction in evaporation and slight increase in precipitation. The humid climate condition in this period has been also detected by pollen analysis in Kumaun Himalaya, and by the higher water level than present identified in the lakes of western Tibet. This humid condition was probably brought by westerlies, the effect of which may have spread farther south than previous estimates based on the distribution of the glaciated area during the last glacial maximum.

Mineralogy and Geochemistry of mafic to hybrid microgranular enclaves and felsic host of Ladakh batholith, Northwest Himalaya: Evidence of multistage complex magmatic processes

Santosh Kumar* and Brajesh Singh

Department of Geology, Kumaun University, Nainital 263 002, Uttarakhand, INDIA

* For correspondence, email: skyadavan@yahoo.com

Felsic magmatisms in the north of Indus-Tsangpo-Suture Zone, referred herein Ladakh granitoids (LG), have been characterized dominantly as calc-alkaline, magnetite to ilmenite series (gradually changing from NW to SE) granitoids derived from partial melting of heterogeneous protoliths in subduction environment. Field relation, petrography, mineralogy and geochemistry of ME and felsic host LG have been carried out along various transects covering Northwest (Dras-Kargil-Silmo-Batalik-Achina Thang), Central (Leh-Ganglas-S. Pullu-KhardungLa-N. Pullu-Khardung), Southeast (Himiya-Litse-Upshi-Karu-Sakti-Zingral-ChangLa) parts of Ladakh batholith in order to understand the physical and chemical processes of mafic and felsic magma interaction in plutonic condition.

The LG can be broadly classified into coarse-grained LG with abundant mafics (hbl-bt), medium-grained LG with low content of mafics, and fine-grained leucocratic LG with very low amount of mafics. Mesocratic to melanocratic, fine to medium grained and porphyritic (xenocrystic) hybrid microgranular enclaves (ME) are found hosted mostly in medium to coarse-grained LG. Double enclaves (one mafic ME into other porphyritic ME) and syn-plutonic disrupted mafic dykes are also hosted in K-feldspar megacrysts bearing LG in the Northwest part of batholith, which record evidence of multiple mafic to hybrid magma injection and thermal rejuvenation of partly crystalline LG. ME are absent or rare in the leucocratic variety of LG. The ME are rounded to elongate commonly having sharp, crenulate, and occasionally diffuse contacts with felsic host, and size varies from a few cm to metres across but cm-sized ME ($d < 30$ cm) are common, which strongly suggest that several pulses of crystal-charged mafic and felsic magmas, coexisted, hybridized, co-mingled into plutonic setting. Most hybridized parts (active mixing region) of LG do not contain ME whereas isolated mixing regions of LG contain variable sizes of mingled and stretched (sine flowage) ME. The ME (diorite, quartzdiorite) and felsic host LG (granodiorite, monzogranite) bear common mineral assemblages (hbl-bt-pl-kfs-qtz-ap-zrn-mt \pm ilm) but differ in their mineral proportions. The ME lack cumulate-like texture and are fine to medium grained, and therefore oppose their co-genetic link with LG. Presence of patchy zoned (spongy, cellular) plagioclase xenocrysts, quartz ocelli and apatite needles in porphyritic ME strongly indicate mingling and undercooling of hybridized ME globules into cooler felsic host LG. Grain size differences, crystal index, and size of ME among the ME population, except to those of porphyritic ones, correlate well with degree of undercooling of ME. Disaggregated large ME into several smaller ones

lack fine-grained chilled margin. Biotite composition of ME and LG from Northwest and Central parts represents Mg-Fe biotites stabilized in FMQ and NNO buffers exhibiting Mg=Fe substitution typical to its crystallization in a calc-alkaline (I-type) felsic melt but biotite of LG from Northwest sector is depleted in phlogopite component as compared to LG biotite of Central part. Biotites of ME and LG from Southeastern part of batholith also represent Mg-Fe biotite but are slightly enriched in Al-Ti-Fe contents and bimodal in nature exhibiting $2Al=3Fe^{2+}$ and Mg=Fe substitutions typical to their crystallization in peraluminous (S-type) and calc-alkaline (I-type) felsic melts respectively. This is because ilmenite series granites dominants over magnetite series granites in the Southeastern transects. The LG batholith predominantly crystallized at elevated fO_2 (magnetite series) and subordinately at low fO_2 (ilmenite series) more prevalent in the Southeastern part. Amphiboles in ME and LG belong to calcic amphibole (magnesian hornblende slightly approaching to ferrohornblende). Changing fO_2 conditions of melt have indeed affected temperature-sensitive exchange vector $Fe^{3+}=Al^{vi}$ of hornblende and thus also have affected the Al-in-hornblende barometers. Taking into account of such limiting factors the Al-in-hornblende barometer estimates emplacement of Northwest LG at $P=2.5-3.5$ (± 0.6 kbar), Central LG at $P=3-4$ (± 0.6 kbar) and Southeastern LG at $P=3.5$ (± 0.6 kbar) suggesting differential unroofing of LG magmachamber(s). The ME globules are mingled and undercooled more-or-less at the same level of LG emplacement but hybrid (ME) magma zone must occur sufficiently below it as some small sized ME have undercooled enroute at ca $P=5.0$ (± 0.6 kbar). Whole rock composition of LG is calc-alkaline, largely metaluminous I-type (mol A/CNK < 1.0) to slightly peraluminous S-type (mol A/CNK > 1.05) but ME are highly metaluminous (mol A/CNK > 0.9) and markedly differ from diorite, gabbro and mafic dykes of the region. Near linear to curvilinear compositional trends observed for TiO_2 , CaO, Fe_2O_3 , MgO, against SiO_2 can be attributed to mafic-felsic magma mixing whereas data scatter for Al_2O_3 , alkalis, MnO, P_2O_5 , Rb and Ba are caused by combined effect of chemical diffusion and modal mineral variations between ME and LG. However, LG and ME might have experienced internal fractional differentiation prior to and during the mixing event. Wide data scatter observed for Nb, Yb, Zr in ME and LG are result of modal abundance of accessory phases (e.g. zircon) hosting these elements. K-feldspar megacrysts bearing LG in Northwest part and its porphyritic ME are Zr-Nb-U-Th-Rb-Ba-Sr-LREE enriched as compared to other LG-ME samples most likely due to retention and recycling of residual mineral

phases hosting these elements mainly during mafic-felsic magma mixing event. The ME and LG from Northwest part of batholith exhibit almost flat REE patterns with low-degree of negative Eu-anomalies as compared to slightly inclined LREE and flat HREE patterns of LG and ME from central and southeast parts of the batholith. Identical trace and REE patterns of ME and LG, and higher sum of REE in ME compared to felsic host LG may be attributed to diffusion mechanism during postentrapment cooling

and mingling of ME magma globules into partly crystalline felsic host LG. Gabbro, diorite and a few LG are depleted in sum of REE and exhibit positive Eu-anomaly, which strongly oppose a cognate origin for ME. Several lines of evidences suggest that calc-alkaline Ladakh granitoids and their microgranular enclaves are product of complex magmatic processes such as multistage magma mixing of multiple pulses of mantle- and crustal-derived magmas concomitant fractional differentiation, contamination, mingling, and diffusion mechanisms.

Geochemistry and Petrogenesis of Granitoids from Kameng Corridor of Arunachal Himalaya, Northeast India

Santosh Kumar* and Manjari Pathak

Department of Geology, Kumaun University, Nainital 263 002, Uttarakhand, INDIA

* For correspondence, email: skyadavan@yahoo.com

Felsic magmatism in Kameng Corridor of Arunachal Himalaya are mainly represented by extensively exposed Palaeoproterozoic granite gneiss (GGn), small stock-like undeformed Mesoproterozoic biotite granite (BG) and veins and pods of Tertiary leucogranite (TLg). The magnetic susceptibility (MS) measurements and whole rock geochemistry of these felsic magmatic bodies have been carried out in order to evaluate nature of granite series and petrogenesis of these felsic rocks with its implication on collisional tectonics.

The GGn records average MS of 0.243×10^{-3} SI at Bomdila proper corresponding to ilmenite series (reduced type) granites, which further reduced ($\chi = 0.076 \times 10^{-3}$ SI) in close contact with black shales of Salari Group. The BG measures MS values between 0.156 and 0.120×10^{-3} SI slightly changing from core to margin of the stock suggesting marginal reduction of BG melt at emplacement level. The TLg bears MS values ($\chi = 0.042$ to 2.82×10^{-3} SI) and at places intrudes the hornblende-biotite granite ($\chi = 15.42$ - 27.37×10^{-3} SI) an older lithounit of Sela Group exposed beyond the Main Crystalline Thrust (MCT). Observed MS variations of these felsic magma bodies appear primarily intrinsic to crustal (metasedimentary) source regions, although these melts have been partly reduced at emplacement level as a result of reaction with carbonaceous country rocks.

The modal composition of GGn represents largely monzogranite (ss) whereas BG corresponds to granodiorite, which are related to pre-Himalayan syncollisional and pre-plate collisional tectonics respectively. However, the TLg is ms-bt±tur leucogranite corresponding to peraluminous syncollisional (Himalayan) anatectic melt. Muscovite of GGn represents solid-solution of celadonitic and paragonitic end-members of primary muscovite composition. Empirically estimated Li-content of GGn muscovite relates to Li-mica zinnwaldite. Biotite in GGn is mostly transitional between Fe- and Mg-biotites evolved from FMQ to NNO buffers syn-crystallizing with muscovite, and exhibits dominant Mg=Fe and less pronounced $2Al=3Fe^{2+}$

substitutions typical to its evolution in a peraluminous (S-type) felsic melt. Biotite in BG is, however, ferritite evolved from FMQ to NNO buffers and exhibits pronounced Mg=Fe and less pronounced $3Mg=2Al$ substitutions typical to its crystallization in a calc-alkaline, metaluminous (I-type) felsic melt. GGn biotite is markedly enriched in siderophyllite and depleted in phlogopite components as compared to BG biotite. Tourmaline from GGn belongs to schorl (Fe)-dravite (Mg)-elbaite (Li+Al) end-members solid-solution typically crystallized in a Li-poor felsic melt. Whole rock composition of GGn (molar A/CNK=1.19-1.45) and TLg (molar A/CNK=1.29-1.33) represents typical to peraluminous (S-type) granites whereas BG (molar A/CNK=0.95-0.97) is metaluminous (I-type) in character, strongly suggesting involvement of heterogeneous protoliths in their genesis. Comparison of melts generated by melting experiments of various protoliths suggests that GGn melts might have been generated by melting of biotite-rich metapelites whereas BG melt might have been formed from melting of biotite-rich metapelite and/or plagioclase-rich metagrewacke sources. However, the TLg melt appears formed by melting of muscovite-rich metapelite source. These felsic melts are slightly to strongly reduced-type mostly intrinsic to crustal source regions, but most likely formed in diversified tectonic regimes (pre-plate to syn-collisional). Content of MgO, Fe₂O₃, MnO, CaO, K₂O, Al₂O₃, Sr, Nb, Ba decreases with increasing SiO₂ content of GGn, showing their compatible nature because of fractional differentiation process mainly involving biotite, plagioclase and K-feldspar. This is further evident by varying degrees of negative Eu-anomalies (EuN/Eu* = 0.29-0.47), LaN/LuN = 5.7-14.8, and sum of rare earth elements ($\Sigma REE = 67$ - 209 ppm). However, trace elements characteristics (Y = 1.06-1.56 ppm, Yb = 16-19 ppm, Sr/Y = 14-35, La/Nb = 1.7-3.0, La/Yb = 25-43, Zr/Sm = 34-44) and REE patterns ($La_N/Lu_N = 17$ - 30 , $Eu_N/Eu^* = 0.63$ - 0.75) of BG appear more like an adakite-like melt but partly contains features similar to a classic arc type calc-alkaline components.

Analysis of gravity and magnetic data along Rumtse-Upshi-Leh-Kardung la and Rumtse-Upshi-Igu-Shakti-Chang la – Durbuk profiles – Presence of ophiolites within Ladakh batholith and suture zones

Rambhatla G Sastry* and Md Israil

Department of Earth Sciences, Indian Institute of Technology Roorkee Roorkee-247667, INDIA

* For correspondence, email: rgss1fes@iitr.ernet.in

Our gravity and magnetic profile data sampled at 1-2 km spacing along Rumtse-Upshi-Leh-Kardung La and Rumtse-Upshi-Igu-Shakti-Chang La-Durbuk profiles across Indus formation, Ladakh batholith and Suture zones are analyzed. The gravity data are processed with our variable density Bouguer anomaly computation algorithm. Spectral analysis of gravity data indicates that the high frequency residual anomalies are of shallow origin. A simple modeling of magnetic data indicates that the ophiolites occur as dykes of steep dips at shallow depths within Ladakh batholith and Shyok suture zones. Detailed gravity modeling is not attempted here.

Introduction

The presence of ophiolites in Ladakh Himalaya in different suture zones is a well known fact. However, their presence within Ladakh batholith is conjectural. Here, our closely sampled (1–2 km) gravity and magnetic data along Rumtse-Upshi-Leh-Khardung La and Rumtse-Upshi-Igu-Shakti-Chang La-Durbuk profiles are analyzed to clarify these matters.

Methodology

The regional gravity profiles in Ladakh Himalaya along this traverse (Figure 1) are processed with our algorithm (Sastry,

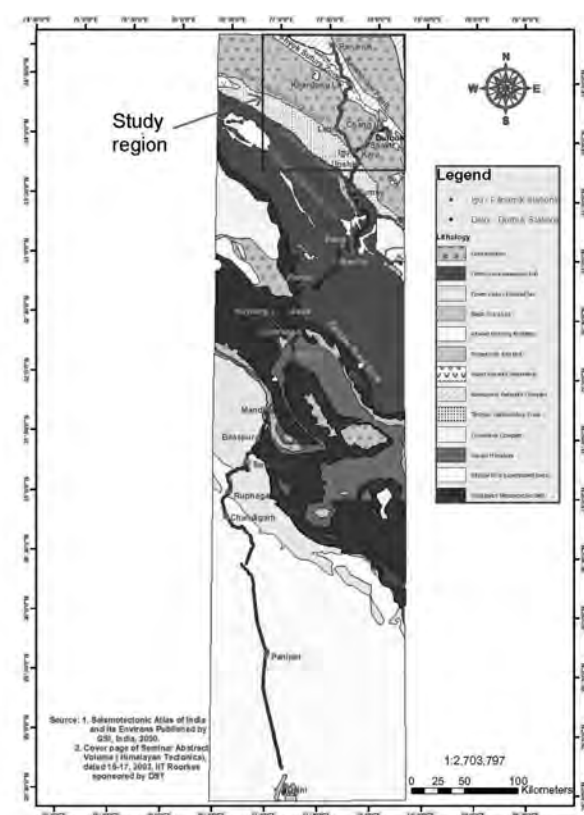


FIGURE 1. The study region is marked with a box in the above map. Both Rumtse-Upshi-Leh-Panamik and Rumtse-Upshi-Igu-Chang La-Durbuk profiles are indicated inside the box. The gravity and magnetic stations are sampled with 1-2 km spacing along these profiles. The background geological map is adapted from two sources, which are indicated on the map itself.

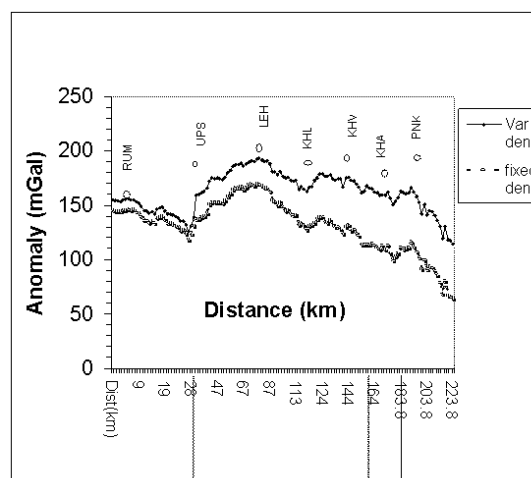


FIGURE 2. Processed gravity data along Rumtse-Upshi-Igu-Leh-Khardung la-Panamik using with conventional constant Bouguer density of 2.67 gm/cc and variable densities (Sastry 2005). For our analysis Bouguer anomaly with variable densities is considered. Index: IF-Indus formation, LB- Ladakh Batholith, SSZ-Shyok suture zone, KB-Karakorum batholith

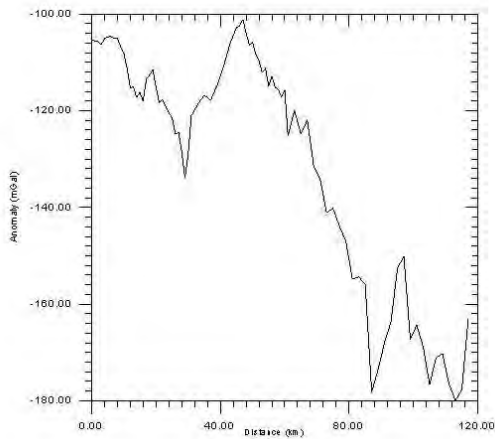


FIGURE 3. Bouguer anomaly gravity profile along Rumte-Upshi-Igu-Shakti-Chang la-Durbuk using variable densities (Sastry 2005).

2005) utilizing ‘GRAVMASTER’ software of ‘GEOTOOLS’. Density measurements of collected representative samples from different geological formations along the profile were utilized for this purpose. The reference Bouguer datum is mean sea level.

The processing of Rumtse-Upshi-Leh-Kardung La (Figure 2) and Rumtse-Upshi-Igu-Shakti-Chang La-Durbuk gravity profiles (Figure 3) are undertaken with two options, viz.

- a) Conventional constant Bouguer density, $D = 2.67 \text{ g/cc}$ (for both Bouguer and terrain corrections)
- b) Variable density for both Bouguer and terrain corrections

For our analysis, we consider gravity profiles processed with the second option. The total-field intensity data along the same profiles is processed as per norms (Figures 4, 5).

Results and Discussion

Spectral analysis of gravity data along both the profiles (Figures 6, 7) have been carried out as per norms. The inferred source of high-frequency part of the anomalies is approximately at 3 km. Similar inference is obtained from spectral analyses of magnetic data (not included here). This has led to a quantitative interpretation of magnetic signatures.

In view of the above, the magnetic anomalies are modeled with an inclined dyke model of infinite-depth extent. The results are included in Figures 4 and 5. These results clearly suggest that the ophiolites with near vertical dips extend from shallow depths

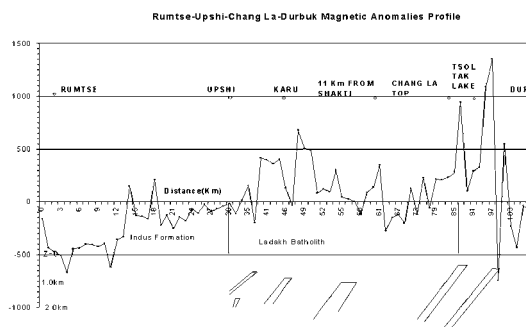


FIGURE 5. Processed magnetic anomaly along Rumte-Upshi-Igu-Shakti-Chang la-Durbuk. Interpreted steeply dipping dykes are located within Ladakh batholith and Shyok suture zone.

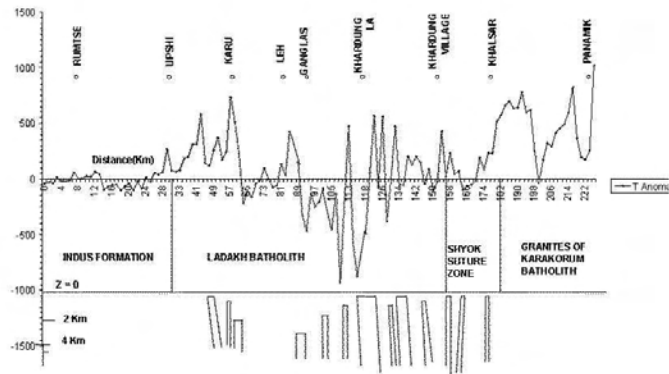


FIGURE 4. Processed magnetic anomaly along Rumte-Upshi-Igu-Leh-Khardung la-Panamik. Interpreted steeply dipping dykes are located within Ladakh batholith and Shyok suture zone.

(0.25-0.4 km) to at least up to 3.0 - 3.5 km from surface within Ladakh batholith and at Shyok suture zone.

Conclusions

The analysis of gravity and magnetic anomalies along Rumtse-Upshi-Leh-Kardung La and Rumtse-Upshi-Igu-Shakti-Chang La-Durbuk profiles clearly suggest the presence of ophiolites within Ladakh batholith and Shyok Suture Zone starting from very shallow (0.25-0.4 km) depths and extending at least up to 3 km from surface.

Acknowledgements

Authors convey their sincere thanks to Sri. DN Awasthi, Chairman, PAMC (DCS), DST, Dr. KR Gupta, Advisor, Dr. Ch. Sivaji, Scientist, DST and all concerned Advisory Committee members of DST “HIMPROBE” team for necessary support and advice. The authors also thank Ms. Neta Chaudhary, Research Associate for assistance in processing. Thanks are also due to DST, New Delhi for sustained encouragement and financial support throughout the implementation of the DST project, of which the present piece of work is an outcome.

References

Sastry RG. 2005. Variable density option in Bouguer anomaly computation. SEG International Exposition and 75th Annual Meeting, Houston, USA, November 2005

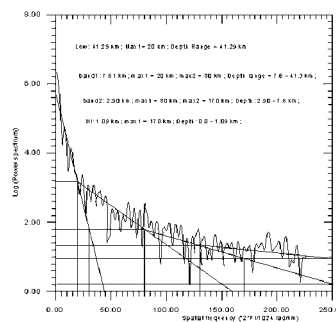


FIGURE 6. Spectral analysis of Bouguer anomaly along Rumtse-Upshi-Igu-Leh-Khardung la-Panamik profile. The high-frequency anomaly source extends up to at least 3.0 km from near surface.

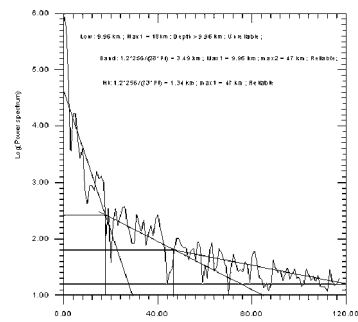


FIGURE 7. Spectral analysis of Bouguer anomaly along Rumtse-Upshi-Igu-Shakti-Chang la-Durbuk profile. The high-frequency anomaly source extends up to at least 3.5 km from near surface.

Analysis of gravity and magnetic data along Mahe-Sumdo-Tso Morari

Rambhatla G Sastry* and Md Israil

Department of Earth Sciences, I.I.T, Roorkee INDIA

* For correspondence, email: rgss1fes@iitr.ernet.in

Our gravity and magnetic profile data sampled at 1 km spacing along Mahe-Sumdo-Tso Morari across Indus-Suture zone to Taglang la formation is analyzed. Gravity data is processed with our variable density Bouguer anomaly computation algorithm. Spectral analysis of gravity and magnetic data indicates that the residual anomaly is of shallow origin. A simple modeling of gravity and magnetic data indicates that the ophiolites has a discordant relationship with ISZ and Taglang la formations. However, the modeled magnetic anomaly could not yield the bottom surface of inclined dyke.

Introduction

Ophiolites presence near Indo suture zone (ISZ) in Ladakh Himalaya is a well-known fact. The geometry and structure delineation of them at different locations by gravity and magnetic signatures could be of specific geodynamic interest. Here, our closely sampled (1 – 2 km) gravity and magnetic data along Mahe bridge – Sumdo - Panamik is analyzed.

Methodology

A regional gravity profile from Ladakh Himalaya along Mahe – Sumdo – Tso-morari (Figure 1) is processed with our algorithm (Sastry 2005) utilizing ‘GRAVMASER’ software of ‘GEOTOOLS’. Density measurements of collected representative samples from different geological formations along the profile were utilized for this purpose.

The reference Bouguer datum is mean sea level.

The processing of Mahe – Sumdo – Tso Morari profile (Figure 2) is undertaken with two options, viz.,

a) Conventional constant Bouguer density, $D = 2.67 \text{ g/cc}$ (for both Bouguer and terrain corrections)

b) Variable density for both Bouguer and terrain corrections

The Bouguer anomaly processed with variable density option clearly reflects (Figure 2) the signature of Nidar ophiolites.

Total-field intensity data along the same profile is processed as per norms (Figure 3).

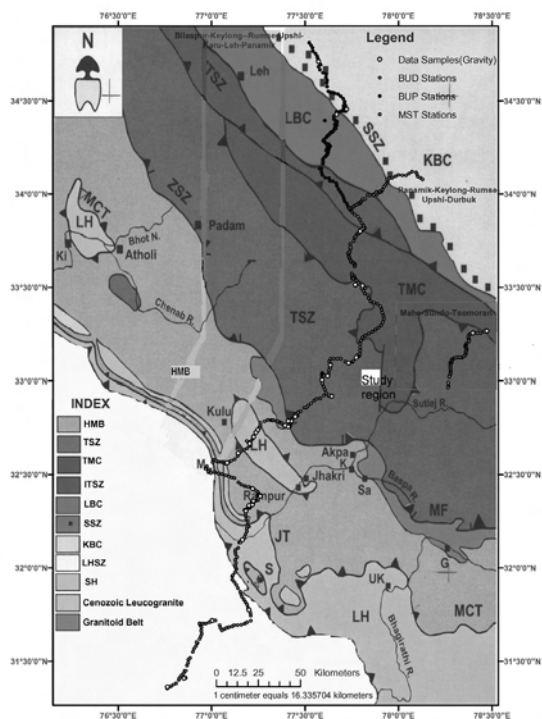


FIGURE 1. Mahe-Sumdo-Tso Morari profile is marked within the box of the above map. Station interval is 1-2 km. Both gravity and magnetic (Total-field intensity) data are acquired along this profile. (After Cover page of Seminar Abstract Volume (Himalayan Tectonics), dated 16-17, 2003, IIT Roorkee)



FIGURE 2. Processed Bouguer anomaly along Mahe-Sumdo-Tso Morari Profile with geological formations. For regional-residual separation sake regional is identified by green line in the above plot. A constraint from spectral analysis also supports the above regional trend.

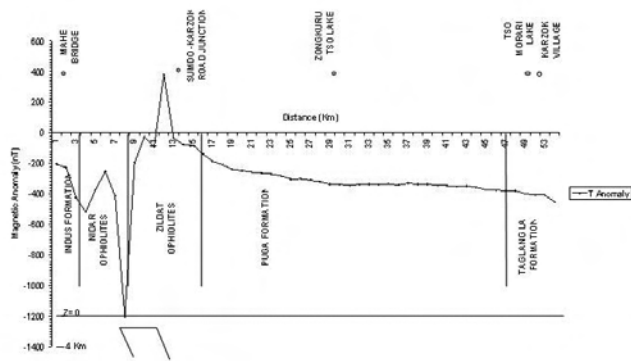


FIGURE 3. Processed magnetic anomaly (Total-field intensity) profile along Mahe-Sumdo-Tso-Morari profile with geological formations. Interpreted dyke model is indicated at the bottom.

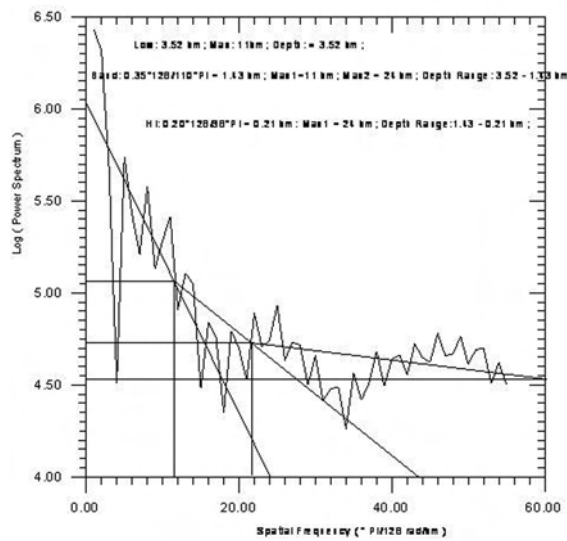


FIGURE 5. Spectral plot for magnetic data along Mahe-Sumdo-Tso-Morari profile. The analysis indicates that residual anomaly source may extend from 0.21-3.5 km. This serves as basis for choice of inclined dyke of infinite-depth extent.

Results and Discussion

Spectral analysis of gravity (Figure 4) and magnetic anomalies (Figure 5) have been carried out as per norms. The inferred source of high-frequency part of the anomalies is approximately 3 km. This has led to quantitative Interpretation of both gravity and magnetic signatures.

By considering both residual gravity and magnetic anomalies, an inclined dyke model is adopted. The residual gravity is modeled with inclined dyke of finite – depth extent (Figure 6). By considering the gravity results, the magnetic anomaly is modeled with a dyke model of infinite-depth extent (Figure 3) as magnetic signature is more influenced by shallow features of the source. The results clearly indicate that the ophiolites extend at least up to 3.5 km from surface.

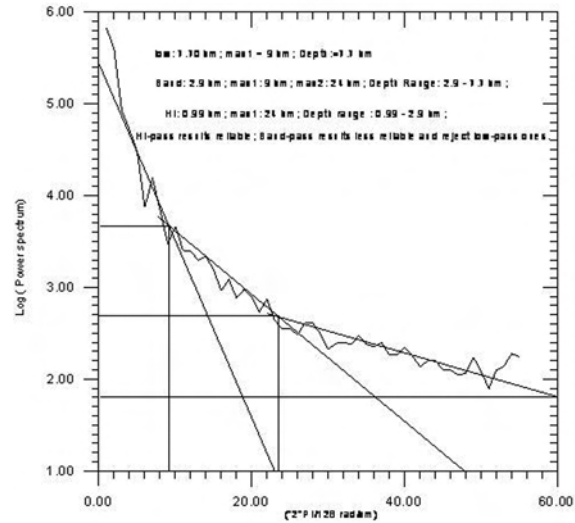


FIGURE 4. Spectral plot for gravity data along Mahe-Sumdo-Tso-Morari profile. The analysis indicates that residual anomaly source may extend from 0.99-3.0 km. This serves as basis for choice of inclined dyke of finite-depth extent.

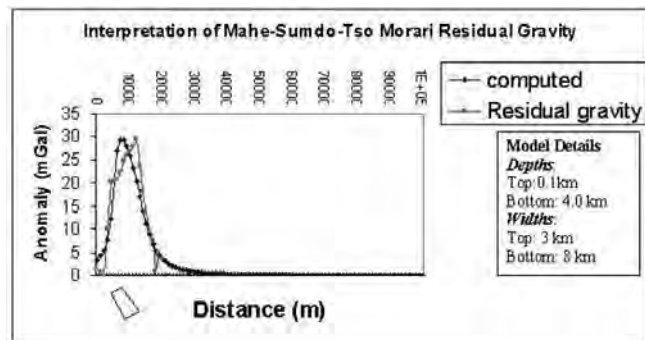


FIGURE 6. Interpreted residual Bouguer gravity along Mahe-Sumdo-Tso-Morari profile. Both field and computed profiles are shown. Ophiolites identified by dipping finite-extent dyke serve as source for the residual gravity anomaly. Thus ophiolites have a discordant relationship with Indus and Taglang la formations in this region

Conclusions

The analysis of gravity and magnetic anomalies along Mahe-Sumdo-Tso Morari profile clearly indicates that the ophiolites have a discordant relationship with Indus and Taglang la formations and they extend up to at least 3 km from surface.

Acknowledgements

Authors convey their sincere thanks to Sri. DN Awasthi, Chairman, PAMC (DCS), DST, Dr. KR Gupta, Advisor, Dr. Ch. Sivaji, Scientist, DST and all concerned Advisory Committee members of DST “HIMPROBE” team for necessary support and advice. The authors also thank Ms. Neeta Chaudhary, Research Associate for assistance in processing. Thanks are also due to DST, New Delhi for sustained encouragement and support throughout the implementation of the DST project, of which the present piece of work is an outcome.

Anatomy, Age and Evolution of the Baltoro granite batholith, Pakistani Karakoram

Michael Searle^{1*}, Andrew Thow¹, Randall Parrish², Steve Noble² and David Waters¹

¹ Department of Earth Sciences, University of Oxford, Oxford OX1 3PR, UK

² Department of Geology, University of Leicester, Leicester LE1 7RH, UK; and NERC Isotope Geoscience Laboratory, British Geological Survey, Keyworth, Nottingham NG12 5GG, UK.

* For correspondence, email: mikes@earth.ox.ac.uk

Geological mapping around the Baltoro granite batholith in North Pakistan has resulted in a more detailed picture of the 3-D anatomy of the batholith. U-Th-Pb geochronology on all the main intrusive phases has resulted in more detailed timing constraints on batholith evolution. The Karakoram terrane in North Pakistan, shows abundant evidence for Middle Jurassic and Cretaceous (170-90 Ma) Andean-type subduction-related granite intrusion (eg: K2, Muztagh Tower gneisses, Hunza granodiorites, Hushe gneisses). Following collision and accretion of first the Kohistan Arc, and later the Indian plate to the southern margin of Asia, crustal thickening along the Karakoram resulted in polyphase deformation, and multiple 'phases' of metamorphism and melting (Searle and Tirrul 1991; Fraser et al. 2001). The major phase of kyanite- and sillimanite-grade metamorphism in the Baltoro region was Oligocene – Lower Miocene (28-22 Ma; U-Pb monazite ages). A widespread network of leucogranitic dykes that cross-cut folds and regional fabrics has been dated at 24.7 ± 0.6 Ma (U-Pb zircon) indicating that major thickening and folding was over by that time. Renewed deformation and heating in the middle-lower crust to sillimanite + K-feldspar grade with migmatization and generation of gem-bearing leucogranite dykes occurred in the deep crustal Dasso gneiss dome in the southern Karakoram between $5.5 - 3.5 \pm 0.2$ Ma (U-Pb zircon, monazite). The Baltoro granite batholith, previously dated between 25-20 Ma (Parrish and Tirrul 1989, Schärer et al. 1990, Searle et al. 1992) also includes Early Miocene granites. New U-Pb monazite ages from crustal melt biotite + muscovite + garnet leucogranites from the Trango Towers, Cathedral peak and Paiyu peak span $19.8 - 17.5 \pm 0.5$ Ma. The youngest leucogranites from the huge

sheeted sill complex that feeds the Masherbrum garnet-bearing 2 mica leucogranite are the youngest dated phases in the Baltoro batholith at 17.6 ± 1.1 Ma. The Masherbrum and K7 granites extend east to the Siachen glacier region where they are cut abruptly by the Karakoram strike-slip fault, indicating that the fault must have initiated after 17 Ma, in common with earlier U-Pb dating constraints from the Tangtse region (Phillips et al. 2004).

References

- Fraser, JE, MP Searle, RR Parrish and SR Noble. 2001. Chronology of deformation, metamorphism and magmatism in the southern Karakoram Mountains. *Geological Society of America Bulletin* 113: 1443-1455
- Parrish, RR and R Tirrul. 1989. U-Pb age of the Baltoro granite, northwest Himalaya, and implications for monazite U-Pb systematics. *Geology* 17: 1076-9
- Phillips, RJ, RR Parrish and MP Searle. 2004. Age constraints on ductile deformation and long-term slip rates along the Karakoram fault zone, Ladakh. *Earth and Planetary Science Letters* 226: 305-319
- Schärer U, P Copeland, TM Harrison and MP Searle. 1990. Age, cooling history and origin of post-collisional leucogranites in the Karakoram batholith: a multi-system isotope study N. Pakistan. *J. Geology* 98: 233-251
- Searle MP and R Tirrul. 1991. Structural and thermal evolution of the Karakoram crust. *Journal of Geological Society, London* 148: 65-82
- Searle, MP, MB Crawford and AJ Rex. 1992. Field relations, geochemistry, origin and emplacement of the Baltoro granite, Central Karakoram. *Transactions Royal Society, Edinburgh* 83: 519-538

Analysis of Climate change from high elevation sites of North West Himalaya based on tree ring data.

Santosh K Shah^{1*}, Amalava Bhattacharyya¹ and Vandana Chaudhary²

¹ *Birbal Sahni Institute of Palaeobotany, 53, University Road, Lucknow-226 007, India*

² *Department of Science & Technology, New Mehrauli Road, New Delhi- 110 016, India.*

* *For correspondence, email: santoshk.shah@gmail.com*

The analysis of tree-ring data of Silver fir (*Abies pindrow* [Royale] Spach.) and Himalayan pine (*Pinus wallichiana* A.B. Jackson) from the sub-alpine forest from Gangotri glacier region, Northwestern Himalayan signifies the importance of August-September temperature in controlling the growth of these trees. Mean temperature in each year for these two months has been reconstructed from A.D. 1995 up to A.D. 1773 based on ring-width and density data. The calibration model explains 44% variance in the instrumental data (1902-1987). The reconstructed temperature series shows annual to multiyear fluctuations punctuated with

colder and warmer periods amongst which A.D. 1830-1852 and A.D. 1961-1972 is the coldest and warmest period respectively. For this region both Little Ice Age cooling of 19th or warming of 20th centuries are recorded as discrete phenomena intermittent with smaller phases of warming and cooling episodes respectively. In contrary to the recent global warming there is cooling phase since A.D. 1973 in the reconstruction. Sequential change-point analysis has been used for the first in the dendroclimatic studies from this region and the result indicates the major regime shifts over the sites at 1783, 1794, 1805, 1827, 1862, 1873, 1898 and 1971.

Geohistory of Tso-Morari Crystalline, Eastern Ladakh, India: a plausible model for ultra-high pressure rocks in the Himalaya

Ram S. Sharma

70/36 Pratap Nagar, Shohpur Road, Jaipur-303906, INDIA

E-mail: sharma.r.sw@gmail.com

The Tso-Morari Crystalline (TMC), eastern Ladakh, is located between the ophiolitic rocks of the Indus-Tsangpo Suture Zone (ITSZ) in the north and the Zaskar sedimentary unit (Tethyan sedimentary zone) in the south. The TMC represents the northern Himalayan Crystalline. It is composed of quartzo-feldspathic gneiss, mostly augen-gneiss, derived from granitoids. Associated with these gneisses are the biotite schist and sillimanite-kyanite gneiss, which occur as discontinuous metasedimentary layers concordant with the banding of the gneisses. The Tso-Morari gneiss complex is heterogeneously deformed and show magmatic to mylonitic texture with dominant S-surface that is domed by NW-SE antiform. The TMC gneisses form the core of this vast dome. The Tso-Morari dome plunges in the west under metasediments, mainly garnet-bearing metapelites of the Phe or Haimanta Formation (Precambrian to Cambrian age). The U-Pb isotope on zircons, single grain as well as small multigrain fractions from the gneiss (deformed granite) yielded magmatic age of 479 ± 2 Ma (Girard and Bussy 1999). Similar age is also reported in the nearby located Polokongla granite. The transition between the Polokongla granite and the Tso-Morari gneiss is gradual, devoid of any intrusive contact with the gneiss. This field occurrence together with their geochemical similarities, identical zircon morphology and same age, suggest that the Polokongla granite is the undeformed facies of the Tso-Morari gneiss. Other granite in the terrain is the Rupshu metagranite which is metaluminous with U-Pb zircon age of 482.5 ± 1 Ma (Girard and Bussy 1999). Strikingly, there are no aplite or pegmatite dykes related to the granite-gneiss association in the TMC terrain. The Tso-Morari gneiss complex encloses eclogitic lenses (1–13 m long and 0.5–4 m thick), aligned parallel to the gneissic fabric. The eclogites, mostly retrograded, are scattered throughout the complex. They are found mainly within the Tso-Morari gneiss and also in the first few hundred meters of metasediments above, which prompted Steck et al. (1998) to designate the Tso-Morari complex as Tso-Morari Nappe – a tectonic unit of high pressure metamorphism. Because of the eclogitic lenses within the Tso-Morari dome, it is obvious that the high pressure metamorphism also affected the Tso-Morari gneisses. The garnet (45–55 vol.%) in the eclogites is rimmed by glaucophane (5–7 vol.%) paragonite (<10%), and omphacite (25–35 %). These minerals also form matrix in the eclogitic rock (Sachan et al., 1999). Glaucophane is also surrounded by tremolite-actinolite as retrogression products (De Sigoyer et al. 1997). In some eclogites, the garnet core contains inclusion of quartz, quartz-coesite or coesite only (Sachan et al. 2004), suggesting coesite formation from quartz during subduction. The eclogite garnets invariably show chemical zoning with Mg increasing and Fe decreasing from core to rim (Sachan et al. 2004). This cation profile of coesite-bearing garnet clearly suggests prograde nature of the ultra-high pressure

metamorphism in the TMC unit. The occurrence of quartz to coesite from core to rim of the garnet together with the chemical zoning of garnet unambiguously suggest prograde nature of the ultra-high pressure metamorphism (UHP).

P-T conditions for the UHP metamorphism are estimated at 20 ± 3 kbar, $580 \pm 60^\circ\text{C}$ for the Tso-Morari gneisses (De Sigoyer et al. 1997, Guillot et al. 1997, Sachan et al. 2004). The UHP metamorphism in the Tso-Morari area has been dated at 55 ± 17 Ma (U-Pb on allanite) and 55 ± 12 Ma (Lu-Hf on garnet-cpx-rutile) (De Sigoyer et al. 2000). Analogous occurrence in the Kaghan valley, Pakistan, the eclogite yielded a Sm/Nd age on garnet-cpx pair of 49 ± 6 Ma (Tonarini et al. 1993). Eclogitization therefore occurred during subduction of the Indian plate beneath Asia.

From the field occurrence of eclogites (metamorphosed basalt) and the presence of coesite with or without quartz in silicate rocks and in pyrope rich garnet suggest rapid subduction of the Indian Precambrian crust to near 100 km depth. With continued subduction, when Indian continental landmass came to collision against Asia (45 – 50 Ma), Proterozoic to Lower palaeozoic cover sequences of northern Indian plate slipped under Asian plate and the Ladakh-Kohistan island arc. In this event, the oceanic lithosphere is assumed to have dragged down a hooked-component of the continental crust of the northern Indian plate margin to great depths, within the coesite stability field. Consequently, UHP mineral assemblages developed in silicate-bearing rocks, especially coesite in garnets (Mukherjee and Sachan 2007) and eclogites in the root of subducting plate. With the slab detachment in depth, the continent-continent collision of India-Asia terminated and the “sunkun” crustal rocks had a rapid return toward shallower depths enabling them to preserve their UHP mineralogy. This movement was akin to that experienced by the contestants in a tug of war with sudden breaking of the rope across the marking line. In the proposed slab-breakoff process, the subducted material possibly exhumed in form of varying-sized fragments (eclogite lenses) and emplaced in the TMC adjacent to ITSZ. It is believed that the Indian crust, which had subducted only to a limited depth owing to buoyancy, exhumed first as the recrystallized Tso-Morari crystalline that became the host rock for the next obducted material from greater depth, especially the eclogites. All the eclogite fragments within Tso-Morari gneisses are characterized by incomplete transformation of coesite to quartz and by radial fractures around the silica inclusions within garnet (Sachan et al 2004), supporting rapid exhumation of the eclogites from depth of >90 km. The mechanism finds support from the occurrence of post-orogenic, undeformed basic rocks (as product of decompression melting of up-warped lithosphere) that intruded the Himalayan metamorphics at several places (Sharma 1962) and from the deep mantle anomalies recently discovered by seismic tomography at the base of lithosphere in West Pakistan (van der Voo et al. 1999).

References

- De Sigoyer J, S Guillot, JM Lardeaux, and G Mascle. 1997. Glaucofane-bearing eclogites in the Tso-Morari dome (eastern Ladakh, NW Himalaya). *Eur. J. Mineral.* 9:1073-1083
- De Sigoyer J, V Chavagnac, BJ Toft, IM Villa, B Luais, S Guillot, M Cosca and G Mascle. 2000. Dating the Indian continental subduction and collisional thickening in the northwest Himalaya: multichronology of the Tso-Morai eclogites. *Geology* 28: 487-490
- Girard M and F Bussy. 1999. Late Pan-African magmatism in the Himalaya: new geochronological and geochemical data from the Ordovician Tso-Morari metagranites (Ladakh, NW India). *Schweiz. Mineral. Petrogr. Mitt.* 79: 399-418
- Guillot S, J De Sigoyer, JM Lardeaux and GJ Mascle. 1997. Eclogitic metasediments from the Tso-Morari area (Ladakh, Himalaya): evidence for continental subduction during India-Asia convergence. *Contrib. Mineral. Petrol.* 128: 197-212
- Mukherjee BK and HK Sachan. 2007. Tracing of Indian continental crust in the mantle and back: a semantic approach. *Himalayan Geology* 28(3): 21-22
- Sachan HK, RJ Bodnar, R Islam, Cs Szabo and RD Law. 1999. Exhumation history of eclogites from Tso-Morari crystalline complex in eastern Ladakh: mineralogical and fluid inclusions constraints. *J. Geol. Soc. India* 53: 181-190
- Sachan HK, BK Mukherjee, Y Ogasawara, S Maruyama, H Ishida, A Muko and N Yoshioka. 2004. Discovery of coesite from Indus Suture Zone (ISZ), Ladakh, India: evidence for deep subduction. *Eur. J. Mineral.* 16:235-240
- Steck A, JL Eppard, JC Vannay, J Hunziker, M Girard, A Morard and M Robyr. 1998. Geological transect across the Tso Morari and Spiti areas: the nappe structures of the Tethys Himalaya. *Eclogae, geol. Helv.* 91: 103-121
- Sharma RS. 1962. On the occurrence of an olivine-dolerite laccolith at Ranikhet, dist. Almora (U.P.). *Jour. Sci. Res.* 12(2): 231-237
- Tonarini S, IM Villa, F Oberli, M Meier, DA Spencer, U Pognante and J Ramsay. 1993. Eocene age of eclogite metamorphism in Pakistan Himalaya: implication for India-Eurasia collision. *Terra Nova* 5: 13-20
- Van der Voo R, W Spakman and H Bizwaard. 1999. Tethyan subducted slab under India. *Earth Planet. Sci. Lett.* 171:7-20

Soft sediment deformation structures in the Late Quaternary sediments of Ladakh: evidence of multiple phases of palaeoearthquakes in the North western Himalayan Region

Binita Phartiyal and Anupam Sharma

Birbal Sahni Institute of Palaeobotany, 53-University Road, Lucknow-226007, UP, INDIA

Ladakh, situated in the tectonically active terrain, in the vicinity of the Indus Suture Zone (ISZ), Shyok Suture Zone (SSZ) and Karakoram Fault (KF), is rich in Quaternary deposits and is truly a treasure trove for Quaternary researchers. This work presents the palaeoseismic signatures as recorded in the Quaternary sediments of the Spituk-Leh (along ISZ) and the Khalsar palaeolakes (along SSZ and KF). These two palaeolakes were a result of a regional tectonic activity at 35,000-40,000 yrs BP. 9 levels of soft-sediment deformation structures (seismites) are recorded from a >27m thick, clay, sand sequence of the Spituk-Leh palaeolake. The deformation levels are confined to the lower 13 m of the sequence (0.5, 2.7, 3.2, 3.6, 5.5, 8.1, 9.8, 12.2 and 13.1 meters). The upper part of the paleolakes seems to have stable tectonic conditions. About 90 km north of this section

and separated by the Ladakh batholith, in the ~11 m thick section of Khalsar palaeolake shows 8 levels of soft-sediment deformation structures at 1.2, 1.5, 4.2, 4.5, 5.4, 8.8, 9.2 and 10.8 m levels. Deformation sediments are composed of alternations of clay, silts and sand and are restricted to single stratigraphic layers bounded by undeformed beds suggesting synsedimentary deformation. They are simple and complex convolutes, pinch and swell bedding, microfolds and microfaults, flame-like structures, pseudonodules or cycloids, clay diapirs, ball and pillow structures, pillar structures, sedimentary dykes, mud lenses, etc. Lying in the vicinity of the active faults the ISZ, SSZ and KF, these two palaeolake systems record multiple phases of seismic tremors of magnitude >5 due to release of stress along these fault systems during the late Quaternary times.

Remote Sensing based Study of Retreat of and Accompanying Increase in Supra-glacial Moraine Cover over a Himalayan Glacier

A Shukla¹, RP Gupta¹ and MK Arora²

¹ Department of Earth Sciences, Indian Institute of Technology Roorkee, Roorkee, INDIA

² Department of Civil Engineering, Indian Institute of Technology Roorkee, Roorkee, INDIA

* For correspondence, email: 1aslesdes@iitr.ernet.in

Glaciers are prime reserves of freshwater and amass about 75% of the world's freshwater. As a major consequence of global warming, glaciers all over the world have been experiencing recession at varying intensities. Owing to this high sensitivity of glaciers for changes in the climatic environment, they are considered as excellent indicators of prevailing climatic changes in a region. Thus mapping and monitoring of glaciers has great significance. Remote sensing is perhaps the only effective tool for comprehensive and repetitive study of mountain glaciers in a cost effective manner.

Mapping of glaciers through remote sensing data can be carried out using visual demarcation, segmentation of ratio images via thresholds, NDSI (Normalised Difference Snow Index) based algorithms and digital image classification. Each has some merits and demerits. Demarcation of snow covered areas through visual interpretation is extremely tedious and time consuming. Segmentation of ratio images is used for segregation of land cover including snow, ice, ice-mixed-debris, and debris. Digital image classification using statistical classifiers are also being used for snow and glacier cover mapping.

In this paper, recent recession of a Himalayan glacier from 1976 to 2004 has been studied. Three remote sensing images one each from IRS-1C LISS-III (date of acquisition: 13th September, 2001), IRS-P6 AWiFS (date of acquisition: 7th September, 2004), TERRA ASTER (date of acquisition: 8th September, 2004) images and Survey of India topographical maps (year of preparation: 1976) of Samudratapu glacier, Chenab basin, Himalayas, have been procured. In a rugged terrain such as Himalayas with highly undulating surface and steep slopes, the radiance reaching the sensor greatly depend on the orientation (slope and aspect) of the target. Therefore, for the optimal recognition of the classes for their effective mapping, the digital numbers have to be converted into topographically corrected reflectance images. The C-correction method, generally reported to be the best amongst the various other methods of topographic correction, has been used in the present work for topographic normalization.

Supervised classification of topographically-corrected reflectance images enabled the mapping of various land cover classes such as snow, ice, ice-mixed-debris, moraine, valley-rock, and water in the glacier terrain, together with the extent of the glacier. Since the extent of glacier, mapped from remote sensing images and topographic map varies in time, thus their inter-

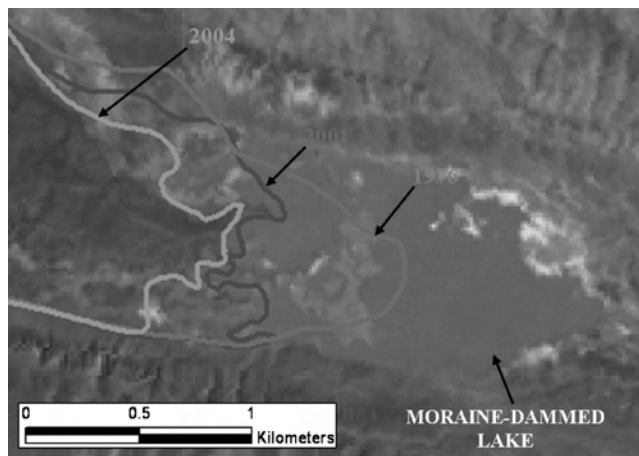


FIGURE 1. Change detection of glacier snout. The position of glacier snout has been mapped in years 1976 (S.O.I toposheets), 2001 (IRS-1C LISS-III image) and 2004 (IRS-P6 AWiFS image).

comparison highlights the varying recessional trends of the glacier in recent past.

Analysis of the results reveals that from 1976-2004 the glacier has receded by about 756.23 m with an average rate of 27 m/yr (Figure 1). An overall depletion in the areal extent is also observed during the said period, reducing the glacier area from 110 km² to 96 km² with the overall deglaciation amounting to 12.34% of the total area covered by the glacier. Interestingly, the glacier retreat has also been accompanied by a marked increase in the extent of moraine cover over the glacier, which has increased from 7.52 km² to 13.27 km² i.e. about 76% increase in just three years (2001-2004).

Thus, the rates at which various surface characteristics of the glacier are changing warrants their effective mapping and monitoring since they might profoundly influence the glacier mass balance, response of the glacier towards climatic fluctuations and also the triggering of various glacier-related hazards. The study highlights the potential of advanced image processing techniques in precise mapping and monitoring of varying glacier extents in time using remote sensing data.

Vertical stratigraphic variations and sedimentation model of the Lower Siwalik sequence in Kumaun Himalaya, India

UK Shukla^{1*} and DS Bora²

¹ *Department of Geology, Banaras Hindu University, Varanasi-221005, INDIA*

² *Schlumberger Asia Services Limited, DCS, Mumbai, INDIA*

* *For correspondence, email: shukla_umakant@yahoo.com*

Lower Siwalik sequence of Kumaun Himalaya is about 300–900 m thick and shows characteristic stratigraphic changes in sedimentation pattern. Available magnetostratigraphic dates indicate Late Miocene age. Based on detailed facies analysis four depositional settings are identified namely Sandstone Succession (Channel deposits), Mudstone Succession (Floodplain deposits), Mottled Mudstone Succession (Palaeosols), and Mottled Siltstone Succession (Interfluvial deposits). Stratigraphic succession shows systematic changes of facies association, palaeocurrent and petrography and palaeochannel patterns. Starting from base, about 500 m thick, coarsening upward Megacycle A is internally made up of two Mesocycles I and II. The sequence is made up of meandering and anastomosing rivers towards the base (Mesocycle I) that gradually evolve into braided towards top (Mesocycle II). This megacycle indicates sedimentation in a narrow subsiding basin by prograding mega fans. The Megacycle evolved under initially more pronounced tectonic activation in the source

terrain (hinterland tectonism) and sub humid climatic conditions, gradually followed by episodic tectonics and more humid climate towards the later phases of sedimentation.

In contrast, following about 400 m thick Megacycle B, made up of two Mesocycles III and IV, is fining upward. This sequence is made up of thickly developed meandering – braided river systems at the base interbedded with thick interfluvial and distal flood plain deposits (Mesocycle III) that gradually becomes thinner towards top, and river system changes to predominantly meandering type (Mesocycle IV). Megacycle B seems to represent sedimentation in a rather wide and tectonically active basin, characterized by incision of rivers. The Megacycle evolved under intense intrabasinal tectonism, and humid climatic conditions in the beginning that gradually changed to rather drier phases. The eustatic changes of more than 140 m during the Lower Siwalik times may have also contributed to base-level changes leading to incision of rivers particularly away from the orogen in the distal alluvial plain settings.

Amphibole compositions as indicators of deep crustal and mantle processes in subduction zones: case study – Tso Morari metamafics, Ladakh, Himalaya

Preeti Singh^{1*}, NC Pant², A Kundu², T Ahmad¹ and PK Verma¹

¹ Department of Geology, University of Delhi, Delhi-110007, INDIA

² EPMA Laboratory, Geological Survey of India, NH-5, Faridabad N.I.T.- 110005, INDIA

* For correspondence, email: preetisingh64@yahoo.co.in

Amphiboles have large number of cationic sites where substitution by various elements is a rule in response to changes in environmental conditions (Veblen 1985). The environmental conditions include hydrostatic pressure, temperature, $\mu_{\text{H}_2\text{O}}$, f_{O_2} etc. Experimental and empirical data are available to correlate these factors with mineral compositions for many amphibole species. These criteria have been utilized to study a natural example of ultra-high pressure metamorphism from the Himalaya.

A small area in SE Ladakh, just south of the Indus Suture Zone has been a subject of intense study recently (de Sigoyer et al. 2000, 2004, Guillot et al. 2000, 2008, Jain et al. 2003) because of the implications of geologic and geochronologic studies on the tectonic nature of Plate Subduction mechanism. Singh and Verma (2006) have shown for this area how compositions of phengite and biotite of metamafics (forming boudins in the host feldspar gneisses) and the host rocks respond to various stages of subduction and exhumation of plates.

Amphiboles are also important constituents of the metamafic boudins present in the Tso Morari region. From the point of view of phase relationships Verma et al. (2008) have shown that the metamafics are characterized by five assemblages. Two of these five assemblages are UHPM indicators while one belongs to HPM.

In the present study, a large dataset of chemical composition data through EPMA on relevant phases including amphiboles has been utilized to fine-tune the P-T- $\mu_{\text{H}_2\text{O}}$ - f_{O_2} values of the P-T-t path (subduction as well as exhumation components). Na-amphibole including glaucophane (Amphibole nomenclature after Leake et al. 1997) is present in cores of the zoned garnets in assemblage i) where it coexists with epidote and paragonite (HPM assemblage). Assemblage ii) is UHPM assemblage without any amphibole. Na-Ca amphiboles, taramite and magnesiokataphorite form assemblage iii), where these occur with garnet and phengite (UHPM assemblages). These amphiboles also occur as inclusions in some garnet grains. A continuous progressive reaction has even generated barroisite and rare winchite compositions in amphiboles that form part of this assemblage in the matrix. Ca-amphiboles occur as part of assemblages iv), and v) which contain albite, chlorite and biotite with another continuous reaction

sequence in amphiboles, chlorites and biotite. These assemblages are correlated with different stages of subduction and exhumation on the basis of textures as well as thermobarometry.

References

- de Sigoyer J, V Chavagnac, JB Toft, IM Villa, B Luais, S Guillot, M Cosca and G Mascle. 2000. Dating the Indian continental subduction and collisional thickening on the NW Himalayas-Multichronology of the Tso Morari eclogites. *Geology* 28: 487-490
- de Sigoyer J, S Guillot and P Dick. 2004. Exhumation of the Ultrahigh-Pressure Tso Morari unit in eastern Ladakh (NW Himalayas): A case study. *Tectonics* 23: 1-18
- Guillot S, KH Hattori and J de Sigoyer. 2000. Mantle wedge serpentinization and exhumation of eclogites: Insights from Eastern Ladakh, NW Himalayas. *Geology* 28: 199-202
- Guillot S, G Maheo, J de Sigoyer, KH Hattori and A Pecher. 2008. Tethyan and Indian subduction viewed from the Himalayan high to ultra-high pressure metamorphism. *Tectonophysics* 451: 225-241
- Jain AK, S Singh, RM Manickavasagam, M Joshi and PK Verma. 2003. HIMPROBE Programme: Integrated studies on geology, petrology, geochronology, and geophysics of the Trans Himalaya and Karakoram. *Memoir Geological Society of India* No 53: 1-56
- Leake BE, AR Woolley, CES Arps, WD Birch, MC Gilbert, JD Grice, FC Hawthorne, A Kato, HJ Kisch, VG Krivovichev, K Linthout, J Laird and J Mandarino. 1997. Nomenclature of amphiboles. Report of the subcommittee on amphiboles of the International Mineralogical Association: Commission on new mineral names. *Mineralogical Magazine* 61: 295-321
- Singh P and Verma PK. 2006. Petrogenetic Significance of Phengite and Biotite from the Ladakh UHP Terrain, Northwest Himalayas. *Indian Journal of Geochemistry* 2(1): 25-48
- Veblen DR. 1985. Amphiboles and other hydrous pyriboles-mineralogy. *Reviews in Mineralogy, Mineralogical Society of America* 9A, 372 pp
- Verma P, AB Thompson, P Singh, N Pant, A Kundu, T Ahmad, S Sengupta, A Saikia, S Deol. 2008. New insights on the mechanism of exhumation of deep crustal rocks in the light of new petrologic data on eclogites and coesite locations in the Lake Morari region, NW Himalayas. (Under Review)

Tectonic Activity In The Ganga Plain Foreland Basin During Quaternary

Indra Bir Singh

Geology Department, Lucknow University, Lucknow-226007, INDIA

Indo-Gangetic Plains, the largest active foreland basin of the Himalaya, developed on an old, cold and rigid Indian lithosphere showing high variability in the down-flexing characteristics. The Ganga Plain making the central part of this foreland basin system shows a diverse fluvial landscape of Late Quaternary age with a variety of fluvial systems. The fluvial geomorphic features often exhibit tectonic control and evidences of active tectonics. Thicknesses of the alluvial fill in the Ganga Plain show control of basement highs. Pattern and orientation of tectonics varies from Himalayan orogen to the Craton margin in the form of compressional tectonics to extensional tectonics respectively. The Craton margin exhibits prominent tectonic movements manifested in the form of vertical uplift, kilometer-scale warping, tilting of blocks, conjugate fractures and gravity faults.

A tectonic event, dated 8-5 kyrs disrupted number of drainages, converting channels into linear lakes; and produced an undulatory topography showing kilometre scale warping. The present-day active rivers show strong control of tectonics in the form of distorted channel segments, uneven height of cliffs along the valley margin. There are distinct zones of more intense tectonics in the form of warping. Often warping is very pronounced along the river channels. The southern part of the Ganga Plain shows several well-defined belts of intense and closely-spaced warping. Tectonic lineaments are mostly well-defined; at few places evidence of faulting is also present. The active tectonics of Holocene in the Ganga Plain has strongly controlled the regional patterns of fluvial facies and sediment transfer. The relationship between tectonic features of the Ganga Plain to the Himalayan tectonics and response of basement are not yet properly understood.

Weathering in the Ganga Alluvial Plain: Geochemical signatures linking of the Himalayan source and the Bay of Bengal sink

Indra Bir Singh¹, Sandeep Singh² and Munendra Singh¹

¹ *Centre of Advanced Study in Geology, University of Lucknow, Lucknow 226 007, INDIA*

² *Department of Earth Science, Indian Institute of technology, Roorkee 247 667, INDIA*

The Ganga Alluvial Plain is basically formed by the Himalayan-derived sediments and serves as transient zone between the Himalaya (source) and the Bay of Bengal (sink). The plain experiences a strong geochemical weathering leading to fractionation and elemental partitioning under sub-tropical climatic conditions controlled by heavy monsoon rainfall with long periods of drought and high ambient temperatures. It plays an important role in geochemical dynamics of this region as compared to the Himalayan area. The chemical weathering of the Ganga Alluvial Plain sediments is more intense than in the Himalaya. In the Ganga Alluvial Plain, the loss of Na, Ca and Sr during weathering is noticeable. Weathering products of the Ganga Alluvial Plain are the results of incomplete alteration of deposited alluvial sequences under humid sub-tropical climate. Annual physical and chemical denudation rates, based on total suspended matter (40 mg/L) and total dissolved solid (260 mg/L), are 9.7 tons/km² and 63.1 tons/km², respectively. In spite of high lithological, climatological and tectonic variability in the Himalayan region, the denudation rates in the Ganga Alluvial Plain are higher (26 % in physical erosion rate) and (73 % in chemical erosion rate) than the Ganga River catchment in the Himalaya. The Gomati

River sediments experience incipient to moderate intensity of the Chemical Index of Alteration (CIA) leading to higher CIA values than those of the Himalayan derived rivers.

The Gomati River, an important alluvial tributary of the Ganga River, drains nearly 30, 500 km² area of the Ganga Alluvial Plain. The river recycles the Himalayan derived sediments and transports its weathering products into the Ganga River to be transferred to the Bay of Bengal. The Gomati River water has dissolved Sr concentrations 375 µg/L, which is more than five times higher than the world's average of river water (70 µg/L) and nearly three times higher than the Ganga river water in the Himalaya (130 µg/L). Dissolved Selenium concentration is also reported as high as 1120 µg/L.

The Ganga Alluvial Plain is a significant geochemical linkage between the source (the Himalaya) and the sink (the Bay of Bengal). At present, most of the interpretation dealing with the sinks of the Ganga Fluvial System is profoundly linked with the geological processes operating in the Himalayan region alone. The importance of monsoon controlled hydro-geochemical processes operating in the Ganga Alluvial Plain, therefore, should be emphasized in interpretation of elemental mobility, cycling and budgets of the Ganga Fluvial system.

Geomorphic indicators of active growth and lateral propagation of fault-related folds: Mohand Ridge anticline, NW Himalaya

Tejpal Singh and A K Awasthi

Department of Earth Sciences, IIT, Roorkee-247667, INDIA

The Himalayan orogen is a result of collision of Indian and Eurasian plates. The collision and continued convergence has resulted in development of three south verging crustal-scale thrust faults all along the E-W trending orogen dividing into three litho-tectonic units *viz.* Higher Himalaya, Lesser Himalaya and Sub-Himalaya from north to south in that order. The Sub-Himalayan zone is characterized by the presence of fault-related folds that are conspicuously marked by the linear ridges running parallel to the orogen. These fault-related folds are segmented by a number of transverse strike-slip faults. The present study investigates the geomorphology of the Mohand Ridge anticline, bound between the two strike slip faults i.e. Yamuna fault towards the west and Ganga fault towards the east. The geomorphic

features related to the interaction of pre-existing through-going drainage, tributary pattern on the ridge and topographic profiles suggest that the Mohand Ridge anticline is growing towards west. Further this information is also supported by morphometric data of watersheds developed on the ridge. A progressive decrease in drainage density (Dd) of watersheds from east to west has been observed in addition to an increase in hypsometric integral (HI) values in that direction. Both these parameters (Dd and HI) have been demonstrated to evolve with time in response to neotectonic activity. Hence based on the geomorphic observations and lateral variation in morphometric data it is inferred that the Mohand Ridge anticline has evolved through by vertical growth and lateral propagation from east towards west.

Neotectonic activity and its geomorphic response in the Tangtse valley, Ladakh Himalaya

Vimal Singh

Wadia Institute of Himalayan Geology, 33 GMS Road, Dehra Dun-248001, Uttarakhand, INDIA, and Centre for Earth Sciences, Indian Institute of Science, Bangalore-5600012, Karnataka, INDIA

E-mail: vimalgeo@gmail.com

The ~800 km long dextral Karakorum fault bounding the southwestern margin of Tibet is commonly considered to be a discrete narrow fault zone. However, this fault is bifurcated between 33.5° N and 34.5° N into two parallel strands namely: the Pangong Tso and the Tangtse (Rutter et al. 2007). Slip rates inferred on the Karakorum fault ranges from 30-35 mm/yr to 3-4 mm/yr (Molnar and Lyon-Caen 1989, Avouac and Tapponnier 1993, Liu et al. 1992, Liu, 1993, Searle et al. 1998 Tapponier et al. 2001, Banerjee and Bürgmann 2002, Brown et al. 2002, Jade et al. 2004). Rutter et al. (2007) have shown evidences of shallow brittle deformation (such as clay-bearing gouges, cataclasite) along the Pangong strand but could not find comparable evidences along the Tangtse strand. Based on this observation, most recent slip is suggested to have been recorded only along the Pangong strand. However, preliminary data collected in this study from deformed fluvio-lacustrine Quaternary deposits cut by Tangtse strand suggest recent earthquake displacement to have occurred after ~13 ka.

In Tangtse valley, fluvio-lacustrine Quaternary deposits are exposed for a length of ~30 km along the Tangtse River. This thick sediment sequence, formed possibly due to damming of Tangtse River, attains a thickness of up to 70 m. Recent activity in Tangtse strand is expressed in the form of changed river course, deformed and displaced sediments, and development of fault gouge. Optically stimulated luminescence age of ~13 ka obtained from deformed lake sediments provides a firm lower bound, on the tectonic activity of Tangtse strand to after ~13 ka. Tectonic activity at ~50 ka, ~35 ka, and ~25 ka has already been inferred from deformation seen at different levels in these type of deposits in adjacent valleys (Shyok Valley and Indus Valley near Leh) (Phartiyal et al. 2005). In the light of these new data, it is inferred that the Tangtse strand has been active during the past ~15 ka.

References

- Avouac JP and P Tapponnier. 1993. Kinematic model of active deformation in central Asia. *Geophysical Research Letters* 20: 895-898
- Banerjee P and R Bürgmann. 2002. Convergence across the Northwest Himalaya from GPS measurement. *Geophysical Research Letters* 29(13): doi: 10.1029/2002GL015184
- Brown ET, R Bendick, DL Bourlès, VK Gaur, P Molnar, GM Raisbeck and F Yiu. 2002. Slip rates of the Karakorum fault, Ladakh, India, determined using cosmic ray exposure dating of debris flows and moraines. *Journal of Geophysical Research* 107: doi: 10.1029/2000JB000100
- Jade S, BC Bhatt, Z Yang, R Bendick, VK Gaur, P Molnar, MB Anand and D Kumar. 2004. GPS measurements from the Ladakh Himalaya, India: preliminary tests of plate-like or continuous deformation in Tibet. *Geological Society of American Bulletin* 116: 1385-1391
- Liu Q. 1993. *Paléoclimat et contraintes chronologiques sur les mouvements récents dans l'Ouest du Tibet: Failles du Karakorum et de Longmu Co-Gozha Co, lacs en pull-apart de Longmu Co et de Sumxi Co* [Ph.D. dissertation]: Paris, Université Paris, v. VII. 358 p
- Liu Q, JP Avouac, P Tapponnier and Q Zhang. 1992. Holocene movement along the southern part of the Karakorum fault: Abstracts, International Symposium on the Karakorum and Kunlun Mountains, June 5-9, 1992, Kashi [sic], China. 91 p
- Molnar P and H Lyon-Caen. 1989. Fault plane solutions of earthquakes and active tectonics of the Tibetan Plateau and its margins. *Geophysical Journal International* 99: 123-153
- Phartiyal B, A Sharma, R Upadhyay, Ram-Awatar and AK Sinha. 2005. Quaternary geology, tectonics and distribution of palaeo- and present fluvio/glacio lacustrine deposits in Ladakh, NW Indian Himalaya - a study based on field observations. *Geomorphology* 65: 241-256
- Rutter EH, DR Faulkner, KH Brodie, RJ Phillips and MP Searle. 2007. Rock deformation processes in the Karakoram fault zone, Eastern Karakoram, Ladakh, NW India. *Journal of Structural Geology* 29: 1315-1326
- Searle MP, RF Weinberg and WJ Dunlap. 1998. Transpressional tectonics along the Karakoram fault zone, northern Ladakh: constraints on Tibetan extrusion. In: Holdsworth RE, RA Strachan, JF Dewey. (Eds.). *Continental Transpressional and Transtensional Tectonics. Geological Society of London, Special Publication* 135: 307-326
- Tapponnier P, ZQ Xu, F Roger, B Meyer, N Arnaud, G Wittlinger and JS Yang. 2001. Oblique stepwise rise and growth of the Tibet Plateau. *Science* 294: 1671-1677

Sediment sourcing in the Gangetic alluvium, Himalayan Foreland Basin – competition between Himalayan and cratonic hinterland

R Sinha^{1*}, Y Kettanah², MR Gibling², SK Tandon³, M Jain⁴, PS Bhattacharjee¹, AS Dasgupta¹ and P Ghazanfari⁵

¹ Engineering Geosciences Group, Indian Institute of Technology, Kanpur 208016, Uttar Pradesh, INDIA

² Department of Earth Sciences, Dalhousie University, Halifax, Nova Scotia B3H 3J5, CANADA

³ Department of Geology, University of Delhi, Delhi 110007, INDIA

⁴ Risø National Laboratory, Radiation Research Department, P.O. Box 49, DK-4000 Roskilde, DENMARK

⁵ Geology Department, Natural Sciences Faculty, Tabriz University, Tabriz, IRAN

* For correspondence, email: rsinha@iitk.ac.in

The Ganga plains in the Himalayan foreland basin have been built by sediments derived from the Himalayan orogen to its north as well as from the cratons to its south. The size of the Himalayan hinterland that receives high precipitation and from where large, sediment-charged rivers originate give the impression that the cratonic rivers have contributed little to the basin compared with Himalayan drainages. However, the Betwa, Chambal and other rivers, which drain northward into the Yamuna, are vigorous monsoonal rivers with large catchments and have contributed significantly to the basin fill during the Quaternary. Our research is based on three cliff sections, seven sediment cores and modern river sand samples in the Ganga-Yamuna-Betwa interfluvial region between Kanpur and Kotra in Uttar Pradesh, with an age model from 35 calibrated radiocarbon dates, OSL dates on quartz and feldspar, and TL dates. We have also used published water well data to map the extent of the cratonic sand wedges in the subsurface. A variety of petrographic methods have been used, viz. framework grain and dense mineral analysis, mica counts, and clay-mineral proportions. Unlike some geochemical methods, these petrographic methods do not allow precise modeling of Himalayan and cratonic contributions to sand and clay samples or sample groups, nor do they allow any source to be ruled out completely. However, our approach explores directly the links between the mineralogy of sediments and their potential source areas and, taking into account multiple criteria, allows a qualitative source-area assessment.

Some of the key questions investigated in this research are: (a) Can modern cratonic (Betwa and Chambal) and Himalayan (Ganga) river sands be distinguished on petrographic criteria? (b) Does older Quaternary alluvium below the Ganga Valley (Ganga Gray) resemble modern Ganga sediment? (c) Does older Quaternary red sand (Yamuna Red) resemble modern Betwa sand derived from the craton? (d) Does older Quaternary gray sediment south of the Ganga (Yamuna Gray, Chambal Gray, Sengar Gray, Rind Gray) resemble sand from any of the modern rivers? (e) During the past ~120 ka, how far north did cratonic sediment reach onto the Ganga Plains, and how far south did Himalayan sediment reach?

Stratigraphic and petrographic evidences show that subsurface bodies of cratonic sediment derived largely from these rivers extend north of the axial Yamuna River. Red feldspathic sand and gravel underlies much of the southern foreland basin at shallow depth (>30 m), where it is dated at 119.2 ± 12 ka B.P., and extends at deeper levels (>500 m) to about one-third of the distance across the foreland basin. Dense mineral analysis confirms a match with modern Betwa River sands, which derive their feldspar from granitic gneisses of the Bundelkhand Complex.

Along the Yamuna Valley, gray alluvium dated at 82 to 35 ka B.P. yields a cratonic signature, with large amounts of smectite derived from the Deccan Traps, and cratonic contributions can be detected in alluvium as young as 9 ka B.P. in a section ~25 km north of the Yamuna. The gray cratonic sands were probably deposited in part by the Chambal River, which transports high-grade metamorphic minerals from the Banded Gneiss Complex of the Aravalli belt. Cratonic sediment appears to interfinger with Himalayan detritus at shallow depth below the Ganga – Yamuna Interfluvium.

Archeological evidence suggests that the Yamuna River may have avulsed into its present position about 4,000 years ago, having previously flowed west of the Delhi-Hardwar Ridge. If so, much of the southwestern basin margin may have lacked an axial river system connected to the Himalaya prior to that time, and axial drainage would have been provided by cratonic rivers. The penetration of Himalayan sediment to the distal foreland basin may owe as much to avulsion along the fault-bounded ridge as it does to dynamic transverse drainage systems from the Himalaya pushing the axial drainage to the feather-edge of the basin. The wide spread of cratonic sediment would have been enhanced by slow subsidence in the distal foreland basin, focusing of rivers into a basin re-entrant, and the modest stream power of opposing Himalayan rivers in the western part of the basin.

We conclude that the dynamic cratonic rivers have been undervalued as contributors to the Himalayan Foreland Basin. They appear to have competed actively with the Himalayan systems in the southwestern part of the basin, where they are opposed to less vigorous rivers than those of the eastern plains (Gandak, Baghmata, and Kosi) and where the low subsidence rate enhances the areal extent of sediment wedges. It has been suggested before that dynamic transverse drainages from the Himalaya pushed the axial rivers to the feather-edge of the basin. However, the penetration of Himalayan rivers and sediment to the southwestern foreland basin may also reflect opportunistic avulsion along the fault-bounded Delhi-Hardwar Ridge. Prior to Yamuna avulsion, cratonic rivers may have contributed a considerable amount of sediment to the Ganga River and Bay of Bengal. Although the Himalaya undoubtedly provided the great bulk of sediment to these systems, more detailed geochemical characterization of northern cratonic source areas and sediment is needed in order to evaluate the cratonic contribution reliably. There may also be overlap between geochemical signatures from orogenic and cratonic sources, precluding an easy finger-printing of sediment from the two areas.

Silurian acanthomorphitae acritarch from the Shiala Formation, Tethys Garhwal Himalaya, India

HN Sinha

Department of Geology, Vinoba Bhave University, Hazaribag-825301, Jharkhand, INDIA
E-mail: hnsinha2003@yahoo.co.in

The Tethyan-Tibetan sedimentary belt extends from Nanga Parbat in the west to Namcha Barwa in the east and divisible into five sub basins, which are resting over the Central Crystalline basement in the south. These continuous sedimentary sequences vary in thickness from 5000 to 16000 m and range in age from Precambrian to Eocene (?). In north they are terminated by the Indus-Tsangpo Suture Zone. The five subdivisions are developed in the Kashmir, Zaskar, Spiti-Kinnur and Garhwal-Kumaon Basin. The present study is confined to the Lower Palaeozoic sequences of Garhwal-Kumaon basin, which is best known for biostratigraphy and sedimentological studies (Shah and Sinha 1974, Sinha 1989, Sinha et al. 1998, Sinha et al. 2005, Sinha and Mishra 2006, Bagati et al. 1991, among others) in the Tethyan-Tibetan belt.

The Ordovician-Silurian strata known as Shiala Formation in the Garhwal-Kumaon basin vary from 400-500 m thickness and are not easily accessible for field work. The Shiala Formation conformably overlies the Garbyang Formation, which is characterised by green shales at the bottom and arenaceous component increases gradually reflecting coarsening upward sequence.

The Shiala Formation has been assigned a mid to late Ordovician age based on index forms of brachiopod taxa (Sinha 1989). Goel et al (1987) assigned a mid Ordovician age on the basis of conodont species, whereas Sinha et al (1998) demarcated Ordovician-Silurian boundary within Shiala Formation itself based on stratigraphically acritarch forms.

The present study reveals the recovery of two acanthomorph acritarch species from the siltyshale discrete horizons. These forms have not been described earlier (Sinha et al. 1998). The recovered forms are *Multiplicisphaeridium eltonense* Dornig 1981 and *Micrhystridium stellatum* Deflandre 1945.

The systematic paleontology is as follow of the recovered forms:

Group: ACRITARCHA Evitt, 1963

Subgroup: Acanthomorphitae Downie et al. 1963

Gegus: Micrhystridium Deflandre 1937

Type species: *Micrhystridium inconspicuum* Deflandre 1937

Micrhystridium stellatum Deflandre 1945

Range: *M. stellatum* has cosmopolitan in distribution and long ranging (Silurian-Mesozoic).

Occurrence: It is rare from the siltyshale lithounit of the Shiala Formation, Garhwal Tethys Himalaya.

Genus: *Multiplicisphaeridium* (Staplin) Lister, 1970

Type species: *Multiplicisphaeridium ramispinosum* Staplin 1961

Multiplicisphaeridium eltonense Dornig 1981

Range: Ludlow type area (Dornig, 1981); Elton group, Ludlow Series (Mullins, 2001).

Occurrence: It is rare from the siltyshale lithounit of the Shiala Formation, Tethys Garhwal Himalaya, India.



FIGURE 1. Cyst circular to subcircular in outline, originally spherical; wall thin, surface laevigate; 10-14 hollow, homomorphic, slightly flexible, spine like, laevigate processes drawn out from and freely communicating with vesicle interior; processes 4-7 m long, 1-2 m wide at sub circular base; processes tips sharply acute, excystment by simple splitting of vesicle wall. Diameter of cyst 14 m.

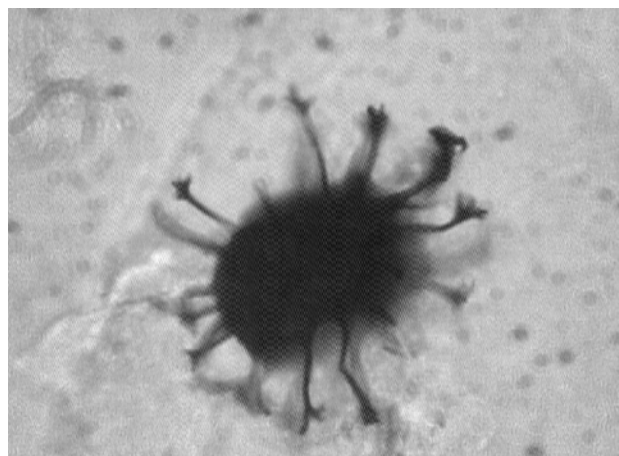


FIGURE 2. Cyst sub spherical, 25 m in diameter, laevigate; 10-18 laevigate, long processes which taper to simple and branched tips; process cavities open to the vesicle interior. Branching generally occurs at 2/3rds the way along the processes; branches ramified up to 3rd order. Pylome not distinct possibly due to over maturation.

Age and Palaeoenvironment

The yield of *Micrhystridium stellatum* and *Multiplicisphaeridium eltonense* from the study section reveals the Silurian age for the Shiala Formation, which is consistent with earlier age (Sinha et al. 1998) assigned.

Several studies have been carried out on the relationship between microplankton species and paleoenvironment. Vecoli (2000) used the distribution of microplankton to interpret the palaeoenvironment of the Cambrian-Ordovician sequence of the Sahara Platform. He found the near shore environment is dominated by thin walled sphaeromorphs, whereas outerself settings were typified by increased acritarch assemblage, high diversity and greater morphological complexity. The recovered forms from the Shiala Formation reveal the outer shelf to open marine environment. These forms are dark indicating high thermal maturation as well as the forms is oxidized prior to final burial in shallow outer shelf settings.

Acknowledgement

The study is financially supported by DST (Government of India) project No.SR/S4/ES-91/2004. The author thanks to Dr L Shiveshwari for her kind support in many ways.

References

- Bagati TN, Rohtash Kumar and SK Ghosh. 1991. Regressive-transgressive sedimentation in the Ordovician sequence of the Spiti (Tethys) basin, Himachal Pradesh, India. *Sedimentary Geology* 73: 171-184
- Deflandre G. 1937. Microfossiles des silex Cretaces. Deuxieme partie. Flagelles incertae sedis Hystrichosphaerides Sarcodines. Organismes-Divers. *Ann. Paleontol.* 26:51-103
- Deflandre G. 1945. Microfossiles des calcaires Siluriens de la Montagne Noire. *Ann. Paleontol.* 31: 39-75
- Dorning KJ. 1981. Silurian acritarchs from the type Wenlock and Ludlow of Shropshire, England. *Rev. Palaeobot. Palynol.* 34: 205-208
- Downie C. 1963. 'Hystrichospheres' (acritarchs) and spores of the Wenlock Shales (Silurian) of Wenlock, England. *Palaeontology* 6(4): 625-652
- Evitt WR. 1963. A discussions and proposals concerning fossil dinoflagellates, hystrichospheres and acritarchs. *Proceed. National Academy of Sciences USA* 49: 158-164
- Geol RK, M Kato, AK Jain and SS Srivastava. 1987. Fauna from the 'Muth Quartzite' Garhwal Himalaya, India. *Journal of the Faculty of Science, Hokkaido University* 22(2): 247-257
- Lister TR. 1970. A monograph of the acritarchs and chitinozoa from the Wenlock and Ludlow Series of the Ludlow and Millichope areas, Shropshire. *Palaeontograp. Soc. (Monograph)* 124(1): 1-100
- Mullins GL. 2001. Acritarchs and prasinophyte algae of the Elton group, Ludlow Series, of the type area. *Palaeontograp. Soc. (Monograph)* 155: 1-154, plates 1-18
- Shah SK and AK Sinha. 1974. Stratigraphy and tectonics of the 'Tethyan' Zone in a part of western Kumaun Himalaya. *Himalayan Geology* 14: 1-27
- Sinha AK. 1989. Geology of the Higher Central Himalaya. Wiley, 219pp
- Sinha HN, Bijai Prasad and SS Srivastava. 1998. Ordovician-Silurian acritarch biostratigraphy of the Tethyan Garhwal Himalaya, India. *Rev. Palaeobot. Palynol.* 103: 167-199
- Sinha HN, SS Srivastava and James Peters. 2005. Palaeoenvironmental deductions of microfossil flora and fauna of the Shiala and Yong formations, Tethyan Garhwal Himalaya. *Journal of the Geological Society of India* 65: 26-42
- Sinha HN and PK Mishra. 2006. Prismocorollina sp. From the Early Ordovician Thango Formation of Tidong Valley, Kinnaur Tethyan Himalaya, Himachal Pradesh. *Journal of the Geological Society of India* 68: 774-778
- Staplin FL. 1961. Reef-controlled distribution of Devonian microplankton in Alberta. *Palaeontologist* 4(3), 392-424, pls 48-51
- Vecoli M. 2000. Palaeoenvironmental interpretation of microphytoplankton diversity trends in the Cambrian-Ordovician of the northern Sahara Platform. *Palaeogeography, Palaeoclimatology and Palaeoecology* 160: 329-346

Landslides in the Kashmir Earthquake of 8th October 2005

Amita Sinvhal*, Ashok D Pandey and Sachin M Pore

Department of Earthquake Engineering, Indian Institute of Technology Roorkee Roorkee-247 667, Uttarakhand, INDIA

* For correspondence, email: amitafeq@gmail.com

The Event

A devastating earthquake (MW 7.3) occurred on 8 October 2005 at 03h 50m 38.63s UTC, (09:20:38, Indian Standard Time), with epicenter at Muzaffarabad, 34.432° N, 73.537° E (NEIC), in Kashmir. The epicenter was located 125 km WNW of Srinagar, more than 700 km from Delhi and 90 km NE of Islamabad. The earthquake devastated the Kashmir valley on both sides of the Line of Control (LoC). Neighboring Afghanistan was also partly affected.

Seismotectonic aspects of the damaged area

The Himalayan arc is one of the most seismically active regions on the continental crust. Seismicity in this inter-plate environment is attributed to seismotectonic evolution of the Himalayas. These rugged mountain ranges were formed as a result of several tectonic upheavals that were spread through several geologic eras. It started with the movement of the Indian plate through the Tethys Sea, which led to subduction of the oceanic part of the Indian plate below the Eurasian plate, and eventually continent – continent collision between the two plates. Thus, rocks that show evidence of sedimentary, igneous (volcanic) and metamorphic activity in different orogenic episodes are found juxtaposed with each other within the various mountain ranges of the Himalayas. This has caused faulting, thrusting, shearing, folding, fissuring, jointing and alluvial fills in the Himalayan compression zone. This seismotectonic situation, together with action produced by rivers and glaciers over geological time, has rendered mountain ranges in this region vulnerable to steep and precarious slopes, which are sometimes almost vertical, prone to landslides, rock slides, rock falls, mud slides, debris fans, and ground fissures.

The Main Boundary Fault (MBF) and the Main Central Thrust (MCT) defines the southern flank of the entire Himalayan arc. The MBF separates the rugged mountains of the Lesser Himalayas from the sedimentary sequence of the Sub-Himalayas. In the eastern and western extremities of the Himalayas, the Himalayan arc and with it the MBF, take a sharp southward bend. This makes the tectonics in this region more complex than in the rest of the Himalayas. In the area affected by the Saturday morning earthquake the Kashmir syntaxis is the most prominent tectonic feature. The epicentral region, defined by the Balakot – Muzaffarabad region, is on the southern flank of this syntaxis.

Landslides

Shaking produced by the inter-plate earthquake of October 8, 2005 in this kind of a geological setting triggered numerous gigantic landslides (Figure 1). These were of unusual dimensions and were spread in a wide geographical region on both sides of the LoC. These included the rugged Pir Panjal and Shamshabari mountain ranges and several river courses, water tributaries and valleys of the Jhelum, Kishan Ganga, Neelam, Qazi Nala and

Kahmil and their many tributaries within Uri and Tangdhar bowls and became more severe beyond that, towards the epicenter. Their incidence and volume of debris increased towards the epicenter, which is in the MBF and MCT region.

The depth of river and valleys ranges from 30 to 70 m with nearly vertical sidewalls in Jhelum between Baramulla and Uri at several places. Landslides in this stretch were with almost vertical faces as if knife cut, and the starting point was a rotational landslide. Soil profile exposed in landslides, road cuttings and along rivers cuttings revealed an abundance of either highly weathered rocks, including sandstone and conglomerates that were highly heterogeneous in nature. The latter sometimes appeared to be studded with angular or rounded boulders and stones of varying sizes ranging from 50 mm (size of pebbles) to 500 mm (boulders) and at many locations huge boulders of size even up to 2.0 m were encountered. These were embedded in gravel, sand of native rock material, silt, clay and other suspended matters that rivers and streams or glaciers have carried over millennia. The color of exposed soil deposits varied from white-gray to light brown to dusty pink. Isolated patches of very fine and jet-black colored soil deposits were noticed at Kamalkot.

Effects

The earthquake on 8th October, 2005 triggered massive landslides in the surveyed region and caused havoc in hills surrounding Uri, Baramulla, Salamabad, Kamanpost, Kamalkot, Nasta Chun Pass, Tangdhar and Tithwal. Rolling down of debris and large size stones which occurred near places of habitat or where life line structures were present caused roadblocks and extensive damage due to boulders finding their way into or through structures causing loss of life and property. Several human settlements were buried, rivers were partly obstructed and roads were blocked.

Roads connecting major urban locations are of permanent type with flexible pavements. Few stretches along the valley are without provision of pavement. No structural failure of these roads was observed. Obstruction to traffic was mainly due to deposition of debris on account of landslides from adjacent hills. Landslides blocked national highway NH1A, between Baramulla and Uri, but roads were cleared within two days of the earthquake. Ample evidence supporting this fact was present by the roadside. Damage to roads due to numerous landslides was of local extent in spite of large size boulders leaping and rolling down hill slopes and hitting the road surface. This shows a desirable performance of forming the embankments with necessary compaction and stabilization.

Landslides adversely affected several fair weather roads also, including the strategically vital road link to Tangdhar and Tithwal. This zigzag road was stabilized with protection walls, made of random rubble stone masonry. It was covered with debris produced by earthquake induced translational type of landslide,

and was cleared immediately after the main event, but was prone to after shocks. In these places old and new trees showed a peculiar trend, curving of trunk at its base, symptomatic of continuing creep on steep hills. Various kinds of landslides were observed at different places, e.g. debris flow at Kamalkot, earth flow at Salamabad, crescent shaped crown of landslides at Tangdhar, and toples near Tithwal, etc.

Road embankments at several locations failed partially on slopes. Landslides and embankment slope failures blocked roads at many spots over stretches extending 100 m at some places. Moderate to severe damage was also observed to slope protection works in the areas surveyed. Failure of stone pitching, breast walls, gabion walls and wing-walls of bridge abutments were observed between Salamabad and Kamalkot as well as on the route to Tangdhar-Tithwal.

On account of the size, and quantity of observed landslides, rockfalls, mudslides, ground fissures etc. in the Pir Panjal and the Shamsabari ranges and in the valleys of Jhelum and Kishanganga and their tributaries, and damage to the built environment in the surveyed region intensities were assigned to various places on the MSK scale, and it varied from MSK XI to MSK VII. At Kamalkot, Salamabad, Uri, Panzgam, Naichian, Tangdhar, Chamkote, Tithwal, Nasta Chun Pass it was XI, at Lagama it was X, at Mohura, Rajarwani, Kupwara, it was IX, at Boniyar, Chandanwari, Rampur, Handwara it was VIII and at Baramula, Srinagar and Pattan it was VII.

Conclusions

The seismotectonic environment of the region makes it extremely prone to seismic events of varying magnitudes with regular frequency. The extensive landslides, slope failures and rock fall as observed in the surveyed region are an indication of its vulnerability to repeated occurrences of such phenomena and associated damage.

Acknowledgements

The authors are indebted to the following whose help and support made this field visit possible: The people of Jammu and Kashmir, the Director, IIT Roorkee, the Head, Department of Earthquake Engineering, IIT Roorkee, and Officers and Ranks of the Indian Army.

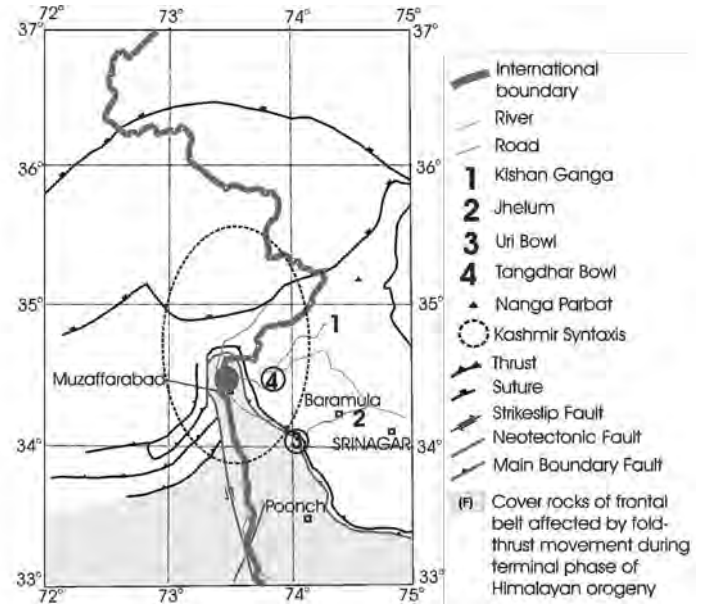


FIGURE 1. Map shows epicenter of Kashmir earthquake of 8th October 2005. Epicentral distance of nearest point of Tangdhar and Uri bowl is approximately 25 and 60 kilometers, respectively. International boundary is redrawn according to Sol sheet 43. Tectonics is redrawn and simplified after Seismotectonic Atlas of India (GSI 2000).

Neogene sedimentary evolution of the Guide Basin and its implications on uplift of the NE Tibetan Plateau, China

Chunhui Song^{1,2}, Qingquan Meng¹, Xiaomin Fang^{2*}, Shuang Dai¹ and Junping Gao¹

¹ Key Laboratory of Western China's Environmental Systems (Ministry of Education) and College of Resources and Environment, Lanzhou University, Lanzhou, Gansu 730000, CHINA

² Center of Basin and Environment, Institute of Tibetan Plateau Research, Chinese Academy of Sciences, Beijing 100085, CHINA

* For correspondence, email: fangxm@itpcas.ac.cn

The Cenozoic Guide Basin in Qinghai Province (northwestern China), an important key site in the northeastern Tibetan Plateau is tectonically controlled in framework by the two big sinistral Kunlun fault and Altyn Tagh – South Qilian (Nan Shan – Qinghai Nan Shan) faults, is filled with huge thick Cenozoic sedimentary sequence that records the important signatures on the deformation and uplift of this part of the plateau. Here we present the results of a detailed lithostratigraphical investigation of the Neogene sedimentary rocks on the northern basin and discuss the style of sedimentation during its deposition. Depend on the mammal fossils and the magnetostratigraphic dating in typical section, detailed sedimentary study has revealed nineteen lithofacies, and five sedimentary environments have been distinguished: braided river, delta, shallow and half-deep lake, fan delta and piedmont proluvial systems. Five stages of the basin evolution have been revealed since 21Ma, they are the basin downfaulted and expanded stage (20.8-13 Ma), the basin developed stage (13-7.8 Ma), the basin shrank stage (7.8-3.6 Ma), basin died out stage (3.6-2.6 Ma) and the intermontane basin and the river terrace developed stage (2.6-0 Ma). The responding relationship between the sedimentation of the Guide basin and the tectonic uplift reveals that there are six important tectonic events at least about >20.8, 13, 7.8, 3.6, 2.6 and <1.8 Ma since late Cenozoic in the north of

Tibetan plateau. But the events are extraordinary important since 7.8 Ma, they gradually induced the marginal growth faults toward basin formed, Lajishan uplifted and the basin shrank. Especially, the tectonic event about 3.6 Ma made the surrounding mountains uplifted on a large scale. The intense tectonic event about <1.8 Ma induced the Songba Gorge formed through the process that the retrogressive erosion of Yellow River dissected the east mountains of the Guide basin, the palaeo-lake of the Guide Basin was cut through, the lake water was drained and the lake disappeared, and the Yellow River appeared in the Guide Basin. In the period of <1.8-0 Ma, the gradual uplifts of the Guide Basin made the Yellow River cut down about 900 m into the Cenozoic strata and the Triassic and Precambrian basement rocks, and have formed seven Pleistocene terraces.

Acknowledgements

This study was co-supported by the Knowledge Innovation Program of the Chinese Academy of Sciences (grant no. kzcx2-yw-104), Chinese National Science Foundation Grants (nos. 40721061 and 40334038), National Basic Research Program of China (grant no. 2005CB422001), and Science and Technology Key Project of Ministry of Education of China (grant no. 306016).

A possible Permian suture in the Lhasa Block, Tibet: Evidence from eclogites and probable ophiolite

Chen Songyong, Yang Jingsui, Li Tianfu, Xu Xiangzhen, Li Zhaoli, Ren Yufeng

Key Laboratory for Continental Dynamics of Ministry of Land and Resources, Institute of Geology, Chinese Academy of Geological Sciences, Beijing 100037 CHINA

The Sumdo eclogite belt was found recently in the Lhasa block, Tibet, over 100 km northeast of the city of Lhasa. Most of the Sumdo eclogites are massive, coarse-grained and fresh, occurring as tectonic slices in garnet-bearing mica-quartz schist. And three distinct types are recognised: phengite eclogite, quartz eclogite and rutile eclogite.

The mineral assemblage of the Sumdo eclogite is garnet + omphacite ± epidote ± phengite ± quartz ± rutile. The rock has been intensely retrograded and the retrograde minerals include amphibole, epidote, quartz, albite and chlorite. Growth zonation can be seen in garnet porphyroblasts. The garnet porphyroblasts and matrix garnet mainly plot in the group C eclogite field, but some rims of garnet porphyroblasts and some matrix garnet plot in the group B eclogite field. Clinopyroxenes are mainly omphacite with minor augite of generations [] and []. According to the garnet-omphacite-phengite geothermobarometer, the P-T estimations are 2.58-2.70 °C Gpa and 630-777 °C Gpa, suggesting that the condition of peak metamorphism are close to the phase boundary between quartz and coesite. Petrographic observation and P-T estimation indicate that the protolith of the eclogites experienced a metamorphic process from high greenschist facies through amphibolite facies, eclogite facies and amphibolite facies to high greenschist facies metamorphism, which suggests that there occurred progressive metamorphism concerning subduction related to the closing of the ocean and subsequent retrogressive metamorphism concerning exhumation.

Petrochemistry and Sr-Nd isotope analysis suggest that its protolith was typical MORB, derived from the depleted mantle. All of the rocks have whole-rock chemical compositions similar to tholeiitic MORB with 45.3-50.6 wt % SiO₂, 12.93-14.27 wt% Al₂O₃ and 1.3-2.8 wt% total alkalis (K₂O + Na₂O). Generally, it has the compositional features of basaltic or gabbroic rocks, belonging to the calc-alkaline suite, and shows the features of MORB, indicating that its protolith came from the oceanic basalt. The chondrite-normalized REE patterns of most samples show depletion in LREE and no pronounced Eu anomaly, with flat HREE patterns. The MORB-normalized trace element spidergrams show depletion in LREE, with flat patterns from Zr to Yb, and no fractionation of the fraction. The La_N/Yb_N, La_N/Ce_N and La_N/Sm_N ratio are 0.19-0.56, 0.75-0.81 and 0.37-

0.81 respectively, the three ratios being all <1. The Hf/Th ratios of most samples are 11.10-33.97, being >8. The Ce/Nb ratios are 2.72-19.02, all being >2. The Th/Yb ratios are 0.01-0.10, all being <1, and ¹⁴³Nd/¹⁴⁴Nd=0.513000-0.5131777. This also shows that its protolith has the features of typical MORB. And the (⁸⁷Sr/⁸⁶Sr)_i=0.703574-0.705478 suggests the protolith derived from the depleted mantle.

The SHRIMP U-Pb zircon dating of the eclogite yielded ages from 242.4±15.2 Ma to 291.9±12.8 Ma, with a mean age of 261.7±5.3 Ma. According to the regional geological data, it is inferred that the eclogite protolith is Carboniferous-Permian in age. All of the zircons contain abundant inclusions, typically concentrated in the cores of grains. Garnet is by far the most common and widespread inclusion, followed by quartz, apatite, rutile and omphacite. Other common inclusions include amphibole, sphene, phengite and albite. Three main inclusion assemblages are recognized: Grt+Omp+Rt+Phe (eclogite facies), Amp+Spn+Ab (amphibolite facies) and Qtz+Ap (uncertain facies). The compositions of the inclusions are identical to the compositions of the same minerals in the bulk rock. The concentration of the inclusions in the cores of the zircon grains and the abundance of eclogite facies minerals indicate that the zircons grew during, or shortly after, peak metamorphism. All of the zircons have very low Th/U ratios consistent with their metamorphic origin in the Permian.

During the field period, we have found blocks of serpentinite, cumulates of gabbro and pyroxenite, and basic volcanic rocks, which occur together with the eclogites. We presume these blocks belong to ophiolite units, but they need to be proved by petrochemical data soon after.

On the other hand, we also checked the island arc basalt reported in Chinese journal, and collected the samples. Although we have not completed the chemical analysis on these rocks yet, based on the field occurrences, we agree the conclusion from previous publication.

In general, there are different lithologic units, including MORB-type eclogite, ophiolite, and island arc volcanic rocks in the same zone, which most likely indicate a suture in the region. Based on the available age data, it is probable a Permian suture.

Long Term GPS Deformation Rates in the Karakoram terrane of Ladakh

Sridevi Jade^{1*}, VK Gaur^{1,2}, MSM Vijayan¹ and P Dileep Kumar¹

¹ CSIR Centre for mathematical Modelling and Computer Simulation, (CMMACS), Bangalore, 560 037, INDIA

² Indian Institute of Astrophysics, Bangalore 560 034, INDIA

* For correspondence, email: sridevi@cmmacs.ernet.in

.....

We present long term deformation rates in the Karakoram terrane of Ladakh, derived from a decade (1997-2008) of GPS measurements, made at two continuous stations and ten campaign sites. GPS measurements over this eleven year period give well constrained present day deformation rates in this region with errors of less than 0.3mm. The results provide a fairly clear picture of the Trans-Himalayan kinematics and deformation mechanism in this region by producing an well constrained annual slip rate along the Karakoram fault, convergence rate across the Himalaya and east-west extension across the whole of

southern Tibet. Eleven years of campaign measurements along the Karakoram fault zone indicate a well constrained dextral slip rate of 2.5 mm/yr in the Panamik Segment and 1.8 mm/yr in the southeastern Tangste segment of the fault. The results also indicate insignificant internal deformation within Ladakh, other than that associated with the slip rate of the Karakoram fault. Ladakh sites indicate a convergence rate of 15 to 18 mm/yr with respect to south India, 12 to 15 mm/yr with Delhi in North India as well as Almora north of MBT and extension of 14 to 15 mm/yr with respect to Lhasa in southeastern Tibet.

The metamorphism of the Tso Morari ultra-high pressure nappe of the Ladakh Himalaya

Albrecht Steck^{1*} and Jean-Luc Epard²

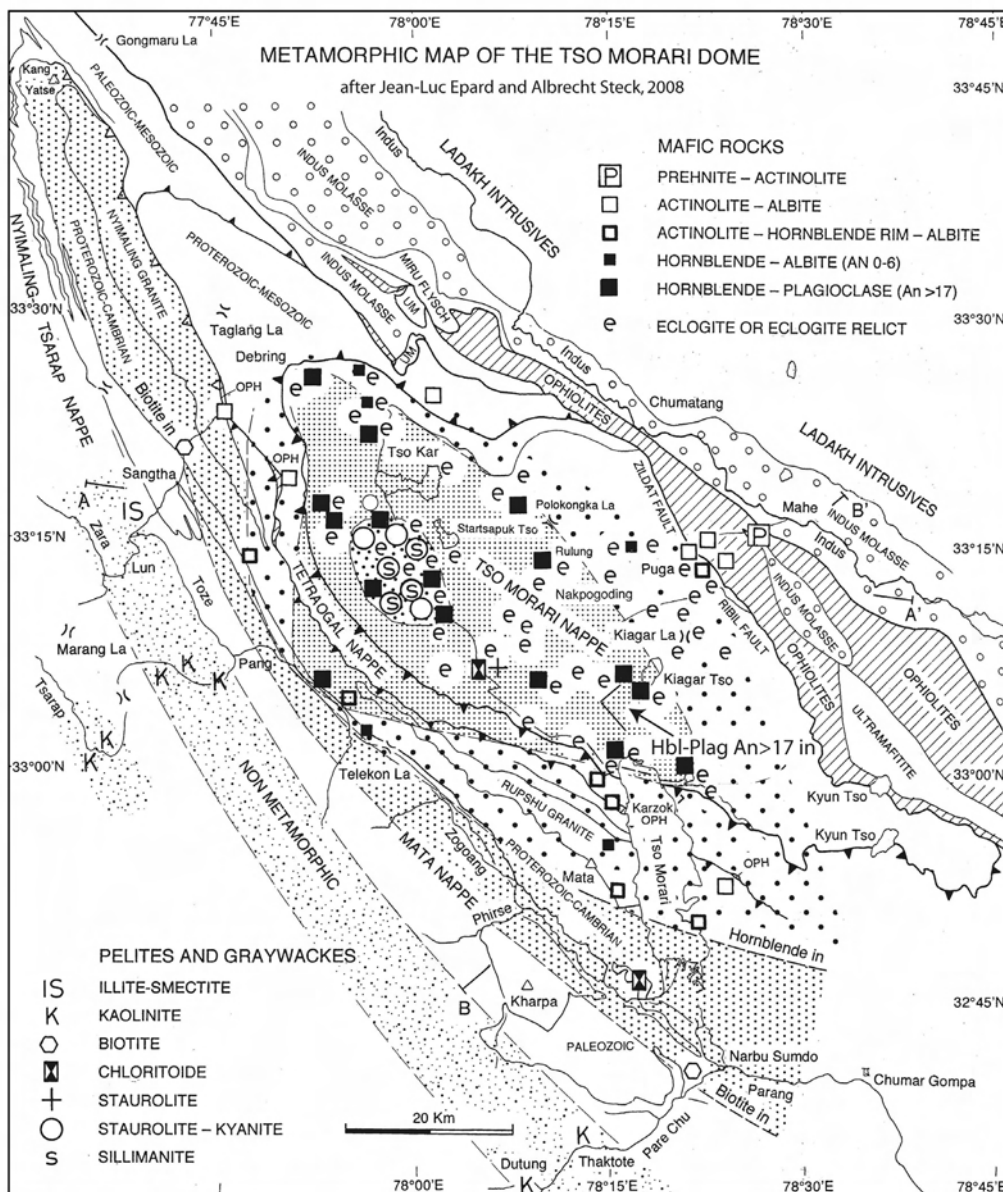
¹ Institut de Minéralogie et Géochimie, Université de Lausanne, Anthropole, CH-1015 Lausanne, SWITZERLAND

² Institut de Géologie et Paléontologie, Université de Lausanne, Anthropole, CH-1015 Lausanne, SWITZERLAND

* For correspondence, email: albrecht.steck@unil.ch

A map of the metamorphic zones of the North Himalayan nappe stack in the Tso Morari region is proposed. The Tso Morari nappe is composed of Late Proterozoic-Cambrian graywackes intruded by the 479 ± 2 Ma Tso Morari granite and mafic dikes (Girard and Bussy 1999). Eclogites and eclogite relicts testify of an oldest ultra-high pressure metamorphism limited to the deepest Tso

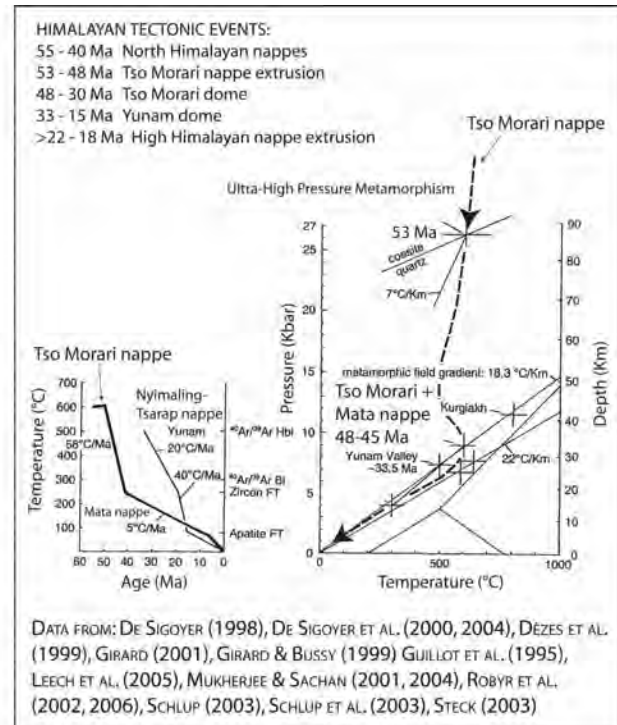
Morari nappe (Epard and Steck 2008). This nappe and the higher Tetraogal, Karzok ophiolite and Mata-Nyimaling-Tsarap nappes are overprinted together by a Barrovian regional metamorphism, that grades from staurolite-kyanite assemblages in the Nuruchan region in the western Tso Morari dome down to metapelites with kaolinite and illite-smectite assemblages in an external zone of



Triassic sediments exposed in the Dutung-Thaktote graben to the SE (Girard 2001, Girard et al. 1999, Steck et al. 1998, Steck 2003). The ultra-high pressure metamorphic rocks with coesite and micro-diamonds are characterized by pressures of over 27 kbars, temperatures of $580 \pm 6^\circ\text{C}$ (De Sigoyer et al. 2004, Mukherjee and Sachan 2001, 2004). The metamorphism is dated of 53.3 ± 0.7 Ma (Leech et al. 2005). The generally non-oriented fabric of the eclogites testify of the static crystallisation of the metabasites at depth of over 90 km. The detachment and extrusion of the low density Tso Morari nappe, composed of 70% of the Tso Morari granite and 30% of graywackes with some eclogitic dikes, occurred by ductile pure and simple shear deformation. It was pushed by buoyancy forces and by squeezing between the underthrust Indian lithosphere and the Asian mantle wedge (Epard and Steck 2008). The extruding Tso Morari nappe reached a depth of over 35 km at the base of the North Himalayan accretionary wedge some 48 Ma ago. There, the whole nappe stack crystallized under amphibolite facies conditions with a metamorphic field gradient of $20^\circ\text{C}/\text{km}$ (De Sigoyer et al. 2004, Girard 2001). The crystallisation of sillimanite needles parallel to the first stretching lineation L1 and after kyanite testify of a pressure drop during the W-directed extrusion of the Tso Morari nappe (Epard and Steck 2008). Zoned amphiboles with an actinolite core and magnesiohornblende border, or a magnesiohornblende core with a tschermakite border indicate a prograde crystallisation during the Barrovian metamorphism (Schlup et al. 2003).

References

- De Sigoyer J, S Guillot and P Dick. 2004. Exhumation of the ultrahigh-pressure Tso Morari unit in eastern Ladakh (NW Himalaya): A case study. *Tectonics* 23: 1-18
- Epard J-L and A Steck. 2008. Structural development of the Tso Morari ultra-high pressure nappe of the Ladakh Himalaya. *Tectonophysics: in press*.
- Girard M. 2001. Metamorphism and tectonics of the transition between non metamorphic Tethyan Himalayan sediments and the North Himalayan Crystalline Zone (Rupshu area, Ladakh, NW India). *Mémoires de Géologie* (Lausanne) 35
- Girard M and F Bussy. 1999. Late Pan-African magmatism in the Himalaya: new geochronical and geochemical data from the Ordovician Tso Morari metagranites (Ladakh, NW India). *Schweizerische Mineralogische und Petrographische Mitteilungen* 79: 399-417
- Girard M, A Steck and P Thélin. 1999. The Dutung-Thaktote extensional fault zone and nappe structures documented by illite crystallinity and clay-mineral paragenesis in the Tethys Himalaya between Spiti river and Tso Morari, NW India. *Schweizerische Mineralogische und Petrographische Mitteilungen* 79: 419-430



- Leech ML, S Sing, AK Jain, RM Klempner and RM Manickavasagam. 2005. The onset of India-Asia continental collision: early stage subduction required by the timing of UHP metamorphism in the western Himalaya. *Earth and Planetary Science Letters* 234: 83-97
- Muckerjee BK and HK Sachan. 2001. Discovery of Coesite from Indian Himalaya: a record of ultra-high pressure metamorphism in Indian continental crust. *Current Science* 81:1358-1361
- Muckerjee BK and HK Sachan. 2004. Garnet response diamond pressure metamorphism from Tso-Morari region, Ladakh, India. *Himalayan Journal of Science* 2/4: 209
- Schlup M, A Carter, M Cosca and A Steck. 2003. Exhumation history of eastern Ladakh revealed by $40\text{Ar}/39\text{Ar}$ and fission track ages: The Indus river-Tso Morari transect, NW Himalaya. *Journal of the Geological Society of London* 160: 385-399
- Steck A, JL Epard, JC Vannay, J Hunziker, M Girard, A Morard and M Robyr. 1998. Geological transect across the Tso Morari and Spiti areas: the nappe structures of the Tethys Himalaya. *Eclogae Geologicae Helveticae* 91: 103-121
- Steck A. 2003. Geology of the NW Indian Himalaya. *Eclogae Geologicae Helveticae* 96: 147-196

The Tectonics of the Tso Morari Ultra High Pressure Nappe in Ladakh, NW Indian Himalaya

Albrecht Steck^{1*} and Jean-Luc Epard²

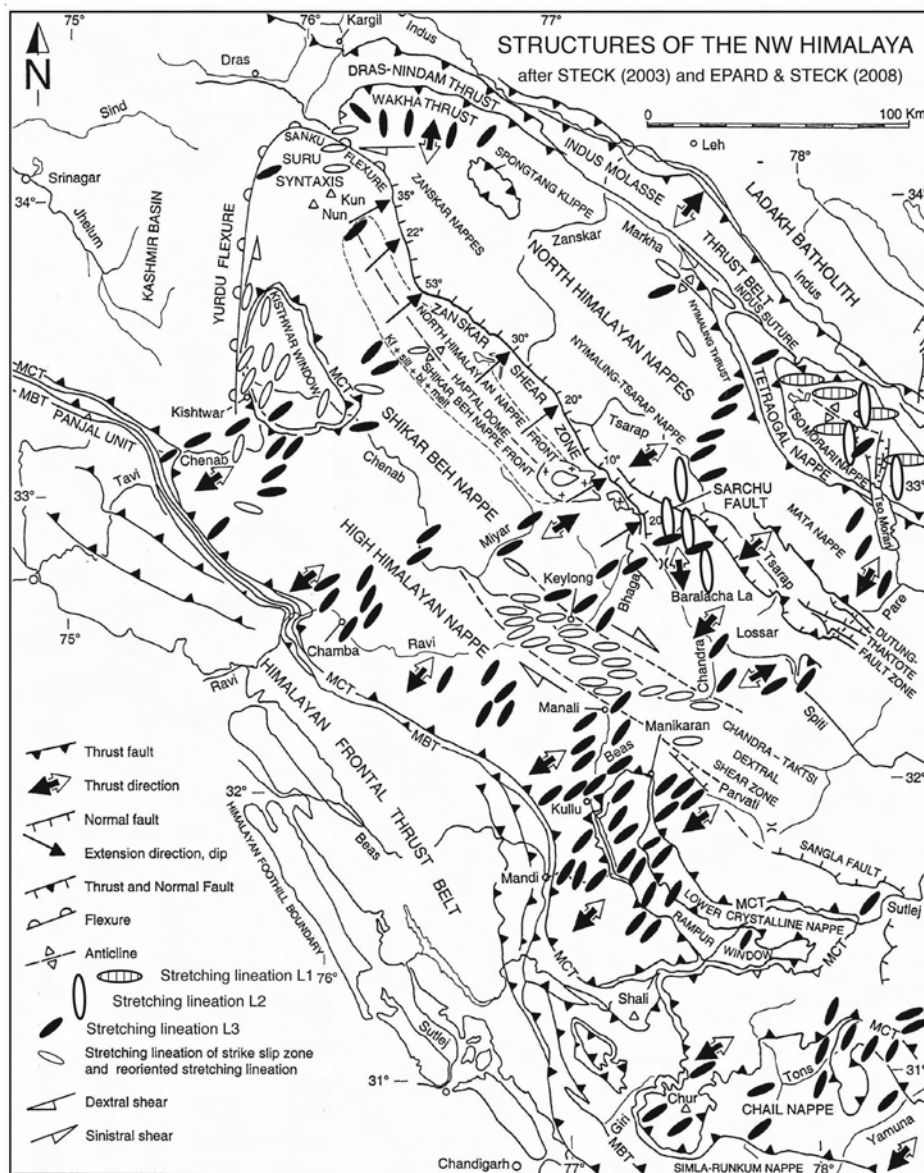
¹ Institut de Minéralogie et Géochimie, Université de Lausanne, Anthropole, CH-1015 Lausanne, SWITZERLAND

² Institut de Géologie et Paléontologie, Université de Lausanne, Anthropole, CH-1015 Lausanne, SWITZERLAND

* For correspondence, email: albrecht.steck@unil.ch

A tectonic model for the structural development of the Tso Morari ultra-high pressure nappe is proposed. It is integrated into the context of the formation of the North Himalayan nappes of the Ladakh Himalaya. In the area, this stack of nappes is composed by, from base to top, the Tso Morari, Tetraogal, Karzok ophiolite, Nyimaling-Tsarap and Mata nappes (Steck et al. 1998, Steck 2003). Four stretching lineations, L1 – L4, are successively developed on

the main schistosity in the North Himalayan nappes (Epard and Steck 2008). L1, with its top-to-the E shear indicators, was formed during the W-directed high temperature extrusion of the ultra high pressure Tso Morari nappe. L2, with its top-to-the S shear indicators, was formed during an early N-directed underthrusting of India below Asia. It is developed in the roof of the Tso Morari nappe as well as at the base and frontal part of the Nyimaling-



Tsarap nappe in the area of Sarchu and Baralacha La. L3, with top-to-the SE shear indicators, was developed in the whole North Himalayan nappe stack during a NE-directed underthrusting of India below Asia. The same NE-directed L3-stretching lineation was also developed in the younger High Himalayan nappes during their SW-directed extrusion and emplacement between about 40 and 18 Ma. L4 is related to active NW-directed low temperature, dextral strike-slip movements. The observed change of underthrusting direction showed by the orientation of L2 and L3 is compatible with paleomagnetic models suggesting an anticlockwise rotation of the Indian continent between 52 Ma and 35 Ma. These two time-constraints are given by the age of the ultra high pressure metamorphism and the Tso Morari dome uplift to a depth of 10 km respectively. The warping of the Tso Morari dome started already some 48 Ma ago with the formation of an extruding nappe at depth. The Tso Morari dome reached a depth of 15 km about 40 Ma ago in the eastern Kiagar La region and 30 Ma ago in the western Nuruchan region (Schlup et al. 2003). The extrusion rate was of about 3 cm/yr between 53 and

48 Ma, then 1.2 mm/yr between 48 and 30 Ma and 0.5 mm/yr after 30 Ma. The Tso Morari dome is still affected by faults, open regional dome, basin and pull-apart structures, coeval with a zone of dextral transpression parallel to the Indus Suture zone (Epard and Steck 2008).

References

- Epard JL and A Steck. 2008. Structural development of the Tso Morari ultra-high pressure nappe of the Ladakh Himalaya. *Tectonophysics*: (in press)
- Schlup M, A Carter, M Cosca and A Steck. 2003. Exhumation history of eastern Ladakh revealed by $^{40}\text{Ar}/^{39}\text{Ar}$ and fission track ages: The Indus river-Tso Morari transect, NW Himalaya. *Journal of the Geological Society of London* 160: 385-399
- Steck A, JL Epard, JC Vannay, J Hunziker, M Girard, A Morard and M Robyr. 1998. Geological transect across the Tso Morari and Spiti areas: the nappe structures of the Tethys Himalaya. *Eclogae Geologicae Helveticae* 91: 103-121
- Steck A. 2003. Geology of the NW Indian Himalaya. *Eclogae Geologicae Helveticae* 96: 147-196

The Trans-Hudson Orogen of North America and the Himalaya-Karakoram-Tibetan Orogen of Asia: Structural and thermal evolution of the collisional lower and upper plates

Marc St-Onge^{1*}, Michael Searle², Natasha Wodicka¹, Jeroen van Gool³, Adam Garde³ and David Scott¹

¹ Geological Survey of Canada, Natural Resources Canada, Ottawa K1A 0E8, CANADA

² Department of Earth Sciences, University of Oxford, Oxford OX1 3PR, UK

³ Geological Survey of Denmark and Greenland, Copenhagen-K 1350, DK

* For correspondence, email: mstonge@nrcan.gc.ca

The Trans-Hudson Orogen (THO) of North America and the Himalaya-Karakoram-Tibetan Orogen (HKTO) of Asia preserve a Paleoproterozoic and Cenozoic record, respectively, of continent-continent collision that is notably similar in scale, duration, and character (St-Onge et al. 2006). In THO, the tectonothermal evolution of the lower-plate involves (1) early thin-skinned thrusting and Barrovian metamorphism, (2) out-of-sequence thrusting and high-T metamorphism, and (3) fluid-localized re-equilibration, anatexis and leucogranite formation. The crustal evolution of the Indian lower-plate in HKTO involves (1) early subduction of continental crust to UHP (ultra-high pressure) eclogite depths, (2) regional Barrovian metamorphism, and (3) widespread high-T metamorphism, anatexis and leucogranite formation. The shallow depths of the high-T metamorphism in HKTO are consistent with early to mid-Miocene ductile flow of an Indian lower-plate mid-crustal channel, from beneath the southern Tibetan plateau to the Greater Himalaya. Melt weakening (Jamieson et al. 2004) of the lower-plate in THO is not observed at a similar scale probably due to the paucity of pelitic lithologies, and consequently formation of a mid-crustal channel is not required to account for the documented tectonothermal evolution of THO's lower plate.

Tectonothermal events in the upper-plate of both orogens include pre-collisional accretion of crustal blocks, with for example the North Atlantic craton of Greenland and Canada being in a similar tectonic position to the South China block in Asia (St-Onge et al., 2008), emplacement of cumulative Andean-type plutonic suites, and consequent, multiple phases of high-T metamorphism (St-Onge

et al. 2007). Syn- to post-collisional events include emplacement of garnet-biotite-muscovite leucogranites, anatectic granites, and sporadic metamorphism (up to 90 Ma following the onset of collision in THO). Comparing the type and duration of tectonothermal events for THO and HKTO supports the notion of tectonic uniformitarianism for at least the later half of dated Earth history (from the early to middle Paleoproterozoic onward), and highlights the complementary nature of the rock record in an older "exhumed" orogen compared to one undergoing present day orogenesis.

References

- Jamieson RA, C Beaumont, S Medvedev and MH Nguyen. 2004. Crustal channel flows: 2. Numerical models with implications for metamorphism in the Himalayan-Tibetan orogen. *Journal of Geophysical Research* 109: B06406, doi:10.1029/2003JB002811
- St-Onge MR, MP Searle and N Wodicka. 2006. Trans-Hudson Orogen of North America and Himalaya-Karakoram-Tibetan Orogen of Asia: Structural and thermal characteristics of the lower and upper plates. *Tectonics* 25: doi:10.1029/2005TC001907, 22 p
- St-Onge MR, N Wodicka and O Ijewliw. 2007. Polymetamorphic evolution of Trans-Hudson Orogen on Baffin Island, Canada: constraints from petrology, structure and geochronology. *Journal of Petrology* 48: doi:1093/petrology/eg1060, 32p
- St-Onge, MR, JAM van Gool, AA Garde and DJ Scott. 2008. Correlation of Archaean and Palaeoproterozoic units between northeastern Canada and western Greenland: constraining the pre-collisional upper plate accretionary history of the Trans-Hudson orogen. *Geological Society of London Special Publication*, (in press).

Melting and Exhumation of the upper structural levels of the Greater Himalaya Sequence and Makalu granite: constraints from thermobarometry, metamorphic modeling and U-Pb geochronology

Michael J Streule^{1*}, Michael P Searle¹, Matthew SA Horstwood² and David Waters²

¹ Department of Earth Sciences, University of Oxford, Oxford OX1 3PR, UK

² NERC Isotope Geoscience Laboratory, Keyworth, Nottingham, NG12 5GG, UK

* For correspondence, email: michaels@earth.ox.ac.uk

The Makalu massif of Eastern Nepal displays a complex suite of Leucogranites and host sillimanite grade gneisses. These leucogranites are linked to the intrusions at the base of the Everest-Lhotse-Nuptse massif immediately to the west (Searle et al 2003) The Makalu intrusion is multiphase and forms the structurally highest foliation-parallel sheets of leucogranite along the top of the Greater Himalayan Sequence on the Nepal-Tibet border. It is comprised of massive Grt + Tur + Ms ± Bt leucogranites that also occasionally contain large cordierite crystals. The abundance of cordierite in the upper granite sheet is unlike other granites in the Nepalese Himalaya. The cordierite bearing leucogranite overlies lower sheets of 'normal' Himalayan granites intruded into black sillimanite gneisses and is thought to be the most recent phase of magmatism. A few cross-cutting feeder dykes mapped adjacent to the upper Barun glacier have channeled magma to the upper sheet. Petrology shows evidence for muscovite dehydration melting (~<700°C) in the upper part of the Barun gneiss which is a likely mechanism by which to produce the Makalu granite melts. Host gneisses retain biotite and so melting temperatures did not exceed 800°C (White et al. 2001). Secondary cordierite rims around garnets in these gneisses and the presence of cordierite in leucogranites record the last low pressure phase of melting. We use these field and petrographic observations for the basis of detailed metamorphic modeling of decompression and geochronology work for the upper parts of the GHS.

P-T determinations (THERMOCALCv.3.30) detail peak sillimanite grade metamorphism at 713°C, 5.9 kbar, with a secondary cordierite overprint, only partially equilibrated in some samples, at 618°C, 2.1 kbar (Figure 1). Thus rapid decompression of the GHS was associated with little temperature reduction. Monazite, zircon and xenotime geochronology directly links the timing of the low pressure cordierite event in the host rocks to those of the cordierite leucogranites; the main phase of leucogranite production and sillimanite grade metamorphism occurred from 25 to 18 Ma, whilst the most recent melt signature can be seen in the cordierite leucogranite and cordierite overprinted gneiss at 15.56±0.10 Ma (Figure 1). Y mapping of monazites in cordierite overprinted rocks implies that the breakdown of garnet released Y into the metamorphic system to trigger monazite growth during this event.

This initial phase of high temperature induced melt production, followed by decompression induced melt production was modeled theoretically using THERMOCALC. Pseudosections, drawn with melt production accurately model the change in assemblage of the host metamorphic rocks, and the composition of the extracted melt. We therefore use this detailed study of geochronology and metamorphism to relate to current Channel Flow models of Himalayan orogenesis (e.g. Beaumont et al 2001, Law et al. 2006, Grujic 2006); In Nepal our data shows that melt weakening facilitated channel flow in the middle

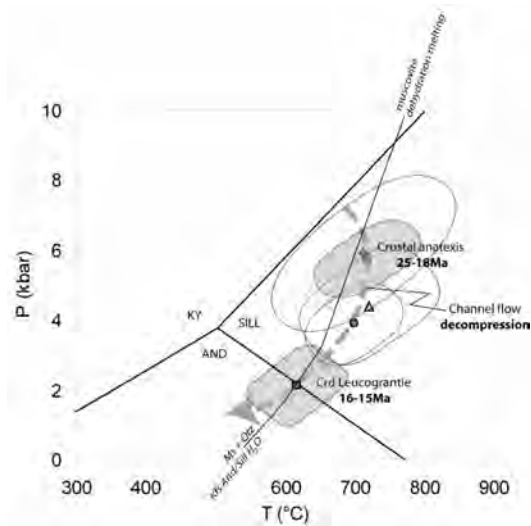


FIGURE 1. P-T-t data from Makalu: Crustal anatexis at 25-18Ma is correlated to peak Sillimanite grade metamorphism (♦, ◻, ◻). Two samples are partially re-equilibrated to lower pressure (Δ, ○) whilst one sample details complete metamorphic overprinting (◻) which is correlated to Cordierite granites at 16-15Ma. The muscovite dehydration melting curve from White et al 2001.

crust. Timing of extrusion of the GHS corresponds with timing of melt production so we propose that channel flow occurred from 25-15 Ma.

References

- White R, R Powell and T Holland. 2001. Calculation of partial melting equilibria in the system $\text{Na}_2\text{O}-\text{CaO}-\text{K}_2\text{O}-\text{FeO}-\text{MgO}-\text{Al}_2\text{O}_3-\text{SiO}_2-\text{H}_2\text{O}$ (NCKFMASH). *Journal of Metamorphic Geology* 19(2), 139–153
- Searle, MP, RL Simpson, RD Law, RR Parrish and DJ Waters. 2003. The structural geometry, metamorphic and magmatic evolution of the Everest massif, High Himalaya of Nepal-South Tibet. *Journal of the Geological Society*, 160(3), 345–366
- Beaumont C, RA Jamieson, MH Nguyen and B Lec. 2001. Himalayan tectonics explained by extrusion of a low- viscosity crustal channel coupled to focused surface denudation. *Nature* 414, 739–742
- Law RD, MP Searle and L Godin (eds). Channel Flow, Ductile Extrusion and Exhumation in Continental Collision Zones. *Geological Society London, Special Publications* 268
- Grujic D. 2006. Channel flow and continental collision tectonics: an overview. In: Law RD, Searle MP and Godin L (eds). Channel Flow, Ductile Extrusion and Exhumation in Continental Collision Zones. *Geological Society London, Special Publications* 268: 25–37

Strong ground motion observation and estimation: From predictive relationships and modelling to real-time shakemaps

Suhadolc Peter*, Costa Giovanni and Moratto Luca

Department of Earth Sciences, University of Trieste, Via Weiss 1, 34127 Trieste, ITALY

** For correspondence, email: suhadolc@units.it*

After a brief review on strong ground motion observation and estimation in continental convergence areas, predictive relationships are discussed with a special emphasis on the near-source areas of large earthquakes. A comparison with relationships derived for low-magnitude events is made and it is demonstrated that the latter cannot be used to extrapolate the ground motion level for large-magnitude events.

The acceleration at low frequencies can be successfully estimated through a deterministic modeling, given an appropriate knowledge about the velocity structure and earthquake source parameters. In particular, the question of the appropriateness of the velocity model is addressed. A series of tests to evaluate how well different 1D approximations of a 2D structural model reproduce the ground motion, in particular its peak amplitude,

is discussed. The deterministic modeling can produce ground-shaking synthetic maps, or scenarios. Examples for some important past seismic events in the Southern Alps area are discussed.

Finally, the strong ground motion level can nowadays be addressed with ShakeMaps, that are generated within few minutes from the earthquake occurrence. They are based on the TriNet "ShakeMap" software of Wald et al. (1999) and interfaced with a real-time acquisition system, that retrieves the real-time waveforms and posts results automatically on the web page. For the calibration of the Shake Maps regional model in the Southern Alps area a simple geological classification scheme and two ground-motion relations for different magnitude ranges are used. The system has been successfully tested for medium to moderate events ($ML < 4.5$).

Degree of Magnetic anisotropy as a strain intensity gauge: An example from the Footwall of MCT Zone along Bhagirathi valley, Garhwal Himalaya, India

Nihar R Tripathy* and Tejpal Singh

Department of Earth Sciences, Indian Institute of Technology, Roorkee-247667, INDIA

* For correspondence, email: tripathynr@gmail.com

In the Garhwal Himalaya, the footwall of the Main Central Thrust (MCT) Zone bears a wide zone (4 to 5 km) of mylonitic quartzite (Figure 1). These mylonites are inferred to have developed due to intense non-coaxial deformation followed by grain refinement through dynamic recrystallisation (Singh and Thakur 2001) and represent deep-level tectonites. These tectonites are devoid of strain markers (in the present case quartz clasts no longer preserved their outer boundaries). As a consequence, estimating finite strain in them is a challenge. Therefore, strain in such rocks needs to be estimated using some alternative techniques. The measurement of anisotropy of magnetic susceptibility (AMS) is one such technique that has been recently used to gauge strain in rocks that are devoid of strain markers (e.g. Hrouda 1993, Tarling and Hrouda 1993, Archanjo et al. 1995, Borradaile and Henry 1997, Mukherji et al. 2004, Sen et al. 2005, Sen and Mamtani 2006).

In the Garhwal Himalaya, MCT Zone is characterized by a 10-12 km thick NNE-dipping shear zone (Figure 1b). The lower boundary of MCT Zone corresponds to MCT (Heim

and Gansser 1939) or Munsiri Thrust (MT: Valdiya 1980). The northerly dipping MCT or MT separates the crystalline rocks of the Munsiri Group (Metcalf 1993) from the quartzites and metavolcanics of the Garhwal Group (Jain 1971). Further north, rocks of Munsiri Group are separated by the rocks of Vaikrita Group, of Higher Himalaya, along the Vaikrita Thrust (VT: Valdiya 1980). The area under investigation comprises of quartzites (referred as the Berinag quartzites; Valdiya 1980) and epidiorites of the Garhwal Group (Jain 1971) and form a part of the footwall of MCT Zone, along the Bhagirathi valley (Figure 1c). Further, these quartzites and epidiorites of the Garhwal Group are separated from the granitic gneiss and amphibolites of the Munsiri Group by the MCT.

Three phases (D1- D3) of deformation have been deciphered from the analysis of structural elements from the footwall of MCT Zone (Tripathy 2006). The earliest deformation (D1) is represented by co-axial strain. The D2 deformation is non-coaxial, characterized by ductile shearing but the degree of shearing varies considerably and has produced mylonites on either side of the MCT. Due to intense shearing, the early formed structures have reoriented and a strong mylonitic foliation (S2) and stretching lineation (L2) has developed on the pre-existing foliation plane (S1). D3 deformation, followed D2, has led to the development of non-penetrative structures mainly faults and joints.

Two-dimensional finite strain was determined using quartz clasts, for each of two mutually perpendicular thin sections (i.e. along XY, parallel to S2 and YZ is perpendicular to S2 and L2) prepared from 20 oriented hand specimens of mylonitic quartzite collected from different locations (shown in Figure 1c) from the area under study. The enlarged photomicrographs taken from thin sections and two-dimensional data were obtained by Center-

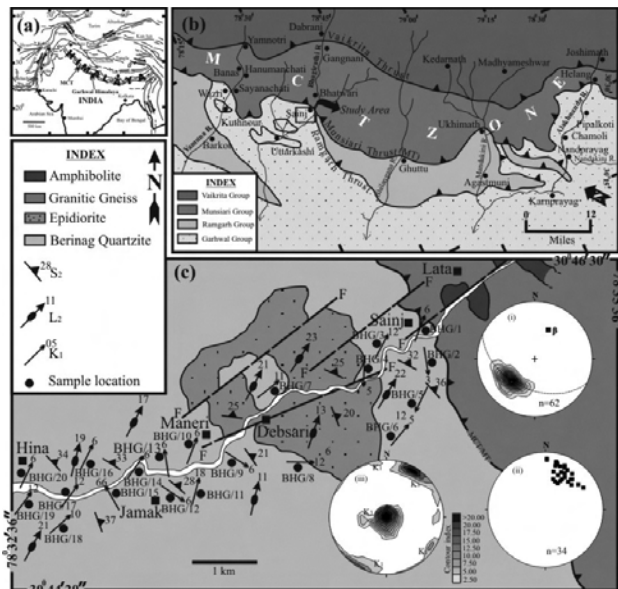


FIGURE 1. (a) Simplified tectonic map of the Himalaya (b) Simplified tectonic map of Garhwal Himalaya (modified after Valdiya 1980) (c) Geological map of the area, along Bhagirathi valley. Inset (i) and (ii) are lower hemisphere equal area projections of mylonitic foliation (S₂) and stretching lineation (L₂) and inset (iii) is the orientation of K₁ and K₃ axis in the footwall of MCT Zone of Bhagirathi valley.

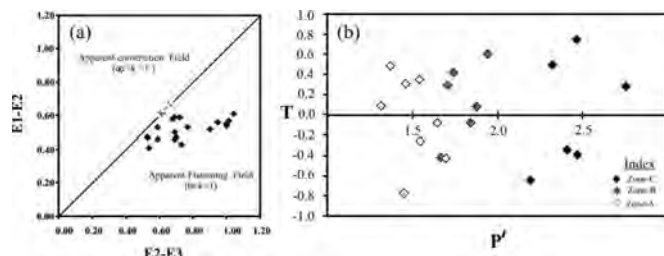


FIGURE 2. (a) Data from R_{xy} vs. R_{yz} of mylonitic quartzites from 20 samples plotted on a Flinn graph and (b) Jelinek plot (P' vs. T) representing the shape of magnetic susceptibility ellipsoids in the investigated mylonitic quartzite

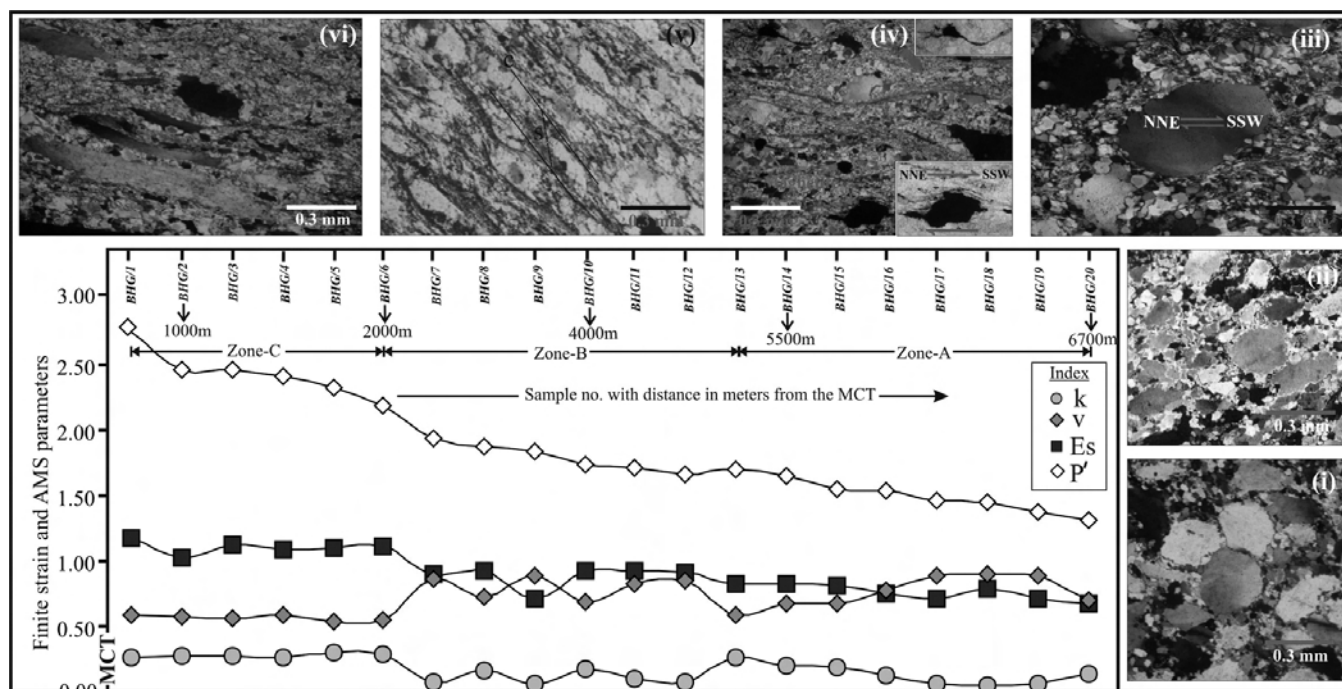


FIGURE 3. Plot showing the spatial variation of petrofabric strain parameters (E_s , k and v) and AMS parameter (P') of the respective samples to the relative position from the Main Central Thrust (MCT). Inset-i to vi shows the progressive development of mylonitic structures with respect to increasing in strain (E_s).

to Center method as suggested by Fry (1979). Three dimensional strain ellipsoids were calculated using two-dimensional strain data from the three mutually perpendicular planes and estimated different finite strain parameters i.e. E_s , k and v (Ramsay and Huber 1983). The deduced shape of the strain ellipsoids falls in the apparent flattening field ($0 < k < 1$, $+1 > v > 0$) of Flinn plot (Figure 2a) (Flinn 1956) and exhibits a high strain intensity. Figure 3 is a plot of strain parameters (E_s , k and v) with respect to the location of collected samples. In the present case the samples (BHG/1 to BHG/20) were collected up to 6700 m (perpendicular distance) from the MCT plane at regular intervals of distance. It has been observed that in between 6700 to 2000 m distance there is a gradual increase in strain towards the MCT. Further from 2000 m to close to the MCT (BHG/6 to BHG/1) there is no significant variation in strain values. In such a strain gradient the microstructural variation (inset-i to vi in Figure 3) was observed in accordance with the increase in strain intensity (E_s).

For the purpose of present magnetic fabric analysis, multiple cylindrical cores were drilled from each oriented quartzite sample (previously used for finite strain analysis) and a total of 63 cores were obtained. AMS analyses of cylindrical specimens of quartz mylonites were carried out with a KLY-3S Kappabridge (AGICO, Czech Republic) at the Wadia Institute of Himalayan Geology (Dehradun, India). The analysis yields orientations and magnitudes of the three principal axes of the magnetic susceptibility ellipsoid viz. K_1 , K_2 and K_3 ($K_1 \geq K_2 \geq K_3$). From these data, the mean susceptibility (K_m), degree of magnetic anisotropy ($P \geq$) and shape parameter (T) are computed using the formulae given by Tarling and Hrouda (1993) and Hrouda et al. (2002). In order to know the source of anisotropy carrier for the development of AMS fabric, the cylindrical core samples were again selected for petrographical

and rock magnetic studies: Isothermal Remanent Magnetization (IRM) and Saturation Isothermal Remanent Magnetization (SIRM).

Figure 2b is the Jelinek plot ($P' \text{ vs. } T$). It graphically represents the shape of magnetic susceptibility ellipsoids in the aforesaid samples. The well scattered T values with respect to P' within the study area document L-S tectonites. The orientation of K_1 (magnetic lineation) and K (pole to magnetic foliation plane i.e., K_1 - K_2 plane) in lower hemisphere equal area projection (inset-iii in Figure 1c), reveal that the magnetic fabrics are well in correspondence to the structural elements of the area under study (Figure 1c, inset-I and ii). It has been noticed that the P' value consistently increases in a finite strain gradient. Whilst the highest P' value is noted in sample no. BHG/1 located 500 m from the MCT, the lowest P' value is noted in the sample no. BHG/20 that lies farthest (6700 m) from the MCT (Figure 3). However, a significant variation in P' values (2.19 to 2.75) can be observed even if the finite strain values are saturated at a distance of 2000m from the MCT and the ductile zone acted as a strain observer (Figure 3).

The studied rock magnetic and chemical parameters; $B0Cr$ (remanence coercivity), $HIRM/\mu_{fr}$ and IRM_{soft} , indicate a good proportion of ferrimagnetic and antiferromagnetic minerals (Figure 4A-C). Whereas, the low K_m (Figure 4D) values ($2.52 \mu SI$ to $29.90 \mu SI$) allow to guess that the total anisotropy is due to presence of magnetite as elongated porphyroclast and lattices inclusion in quartz and mica grains. Since the objective of the present study is to demonstrate weather P' can be used as a strain intensity gauge in a saturated finite strain zone, the study area was divided in to three zones i.e. Zone-A to C for better comparison and discussion of the results obtained from finite strain, rock magnetism and AMS fabrics studies.

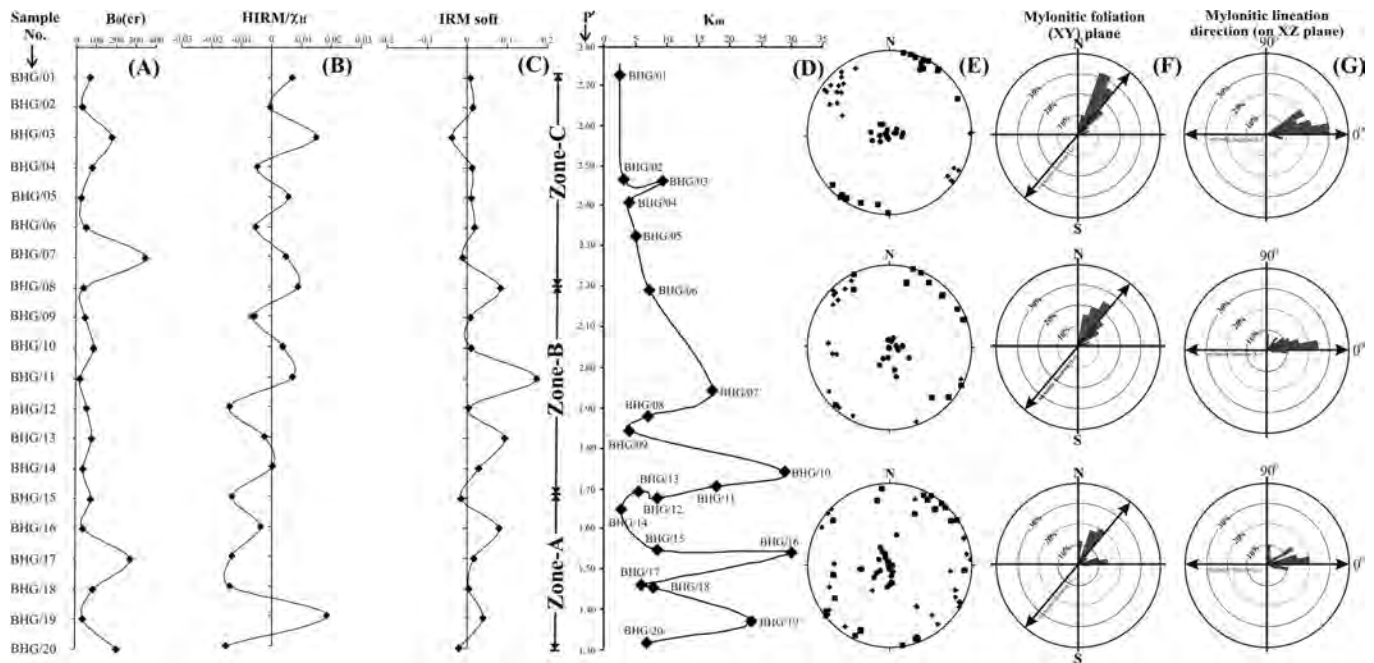


FIGURE 4. Plot of the rock magnetic and chemical parameters (A) B0Cr (remnance coercivity), (B) HIRM/ μ_r , (C) IRMsoft, (D) plot of Km vs. P^{\wedge} , (E) the distribution of susceptibility axes (K_1 , K_2 and K_3) from multiple core samples within the site were plotted on equal area projection for all the three Zones and (F and G) Ross diagram of orientation of long axes of magnetite grains with respect to the mylonitic foliation plane (XY plane) and with respect to the mylonitic lineation (L_2) direction.

Correlation between P^{\wedge} and strain in quartz mylonites has been a matter of debate. To apply P^{\wedge} as a strain-intensity gauge, it is most important to demonstrate that P^{\wedge} is independent to Km. Moreover, it is essential to examine a consistent relationship between P^{\wedge} and shape ratio of magnetite grains which may lead to magnetic interaction in AMS fabric (Ruff et al. 1988, Archanjo et al. 1995). A comparison of P^{\wedge} values with Km reflects a considerable higher P^{\wedge} with low Km values in Zone-C than in Zone-A and B (Figure 4D). Again in Zone-A and B, Km values show much variation from one to another with low P^{\wedge} . This indicates the role of strain being responsible for high P^{\wedge} values rather than rock magnetic interaction. In consequence, the development of AMS fabric (directional data) due to the preferred orientation of the magnetite grains was examined by measuring the orientation of long axes of magnetite grains with respect to the mylonitic foliation plane (XY plane) and with respect to the mylonitic lineation (L_2) direction (on XZ plane). The distribution of susceptibility axes (K_1 , K_2 and K_3) from multiple core samples within the site were plotted on equal area projection for all the three zones (Figure 4E). In Zone-A, a prolate magnetic fabric has developed, resulting in well defined K_1 axis directions whereas the K_2 and K_3 directions lie in the plane perpendicular to the K_1 direction, but are not isolated from each other. However, in an increasing strain gradient from Zone-A to Zone-C, the susceptibility axes have become increasingly isolated from each other. This suggests that with increasing finite strain and P^{\wedge} values from Zone-A ($E_s=0.67-0.83$, $P^{\wedge}=1.32-1.65$) to Zone-C ($E_s=0.90-1.18$, $P^{\wedge}=1.94-2.75$), elongate magnetite grains are rotated into the mylonitic foliation (Figure 4F) and towards the mylonitic lineation direction (Figure 4G). Thus, the development of preferred alignment is predominantly accomplished by rotation

of mica cleavage planes into mylonitic foliation. Since much of the elongate magnetite is incorporated within the mica cleavage planes, rotation of the mica will also rotate the included magnetite into the mylonitic fabric. These observations suggest that the AMS fabric was controlled by the reorientation of originally randomly oriented elongate magnetite grains into the mylonitic foliation and lineation directions with increasing strain. Thus, the above observations suggest that the development of AMS fabric is influenced by the passive rotation of magnetite grains as a function of strain. Hence P^{\wedge} can be used as a strain-intensity gauge at least on the outcrop scale, where a systematic variation in P^{\wedge} values can be noticed.

References

Archanjo CJ, P Launeau and JL Bouchez. 1995. Magnetic fabric vs. magnetite and biotite shape fabrics of the magnetite-bearing granite pluton of Gamelerias (Northeast Brazil). *Physics of the Earth and Planetary Interiors* 89: 63-75

Borradaile GJ and B Henry. 1997. Tectonic applications of magnetic susceptibility and its anisotropy. *Earth Science Reviews* 42: 49-93

Fry N. 1979. Random point distribution and strain measurements. *Tectonophysics* 60: 89-105

Hrouda F. 1993. Theoretical model of magnetic anisotropy to strain relationship revisited. *Physics of the Earth and Planetary Interiors* 77: 237-249

Ruff AS, SJ Naruk, RF Butler and GJ Calderone. 1988. Strain and magnetic fabric in the Santa Cataline and Pinaleno mountains metamorphic core complex mylonite zones, Arizona. *Tectonics* 72: 235-248

Singh K and VC Thakur. 2001. Microstructure and strain variation across the footwall of the Main Central Thrust Zone, Garhwal Himalaya, India. *Journal of Asian Earth Science* 19: 17-29

Petrology and geochronology of eclogitic and retrograde micas from Tso Morari UHP Complex, Ladakh Himalaya

Igor M Villa^{1,2*}, Julia de Sigoyer³ and Stéphane Guillot⁴

¹ *Universität Bern, 3012 Bern, SWITZERLAND*

² *Università di Milano Bicocca, 20126 Milano, ITALY*

³ *ENS-CNRS, Labo. Géologie, 75005 Paris, FRANCE*

⁴ *CNRS-Université Grenoble 1, 38031 Grenoble, FRANCE*

* *For correspondence, email: igor@geo.unibe.ch*

The Tso Morari UHP Complex in Ladakh (NW Himalaya) recorded the very early evolution of the Himalayan range. Based on sedimentological and geochemical arguments the Tso Morari Complex can be related to the polymetamorphic Indian continental margin. Dating its UHP metamorphic peak and its retrogression allow to discuss the geometry of the subduction zone, the geometry of the Indian margin before the collision, and the exhumation processes of UHP complex.

The Tso Morari UHP complex consists of coesite-bearing meta-crustal rocks (mostly metagranites and a thin metasedimentary cover). The eclogitic paragenesis proper is coesite-garnet-omphacite-quartz-phengite-rutile, in metabasic rocks, and garnet-jadeite-chloritoid-phengite in metapelitic rocks.

The age of peak metamorphism was established to be near 55 Ma by multichronometry (de Sigoyer et al. *Geology* 28 2000). Successive zircon SHRIMP dating refine the age of peak metamorphism close to 53 Ma (Leech et al. *EPSL* 234: 2005) or close to 49 Ma (O'Brien, *EPSL* 245: 2006).

Among the findings by de Sigoyer et al. (2000) were the observation of an amphibolitic paragenesis on the exhumation path, and of a subsequent greenschist facies retrogression, which both constrained a P-T-t path.

The ³⁹Ar-⁴⁰Ar analysis of the micas in the different rock types of the Tso Morari Complex can give decisive understanding on the processes that affected the UHP rocks. Here we focus on the amphibolite/greenschist parageneses.

The greenschist facies retrogression reactions are dated at 30-31 Ma in the southern part of the Tso Morari massif. Greenschist facies rocks are pervasively recrystallized, and biotite (not an eclogitic mineral in the metapelitic rocks) can be used as an index mineral for the chemically open-system recrystallization. Biotite-bearing metapelites have low-Si muscovites (Si < 3.1 apfu), again showing that the high-Si HP phengites were recrystallized. One such sample, LK93-42, gave a "plateau" at 30.6 ± 0.4 Ma, with a noticeable age increase in the high-temperature steps. This age increase correlates with the Ca/K and Cl/K ratios and therefore, following Villa (Lithos, 55: 2001), we presumed that it consisted of a heterochemical mixture of more than one white mica generation. Electron microprobe analyses confirmed that high-Si and low-Si mica grains were present. The separate was therefore subjected to

density separation, and a light (L) and a heavy (H) fraction were analyzed both by ³⁹Ar-⁴⁰Ar and by electron microprobe. The two age spectra were found to be remarkably different. LK93-42H was almost flat, with an age of 30.6 Ma. LK93-42L on the other hand had a much more pronounced high-temperature age discordance, with high-temperature steps up to ca. 40 Ma. The Cl/K and Ca/K indicators of heterochemical contaminants were much higher for -L than for -H. The straightforward explanation is that the different white mica generations were physically separated. Indeed, the BSE images show that the L fraction contains about 10% pure low-Si muscovite and 90% grains containing Si-rich phengite inclusions. The H fraction consists of about 66% pure muscovite grains and only 34% inclusion-bearing grains. We are forced to identify the eclogite and/or amphibolite facies (older) HP phengite relics as the carriers of inherited ⁴⁰Ar.

The amphibolite facies event is well constrained by multichronometry to have occurred at 47 ± 3 Ma (De Sigoyer et al. 2000). The amphibolite-facies, intermediate pressure (ca. 10 kbar) phengite samples (Si > 3.3 apfu) mostly give discordant age spectra ranging from Eocene to Early Cretaceous; ages never cluster towards what could be viewed as a well-defined age estimate. Moreover, the Cretaceous ages conflict with the other Eocene ages for the amphibolite facies retrogression. It is a very common observation (Di Vincenzo et al. *J Petrol* 145: 2004) that eclogitic white micas can preserve inherited ⁴⁰Ar contained in pre-eclogitic relics. In our case, minor inheritance of a very much older mica population can easily bias young phengites to a significant extent. It can be easily detected, fortunately, by the same Ca/Cl/K-age diagrams that successfully unravelled the greenschist-facies mixture. Most samples show Cl/K and/or Ca/K clusters, but never simple binary mixing, indicating that the pre-eclogitic mica relics were themselves heterogeneous. BSE mapping will examine this possibility.

In conclusion, the Tso Morari Complex consists of rocks that record different peak and retrograde reactions. The combination of petrology and geochronology allows the self-consistent reconstruction of its tectonic history. Its exhumation from > 27 to ca. 10 kbar occurred "quickly" before ca. 47 Ma, at a minimum average rate of (17 ± 2 kbar)/(4 ± 4 Ma). Subsequent exhumation to greenschist facies (ca. 4 kbar) was almost one order of magnitude slower, at a rate of 6 kbar/16Ma.

Examining the Tectonic Wedging Hypothesis in the NW India Himalaya

A Alexander G Webb* and An Yin

Department of Earth and Space Sciences and Institute of Geophysics and Planetary Physics, University of California–Los Angeles, Los Angeles, California 90095-1567, USA

* For correspondence, email: awebb@ess.ucla.edu

A specific structural correlation of the Main Central thrust and the South Tibet detachment is observed in the central Himalaya, where the two faults stack three units. The high grade Greater Himalayan Crystalline complex (GHC) overlies the low grade Lesser Himalayan Sequence (LHS) along the Main Central thrust and underlies the low grade Tethyan Himalayan Sequence (THS) along the South Tibet detachment. Current tectonic models of the Himalaya (i.e., wedge extrusion, channel flow) envision the high grade middle unit (GHC) as a “pipe to the surface” of middle crustal rocks, with the two bounding faults active at the surface and without cut-off relationships. However, some regional syntheses of the western Himalayan geology suggest that the GHC is discontinuous there, in conflict with the “pipe to the surface” geometry. A new “tectonic wedging” hypothesis (à la Price 1986) may explain this structural geometry and have wide-reaching implications for the evolution of the Himalayan orogen (Yin 2006, Webb et al. 2007). In the tectonic wedging kinematic model, the GHC is emplaced at depth as a thrust horse bound below by the Main Central thrust, above by the South Tibet detachment, and up-dip (to the south) by the merging of these two faults.

Field observations and analytical data from the NW India Himalaya support a tectonic wedging kinematic model for the evolution of the Himalayan orogen. In NW India, the GHC pinches out laterally from east to west where the Main Central thrust places the THS directly on top of the LHS. Field mapping shows that this relationship results from up-dip merging of the top-south Main Central thrust below and the South Tibet detachment, with alternating top-south and top-north shear, above. Analytical data suggest stratigraphic correlations exist across the Main Central thrust and South Tibet detachment. U-Pb zircon geochronology shows that ~1.85 Ga granite and granitic gneiss occur above and below the Main Central thrust. U-Pb geochronology of detrital zircons suggests that correlative Late Proterozoic strata occur above the STD, below the MCT, and between these two faults. Consistent detrital zircon age populations suggest that the metasedimentary rocks of the MCT hanging wall southwest of the MCT-STD merger may belong to

a single lithologic unit, supporting field evidence that includes these rocks in the basal THS. Thermobarometry of these same rocks yields temperatures of 450 to 560 °C with pressures of 7 to 9 kbar, and Th-Pb monazite geochronology shows that this metamorphism occurred in two similar phases, one in the Paleozoic and the other in the early/middle Cenozoic. These P-T-t results are consistent with similar work on THS rocks to the north, i.e., from the STD hanging wall. The metamorphic evolution of basal THS rocks is broadly correlative to that of the GHC prior to the Late Oligocene / Early Miocene, providing another link between these sequences.

These results are synthesized into a new model of the pre-India-Asia collision stratigraphic framework of this region and a tectonic wedging kinematic model for the evolution of the Himalayan orogen. The tectonic wedging model has broad implications for exhumation and foreland sedimentation history across the entire Himalayan orogen. Since basal THS rocks and GHC rocks represent correlative strata which have experienced similar metamorphism, detritus from these units may only be distinguished by the few high grade minerals that occur exclusively in the GHC. Also, because the proposed kinematic evolution matches that of thrust systems developed in the upper 5-10 km of the crust (Price 1986), a large strength contrast between the middle crust (GHC) and upper crust (LHS, THS) is not required.

References

- Price RA. 1986. The southeastern Canadian Cordillera: thrust faulting, tectonic wedging, and delamination of the lithosphere. *Journal of Structural Geology* 8: 239–254
- Webb AAG, A Yin, TM Harrison, J Célérier and WP Burgess. 2007. The leading edge of the Greater Himalayan Crystallines revealed in the NW Indian Himalaya: Implications for the evolution of the Himalayan Orogen. *Geology* 35 (10):955-958
- Yin A. 2006. Cenozoic tectonic evolution of the Himalayan orogen as constrained by along-strike variation of structural geometry, exhumation history, and foreland sedimentation: *Earth Science Reviews* 76: 1-131

Tectonic sequence diagrams and the constraints they offer for the structural and metamorphic history of the Kullu Valley, NW India

L White^{1*}, G Lister¹, M Forster¹ and T Ahmad²

¹ *Research School of Earth Sciences, The Australian National University, Canberra, AUSTRALIA*

² *Department of Geology, University of Delhi, Delhi, INDIA*

* *For correspondence, email: lloyd.white@anu.edu.au*

Recent fieldwork between the Rohtang Pass and the town of Kullu in Himachal Pradesh, India was conducted to gain an understanding of the tectonic and metamorphic history of the region. Particular attention was paid to structural cross-cutting relationships, mineral growth and evidence of metamorphic overprinting to produce tectonic sequence diagrams (Forster and Lister 2008). The aim was to evaluate three competing hypotheses as to the tectonic evolution of this part of the Himalaya: a) the undeformed ramp and flat thrust sheet model advocated by Webb et al. (2007), b) the Alpine nappe model advocated by Epard et al. (1995) and c) the imbricated thrust stack hypothesis, as suggested by Ahmad et al. (2000). These models differ widely in their consideration of factors as fundamental as the location of the actual MCT (with up to 200 km difference in location) or as to the nature and significance of the deformation associated with Himalayan orogenesis.

Our data suggest that the model advocated by Webb et al. (2007) does not apply. Their fold of the South Tibetan Detachment amounts to a forced correlation, and thus an imposed geometry based on the following assumptions: (1) that the rock units of the Kullu Valley are part of the Tethyan Himalaya and not the Jutogh Group (Lesser Himalayan Sequence) (e.g. Valdiya 1980); (2) the Vaikrita or Jutogh thrust is the MCT; and (3) shear zones reactivate with the different senses of movement during different tectonic events or periods of time, based on locally determined sense-of-shear criteria.

In contrast, the model advocated by Epard et al. (1995) more faithfully reflects observations that can be made in the field. The Phoal recumbent antiform is not a late stage incidental structure as proposed by Webb et al. (2007) but in fact formed subsequent to the first major foliation, and folded Barrovian isograds. This is a nappe-like structure, especially if we include a basal thrust, in the position as inferred by Thakur (1992)

The major difference in the Webb et al. (2007) and Epard et al. (1995) interpretations lies in the location of the MCT. This is located on the basis of Barrovian assemblages and the definition of lithotectonic units (i.e. Lesser Himalayan Sequence *vs.* Tethyan Himalayan Sequence). We follow the interpretation of Thakur (1992) and place the MCT equivalent at the foot of the Rohtang Pass, coincident with the Vaikrita Thrust.

The tectonic sequence diagrams suggest that early Barrovian facies metamorphism led to mineral growth that overprinted an intense fabric that was subsequently at least twice recumbently folded. These folds were themselves overprinted by intense shear zone related fabrics during Himalayan orogenesis.

References

- Ahmad T, N Harris, M Bickle, H Chapman, J Bunbury and C Prince. 2000. Isotopic constraints on the structural relationships between the Lesser Himalayan Series and the High Himalayan Crystalline Series, Garhwal Himalaya. *Geological Society of America Bulletin* 112: 467-477
- Epard JL, A Steck, JC Vannay and J Hunziker. 1995. Tertiary Himalayan structures and metamorphism in the Kulu Valley (Mandi-Khoksar transect of the Western Himalaya) – Shikar Beh Nappe and Crystalline Nappe. *Schweizerische Mineralogische und Petrographische Mitteilungen* 75: 59-84
- Forster MA and GS Lister. 2008. Tectonic sequence diagrams and the structural evolution of schists and gneisses in multiply deformed terranes. *Journal of the Geological Society, London* 165: 1-17
- Thakur VC. 1992. *Geology of the Western Himalaya*. Pergamon Press, Oxford, 366p.
- Valdiya KS. 1980. The two intracrustal boundary thrusts of the Himalaya. *Tectonophysics* 66: 323-348
- Webb AAG, A Yin, TM Harrison, J C el erier and W P Burgess. 2007. The leading edge of the Greater Himalayan Crystalline complex revealed in the NW Indian Himalaya: Implications for the evolution of the Himalayan orogen. *Geology* 35: 955-958

Different eclogite types from the Pakistan Himalaya and implications for exhumation processes

Franziska DH Wilke^{1*}, Patrick J O'Brien¹ and M Ahmed Khan²

¹ Institut für Geowissenschaften, Universität Potsdam, D-14476 Potsdam, GERMANY

² University of Sargodha, Sargodha, PAKISTAN

* For correspondence, email: fwilke@geo.uni-potsdam.de

Metabasites were sampled from the Higher Himalayan Crystalline, south of the Main Mantle Thrust, from the Upper Kaghan Valley, Pakistan. These vary from corona dolerites outcropping around Saif ul Muluk in the south to coesite-eclogite close to the suture zone in the north. Peak pressures around 27 kbar, for a temperature of 690–750°C, were obtained by O'Brien et al. (2001) for coesite-bearing (in omphacite) eclogites. The study of newly collected samples reveals coesite in both garnet and omphacite, which was confirmed by in situ raman spectroscopy. Both coesite-bearing and coesite-free eclogites show growth of amphiboles during exhumation. Within newly investigated coesite-bearing eclogites the presence of glaucophane cores within barroisite amphibole is noted. In addition, some eclogite bodies show leucocratic segregations containing phengite, albite, kyanite and/or zoisite consistent with decompression melting as described by Franz et al. (1995) for the Münchberg Massif, Germany: further examples are known from the Eastern Alps and Norwegian Western Gneiss Region. The important implications are not only that the continental crust of the Indian plate was subducted to depths of ~100 km but that the exhumation path is complex and shows stages of cooling (glaucophane) followed by reheating (melting).

The glaucophane- and coesite-bearing eclogite was sampled in Saleh Gali, northwest of Gittidas, only a few hundred metres from the Indus Suture Zone. The very fresh eclogites exhibit a massive, fine grained (<1 mm) matrix with red garnet and dark green omphacite. Overgrowing this early fabric are larger (>1

mm) dark amphiboles. Microscopically anhedral, optical zoned garnets up to 0.8 mm sit within a weakly defined foliation formed by elongate omphacite, phengite and chains of rutile. Omphacite is up to 1 mm in length and mostly inclusion poor, whereas phengite is only 0.5 mm and rimmed by a thin biotite-bearing breakdown rim. Amphiboles with a conspicuous violet core and a dark green rim form small poikiloblasts enclosing the earlier phases. Coesite occurs as inclusions in omphacite and garnet, showing in both cases the typical radiating network of fractures. Coesite inclusions are best preserved in omphacite but only one example has been found in garnet so far. This might be due to a lack of garnet growth in the coesite field.

Optical zoning in garnet is only weakly reflected in mineral chemistry. Ca-poor cores $\text{Alm}_{56}\text{Prp}_{15}\text{Sp}_{15}\text{Grs}+\text{Adr}_{27}$ are surrounded by $\text{Alm}_{31}\text{Prp}_{16}\text{Sp}_{16}\text{Grs}+\text{Adr}_{31}$ rims. The jadeite content of omphacite is in the range $X_{\text{Jd}} 0.36\text{--}0.39$ with $X_{\text{Acg}} 0.08\text{--}0.14$. Violet amphibole cores are glaucophane (see also Lombardo et al. 2000) with a representative composition of $\text{Na}_{0.27}(\text{Na}_{1.59}\text{Ca}_{0.35}\text{Fe}^{2+}0.06)(\text{Mg}_{2.07}\text{Fe}^{2+}_{1.33}\text{Fe}^{3+}_{0.22}\text{Al}_{1.38})(\text{Al}_{0.3}\text{Si}_{7.7})\text{O}_{22}$ zoned to barroisite with $\text{Na}_{0.37}\text{K}_{0.03}(\text{Na}_{1.17}\text{Ca}_{0.76}\text{Fe}^{2+}_{0.07})(\text{Mg}_{2.29}\text{Fe}^{2+}_{1.35}\text{Fe}^{3+}_{0.32}\text{Al}_{1.03})(\text{Al}_{0.59}\text{Si}_{7.41})\text{O}_{22}$.

Leucocratic segregations containing phengite, albite, kyanite and/or zoisite are found in eclogites exposed Gittidas Nala. These generally strongly deformed and retrogressed rocks exhibit a very fine-grained, dark green to gray matrix with up to 2 mm black amphiboles overgrowing this fabric. Conspicuous are several

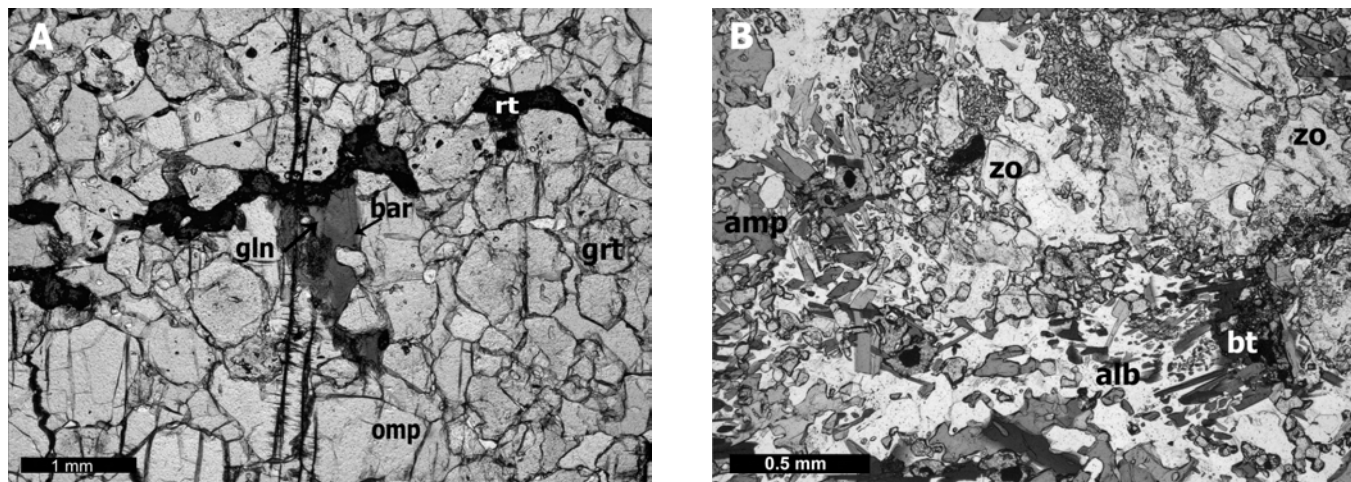


FIGURE 1. (A) Photomicrograph of a fresh eclogite containing glaucophane, rimmed by barroisite, omphacite and optically-zoned garnet disrupted by a chain of rutile. Scattering vertical cracks showing the last retrogression under greenschist facies conditions. (B) Leucocratic segregations containing zoisite, albite and biotite (after phengite).

mm-sized clinozoisite crystals wrapped by the strongly developed foliation. In addition, the rock is cut by light-coloured veinlets containing phengite, albite, kyanite and locally also cm-sized rutile grains. In the microscope, anhedral, un-zoned garnets are mostly smaller than 0.25 mm. There is no preferred orientation but garnet often forms bands especially around the margins of the large clinozoisites. Relicts of omphacite occur mainly as tiny inclusions in clinozoisite although locally primary coarse omphacite-bearing bands are still preserved. Amphibole exists in several generations: as inclusions in clinozoisite; as large, pale green porphyroblastic grains with partly irregular, retrograded outer rims; in symplectites after matrix omphacite and as euhedral nematoblastic amphibole of up to 0.1 mm in the melt zones. Phengite is rare and partially transformed to lepidoblastic biotite and albite symplectites. Zoisite is abundant, often up to 2.5 mm in longest dimension and mostly rich in inclusions, showing the complete range of an eclogite mineral assemblage. Kyanite is rare, mostly under 0.75 mm and only occurs in the leucocratic melt lenses.

Interestingly, eclogites containing coesite and/or glaucophane are also described from the Tso Morari area of Ladakh (de Sigoyer et al. 1997, Sachan et al. 2004). Their published P-T evolution is two-step with an isothermal decompression at $580 \pm 60^\circ\text{C}$ from 20 ± 3 to 11 ± 2 kbar followed by an increase in temperature of $\sim 30^\circ\text{C}$ which is reflected by the transformation of glaucophane to calcic amphibole. Based on our new observations we favour an S-shaped P-T path that starts from the coesite field, cools and decompresses into the glaucophane field (15–20 kbar/ $\sim 550^\circ\text{C}$) and

later is reheated to 8–10 kbar/ 700°C within the amphibolite field, to cause melting. These conditions cover the finding of coesite, later grown glaucophane that gives way to a barroisite amphibole and the newly discovered melt segregations. Tectonically, this could reflect stacking of the crustal units at depth (i.e., cooling) followed by partial relaxation (heating) before final exhumation.

References

- de Sigoyer J, S Guillot, J-M Lardeaux and G Mascle. 1997. Glaucophane bearing eclogites in the Tso Morari dome (eastern Ladakh, NW Himalaya). *European Journal of Mineralogy* 9: 1073-1083
- Franz G and EA Smelik. 1995. Zoisite-clinozoisite bearing pegmatites and their importance for decompressional melting in eclogites. *European Journal of Mineralogy* 7: 1421-1436
- Lombardo B, F Rolfo and R Compagnoni. 2000. Glaucophane and barroisite eclogites from the Upper Kaghan nappe: implications for the metamorphic history of the NW Himalaya. In: Khan MA, PJ Treloar, MP Searle, MQ Jan (eds), Tectonics of the Nanga Parbat Syntaxis and the Western Himalaya. *Geological Society, London, Special Publications* 170: 411-430.
- O'Brien PJ, N Zotov, R Law, Khan M Ahmed and Jan M Qasim. 2001. Coesite in Himalayan eclogite and implications for models of India-Asia collision. *Geology* 29: 435-438
- Sachan HK, BK Mukherjee, Y Ogasawara, S Maruyama, H Ishida, A Muko and N Yoshioka. 2004. Discovery of coesite from Indus Suture Zone (ISZ), Ladakh, India: Evidence for deep subduction. *European Journal of Mineralogy* 16: 235-240

River discharge and erosion rates in the Sutlej basin, NW Himalaya

Hendrik Wulf^{1*} and Dirk Scherler²

¹ Department of Geoecology, University of Potsdam, GERMANY

² Department of Geosciences, University of Potsdam, GERMANY

* For correspondence, email: Hendrik.Wulf@uni-potsdam.de

Several studies have suggested couplings between climate and tectonics in the Himalayas, where high amounts of rainfall often coincide with high exhumation rates (Wobus et al 2003 Thiede et al 2004). In central Nepal, for example, fluvial erosion has been proposed to localize tectonic strain near the Main Central Thrust (Wobus et al., 2003, Hodges et al 2004). However, Burbank et al (2003) found uniform mineral cooling ages across a pronounced precipitation gradient and suggested to decouple rainfall and erosion.

The aim of this study is to explore and quantify the relationship between precipitation, discharge, topography and erosion within the Sutlej basin in the western Himalaya. The Sutlej River originates on the Tibetan Plateau and transects the Great Himalaya in a deep and steep valley before reaching the mountain front. Its catchment spans 52,798 km² and is therefore, after the Brahmaputra-Tsangpo and the Indus, the third largest catchment in the Himalayas (Bookhagen and Burbank, in review).

Climate in the Sutlej region is characterized by two main precipitational regimes. The Indian summer monsoon delivers large amounts of moisture from the Bay of Bengal, from mid June to mid September (Bookhagen and Burbank 2006). The rainfall amounts gradually decrease across the Himalayas from 3 m/yr at the front to 0.3 m/yr behind the orographic barrier (Bookhagen et al. 2005). Winter precipitation mainly derives from Western Disturbances, which are upper-tropospheric synoptic-scale waves that can undergo orographic capture as they pass over south central Asia (Lang and Barros 2004). Above 2000 m, Western Disturbances mostly provide snowfall with snow water equivalents (SWE) of up to ~1 m measured at valley weather stations in the Greater Himalaya (Singh and Kumar 1997). These SWE values are likely to increase at mountain peaks and ridges and may be regarded as a lower estimate of the principal moisture source for the high elevations in the Greater Himalayas of the Sutlej region.

To quantify the interactions between precipitation, discharge and erosion on a large spatial scale we used the following approach. We model discharge along the transition of fluvial to nivo-glacial dominated tributary catchments. To capture the different sources of river discharge over a large region we utilized remote sensing data in combination with ground-based measurements. TRMM (Tropical Rainfall Measuring Mission) data provide mean rainfall amounts over the period 1998 to 2006 (Bookhagen and Burbank in review). Interannual variability was derived on the basis of daily precipitation measurements from 15 weather stations within the Sutlej catchment. To take evapotranspiration into account, we used MODIS (Moderate-resolution Imaging Spectroradiometer) derived estimates (Mu et al. 2007). Furthermore, the MODIS snow cover product serves as a proxy for snowfall from which we

infer differences in annual snow melt. We plan to model glacier melt based on MODIS-derived daytime temperature, the snow cover products and glacial cover that we mapped using Landsat satellite imagery. Based on discharge measurements from several tributaries along the Sutlej we aim to calibrate our model to estimate discharge on other large (> 100 km²) tributary catchments along the Sutlej River.

Eventually, we gain insights into discharge formation along the Sutlej and across different climatic sectors of the orogen. Additionally, we discuss potential sediment sources based on geological maps, digital terrain analysis and spectral classification, taking into account surface and exposure characteristics, such as soil cover, lithology, vegetation and morphometric characteristics. This approach allows us to subdivide and categorize the tributary catchments into morphological units, which characterizes the catchments susceptibility to erosion (Märker 2001). Finally, we combine the river discharge and suspended sediment concentration (SSC) data, acquired from HPSEB (Himachal Pradesh State Electricity Board) to derive erosion rates for the investigated tributaries and time periods

Our results show that there exists a transitional zone in the Sutlej transect, which receives considerable amounts of monsoonal rainfall (~1 m/yr), and which concurrently benefits from large amounts of snow and glacier melt. This results in increased erosion rates in a high, heavily glacierized tributary catchment (Wanger) in the transitional zone compared to a rather low lying, fluvially shaped tributary catchment (Ganvi) in the rainfall dominated zone. Although the lower basin transports more suspended sediment and receives higher amounts of rainfall, the higher basin gains additional snow- and glacier melt, which sustain high discharge for a longer period than in the lower catchment.

References

- Bookhagen B, RC Thiede and MR Strecker. 2005. Abnormal monsoon years and their control on erosion and sediment flux in the high, arid northwest Himalaya. *Earth and Planetary Science Letters* 231: 131-146
- Bookhagen B and DW Burbank. 2006. Topography, relief, and TRMM-derived rainfall variations along the Himalaya. *Geophysical Research Letters* 33: L08405
- Bookhagen B and DW Burbank. (in review). Controlling factors for monsoonal rainfall distribution and its implication for specific stream power amounts in the Himalaya. *Journal of Geophysical Research - Earth Surface*
- Burbank DW, AE Blythe, JL Putkonen, BA Pratt-Situala, EJ Gabet, ME Oskin, AP Barros and TP Ohja. 2003. Decoupling of erosion and climate in the Himalaya. *Nature* 426: 652-655
- Hodges KV, C Wobus, K Ruhl, T Schildgen and K Whipple. 2004.

- Quaternary deformation, river steepening, and heavy precipitation at the front of the Higher Himalayan ranges. *Earth and Planetary Science Letters* 220: 379–389
- Lang TJ and AP Barros. 2004. Winter Storms in the Central Himalayas. *Journal of the Meteorological Society of Japan* 82(3): 829
- Märker M. 2001. *Regionale Erosionsmodellierung unter Verwendung des Konzepts der Erosion Response Units (ERU) am Beispiel zweier Flusseinzugsgebiete im südlichen Afrika*. Ph.D. Dissertation, Friedrich-Schiller-University of Jena, Chemistry and Geoscience Faculty
- Mu Q, FA Heinsch, M Zhao and SW Running. 2007. Development of a global evapotranspiration algorithm based on MODIS and global meteorology data. *Remote Sensing of the Environment* 111(4): 519-536
- Singh P and N Kumar. 1997. Effect of orography on precipitation in the western Himalayan region. *Journal of Hydrology* 199: 183-206
- Thiede, R.C., Bookhagen, B., Arrowsmith, J.R., Sobel, E.R., Strecker, M.R., 2004. Climatic control on rapid exhumation along the Southern Himalayan Front. *Earth Planet. Sci. Lett.* 222: 791–806
- Wobus, C. W., K. V. Hodges, and K. X. Whipple, 2003. Has focused denudation sustained active thrusting at the Himalayan topographic front. *Geology* 31(10): 861–864.

The Central Crystallines Around Hapoli, Subansiri, Eastern Himalayas

An Yin¹, C S Dubey², A A G Webba¹, P K Verma², T K Kelty³ and T M Harrison¹

¹ Department of Earth and Space Sciences and Institute of Geophysics and Planetary Physics, University of California, Los Angeles, 90095-1567, CA

² Department of Geology, University of Delhi, Delhi-110007, INDIA

³ Department of Geological Sciences, California State University, Long Beach, 90840-3902, CA

Despite a long research history, our understanding of the Himalayan tectonic evolution remain incomplete that can be attributed largely to the lack of geologic constraints on the structural style and timing of deformation in the eastern Himalaya. To overcome this problem, we conducted geologic investigation along traverse from Kimin to Geevan in the District of Upper Subansiri. Prior to our study, researchers had debated on the location of the Main Central Thrust (MCT) across the traverse, with the fault either being placed near the crest line of the Himalayan Range north of latitude 28°N or a broadly folded thrust with its frontal trace exposed south of latitude of 27°N. The above confusion may be attributed to the fact that orthogneiss units, widely exposed in the area, exhibit similar lithology and structural fabrics and are difficult to be determined if they lie in the hanging wall or footwall of the MCT. We address this problem by conducting detailed structural observations and systematic U-Pb zircon dating of the orthogneiss units and leucogranites that intrude them. Our mapping reveals that the MCT hanging wall is composed of schist, garnet-biotite gneiss, quartzo-feldspathic gneiss, mylonitic augen gneiss and foliated biotite granitoid. All of the above units are closely associated with Tertiary leucogranites. The MCT is a folded structure expressed as a large half window opening to the west and a small klippe that lies within the half window. The north-south width of the MCT half window requires >60-km southward slip on the MCT. The MCT hanging wall consists of a prominent ductile thrust shear zone with a thickness >200 m at the northern end of our traverse near Geevan. It correlates along strike with the Zimithang shear zone in Tawang and the Kakhtang thrust zone in northern Bhutan. This correlation requires a >300-km east-west length of the Zimithang-Kakhtang thrust zone in the eastern Himalaya and implies significant amount of crustal shortening within the MCT hanging wall.

We analyzed six orthogneiss samples from the Kimin-Geevan traverse using the ion microprobe mass spectrometer at UCLA. Sample 1 is from an orthogneiss unit in the MCT hanging wall near Hapoli. We obtained 17 spot analyses on 15 zircons, of which fifteen yield ²⁰⁷Pb/²⁰⁶Pb ages ranging from 460.5 Ma to 546.1 Ma with a weighted mean age of 504.9 ± 8.3 Ma. These fifteen analyses are concordant or reversely discordant on the U-Pb concordia plot; the increased reverse discordance is associated with higher U concentrations. The other two analyses yield ²⁰⁷Pb/²⁰⁶Pb ages of 836.9 ± 13.2 Ma and 730.2 ± 13.1 Ma and plot along the concordia. Th/U ratios of all of the above analyses are >0.01, with more than half of them over 0.1. The grain that yields 826-Ma age is subhedral and its cathodoluminescence image shows distinct domains without clear definition of the core

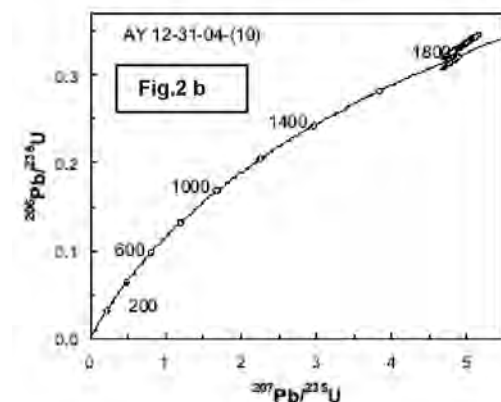
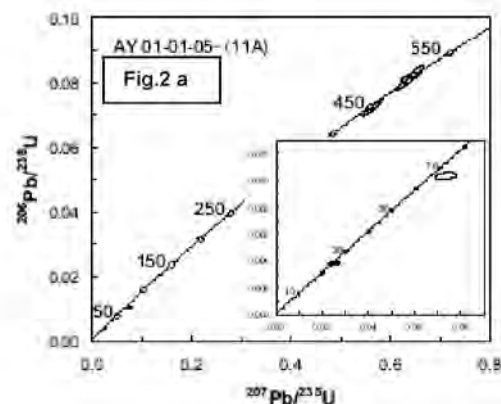
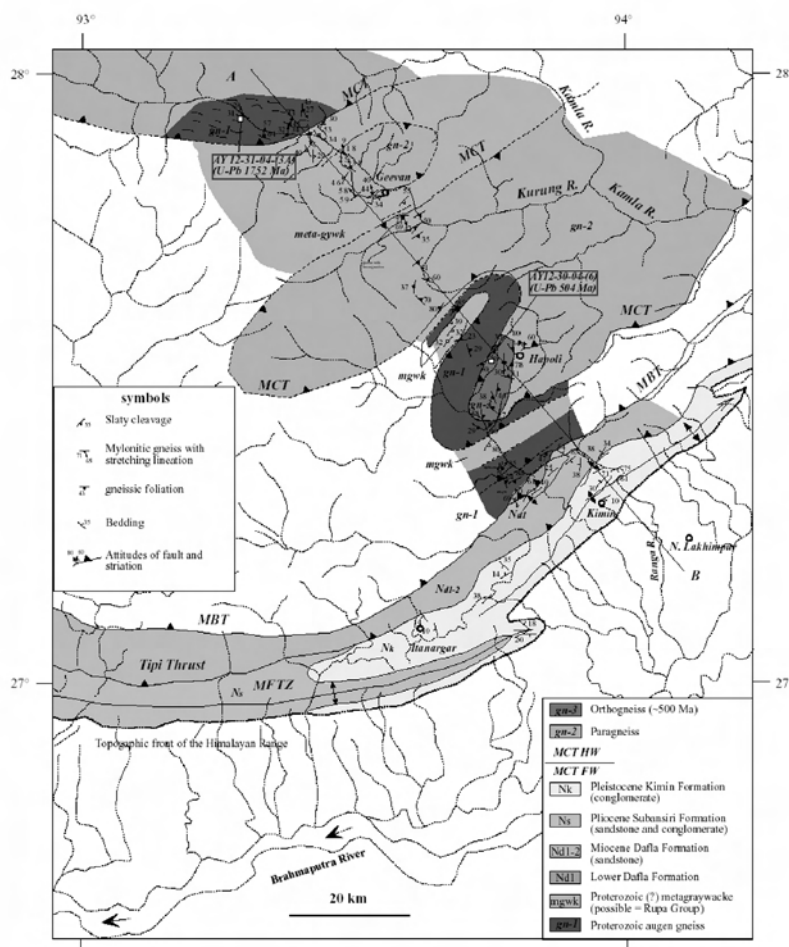
from the rim. A spot yielding the 836.9 ± 13.2 Ma ²⁰⁷Pb/²⁰⁶Pb age corresponds to a high Th/U ratio of 0.419 and is typical of igneous origin. Another spot analysis from the same grain yields a reversely discordant result with a 505.8 ± 8.3 Ma ²⁰⁷Pb/²⁰⁶Pb age; it corresponds to a low Th/U ratio of 0.034 and a UO/U ratio below the range of the calibration. The dominant age population of the fifteen out of seventeen analyses and moderate-to-high Th/U ratios all indicate the crystallization age of the augen gneiss at ~505 Ma with one inherited grain at 836 Ma. As a 825-Ma plutons exist in the Bhutan Himalaya and a 878-Ma augen gneiss is present in the Bhalukpong-Zimithang traverse, the 836-Ma zircon may have come from a pluton emplaced during the same igneous event. This interpretation implies that the eastern Himalayan region experienced a magmatic event during 825-878 Ma. Sample 2 was collected from a mylonitic augen gneiss unit in the MCT hanging wall. Of the 15 total analyses from 15 zircons, 13 yield ²⁰⁷Pb/²⁰⁶Pb ages ranging from 1703 Ma to 1780 Ma, with a weighted mean age of 1752 ± 12 Ma. Of these 13 analyses, the one with the lowest Th/U ratio (0.038) is strongly discordant, plotting along a discordia line with a projected intersection of a Phanerozoic age along the concordia curve. The remaining two analyses have ²⁰⁷Pb/²⁰⁶Pb ages of 1921 ± 13 Ma and 2515 ± 12 Ma; while the younger analysis is nearly concordant, the older one is strongly discordant. We consider these analyses to represent older, wall rock zircons assimilated during emplacement of the granitoid at ~1752 Ma. The discordant, low Th/U analysis hints a Phanerozoic metamorphic event. Sample 3 was collected from an augen gneiss unit directly above the MCT. We analyzed six spots of different zircons from sample that yield a discordia line with intercepts on the concordia at 28 ± 13 Ma and 512 ± 14 Ma (MSWD = 1.3). Four spot ages cluster near the upper intercept, one plot near the lower intercept with a low Th/U value, and one plot between the two age groups. We interpret these results to indicate crystallization of the augen gneiss at ~512 Ma succeeded by a thermal event at ~28 Ma. Sample 4 was from mylonitic augen gneiss in the MCT footwall. We acquired five spot analyses from different zircons. Three analyses cluster together along the concordia, yielding a weighted mean ²⁰⁷Pb/²⁰⁶Pb age of 1747 ± 7 Ma. The other two ages are discordant, potentially drawn down from ~1750 Ma towards the Phanerozoic portion of the concordia. We interpret these results to indicate crystallization of the granitic protolith at ~1747 Ma and a later Late Proterozoic or Phanerozoic Pb-loss event that may correlate with metamorphism. Sample 5 was collected from a biotite-quartz mylonitic granitoid that lies directly above the MCT Geevan klippe. We analyzed five spots of different zircons and four of them clustering on the concordia yield

a weighted mean $^{207}\text{Pb}/^{206}\text{Pb}$ age of 1743 ± 7 Ma. One spot age is slightly older with a $^{207}\text{Pb}/^{206}\text{Pb}$ age of 1939 ± 9 Ma. We interpret these results to indicate crystallization of the granitic protolith at ~ 1743 Ma, with the single older age representing an inherited component. Sample 6 was from an augen gneiss directly above the MCT and north of sample 5. We acquired four spot analyses from different zircons. Three analyses cluster on the concordia indicating a weighted mean $^{207}\text{Pb}/^{206}\text{Pb}$ age of 1772 ± 6 Ma (2σ) (Figure 1). We interpret these results to indicate crystallization of the granitic protolith at ~ 1772 Ma.

In addition to dating the orthogneiss, we also obtained U-Pb ages from leucogranites in our study area. The first sample was from a leucogranite that intrudes a 1752-Ma augen gneiss in the MCT hanging wall. Of the fourteen zircon analyses we obtained, six are discordant, four have UO/U values exceeding the range of calibration, and another four have Th/U values below 0.1. The data plot along a discordia line that intercepts the concordia curve at 373 ± 59 Ma below and 1759 ± 36 Ma above (MSWD = 1.4). The upper intercept age overlaps with the crystallization age of the host rock at 1752 ± 12 Ma and likely reflects inheritance of wall-rock zircons. The wall-rock zircons may have experienced Phanerozoic metamorphism during zircon growth as indicated by moderate to low Th/U values. Considering the large uncertainty for this age, it is likely that the metamorphic event was related to the widespread Cambro-Ordovician plutonism and metamorphism across the Himalaya. Thus, the above interpretation suggests that some Himalayan leucogranite may have emplaced in the early Paleozoic as well. Our second leucogranite sample was from

a vein that intrudes a 500-Ma granitoid in the MCT hanging wall. Five analyses plotted in two concordant clusters, three of which yield a $^{207}\text{Pb}/^{206}\text{Pb}$ weighted mean age of 491 ± 11 Ma (2σ) and the other two featuring very low Th/U ratios yielding $^{238}\text{U}/^{206}\text{Pb}$ weighted mean ages of 24.6 ± 0.5 Ma and 24.4 ± 0.3 Ma. Additional two spot analyses plotted along a discordia line between the two age clusters. The ~ 491 Ma age zircons may represent inherited zircons from the wall rocks and the younger zircons may result from crystallization of the leucogranite at ~ 24 Ma. Our last sample was from a leucogranite intruding high-grade gneiss in the MCT hanging wall. We analyzed nine spots on different zircons (Figure 2). One analysis with a high Th/U ratio yields a $^{207}\text{Pb}/^{206}\text{Pb}$ weighted mean age of 1746 ± 14 Ma (2σ); the rest yield moderate to low Th/U ratios and Cenozoic $^{238}\text{U}/^{206}\text{Pb}$ ages, with a dominant age cluster from ~ 23.5 Ma to ~ 20 Ma. We interpret the ~ 1746 Ma age as reflecting inheritance from the wall rocks and the younger ages indicate crystallization of the leucogranite at 23–20 Ma.

In order to understand the evolution of the Himalaya along the Kimin-Geevan traverse, we constructed a balanced cross section and performed a systematic restoration of the section. Our structural analysis leads to an estimate of 190-km shortening and a corresponding horizontal shortening strain of 76%. As the region may have experienced significant Cambro-Ordovician deformation as indicated by the wide occurrence of 480–500 Ma granitoids, the above shortening estimate should be regarded as a combined effect of early Paleozoic and Cenozoic deformation, thus only placing an upper bound for the actual shortening strain in the Cenozoic.



Surface-tectonic coupling at the Namche Barwa – Gyala Peri massif and geologic hazards associated with a proposed dam on the Yarlung-Tsangpo river in SE Tibet

Peter Zeitler^{1*}, Anne Meltzer¹, Brian Zurek¹, Lucy Brown¹, Noah Finnegan², Bernard Hallet³, Page Chamberlain⁴, William Kidd⁵ and Peter Koons⁶

¹ Dept. of Earth and Environmental Sciences, Lehigh University, Bethlehem, PA 18015, USA

² Dept. of Earth and Atmospheric Sciences, Cornell University, Ithaca, NY 14853, USA

³ Dept. of Earth and Space Sciences, University of Washington, Seattle, WA 98195, USA

⁴ Dept. of Geological and Environmental Sciences, Stanford University, Stanford, CA 94305, USA

⁵ Dept. of Earth and Atmospheric Sciences, University at Albany, Albany, NY 12222, USA

⁶ Dept. of Earth Sciences, University of Maine, Orono, ME 04669, USA

* For correspondence, email: peter.zeitler@lehigh.edu

The Yarlung-Tsangpo River leaves the SE Tibetan Plateau through a deep canyon that it slices across the Himalaya as it drops ~2000 m along an irregular hairpin reach ~100 km in length. We have been examining the geodynamic evolution of this region and have gathered considerable geophysical and geological data on this steep reach of the river and the surrounding Namche Barwa-Gyala Peri massif. In this region, petrological, geochronological, thermochronological, and cosmogenic-isotope data show that very rapid bedrock exhumation at rates of 7 mm/yr or more has exposed granites as young as 1 Ma, and this rapid exhumation has been underway for at least the past 3 m.y.

Detrital-dating evidence shows that these high rates continue at present and that erosion within the massif contributes fully 50% of the modern suspended-sediment load in the Yarlung-Tsangpo at the point where it enters the Assam floodplain (roughly 100 Mt/yr of sediment are derived from the massif). The steep slopes in the massif fail by pervasive landsliding and suggest a steady-state topography where the high erosion rates are balanced by equivalent rates of rock uplift accommodated by numerous active structures.

At a broader scale, GPS results show that steep three-dimensional velocity gradients exist across the region: in the easternmost Himalaya near Namche Barwa >50% of the Indian – Eurasian plate convergence is accommodated within a zone of high strain rates. The 1950 Assam earthquake (M8.6) was one expression of the high local strain rates, and caused considerable damage within the canyon area. Seismic results from our portable deployment show that the area beneath the massif and the Yarlung-Tsangpo canyon is exceptionally active, with over 1000 events ranging in magnitude from 1.0 to 5.6 (mb) taking place over a 15-month period. The events occur almost entirely in the mid to shallow crust and show a range of first motions.

Dynamical modeling and context provided by diverse regional data suggests that the metamorphic massif and steep reach of the Yarlung-Tsangpo at Namche Barwa have persisted for at least 3 m.y. Divergent low-temperature cooling histories within and upstream of the massif suggest that development of a coupled system and pinned knickpoint may have started at roughly 5 Ma.

For a decade anecdotes and media reports have been circulating about a proposed dam in SE Tibet, on the Yarlung-Tsangpo knickzone. The fundamental purpose of the dam is generation of ~40,000 MW of hydropower to be used in diverting a portion of the impounded river to water-starved regions of northern China. It has been argued that any benefits that would accrue from improving water supply in the north would be offset by water-flow and sediment-flux impacts that would be felt downstream in the Brahmaputra system in northeastern India and Bangladesh, as well as by the impacts that a dam and large lake would have on the pristine, ecologically and ethnographically diverse area around the Yarlung-Tsangpo canyon, an area of great significance to Tibetan Buddhists.

Our data show that the Yarlung-Tsangpo canyon is one of the most geologically active regions on Earth, and they suggest that any dam placed there would be at high risk, with the dam being prone to failure due to pronounced seismic hazards and focused deformation. As it fills, water pressure behind the dam could help trigger shallow earthquakes and landslides, and the dam would be difficult to maintain given the high frequency of landsliding and extreme local bedrock exhumation rates that would lead to rapid siltation at the dam site. Further, this impoundment of the Yarlung-Tsangpo would greatly starve the sediment flux downstream in the Brahmaputra, its densely populated flood plain, and ultimately the Bay of Bengal systems.

Paleomagnetic and Geochronologic Results From Late Paleozoic and Mesozoic Rocks of the Central Tibet: Implications for the Paleogeography of the Qiangtang Terrane

Xixi Zhao^{1*}, Pete Lippert¹, Rob Coe¹, Chengshan Wang², Zhifei Liu³, Haisheng Yi⁴, Yalin Li², Bin Deng⁴ and Igor Villa⁵

¹ Department of Earth Sciences, University of California, Santa Cruz, CA 5064, USA

² China University of Geosciences, Xueyuan Lu 29, Beijing 100083, CHINA

³ Laboratory of Marine Geology, Tongji University, CHINA

⁴ Chengdu University of Technology, Chengdu 610059, CHINA

⁵ Institute of Geological Sciences, University of Berne, Erlachstrasse 9a, 3012 Berne, SWITZERLAND

For correspondence, email: xzhao@pmc.ucsc.edu

The Qiangtang terrane of Tibet is a critical region for tectonic reconstruction of Asia. Here, we summarize our paleomagnetic, rock magnetic, and geochronologic data from our study of Late Permian to Late Jurassic rocks from the Qiangtang Terrane in Central Tibet. This study consists of paleomagnetic and geochronologic sampling at 7 localities of volcanic and sedimentary rocks from eastern and southern Qiangtang. All paleomagnetic samples were subjected to detailed progressive thermal and/or alternating field demagnetization to isolate various magnetization components. Rock magnetic measurements suggest that magnetite is the dominant magnetic mineral. Resistance to alternating field demagnetization in several volcanic samples, thermal demagnetization behavior, and magnetic hysteresis data, however, indicate the presence of

significant amounts of hematite as well. In nearly all cases where hematite exists, directions carried in hematite are indistinguishable from those carried in high-unblocking temperature magnetite, suggesting the hematite formed as a result of high-temperature oxy-exsolution at the time of initial cooling. Positive regional fold test and reversal test results all suggest that the stable magnetizations in these rocks are primary. Our paleomagnetic data clearly show that the Qiangtang terrane did not occupy its current position in terms of paleolatitude in both Permian and Jurassic times, and suggest significant separation between Qiangtang and surrounding Asian blocks during Late Permian through Late Jurassic. Our new data reinforce our previous interpretations on block rotations and paleogeography of the Eastern Qiangtang Terrane.

Whole-rock elemental and zircon Hf isotopic geochemistry of mafic and ultramafic rocks from the Early Cretaceous Comei large igneous province in SE Tibet: constraints on mantle source characteristics and petrogenesis

Di-Cheng Zhu^{1,*}, Xuan-Xue Mo¹, Zhi-Dan Zhao¹, Yaoling Niu² and Sun-Lin Chung³

¹ State Key Laboratory of Geological Processes and Mineral Resources, China University of Geosciences, Beijing 100083, CHINA

² Department of Earth Sciences, Durham University, Durham DH1 3LE, UK

³ Department of Geosciences, National Taiwan University, Taipei 106, TAIWAN

* For correspondence, email: dchengzhu@163.com

The Early Cretaceous Comei large igneous province (CLIP) aged from ca. 145 to 128 Ma with peak activity at ca. 132 Ma was recently identified in southeastern Tibet (Figure 1a, Zhu et al. 2008a). The CLIP is dominated by dismembered mafic lava flows, sills and dikes, with subordinate ultramafic and silicic rocks. Seventy mafic and ultramafic

intrusion samples collected via three N-S transects from 28° N to 29° N and 90°30' E to 92° E in the CLIP (Figure 1b) were subjected to detailed geochemical analyses involving whole-rock major and trace elements and Sr-Nd isotopes as well as zircon Lu-Hf isotopic measurements for constraint on mantle source characteristics and petrogenesis.

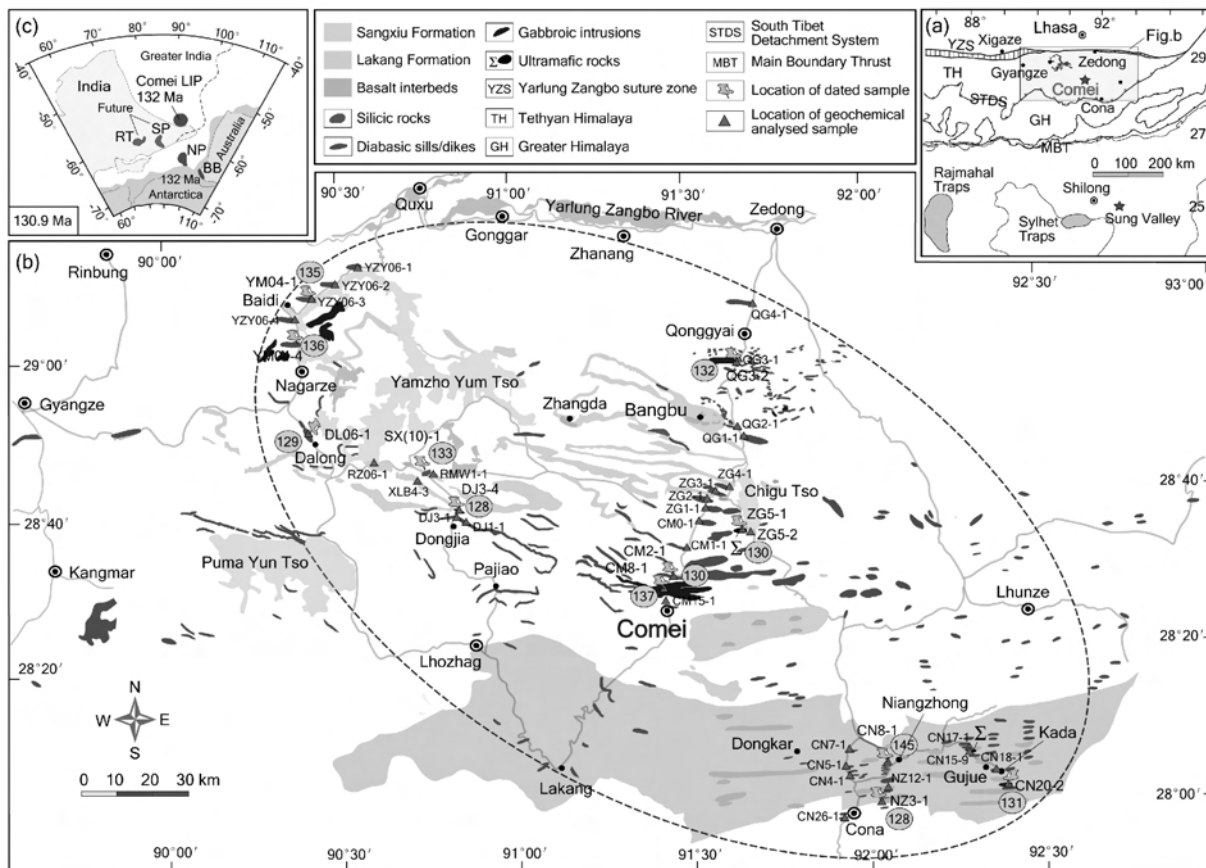


FIGURE 1. The spatial extent (dashed ellipse) of the Comei LIP in SE Tibet (Zhu et al. 2008a). (a). Sketch of the tectonic map in SE Tibet, showing the location of the Comei large igneous province (LIP) compared to the Rajmahal, the Sylhet Traps and the igneous complexes in Sung Valley of NE India (Coffin et al. 2002, Zhu et al. 2008b). (b). Simplified geology map showing the spatial extent (dashed ellipse) and distributions of ~ 132 Ma igneous rocks of the Comei LIP (Zhu et al. 2008a). (c). Plate reconstruction of the southern Indian Ocean region at ~ 130.9 Ma (Coffin et al. 2002). The major Proterozoic terranes for each continental block and the known locations of the Shillong Plateau (SP), Rajmahal Traps (RT), Naturaliste Plateau (NP), and Bunbury Basalt (BB) are labelled. The location of the Comei LIP is shown in view of present-day spatial extent and Cenozoic shortening relative to the Rajmahal Traps province.

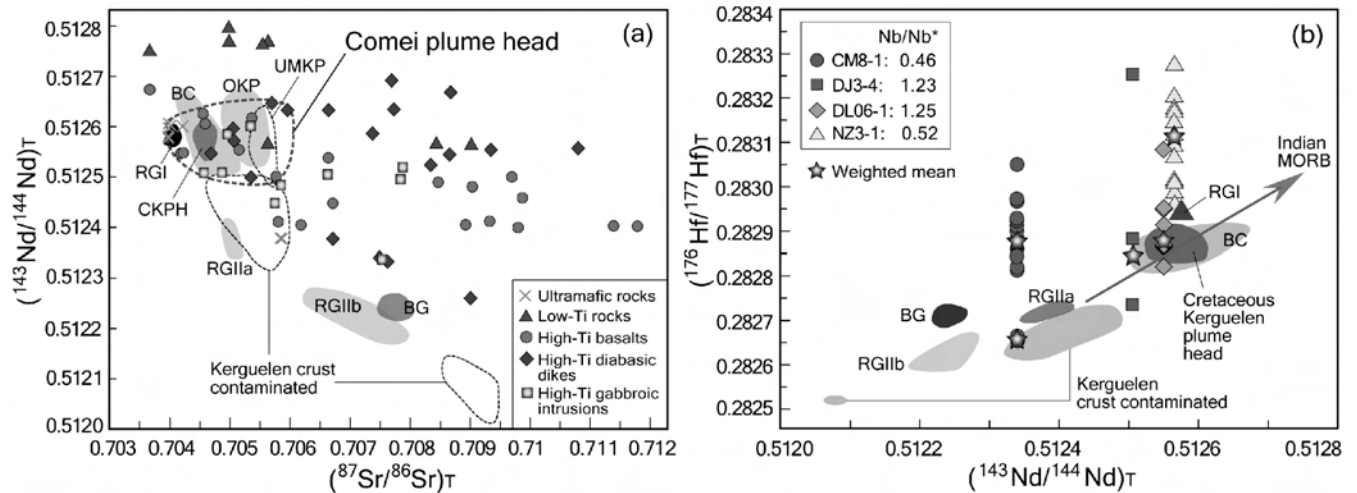


FIGURE 2. Whole-rock Sr-Nd and zircon Hf isotopic compositions of the Comei LIP in SE Tibet. Data sources: Bunbury Casuarina (BC) and Bunbury Gosselin (BG, Frey et al. 1996, Ingle et al. 2004); Rajmahal Group I (RGI) and Rajmahal Group II (RGII, Baksi 1995, Kent et al. 1997, Ingle et al. 2004); Oligocene Kerguelen Plume (OKP, Yang et al. 1998); Upper Miocene Kerguelen Plume (UMKP, Weis et al. 1993); Cretaceous Kerguelen Plume Head (CKPH, Ingle et al. 2004). $Nb/Nb^* = Nb_{PM} / (La_{PM} \times Th_{PM}) / 2$, PM is primitive mantle-normalized (Sun and McDonough 1989). The Sr-Nd isotopic compositions of the Comei plume head are designated by the 17 uncontaminated high-Ti group samples and 6 ultramafic samples (Figure 2a), which are filtered from 51 samples from different sites in the CLIP. The altered and contaminated samples have been excluded by geochemical diagnostic signatures (such as LOI content, and $(Th/Nb)_{PM}$ value) and petrographic observations.

The mafic rocks in the CLIP can be subdivided into two major groups in terms of TiO_2 and P_2O_5 contents, including the dominant high-Ti group ($TiO_2 > 2.4\%$, $P_2O_5 > 0.3\%$) that consists of basaltic lavas, diabasic sills/dikes, and gabbroic intrusions, and the low-Ti group ($TiO_2 < 2.2\%$, $P_2O_5 < 0.2\%$) that consists of basaltic lavas and gabbroic intrusions. Twelve SHRIMP zircon U-Pb age dates indicate that the high-Ti group is persisted from ca. 145 Ma to 128 Ma, and the tholeiitic magmatism is occurred at 132 Ma, and continued to 128 Ma (Zhu et al. 2008a).

Leaving out the altered and contaminated samples from 51 analyses by geochemical diagnostic signatures (e.g., LOI content, and $[Th/Nb]_{PM}$ value, PM is primitive mantle-normalized) and petrographic observations, the Sr and Nd isotopic compositions of $(87Sr/86Sr)_T = 0.70418 \sim 0.70596$, $(^{143}Nd/^{144}Nd)_T = 0.512502 \sim 0.512647$, $\epsilon Nd(T) = 0.67 \sim 3.81$ for seventeen high-Ti group samples with Nb/Y ratios ranging from 0.53-1.07 (majority > 0.68), and 0.70397 \sim 0.70421, 0.512578 \sim 0.512606, 2.13 \sim 2.69 for six layered picrite porphyrite samples with Nb/Y ratios from 0.5 to 0.7, were obtained. It has been recognized that a long period of alkalic magmatism followed by enormous tholeiitic volcanism is typical of many flood-basalt provinces of the world (Sheth and Chandrasekharam 1997). We therefore interpret the isotopic compositions of the uncontaminated high-Ti group with alkalic to transitional nature and ultramafic samples as reflecting the source characteristics of the Comei plume head, which is: $(87Sr/86Sr)_T = 0.70398 \sim 0.70596$, $(^{143}Nd/^{144}Nd)_T = 0.512502 \sim 0.512647$, $\epsilon Nd(T) = 0.67 \sim 3.81$ (Figure 2a). This isotopic composition overlaps those of basalts produced by the Kerguelen plume, e.g., the Cretaceous Rajmahal Group I basalts (Baksi 1995, Kent et al. 1997), the Bunbury Casuarina basalts (Frey et al. 1996), Oligocene (Yang et al. 1998) and upper Miocene Kerguelen plume materials (Weis et al. 1993), as well as the proposed Cretaceous Kerguelen "plume head" (Ingle et al. 2004) (Figure 2a). The geochemical similarity between the Comei plume head and the Kerguelen

plume materials is also supported by the in situ zircon Hf isotopic composition of the uncontaminated high-Ti group samples. Zircons from sample DL06-1 (129.1 ± 1.2 Ma) and DJ3-4 (128.3 ± 1.9 Ma) (Zhu et al. 2008a) have $\epsilon Hf(t)$ values from + 4.6 to + 13.9, and from + 1.5 \sim +19.9, respectively with weighted mean values close to those of the Bunbury Casuarina and the proposed Cretaceous Kerguelen "plume head" (Ingle et al. 2004) (Figure 2b). Although these similarities in elemental and isotopic characteristics could be fortuitous (Frey et al. 1996), they are permissive evidence that the CLIP magmas are derived from the same as, or similar to, mantle sources for lavas from the Kerguelen plume recorded in the eastern Indian Ocean and neighbouring continental margins (Figure 1c).

The prolonged alkaline magmatism of the CLIP favors plume head incubation beneath an originally thick lithosphere, as many flood-basalt provinces of the world would have (Sheth and Chandrasekharam 1997). We propose that the relative wide range of Sr and Nd isotopic compositions of the Comei plume head would ascribe to the relative long incubation of the Comei plume head beneath thick Eastern Gondwana lithosphere at the transition from the Late Jurassic to the Early Cretaceous time.

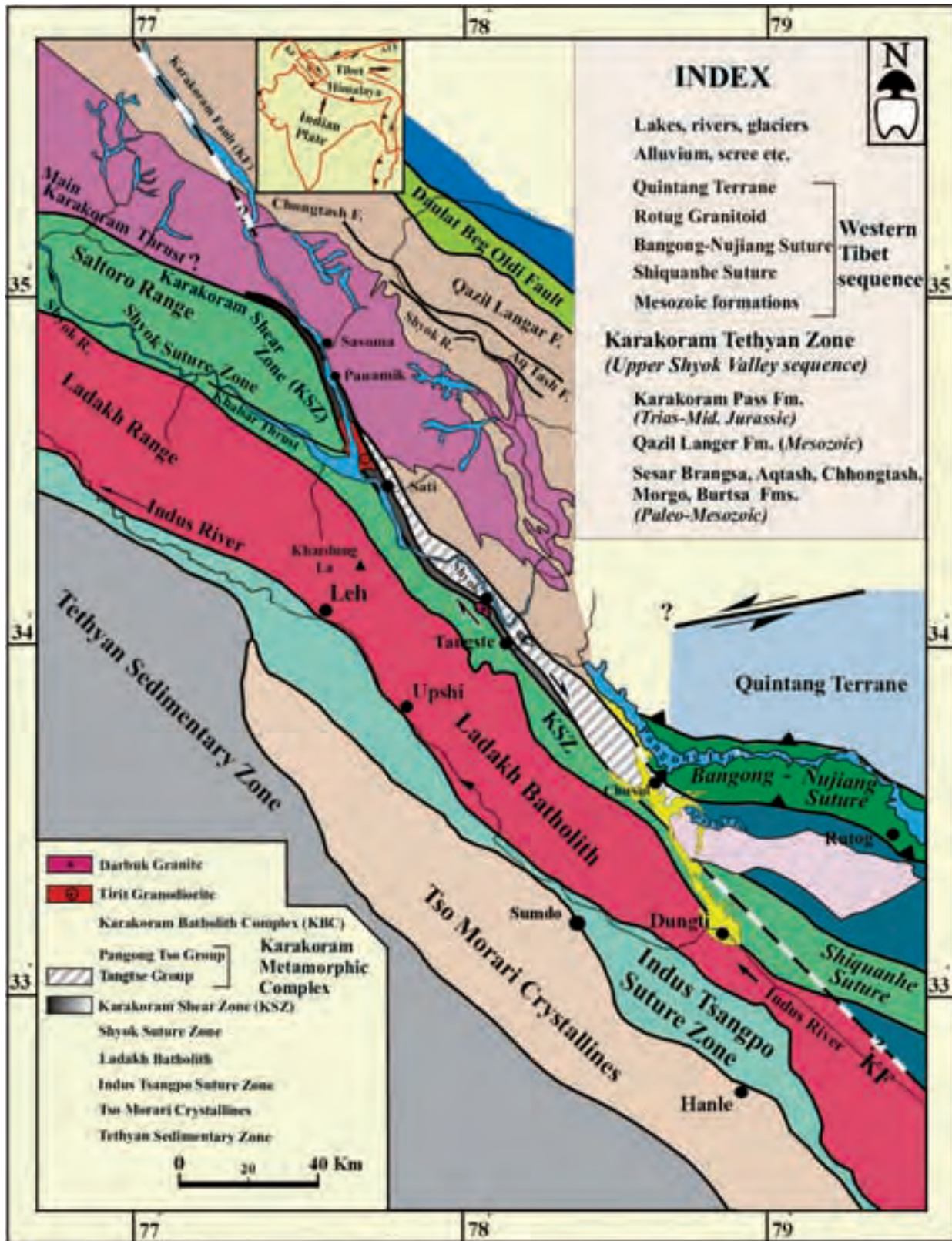
Acknowledgements

The NSFC projects (40503005 and 40473020), and the Programme of Excellent Young Scientists of the Ministry of Land and Resources supported this study.

References

- Baksi AK. 1995. Petrogenesis and timing of volcanism in the Rajmahal flood basalt province, northeastern India. *Chemical Geology* 21: 73-90
- Coffin MF, MS Pringle, RA Duncan, TP Gladchenko, M Storey, RD Müller and LA Gahagan. 2002. Kerguelen hotspot magma output since 130 Ma. *Journal of Petrology* 43: 1121-1139
- Frey FA, NJ McNaughton, DR Nelson, JR Delaeter and RA Duncan. 1996.

- Petrogenesis of the Bunbury Basalt, Western Australia: interaction between the Kerguelen plume and Gondwana lithosphere? *Earth and Planetary Science Letters* 144: 163-183
- Ingle S, JS Scoates, D Weis, G Brüggmann and RW Kent. 2004. Origin of Cretaceous continental tholeiites in southwestern Australia and eastern India: Insights from Hf and Os isotopes. *Chemical Geology* 209: 83-106
- Kent RW, AD Saunders, PD Kempton and NC Ghose. 1997. Rajmahal basalts, eastern India: mantle sources and melt distribution at a volcanic rifted margin. In: Mahoney, JJ and MF Coffin (eds.). Large Igneous Provinces: Continental, Oceanic and Planetary Flood Volcanism. *Geophysical Monograph, American Geophysical Union* 100: 145-182
- Sheth HC and D Chandrasekharam. 1997. Early alkaline magmatism in the Deccan Traps: implications for plume incubation and lithospheric rifting. *Physics of the Earth and Planetary Interiors* 104: 371-376
- Sun, SS and WF McDonough. 1989. Chemical and isotope systematics of oceanic basalts: implications for mantle composition and processes. In: Saunders, AD (eds.). Magmatism in ocean Basins. *Geological Society Publication* 42: 313-345
- Weis D, FA Frey, H Leyrit and I Gautier. 1993. Kerguelen Archipelago revisited: geochemical and isotopic study of the Southeast Province lavas. *Earth and Planetary Science Letters* 118: 101-119
- Yang HJ, FA Frey, D Weis, A Giret, D Pyle and G Michon. 1998. Petrogenesis of the flood basalts forming the northern Kerguelen Archipelago: Implications for the Kerguelen plume. *Journal of Petrology* 39: 711-748
- Zhu DC, SL Chung, XX Mo, ZD Zhao, Y Niu and B Song. 2008a. Kerguelen plume activity identified in southeastern Tibet: The Comei large igneous province. *Geology*, in review
- Zhu DC, XX Mo, GT Pan, ZD Zhao, GC Dong, YR Shi, ZL Liao and CY Zhou 2008b. Petrogenesis of the earliest Early Cretaceous basalts and associated diabases from Cona area, eastern Tethyan Himalaya in south Tibet: interaction between the incubating Kerguelen plume and eastern Greater India lithosphere? *Lithos* 100: 147-173



Geological map of Ladakh and Karakoram Mountains.
 Insert shows extrusion tectonics in Tibet

